U-SERIES DATING OF CARBONATES BY MASS SPECTROMETRY WITH EXAMPLES OF SPELEOTHEM, CORAL AND SHELL

by

JOYCE LUNDBERG, B.A (Mod.), M. Sc.

A Thesis

Submitted to the School of Graduate Studies

in Partial Fulfillment of the Requirements

for the Degree of

Doctor of Philosophy

McMaster University

February 1990

U-SERIES DATING OF CARBONATES BY MASS SPECTROMETRY

DOCTOR OF PHILOSPOHY (1990) McMASTER UNIVERSITY

(Geography) Hamilton, Ontario

TITLE: U-SERIES DATING OF CARBONATES BY MASS SPECTROMETRY WITH EXAMPLES OF SPELEOTHEM, CORAL AND SHELL.

AUTHOR: JOYCE LUNDBERG, B.A. Moderatorship (Trinity College, Dublin); M.Sc. (Australian National University, Canberra).

SUPERVISORS: Dr. D. C. Ford

Dr. H. P. Schwarcz

ABSTRACT

Uranium series dating is a well established technique for dating carbonate deposits of the last 350,000 years. The most common carbonates which have been dated are cave calcites (speleothem) and corals. The technique relies on the build-up of ^{230}Th over time by radioactive decay of ^{238}U and ^{234}U, in materials which were initially free of ^{230}Th. The ratios of the activities of $^{230}Th/^{234}U$ and $^{234}U/^{238}U$ are entered into the standard equation for radioactive decay which is then solved for time. These ratios have traditionally been measured by counting the alpha particle emissions from each isotope. An alpha counting laboratory was set up in McMaster in the early 1970s and is still in operation today. The technique has been improved considerably but the precision of dating by this method is limited by the statistics of counting small numbers of emissions from the trace quantities of isotopes trapped in the carbonate crystal lattice. Typically U ratios can be measured to 1σ precision of 1% and Th ratios to 3%. This leads to an error in the estimated date of ~10%. Alpha counting requires a rather large sample, varying from ~10 g to ~40 g depending on the U content and age of the sample. It also requires extensive chemical preparation of the sample to isolate U and Th from the matrix and to completely separate U from Th.

The development of high resolution and high abundance sensitivity thermal ionization mass spectrometry in the last decade has allowed for the measurement of heavy atom ratios to high precision with very small samples. The McMaster geology department acquired such a machine in the 1980s and it has been adopted for the

measurement of $^{230}Th/^{234}U$ and $^{234}U/^{238}U$ ratios. The typical 1σ precision attainable for U ratio measurement is 0.03% and for Th ratios 0.15%, which leads to an error in the estimated age of only ~0.5%. This is more than an order of magnitude better than that attainable by alpha counting. The sample size required varies from ~0.3 g to ~6 g depending on the U content and age of the sample. Thus sampling can be at higher density or resolution than for alpha counting. The technique requires rigorous purification of U and Th from the matrix but separation of U from Th can be rough, so the chemical preparation is simpler than that for alpha counting and usually involves only anion exchange procedures. Because the samples are so small and the technique so sensitive, contamination must be carefully avoided: all operations take place in a very clean environment.

Uranium and thorium ratios cannot be measured directly. Therefore, a tracer or "spike" of artificial isotopes of U and Th in a known ratio must be added. ^{236}U and ^{229}Th are used. The spike was made and its concentration and isotopic ratio calibrated against four standards of different origin. The accuracy of U ratio measurement was tested by measuring NBS U standards. The accuracy of Th ratio measurement cannot be directly tested because no Th isotopic standards are available. Instead it was tested by dating the McMaster standard speleothem 76001.

The main calcite sample to be dated was a piece of flowstone from -15 m in a flooded Bahamian cave. The many layers of calcite deposition separated by thin coatings of mud indicate that the cave was alternately air-filled (during calcite deposition) and water filled (cessation of calcite deposition) over the last 300,000

years. The drownings occur when sea level rises. The dates on the layers of calcite immediately below and above the mud-coated hiatuses give limits on the times when sea level must have been below -15 m elevation. The periods on non-deposition indicate when sea level was above -15 m. The dates on this sample allowed the construction of a sea level curve for this area of significantly higher precision than was formerly possible. The conclusion was reached that sea level events correlate with the marine foraminiferal isotopic signature which has been fitted to an orbitally-tuned timescale. This gives strong support for the orbital geometry theory (Milankovitch cycles) of climatic change.

The second sample dated was a thermal water calcite crust from Wind Cave, South Dakota. High resolution dating of this 2 cm thick crust suggested that degassing is the principal control on sub-aqueous crust formation and revealed the behaviour of the aquifer over two glacials and one interglacial. This has been modelled in terms of aquifer recharge rate and mixing of waters of surface and deep groundwater origin.

The third sample dated was a layered stalactite from Rat's Nest Cave, Alberta, which promised to yield a record of glacial advance and retreat in the Bow Valley, Rocky mountain foothills. Dating of the very thin layers simply revealed that calcite deposition correlates with interglacial periods and hiatuses correlate with glacials. A sample with thicker layers and a greater number of layers is required for closer resolution of individual advance and retreat events.

The rest of the study involved a small amount of test dating of other

materials. Dating of calcite raft debris from Carlsbad Caverns gave some information on the rate of drawdown of the water table. Dating of corals established that the technique works very well on this medium. Finally, dating of tiny samples of ostrich eggshells from the Sahara demonstrated that U-series dating may work on eggshells if they can be shown to have been closed to isotopic migration for most of their history. It also indicated that this now arid area was wetter during the last interglacial.

Mass spectrometric dating of carbonates is now established at two world centres: Caltech and McMaster. In the future it may completely replace alpha counting for Th/U and U/U dating. However, alpha counting is still the best option for Pa/U dating and other techniques which require the measurement of trace amounts of isotopes with high activities.

ACKNOWLEDGEMENTS

I would like to extend special thanks to Dr. Derek Ford who enabled this work to be undertaken through his academic and financial support. He has provided excellent supervision, stimulated ideas and extended support at all stages. My thanks also go to Dr. Henry Schwarcz for his many perceptive judgements and suggestions; to Wangxing Li for numerous helpful discussions and to Dr. Alan Dickin for help with mass spectrometry problems; to Catharina Jaeger for clean lab companionship and to Jim McAndrew for fixing things so efficiently. Thanks to Bob Bignell for photography, Cliff Brettle for making equipment, Greg Potter for providing spike thorium, Dennis Williams and Chas Yonge for speleothem samples and Lynton Land for coral samples, to Jim Garrett for the furnace test, to Jim Peneston for some proof reading. Thanks to Joan Parker for continuing support over the years and for help with printing.

TABLE OF CONTENTS

LIST OF FIGURES

LIST OF TABLES

Chapter 1

INTRODUCTION

1.1 U-SERIES DISEQUILIBRIUM DATING METHODS: a brief survey[1]

Uranium series dating is based on the radioactive decay of ^{238}U and ^{235}U (Figure 1.1).

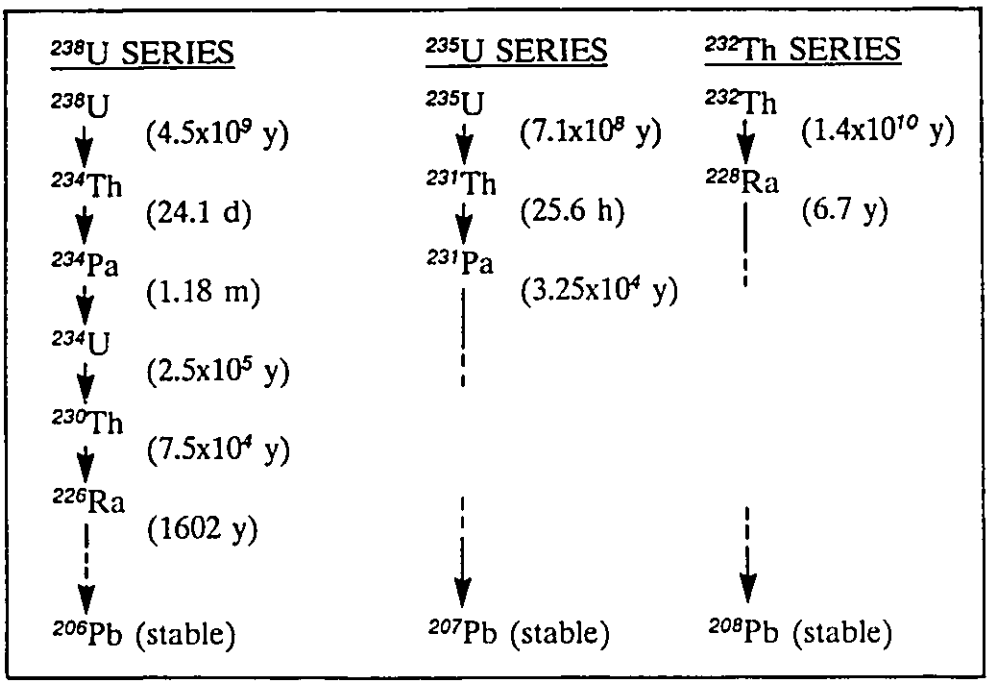

Figure 1.1: URANIUM AND THORIUM DECAY SERIES. The half lives of the isotopes are included in brackets. The dashed line indicates that some of the steps are missing. The intermediate steps between ^{238}U and ^{234}U, and between ^{234}U and ^{230}Th are ignored for U-series dating because they are very rapid.

In the uranium series most radioactive decays occur by the release of alpha particles or beta particles, often accompanied by the emission of gamma radiation. Alpha particles are helium nuclei and consist of two protons and two neutrons. Each

[1]For full discussion see Ku (1976), Ivanovich and Harmon (1982), Gascoyne (1984b) and Gascoyne, Schwarcz and Ford (1984).

alpha emission involves the loss of 4 atomic mass units and two positive charges. The element is transformed into a new isotope[2] of lower atomic mass and atomic number; for example, ^{234}U is transformed into ^{230}Th. Beta particles are electrons. Their emission involves loss of one negative charge, transformation of elements but no loss of mass. Gamma radiation involves loss of energy but neither charge nor mass. For each transformation in the decay series the emitted particle has a characteristic energy (α), or range of energies (β). The presence of a particular isotope is usually detected by measuring its emission at the characteristic energy level. Any of the emissions may be used but alpha particles are the most commonly measured. Their number, normally detected by alpha spectrometry, is a measure of the number of emitting atoms.

This thesis documents a new method for precise measurement of isotopic ratios for U-series disequilibrium dating. This method counts atoms by mass spectrometry, rather than their emissions by alpha spectrometry. The isotope ratios are measured to a precision an order of magnitude or more higher than is possible with alpha counting: the precision by mass spectrometry is 0.04 to 1.0% (2σ) compared to 2 to 10% by alpha counting (Harmon et al 1975). Other parts of the dating procedures have also been significantly improved so that the results are both more precise and more accurate than was formerly possible.

An important difference is in the sample size requirement: mass spectrometry needs only ~0.5 to 5 grams of material whereas alpha counting generally uses 20 to 100 grams. This allows for higher sampling densities and closer resolution of events of interest.

The theoretical basis behind the dating procedure, which is outlined below, is essentially identical for either method of isotopic ratio measurement. However, because it detects atoms by their mass rather than their activity, mass spectrometry

---

[2]An element may exist in several forms or "isotopes" of the same atomic number (i.e. same charge) so that their chemical behaviour is similar, but of different number of neutrons, so that their atomic masses are different.

can ignore many of the problems associated with interference in alpha spectrometry. The preliminary chemical purification for mass spectrometry is principally concerned with the separation of the atoms of interest from other molecules of the same mass; their activities are irrelevant. For alpha counting, atoms whose activities have a similar energy level must be carefully separated by chemical means. Because of this, the chemical preparation for mass spectrometry is simpler than that for alpha counting.

Another concern for alpha spectrometry is the ingrowth of very active daughters during the course of the rather lengthy counting procedure. Where the peak of interest is contaminated by ingrowth of daughters then the daughter must be measured separately and a correction made to the peak of interest. Such problems are of no concern for mass spectrometry.

1.1.1 Equilibrium and dis-equilibrium:

In a decay chain where the half life[3], $t_{½}$, of each successive daughter is less than each parent (i.e. the decay rate gets faster down the chain) there can be no build up of daughters. Where a system has been left undisturbed for a long time (e.g. $> 10 \times t_{½}$) then a balance exists between each decay product and its daughter such that the rate of production is balanced by the rate of decay: the ratio of the activity of daughter to parent is 1.00. This state is called "Secular radioactive equilibrium". The time required to achieve equilibrium for the different decay steps depends on the half lives of the isotopes involved: e.g. in a sample of uranium, ^{234}U will produce ^{230}Th which will in turn decay to ^{226}Ra until the $^{230}Th/^{234}U$ ratio[4] reaches 1.00, in about 600,000 years.

---

[3]The half life is the time required for half of the atoms to disintegrate.

[4] The ratio of the activities of two isotopes is expressed in the form $^{230}Th/^{234}U$ throughout the thesis; to avoid confusion where necessary the words "activity ratio" may be added. Where the ratio of the number of atoms is required this will be specified as $^{230}Th/^{234}U$ atomic ratio.

If a system is disturbed so that the ratios are no longer 1.00 then equilibrium is destroyed. U-series dating is based on measurement of the return to equilibrium of a disturbed system. Typically the system to be dated begins with none, or very low levels, of one of the isotopes. Where the parent was present and the daughter missing at the start of the system ("daughter deficient methods") then a measure of the build-up of daughter gives a measure of the time since the system was created or was reset to zero. Where the daughter/parent ratio is greater than 1.00 ("daughter excess method") then the reduction in levels of the unsupported daughter as it decays gives a measure of time.

1.2 DAUGHTER-DEFICIENT METHODS

1.2.1 $^{230}Th/^{234}U$ decay:

The most common method of radiogenic dating in carbonates, the "daughter deficient" method, is based on the accumulation of decay products of U, where ^{238}U and ^{234}U are present when the system is initiated but ^{230}Th is absent or at very low levels. This separation of mother and daughter is effected through the differing solubility of uranium and thorium. Uranium is soluble in water and thus mobile in the lithosphere and biosphere, while thorium is virtually insoluble in neutral and alkaline waters and is relatively immobile: uranium is carried in solution in soil-, ground- and sea-water while thorium tends to remain adsorbed to detrital particles. During speleothem deposition uranium is deposited from groundwater solution into the crystal lattice but thorium is not. In this way the speleothem system is initiated with parent present but daughter absent. The initial $^{230}Th/^{234}U$ activity ratio is zero. ^{230}Th builds up over time from the decay of ^{234}U, which is itself supplied by the decay of ^{238}U. After about 600,000 years the $^{230}Th/^{234}U$ ratio reaches equilibrium. In the interim, this ratio gives a measure of time elapsed. The limit of the time period which can be measured depends on the accuracy with which the ratio can be measured and the quantities of radionuclides in the sample.

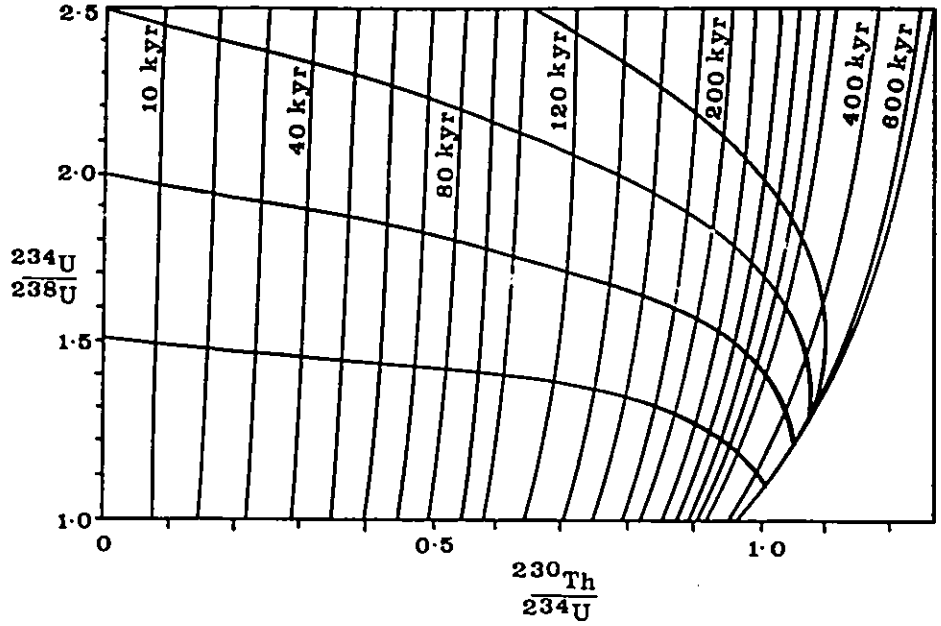

Figure 1.2: GRAPHICAL REPRESENTATION OF THE $^{230}Th/^{234}U$ DATING EQUATION. ^{230}Th grows towards equilibrium with ^{234}U in a closed system which begins with no initial ^{230}Th. The near-vertical lines show isochrons of the time elapsed since the start of the system. The roughly horizontal lines depict the change in $^{234}U/^{238}U$ ratio over time.

Other carbonates are daughter deficient for similar reasons. In the sea, thorium is adsorbed onto detrital particles which settle out rapidly, leaving the water thorium deficient. Dissolved uranium enters the tissue fluid of marine organisms such as coral and becomes incorporated into the carbonate tests, but thorium does not. The shells of land animals such as ostriches will likewise be thorium deficient because thorium is not present in tissue fluid.

The $^{230}Th/^{234}U$ daughter deficient dating method requires estimates of the $^{230}Th/^{234}U$ and the $^{234}U/^{238}U$ activity ratios and the decay constants of the isotopes. The time since initiation of the system is calculated using the standard dating equation (Schwarcz and Gascoyne 1984, Ivanovich 1982):

$$^{230}Th/^{234}U = (1 - e^{-\lambda 230\, t})\ (^{238}U/^{234}U)$$
$$+ [(1 - {}^{238}U/^{234}U) \times \lambda 230/(\lambda 230 - \lambda 234)]\ (1 - e^{-(\lambda 230 - \lambda 234)t})$$

where t is time and $^{230}Th/^{234}U$ and $^{238}U/^{234}U$ refer to the activity ratios of the isotopes today, and $\lambda 230$ and $\lambda 234$, the decay constants. The formula is solved iteratively: an initial estimate for time is entered and the estimate is then improved to a stated limit. A graphical representation of time in relation to both ratios is shown in Figure 1.2.

Alpha spectrometry has been the most important means of measuring activity ratios for U-series disequilibrium dating since the establishment of these dating methods in the early 1950s (Gascoyne 1977a, 1977b and 1984b). Alpha particle emission for each of the nuclides is at a characteristic energy. However, the pulses for ^{230}Th and ^{234}U are too close to resolve because the pulses are somewhat flattened and each has a tail to the low energy side. For this reason the thorium and uranium fractions must be separated chemically and the alpha emissions counted separately.

Uranium and thorium behave differently during chemistry. In order to account for the difference and for any loss during processing, a tracer or "spike" of known concentration, which contains one isotope of uranium and one of thorium, must be added at the start of the chemical procedures. The fate of the spike isotopes then gives a measure of the fate of the sample isotopes: the true ratios of the sample isotopes can be calculated by adjusting the measured ratios according to the difference between the measured ratio and the true ratio of the spike. A commonly used spike is a mixture of artificial ^{228}Th and ^{232}U. It is assumed that all isotopes of a particular element behave in the same way chemically: that fractionation during the chemical processing is negligible. Therefore the yield of the spike isotopes after chemistry is a true indication of the yield of the sample isotopes:

$$[^{230}Th/^{234}U]_{true} = [^{230}Th/^{228}Th]_m \times [^{232}U/^{224}U]_{m} \times [^{228}Th/^{232}U]_s$$

where m is the measured ratio and s is the spike ratio.

The ratio of Th and U in the spike must be accurately known because the precision of the dating method depends largely upon this measure. Calibration of the

spike ratio and concentration is achieved in two ways (Gascoyne 1977b): by measurement against Th and U standards of known isotopic composition and concentration, or by measurement against a uraninite ore standard of "infinite" age whose $^{234}U/^{238}U$ and $^{230}Th/^{234}U$ activity ratios are at secular equilibrium[5].

In order to date a sample the alpha emissions are counted over the range expected; the count for each isotope is summed by integration across the peak. The area to be integrated is decided by the operator. Ideally the counts should fall to zero to either side; in practice the operator has to choose where background noise gives way to the peak limb. The counts must also be adjusted for interpeak counts, detector contamination and background noise, and reagent blank. Detector contamination and background is counted on blanks at regular intervals and an average value used. Reagent blanks are usually counted less often.

For each sample the counts must be done soon after the last chemical step before the short lived daughters of high activity grow in and prevent resolution of the peaks of interest. The daughters which may cause problems are of bismuth which accompanies U and Th during chemistry (Gascoyne 1977a).

The error associated with each count is calculated from Poisson statistics ($\sigma_n = \sqrt{n}$). For a 1σ error of 1% or less the peak must have at least 10^4 counts. The count time depends on the U and Th content of the sample and may vary from around 10^3 minutes to 10^4 minutes. For a very low U sample, increasing the count time beyond this is of no added value because the background count and the error associated with its measurement are too high relative to the sample peaks.

The age equation is solved iteratively by computer program (Gascoyne 1977a). The error associated with the date is a measure of precision associated with counting statistics but includes no estimate of other sources of uncertainty (see chapter 4). The $^{230}Th/^{234}U$ daughter deficient dating method is the principal one used in this thesis.

---

[5]This is further discussed under the section on spike calibration.

1.2.2 $^{231}Pa/^{235}U$ daughter deficient method:

Protactinium dating using the $^{231}Pa/^{235}U$ ratio is another commonly used daughter deficient method (Ivanovich 1982). Protactinium resembles thorium in its solubility and chemical behaviour. It is relatively insoluble in water, so that initial values of ^{231}Pa in speleothem are low or zero. ^{235}U decay produces ^{231}Pa and secular equilibrium is approached after 200,000 years. Since this method has a shorter time scale it is generally used as a cross check on $^{230}Th/^{234}U$ dates. However, it is successful only on samples with a relatively high U content (>1 ppm) because concentrations of source ^{235}U are low (the $^{235}U/^{238}U$ atomic ratio is only .00726). Ku (1968) found this method to be useful for dating unaltered corals: high U levels permitted high precision Pa dating and the ages agreed well with $^{230}Th/^{234}U$ dates.

1.3 DAUGHTER EXCESS METHODS

1.3.1 ^{234}U excess:

Daughter excess dating is based on the decay of unsupported intermediate nuclides in the series: the original system generates a daughter/parent ratio greater than unity. Over time the excess daughters decay and the system returns to secular equilibrium. Provided that the initial daughter to parent ratio is known then the quantity of daughter left provides a measure of the time since deposition. If ^{234}U is at a higher activity level than ^{238}U, and if the initial $^{234}U/^{238}U$ activity ratio is known, then the relationship between the initial and the present-day ratio provides a dating method. Time is measured as the decay of the unsupported ^{234}U towards equilibrium with ^{238}U. The relationship is given by:

$$[(^{234}U/^{238}U)_t - 1] = [(^{234}U/^{238}U)_0 - 1]\, e^{-\lambda 234 t}$$

where λ 234 is the decay constant for ^{234}U, $(^{234}U/^{238}U)_t$ is the present activity ratio and $(^{234}U/^{238}U)_0$ is the initial ratio. This method is used occasionally in this study.

A major source of uncertainty in this method is the estimation of initial

$^{234}U/^{238}U$ activity ratios. For marine deposits it appears that the $^{234}U/^{238}U$ ratio of sea water has been close to 1.144 ± 0.002 (Chen et al 1986) for at least 200,000 years. Marine organisms incorporate this uranium into their tests and, since uranium is not used for any metabolic process and its concentration will therefore be constant throughout the body of the animal, there should be no fractionation. The initial $^{234}U/^{238}U$ is thus 1.144 and time is measured as the change from 1.144 towards 1.00. Equilibrium is reached in about 1.2 million years, so this method gives a potentially long timescale. In theory it is applicable to unaltered corals (e.g. Veeh 1966) but in practice it is less reliable than $^{230}Th/^{234}U$ dating because the initial $^{234}U/^{238}U$ activity ratio cannot be confidently known in old corals (e.g. Harmon et al 1983). Edwards (1988) and Edwards et al (1987, 1986/86 and 1988) found that corals which are thought to have remained closed to isotopic migration have a range of initial $^{234}U/^{238}U$ ratios generally higher than that of seawater.

Ku (1965) investigated the possibility of using this 14.4% excess ^{234}U activity to date pelagic sediments but discovered that the sediments do not form a closed system; ^{234}U migrates after deposition, so this dating method cannot be used in any simple manner.

In speleothem (see Thompson, Ford and Schwarcz 1975 and Harmon, Thompson, Schwarcz and Ford 1978) it is sometimes possible to see a clear trend towards equilibrium in sequential samples. This implies that the $^{234}U/^{238}U$ ratios in the feeder drips were constant over time. If a $^{230}Th/^{234}U$ dated series shows a constant initial $^{234}U/^{238}U$ ratio and this initial ratio is adopted for all of the speleothem, then that part older than 350,000 years but younger than around 2 million years can be dated very approximately. Similarly, if all the speleothem from a region show similar initial $^{234}U/^{238}U$ ratios then the Regional Uranium Best Estimate (R.U.B.E.) technique may allow even more approximate dating of the older samples of the region (Gascoyne et al 1983 and Gascoyne 1984b).

1.3.2 ^{230}Th and ^{231}Pa excess:

These daughter excess methods are used to date deep sea sediment (Ku 1976). ^{234}U and ^{235}U dissolved in sea water decay to the insoluble ^{230}Th and ^{231}Pa. These precipitate onto the sea floor sediment, are buried and subsequently decay. If the sediment builds up at a constant rate then the concentrations of ^{230}Th and ^{231}Pa decrease exponentially with depth. Either of these decay steps may be used as a dating tool. A variation on this theme is the change over time of the unsupported ^{231}Pa/^{230}Th ratio from an initial constant ratio. This gives a dateable range of 150,000 years.

This technique is possible for marine sediments because the U content of sea water has remained reasonably constant over geological time and can be assumed to be constant over the time scale of deep sea sediments from cores. The major drawback is that there must be no input of detrital Th from land sediment; otherwise some of the ^{230}Th may not be from decay of ^{234}U in the water. The technique also assumes that ^{230}Th rains out at a constant rate. There is some evidence that particles of biogenic origin scavenge ^{230}Th more efficiently than detrital particles so dates from cores with high biogenic carbonate content may not be reliable.

The technique cannot be used for inland water sediments or shallow sea sediments because the initial levels of thorium or protactinium cannot be known.

1.4 COMPLICATIONS FOR ^{230}Th/^{234}U DATING

The most commonly used of all these dating techniques is the ^{230}Th/^{234}U daughter deficient method. This is the technique usually implied by the term "U-series disequilibrium dating". It is widely used but proper interpretation of results requires awareness of several problems such as detrital contamination, organic matter effects, weathering effects and open system migration of isotopes.

1.4.1 Detrital contamination:

Any of these dating techniques relies on the assumption that the initial

conditions are known. A pure carbonate sample is deposited with no initial thorium. ^{230}Th builds up over time from U decay and the levels of ^{232}Th are very low. However, detritus carries adsorbed ^{232}Th and, possibly, ^{230}Th. If a sample contains detritus then some ^{230}Th may have been present at the time of deposition in association with the ^{232}Th which was adsorbed onto the detrital particles. The ^{230}Th now detectable in the sample may originate partly from radioactive decay of ^{234}U and partly from the detritus. The initial levels have to be assumed and the age corrected for detrital ^{230}Th. The presence of detritus is detected by high levels of ^{232}Th. In most labs an activity ratio $^{230}Th/^{232}Th$ of < 20 is considered to be the threshold indicating detrital contamination.

Detritus occurs in speleothem mainly around hiatuses where flooding deposited a layer of mud or organic matter. This is particularly unfortunate because these events are usually the most interesting part of the sample and corrections using assumptions of initial ratios are rarely satisfactory. Corals seldom have problems of detrital contamination: sometimes voids are infilled with detritus but these are usually of a distinct colour and can be avoided during sampling.

1.4.2 Correction for detrital contamination:

Most detritus is made up of HNO_3- or HCl- insoluble resistate material which can be dissolved in HF. The detrital and carbonate phases cannot be completely separated chemically. Dissolution of the sample in HNO_3 or HCl will leach some of the thorium (both ^{232}Th and ^{230}Th) and possibly some uranium from the detritus (Ku and Liang 1984). This fraction, the leachate, therefore contains U and Th from the pure carbonate phase and some U and Th from the detrital phase.

Several approaches to correction techniques have been proposed using a variety of analyses: (i) of leachate alone, (ii) of leachate and detrital phases separated, (iii) of leachate and detrital phases mixed.

A very simplistic approach is to measure the current $^{230}Th/^{232}Th$ ratios in modern detritus, assume that this represents the original $^{230}Th/^{232}Th$ ratio of the

detritus contaminating the carbonate, and correct the age accordingly. The sample is dissolved in HNO_3, the insolubles in HF and $HClO_4$ and the mixture analyzed for isotopic ratios. Kaufman and Broecker (1965) found that Lakes Lahontan and Bonneville sediments had a $^{230}Th/^{232}Th$ ratio of 1.70. They used this ratio to correct for non-radiogenic ^{230}Th. This value of 1.7 for the original $^{230}Th/^{232}Th$ activity ratio of detritus has been used in this thesis in the section of the BASIC program AGE.BAS for detrital correction. There is no real justification for adopting it except that the correction is very simple. It only gives an order of magnitude correction and should be evaluated as such. Any correction using an assumed initial ratio is only as good as that ratio. Various labs use different estimates and sometimes change their estimates. Published values range from 1.25 to 1.70; for example, Blackwell and Schwarcz (1986) use 1.25. This correction method is clearly inferior to those described below but is the only one available for a single sample analysis of leachate alone.

Another approach is to dissolve the sample in HNO_3, separate off the insolubles and then dissolve those in HF. The two fractions are analyzed separately. The $^{230}Th/^{232}Th$ ratio of the detrital phase is measured and used to correct the $^{230}Th/^{232}Th$ ratio of the carbonate phase. This ignores any possibility of fractionation of the more soluble ^{230}Th compared to ^{232}Th during dissolution. Ku et al (1979) measured the $^{230}Th/^{232}Th$ ratio in the nitric acid insoluble fraction of caliche samples, assumed secular equilibrium for $^{230}Th/^{234}U$ and $^{234}U/^{238}U$ of detrital phase, allowed for fractionation between U and Th during dissolution but no fractionation of thorium isotopes. They corrected the measured ^{230}Th from the soluble fraction thus:

$$^{230}Th_C = {}^{230}Th_L - {}^{232}Th_L(^{230}Th/^{232}Th_R)$$

$$^{234}U_C = {}^{234}U_L - {}^{232}Th_L(^{230}Th/^{232}Th_R) - f_R/f_L(^{230}Th_R - {}^{234}U_R)$$

$$^{238}U_C = {}^{238}U_L - {}^{232}Th_L(^{230}Th/^{232}Th_L) - f_R/f_L(^{230}Th_R - {}^{238}U_R)$$

where subscripts C, L and R refer to the carbonate phase, the leachate and the resistate (detrital) phase and f is the weight fraction. The terms ($^{230}Th_R$ - $^{234}U_R$) and ($^{230}Th_R$ - $^{238}U_R$) correct for U/Th fractionation during dissolution assuming secular equilibrium. This assumption of secular equilibrium for the detrital phase is debatable: usually ^{234}U is in excess (Szabo and Rosholt 1982).

If the sample is totally dissolved (carbonate and detritus) then differences in solubility of the isotopes are taken into account. The solution contains ^{230}Th of radiogenic origin from the nitric acid soluble phase, ^{230}Th of non-radiogenic origin from the detrital phase and ^{232}Th from the detrital phase (Schwarcz 1979 and 1980). A small proportion of U may have leached from the detritus. The ^{232}Th is an index of the quantity of detritus and a set of equations is derived whose intercepts at ^{232}Th = 0 give the ^{230}Th, ^{234}U and ^{238}U activities of the non-detrital phase:

$$^{238}U_s = [(^{238}U_d - ^{238}U_c) / ^{232}Th_d] \, ^{232}Th_s + ^{238}U_c$$

$$^{234}U_s = [(^{234}U_d - ^{234}U_c) / ^{232}Th_d] \, ^{232}Th_s + ^{234}U_c$$

$$^{230}Th_s = [(^{230}Th_d - ^{230}Th_c) / ^{232}Th_d] \, ^{232}Th_s + ^{230}Th_c$$

where s indicates the whole sample, d the detrital phase and c the carbonate phase.

A different approach to detrital correction requires the analysis of several samples from the same growth layer but with varying proportions of detrital contamination (Osmond et al 1970, Ku and Liang 1984). This is called "Isochron" dating because the samples are presumed to have been deposited during the same time interval. The variety of $^{230}Th/^{232}Th$ ratios represents a variety of carbonate/detritus weightings. The carbonate $^{230}Th/^{232}Th$ ratio is presumed to be the same for each so the variety is contributed by varying inputs from the detrital phase. The radiogenic $^{230}Th/^{234}U$ ratio should be the same for each sample. However the non-radiogenic $^{230}Th/^{234}U$ ratio will vary with the quantity of detritus. The samples may be totally dissolved, or the leachate and detrital phases analyzed separately but the results processed as one, or only the leachate analyzed. The correction requires that U and Th leached from the detrital phase are not

of the resistate material should be the same as the detritus.

The $^{230}Th/^{234}U$ activity ratios are plotted against the $^{232}Th/^{234}U$ ratios for all the analyses: they will show a positive relationship. The line of best fit is propagated back to a $^{232}Th/^{234}U$ ratio of zero. This intersects the Y-axis at the radiogenic $^{230}Th/^{234}U$ ratio. The slope of the line is the $^{230}Th/^{232}Th$ ratio of the detrital component. A plot of $^{234}U/^{238}U$ against $^{232}Th/^{234}U$ (negatively correlated) will yield the $^{234}U/^{238}U$ for zero detritus.

Alternatively, the slope of $^{234}U/^{232}Th$ against $^{238}U/^{232}Th$ gives $^{234}U/^{238}U$ and the slope of $^{230}Th/^{232}Th$ against $^{234}U/^{232}Th$ gives the $^{230}Th/^{234}U$ ratio (Blackwell and Schwarcz 1986 and Schwarcz and Skoflek 1982). These are used to get an estimate of age.

Kaufman (1971) applied these corrections to samples of lake basin marls of varying detrital contamination. The method of correction appeared to be quite successful: by using the estimates for $^{230}Th/^{234}U$ and $^{234}U/^{238}U$ for zero detritus, the whole series was shown to have a constant initial $^{234}U/^{238}U$ ratio.

A further modification is possible where the intercept at $^{234}U/^{232}Th$ of zero gives the $^{230}Th/^{232}Th$ ratio of the leachable part of the detritus (Schwarcz 1980). The original $^{230}Th/^{232}Th$ ratio is given by:

$$^{230}Th/^{232}Th_o = {}^{230}Th/^{232}Th_c \times e^{(-\lambda 230t)}$$

where the subscript o represents "original", and c, "current" $^{230}Th/^{232}Th$ of the leachable part of the detrital thorium

Then:

$$^{230}Th/^{234}U_R = {}^{230}Th/^{234}U_M - {}^{232}Th/^{234}U_M \times {}^{230}Th/^{232}Th_o \times e^{(-\lambda 230t)}$$

where $^{230}Th/^{234}U_R$ is the radiogenic, and $^{230}Th/^{234}U_M$ the measured ratio. The age is then recalculated with the new $^{230}Th/^{234}U$ estimate.

Ku and Liang (1984) observe that this correction method requires no fractionation of U and Th during leaching. They discovered significant fractionation with strong acids but none with weak acids and recommended a preparation procedure to minimize fractionation involving conversion of $CaCO_3$ to CaO in a furnace followed by dissolution in very dilute acid. The resistate fraction is dissolved and analyzed separately. Schwarcz and Latham (1990) observe that it may be difficult to ensure complete freedom from fractionation and that, if any does occur, then the leachate-resistate method will be incorrect. They show that analysis of leachates alone is not adversely affected by fractionation: it does not affect the slopes of the isochrons. The method works providing the detrital component is uniform from one sub-sample to another. Przyblowicz, Schwarcz and Latham (1990) showed that the leachate alone method is superior for artificial mixtures of pure calcites of known age and detrital content.

Isochron dating requires that a large range of ^{232}Th levels be included and that the points plot reasonably close to a straight line. The error on the ratios taken from the extrapolated lines of best fit are calculated from the precision of the regression line. The error on each of the original points tends to have an equal effect on both ordinate and abscissa and so is not included (Schwarcz and Latham 1990). Obviously a date from an isochron plot is less precise than its quoted precision suggests.

Not all samples with high ^{232}Th necessarily need correction. Gascoyne, Ford and Schwarcz (1981) found that a replicate of a highly contaminated sample on a less contaminated sample from the same layer gave a concordant age. This suggests that ^{230}Th did not accompany the ^{232}Th from the detritus and that no correction is required. For the Rat's Nest Cave stalactite sample dated in this thesis, the detrital layers give a date 1.5 to 2% younger than less contaminated replicates. In this case the higher U concentration of the detrital samples suggests that slight ^{234}U contamination from the detritus affected the isotopic ratios more than ^{230}Th contributions.

1.4.3 Organic matter contamination:

Organic matter contamination may affect the dating procedure and the interpretation of results (Bakalowicz 1982, Lauritzen 1983). It may cause loss of spike and poor yields during chemistry. It can also act like detrital contamination in that it may contribute some Th to the sample so that the initial ^{230}Th is not zero.

Organic contaminants are evident where a sample is coloured and/or foamy during dissolution (Gascoyne 1977c). They are usually present as either humic or fulvic compounds (complex, high molecular weight organics derived from soil components). They can chelate U and/or Th. Both are water soluble but in acid conditions humics are insoluble while fulvics are soluble. Thus uranium and/or thorium adsorbed to humics may be lost in chemical preparation during the acid dissolution and centrifuging step. Ether causes a loss in solubility in fulvics so these may be lost during iron extraction with isopropyl ether (Gascoyne 1977b).

For reliable results the chelated U or Th must be extracted before centrifuging. Bakalowicz (1982) tried several methods to breakdown the organics: (i) oxidation of finely-crushed sample by ultra violet light in an oxygen atmosphere was not particularly effective; (ii) dissolution in concentrated HNO_3 followed by exposure to UV light increased U yield; (iii) oxidation by hydrogen peroxide and UV light gave the best improvement for both U and Th but (iv) oxidation by H_2O_2 alone proved to be the best compromise for effectiveness and convenience.

1.4.4 Weathering Effects - Leaching:

Where a sample has been exposed to agents of weathering, either between stages of deposition or after cessation of deposition, then it must be sampled with care and the dates interpreted with discretion. Weathering is mainly expressed as leaching of uranium. It may be apparent in a layer of exceptionally low U concentration or of uncommonly low $^{234}U/^{238}U$ ratio.

In speleothem leaching is usually restricted to the layer immediately beneath a depositional or erosional hiatus where the sample was exposed to re-solution.

Leaching may be hard to detect on a sample taken in isolation: if a series is dated and the date immediately beneath an hiatus is clearly out of chronological order then uranium leaching should be suspected. Leaching will impart a falsely old date because the thorium persists but the supporting uranium has been washed out.

In corals weathering effects will depend on the history of the sample. Most of the corals dated in this study were deposited during high sea stands and are currently exposed at about +5 m above modern sea level. They have been open to weathering at the earth's surface for over 100,000 years. The external, weathered portions can be seen to have a more porous texture and grey appearance compared to the compact, white interior. Surface weathering may cause biological corrosion (e.g. from cyanophyte activity) as well as leaching of uranium. In that case the date may also be affected by remnant organics.

1.4.5 Open systems:

U-series dating generally requires that the crystal remain closed to isotope migration, that there be no movement of U or Th after deposition. This may not always be the case: the system may have been "open" for some or all of its history. Bones and shells are classic examples: the extremely high uranium content of fossil bones and shells compared to the low levels of their living or recently dead counterparts indicates considerable post-depositional uptake of uranium. Broecker (1963) observed such a discrepancy between many species of living and fossil mollusks and concluded that they were not suitable for U-series dating. Szabo and Rosholt (1969) found discordance between ^{230}Th and ^{231}Pa dates on molluscan shells and presumed open system behaviour. Excess ^{231}Pa with respect to ^{235}U indicated that U had migrated after having produced daughters. They presumed that the U which had migrated was of the same ^{234}U/^{238}U ratio as that which remained and proposed a model based on the measured activities of ^{230}Th, ^{231}Pa, ^{234}U and ^{238}U; an initial estimate of time is input to their dating equation and improved on successive iterations. This same model was applied by Szabo, Malde and Irwin-

Williams (1969). However, it was discredited by Kaufman et al (1971) who demonstrated that no system of correction has any notably high success rate. They observed that open systems are indicated by (i) an increase of ^{238}U with time, (ii) an increase of the $^{234}U/^{238}U$ activity ratio over time, and (iii) discordant $^{230}Th/^{234}U$ and $^{231}Pa/^{235}U$ ages. They concluded that (i) U-series dating on mollusks which show open system behaviour is highly questionable, and (ii) modelling the migration of U-series isotopes may be difficult because it is complicated and possible multi-staged.

Uranium is more likely to be mobilised than thorium because of its greater solubility in water. Therefore, open systems where the U has been mobilised and lost would tend to return falsely old dates. If uranium is added to any part of the system then the age will be falsely young. In addition, ^{234}U, being more soluble[6] than ^{238}U, is more likely to have migrated. Therefore the $^{234}U/^{238}U$ ratios might be lower than expected and the $^{230}Th/^{234}U$ ratios higher than expected.

Typically migration might be expected where recrystallization has occurred. Stability of crystal form is a function of grain size because recrystallization is driven by surface energy: the smaller the grain size the greater the relative surface area. This is especially important for corals because they are originally deposited in a fine-grained aragonitic form which is easily changed into more stable coarser-grained calcite. Some shells also recrystallize from aragonite into calcite; Tridacna is one of the few shells which is deposited as calcite and is not so liable to recrystallization. Speleothem is less likely to show recrystallization because it is usually deposited as sparry calcite. If a speleothem shows no signs of recrystallization or re-solution and if the dates are in chronological order then the system is likely to have remained closed to post-depositional isotope migration.

Shells and bones have a strong tendency to absorb U after death of the

---

[6] ^{234}U is more soluble than ^{238}U because it is in sites of lattice damage from alpha particle tracking, because alpha recoil may project the newly decayed atom into solution and because it is slightly less massive and therefore slightly more chemically reactive (Osmond and Cowart 1982).

organism. If the open state were temporary, so that absorption took place in a single step soon after death, then there might be no problem. This appears to have applied in the case of the ostrich egg shells dated in this study. However, usually the pattern of uptake cannot be easily modelled because it depends on diffusion gradients, crystal structure, U concentration in the environment, porosity of substrate, etc. Several models of uptake have been investigated but few have been shown to be applicable beyond the immediate sample (Ku 1965, Szabo and Rosholt 1969, Ivanovich 1982).

1.5 BRIEF HISTORY OF U-SERIES DATING OF CARBONATES BY ALPHA COUNTING

The earliest dating efforts in the 1950s were generally unsuccessful because of the unsuitability of the materials tested (Gascoyne 1984b). Revival of interest in the 1960s led to further research into the potential of U-series dating. Barnes et al (1956) dated corals reasonably successfully using only $^{230}Th/^{234}U$ decay. Cherdyntsev et al (1965) reported that soils and bones were unsatisfactory due to migration of isotopes while calcareous tufas and travertine had the greatest potential. Kaufman and Broecker (1965) tried lake carbonates (gastropods, tufa, marl, ostracods) and reported that, where the ^{232}Th contribution is not "unusually large", dates are reliable; if the initial $^{230}Th/^{232}Th$ ratio can be established, then excess ^{232}Th can be accounted for. Broecker (1963) tested the potential of many types of marine carbonates and concluded that corals and oolites are suitable but fossil mollusks are unsuitable because they are open to post-depositional U uptake. Osmond et al (1965) then dated corals and oolites, again using only the $^{230}Th/^{234}U$ decay.

A wide variety of materials have since been dated with varying degrees of success (Szabo and Rosholt 1982, Gascoyne and Schwarcz 1982). Thompson (1973) demonstrated the successful application to speleothem. Schwarcz et al (1979) and Harmon et al (1980) dated open air precipitated travertines at archaeological sites, Kaufman (1971) dated lake marls, Ku et al (1979) caliche rinds. Gascoyne and

Schwarcz (1982) observed that any mineral which is precipitated from ground or surface water containing uranium but no thorium may be dated by U-series disequilibrium. Sulphates and carbonates of caves are obvious candidates but even evaporites may be dateable. Speleothem and corals remain the most reliable materials for U-series dating.

1.5.1 Applications to geographic problems:

U-series dating of speleothem provides information on the history of the sampled cave but its greater value is realised when it is combined with other information or other techniques such as isotope geochemistry (Gascoyne, Schwarcz and Ford 1978).

The number and variety of applications is large. Harmon (1975), Gascoyne et al (1980) and Gascoyne et al (1981) coupled dating with oxygen isotope chemistry to elucidate variations in paleotemperature over time as recorded in speleothem. Harmon, Ford and Schwarcz (1977), Atkinson et al (1978), Gascoyne (1981), Gascoyne Schwarcz and Ford (1983), Atkinson et al (1986) and Gordon et al (1989) used the distribution of U-series ages on speleothem to show the timing of glacial and interglacial periods. Harmon, Schwarcz and Ford (1978) and Gascoyne et al (1979) elucidated sea level changes by means of dates on drowned Bermudan and Bahamian speleothem. Gascoyne (1980) estimated rates of valley entrenchment from speleothem dates in N. W. England. Gascoyne Ford and Schwarcz (1983) and Gascoyne and Ford (1984) similarly used cave dates to estimate rates of landform development.

The value of speleothem dating is now well established in the scientific literature. The McMaster lab, set up and maintained by D.C. Ford and H.P. Schwarcz, has been an important centre since the early work of Thompson (1973). Harmon (1975), Gascoyne (1979) and Latham (1981) continued to improve the methods. The establishment of the mass spectrometric technique puts McMaster once again in the forefront of dating advances.

The only other successful U-series dating by mass spectrometry is from the Cal Tech laboratory. Chen and Wasserburg (1980 and 1981) measured $^{238}U/^{235}U$ ratios by mass spectrometry on a variety of meteorites and terrestrial basalts. This was the first high precision mass spectrometric analysis of U isotopic ratios with small samples. They moved on to the analysis of sea water and added ^{234}U and ^{232}Th to the list of successfully measured isotopes (Chen, Edwards and Wasserburg 1986). Edwards (1988) and Edwards et al (1986/7 and 1987) added ^{230}Th measurement to date corals using the $^{230}Th/^{238}U$ dating equation. They tested the accuracy of the dating technique by dating very young corals (Edwards et al 1988) which had been dated by other means. Their results were extremely favourable with precisions on age less than 1% (2σ) error. They established the superiority of mass spectrometric U-series dating over alpha counting.

1.6 LIMITATIONS ON U-SERIES DISEQUILIBRIA DATING METHODS

In 1982 Ivanovich could state that "few radiometric techniques can date events in the 300 - 1000 kyr period". Mass spectrometric dating has improved precision so much that the limit is now close to 550 kyr. For example, a high uranium sample (3 - 4 ppm) may yield a $^{230}Th/^{234}U$ ratio with 0.5% error and a $^{234}U/^{238}U$ ratio with 0.2% error; the upper limit of dating resolution would be around 550 kyr with an error margin of around 50 kyr. However, for most samples the limit is closer to 500 kyr with an error of ~70 kyr. The gap between ~500 and 1000 kyr remains. The $^{234}U/^{238}U$ method covers the gap but there are still major problems with its application. Mass spectrometry can improve the precision of this method but cannot remove the uncertainties in the estimation of initial $^{234}U/^{238}U$.

Ku (1965) observed that the absolute dating of deep sea sediments during the Pleistocene is vital but that all the methods then available were limited to less than half of the Pleistocene history. Again mass spectrometry can improve the precision on ratio measurement but the cannot affect the uncertainties of the assumptions on which dates are based. One of the possibilities for further research

is to exploit the small sample size requirement for mass spectrometry to date ocean core foraminiferal tests.

Coral dating by U-series disequilibrium has provided much information on sea level change, rates of tectonism, etc. The relationship of sea level, ice volume, climate and solar insolation and orbital geometry has been of great interest for the last two decades. However, the precision of alpha counting, even on high U coral samples, is too low to allow for clear resolution of the timing of sea level events. Mass spectrometry on corals is now well established and the process of high precision dating of high sea level stands has begun (see section on dating corals). Dating of drowned speleothem (see chapter on Bahamas sea level history) has excellent potential for elucidating the timing of low sea stands. Mass spectrometric dating should provide a suitably precise data base to study the effect of orbital geometry on climate, ice volume and sea level. However, the limit of ~500 kyr still applies.

Most coral dates up to the present have been on colonial corals. These are limited to tropical coastal areas so that the geographical information they provide is necessarily limited. Dating of solitary corals is of interest because these have a wider geographical distribution. This is currently being done by mass spectrometry at Cal. Tech.

Dating of cave mouth or sub-aerial tufas and travertines has always caused great problems for alpha counting. Detrital and/or organic contamination severely constrains the interpretation of results. The smaller sample size requirement of mass spectrometry may allow more selective sampling of less contaminated layers.

Chapter 2

MASS SPECTROMETRY[7]

Mass spectrometry separates charged atoms and molecules according to their masses, based on their motions in magnetic and/or electrical fields. It divides the ions making up a sample into their separate masses, counts the proportions of each and outputs the ratios of the masses. The masses are segregated when a beam of positive ions is deflected by a magnetic field: the ions of lesser mass are deflected more than those of greater mass and thus the beam is divided into sections according to mass.

The mass spectrometer is made up of the ion source, the mass analyzer, the ion detector and the vacuum system. In the ion source the ions are formed, accelerated by means of high voltages and focussed into a narrow beam in the flight tube. The mass analyzer separates the positive ions in the beam according to their mass to charge ratios (m/e). As the ion beam passes through the magnetic field the ions are deflected into circular paths, the radii of which are proportional to $\sqrt{(m/e)}$. The separated ions are collected in the ion detector, converted into an electrical impulse and fed into an amplifier.

If the location of the detectors is not variable then the ion beam must be aligned with the exit slit by changing either the magnet current or the accelerating voltage. Changing the voltage will also change the beam intensity so it is preferable to change the magnet current.

The flight path must be pumped out to high vacuum to avoid scattering due to collisions between residual gases and the ions to be counted. An operating vacuum of at least 10^{-6} Torr is necessary to minimize peak broadening due to scattering. Pressure is increased when the sample is ionized. Preliminary chemical purification will minimize this effect.

---

[7]The following is a very brief account of the general principles of mass spectrometry. Full details may be found in Potts 1987.

All ions having the same m/e value will be collected at approximately the same point. "Isobars" are ions with the same m/e value. If isobars of the ions of interest are present then they will also be counted and the ratio returned will include this isobaric interference. Chemical purification of samples reduces such interference to a minimum.

The principal value of mass spectrometry is (i) that the low background provides for low ion beam detection limits, and (ii) that it can determine abundance ratios of isotopes to high precision. The more sensitive the mass spectrometer the greater the need for extensive chemical pre-treatment to remove isobaric interference. The detection limit is governed by the background count from reagent and environmental contamination; thus chemical procedures should be carried out in extremely clean, controlled conditions.

In order to measure abundance ratios, ions of different m/e value can be collected either (i) simultaneously by several detectors in the multiple collection mode, or (ii) sequentially on the same detector by varying the magnet current strength and thus sweeping the detector with each part of the beam in sequence. This is called the peak jumping mode. Multiple collection eliminates variation in source intensity but is not possible if only one detector is available. During peak jumping, accuracy will be reduced if there is any drift in the intensity of the ion beam between peak counts. Long-term drift is easily allowed for by keeping a running mean of counts. Short-term random fluctuations are eliminated by screening data and rejecting extreme values.

Resolution is a measure of the ability of the mass spectrometer to distinguish between two adjacent mass peaks. The resolving power is the relative mass difference between two adjacent mass peaks of equal intensity, the tails of which overlap at an intensity of 10% of the peak height. For example, to resolve masses 235 and 236 such that the interpeak valley will be at 10% of the peak heights a resolution of [235/(236-235)], or 235, is the minimum necessary. The VG354 in use in the McMaster lab has a resolution of 370. In practice peaks are rarely of equal

intensity so that this definition of resolution is not of great practical use.

Abundance sensitivity is a measure of the instrument's capacity to resolve the tail of a major peak from the measurement of an adjacent minor peak. The abundance sensitivity is the ratio of the intensity of the tail of a major peak, at the mass of the minor isotope, relative to the intensity of the major peak itself. The VG354 has an abundance sensitivity of 2 ppm at mass 237 relative to a peak at mass 238.

2.2 THERMAL IONIZATION MASS SPECTROMETRY

In the last decade thermal ionization mass spectrometry (TIMS) has made an important contribution to geochemistry. The purified sample is loaded onto a rhenium or tantalum filament and ionized by electrical heating. Isotopic ratios are measured directly or by isotope dilution, which involves the addition of a "spike" or tracer of known composition and concentration to the sample.

Isotopes of similar chemical composition but differing mass do not behave in an identical fashion during evaporation of the sample from the filament. The isotopes of lighter mass are more likely to be vaporized and ionized than the heavier ones. Thus the ratio of isotopes in the ion beam does not directly represent the ratio in the sample: there is some discrimination in favour of the lighter isotope. This is called fractionation and must be corrected for in the final data analysis (see section on correction for fractionation and mass discrimination in chapter 4).

The detection system has been greatly improved by the invention of the Daly detector (Daly 1960). However, the Daly causes mass discrimination: i.e. there is a bias in the detection of ions of different mass whereby the abundance of the lighter ion is exaggerated. The correction procedure is described under the section on fractionation and mass discrimination correction.

A thermal ionization mass spectrometer consists of the ion source containing the sample, the deflection system to steer the ion beam, the analyzer with the magnet to segregate the masses, and the collector/detector unit to amplify the signal

and count the ions. The deflection system, analyzer and detector system usually conform to a standard pattern such as that described in Wasserburg et al (1969) and Potts (1987). However, the ion source may be quite variable: the sample may be loaded in different ways, in diverse chemical forms and on metal filaments of varying composition and configuration. Reasons for the variety are discussed below.

2.2.1 The filament metal:

When heated, the sample produces positive metal ions and neutral molecules. The ion beam contains only positive ions; uncharged or negative particles are removed by the vacuum system, or deposited on the chamber walls. In order to maximize the production of positive ions the filament metal should have a high work function (W). The work function is the energy which must be applied to a heated filament to cause free electrons within the filament to escape by overcoming their association with the bulk metal (Potts 1987). The filament metal will evaporate along with the sample. Positive filament metal ions (e.g. Re^+) will interact with neutral sample molecules (e.g. U) and remove an electron. The electron exchange results in a neutral filament metal molecule and a positive sample ion.

$$Re^+ + U = Re + U^+$$

The lower limit of work function depends on the ionization potential of the sample (IP). This is the energy required to remove the most loosely-bound electron from the atom. The sample must give up its electron more easily than the filament metal does: i.e. (W - IP) has to be positive. If IP is low then a relatively low work function metal can be tolerated. However, the ionization potentials of U and Th are high; hence the need for high work function metals.

Uranium and thorium ionize at high temperatures (1500 - 2000°C) so the metal must also have a high melting point.

Only tantalum, tungsten and rhenium have both properties in a suitable range. Experience in the McMaster lab shows that uranium runs best with tantalum and thorium with rhenium.

2.2.2 Loading, chemical form and filament configuration:

The loading procedure affects the rate ot ionization and the production of positive ions. Methods of loading vary considerably, depending on the task and on the laboratory. Two processes are involved: the sample must evaporate, and the vapour must be ionized. Both are affected by temperature but both are not necessarily optimised at the same temperature. Since evaporation is maximised at a lower temperature than is optimal for maximum ionization, temperature is fixed by evaporation rate and ionization efficiency may be reduced. The chemical form of the sample affects its volatility: e.g. chlorides are often highly volatile. Sometimes it is desirable to choose a less volatile form so that the temperature may rise closer to the ionization temperature. Ideally the sample evaporates at a slow controlled rate and a high proportion of the molecules are ionized. However, this may be difficult to arrange because, on a single filament, evaporation and temperature cannot be controlled separately (Inghram and Chupka 1953, Rec et al 1974). Most loading methods seek to encourage ionization by providing a reducing environment while some (e.g. Rec et al 1974) seek to control the rate of evaporation.

(a) Single filament: For most mass spectrometric applications the sample is loaded on a single filament. This method is used for most of the U and Th analyses reported. Chen and Wasserburg (1981) and Edwards et al (1986/87) sandwich the sample between layers of colloidal graphite to inhibit oxide formation during ionization. Gancarz and Wasserburg (1977) used a "V"-shaped rhenium filament, loading the sample with silica gel and phosphoric acid, for uranium analysis. Manhes et al (1984) analyzed thorium in sulphate form with colloidal graphite on a tungsten filament (which yielded lower contaminants than rhenium). Rec et al (1974) improved the ionization efficiency significantly by coating the sample, which had been loaded onto a single rhenium filament by evaporation, with a sputtered-on layer of rhenium.

(b) Double filaments: Inghram and Chupka (1953) achieved greater ionization efficiency, for elements with high ionization potentials, with double filaments than

with a single filament. The sample filament is heated to the temperature of optimal evaporation while the vapour is ionized by the adjacent filament at a much higher temperature. This method is in use in the McMaster lab for U and Th analysis (run separately). The uranium sample is loaded in the phosphate form unto a tantalum[8] side filament while a hot centre rhenium filament provides positive Re^+ ions to reduce any neutral sample ions.

Thorium can cause additional problems because a large proportion of the thorium may be emitted as ThO^{2+} molecules. In this case, Re^+ ions are required to reduce thorium oxide to the positive metal ion.

$$ThO^{2+} + Re^+ = Th^+ + ReO^{2+}$$

The thorium sample is loaded in the phosphate form unto a rhenium filament crimped into a "V" cross-section. This holds the sample better than the more usual flat filament and is recommended by Chen and Wasserburg (1981) for more efficient ionization. A very high current on the centre rhenium filament provides ample Re^+ ions. As an added precaution a second side filament of Re provides another source of positive ions. Thorium beads thus have three filaments of rhenium.

Good quality filament metal is important because a poor filament may cause excessive variability of supply of Re^+ ions which may in turn cause irregular variations in the proportions of metal and oxide ions in the beam.

(c) Triple filaments: Thirlwall (1982) used a triple filament of Re centre and Ta sides, loading the sample on to both side filaments. He observed more stable focus positions and more predictable emission temperatures than with a single filament. This has not yet been tried for the McMaster lab: the control mechanism for the VG354 adjusts both side filaments as a single unit, so that the sample size and thickness for both would have to be as close to identical as possible.

---

[8] Zone refined tantalum and rhenium of 99.997% purity from H. Cross Company are used. The beads (8 pin, glass "Mass spectrometer filament support/assembly") are from Cathodeon Ltd., Cambridge, England.

2.3 U AND Th ISOTOPE RATIO MEASUREMENT

The mass spectrometer in use in the McMaster lab is a VG354 model thermal ionization mass spectrometer. Some details are given in the appendix. The technical manual being prepared as an adjunct to this thesis provides details on the operation of the VG 354 and all the instructions necessary for the dating of carbonates (Lundberg, 1990). Only the more general details are given below.

The samples are loaded onto the filaments in ~1 μl phosphoric acid solution, by evaporation. The acid serves to etch the surface of the metal slightly to enhance sample attachment. The drop is allowed to dry for a couple of minutes at ~1.5 A. The acid remains are then outgassed by heating the filament close to glowing point. For the U samples on the Ta filament outgassing occurs at ~2.5 A, and, for the Th samples on the Re filament, at ~2.2 A. Once under vacuum inside the source chamber, the filaments are preheated for 5 to 10 minutes, the U samples at 1.6 A and the Th samples at 1.8 A. If a sample has high detrital or organic content then it is preheated for 15 minutes.

Two types of detector are available: the Faraday and the Daly. The ions landing on the detector discharge a current in the detector which is amplified to give the signal. The Daly is used for U and Th isotopic ratio analysis. This allows highly sensitive detection of very small currents. In the McMaster lab it is run in the analogue mode: i.e. ion current is measured rather than ion counts. When the Daly is in operation the positive ion beam is deflected to the Daly "knob" by a high negative voltage. A photomultiplier amplifies the signal: an ion beam current of 10^{-13} A will give around 2×10^{-6} A on the last dynode of the multiplier. The detector efficiency is greater than 99%. It can count signals as low as 10^{-17} A (~10 counts per second) and up to 5×10^{-13} A (500,000 counts per second). The response is linear to within 0.25%.

The peak shape is affected by the Daly potential: with low potential it is skewed up mass, with high potential it becomes skewed down mass. The optimum flat shape should occur at a potential of between 17 - 26 kV but this is variable.

The voltage is adjusted regularly to optimize peak flatness: it was around 13.8 kV in 1988 and is currently around 11.6 kV (December 1989). The photomultiplier tube of the detector has a ~1.3 kV supply. This is also adjustable and has varied from 1.030 kV in 1988 to 1.137 kV by December 1989.

The peak jumping mode is used for U and Th analyses with the Daly detector in the axial location. To calculate ratios the beam is adjusted to allow each peak to impinge on the collector in turn. There is thus some loss of information while other peaks are being measured. However the level of precision is still extremely high (standard errors in the order of 0.05% for U ratios and 0.15% for Th ratios).

Data are collected by a process of cyclical interpolation: two complete cycles of data over all the peaks are stored. Ratios are calculated from an average of these two cycles assuming linear decay or growth of ion beam current. The second ratio interpolates between the second and third cycle, etc. This procedure is designed to circumvent any problems of long term drift in the ion beam current.

For each peak the ion count is integrated over a time interval set by the operator. The integration times vary with the size of the peak. For small peaks precision is improved by integrating over a longer time. However, a balance has to be achieved between the improved precision of a longer integration time and the decreased precision of the longer delay between peaks whose ratios have to be calculated. Integration time is 4 seconds for ^{230}Th and ^{234}U, 2 s for the zeroes to either side of these peaks, 2 s for ^{236}U and ^{229}Th, 1 s for the zeroes to either side and 1 s for ^{238}U and ^{232}Th.

Data are screened for exceptional values: all points outside two standard deviations of the mean are rejected, a new mean and sigma are then calculated and the data re-examined. The remaining data must be within two sigma of the new mean. This refining process is repeated until the number of data points left is constant or 15% of the data is rejected. This screening procedure eliminates extraordinary data caused by random fluctuations in the ion beam current. The data are output in the form of isotopic ratios with standard errors expressed as percentage

error. The values are entered into the BASIC program described in the appendix. This corrects for fractionation and mass discrimination and calculates the age.

Isotope peaks are counted at each mass unit. These are corrected for background noise measured at 227.3 mass units (i.e. away from any known peak). They are also corrected for interpeak background and tailing, measured at 0.5 mass units above and below each peak. Interpeak background is presumed to be linear and the correction factor is simply the average of the interpeak counts to either side. Some values for tailing are presented in the section on sources of uncertainty. It is generally negligible. Theoretically any tail has an exponential form, so that the tail correction should be weighted in favour of the lower side. However, for most U and Th analyses, a linear interference correction has been shown to cause insignificant error compared to an exponential correction (Li 1989). Exponential correction may be considered in the future if samples of very high ^{232}Th content are analyzed.

The "rhenium aiming current" specifies the size of the beam of Re^+ ions produced from the centre filament: it is set to 2.5 x 10^{-12} A for U runs and 1.5 x 10^{-11} A for Th runs. This setting for Th has been shown to be the optimum for minimizing ThO^{2+} ions while maintaining a Re^+ beam for 2 to 3 hours (Li 1989).

"Beam growth limit" specifies the beam stability required for data acquisition: it is set to ± 2.5% in 10 seconds for the U runs but to ± 4.5% in 10 s for the Th runs. This extra leeway is required for Th runs because the Th beam tends to be less stable than the U beam: too stringent a beam growth limit may result in little data collection.

Uranium is analyzed, in about 2 hours, in two stages: masses 235, 236 and 238 over 60 cycles, and then masses 234, 235 and 236 over 100 cycles. (The addition of the artificially produced isotopes ^{236}U and ^{229}Th as a spike is discussed in chapter 3.) The first stage measures the atomic ratios $^{235}U/^{238}U$ and $^{235}U/^{236}U$, the second stage, ratios $^{235}U/^{236}U$ and $^{234}U/^{235}U$. $^{234}U/^{238}U$ is then calculated. Levels of ^{234}U in nature are very low in relation to ^{238}U. Thus direct measurement of their ratio

would result in low precision. This two stage run avoids such problems. Each run is monitored and adjusted to keep the ^{234}U beam high and the side filament current in the range 2.0 A to 2.4 A. A typical mass spectrum is shown in Figure 2.1, a.

Thorium is normally run, in 1.5 to 2 hours, in one stage over 100 cycles (masses 229, 230 and 232) but if detrital content is high, interference from the high ^{232}Th necessitates a two-stage run (masses 229 and 232 first, 229 and 230 second). Each run is monitored to yield a stable and long-lived ^{230}Th beam with a current of ~5 x 10^{-17} A (or higher) while keeping the side filament current between 2.2 and 2.6 A. In the single stage run the atomic ratio $^{229}Th/^{230}Th$ may be evaluated in two ways: the direct measure may be used, or it may be calculated from the ratios $^{229}Th/^{232}Th$ and $^{230}Th/^{232}Th$; whichever gives the lowest error is used. In the two stage run the directly measured ratio must be used. A typical scan for a single stage Th run is shown in Figure 2.1, b.

The run is controlled by adjusting the "aiming current", which specifies the size of sample ion beam required. It is the sum of all the isotopes being scanned. The setting may vary for each sample and over the course of a run. For $^{235}U/^{238U}$ and $^{236}U/^{238}U$ ratios it must be reasonably high (e.g. 1.0 to 4.0 x 10^{-13} A) to ensure an adequate ^{236}U count amidst the abundant ^{238}U ions. For $^{234}U/^{235}U$ and $^{236}U/^{235}U$ ratios and for Thorium isotope ratios it can be lower (e.g. 1.0 x 10^{-15} A to 4.5 x 10^{-14} A). However, if ^{232}Th levels are high then the ion beam is dominated by ^{232}Th. In order to get adequate ^{230}Th counts the aiming current may have to be raised up to 4.0 x 10^{-13} A.

The ratios measured include "dummy" ratios, such as 233.3/238 and 229.3/232, which are included to avoid memory effects: they are measured simply to give a delay while high peaks die before the next low peak is measured.

Instructions for different types of runs are contained in Procedure files and Sequence Type files. These are explained in the appendix and some examples are given.

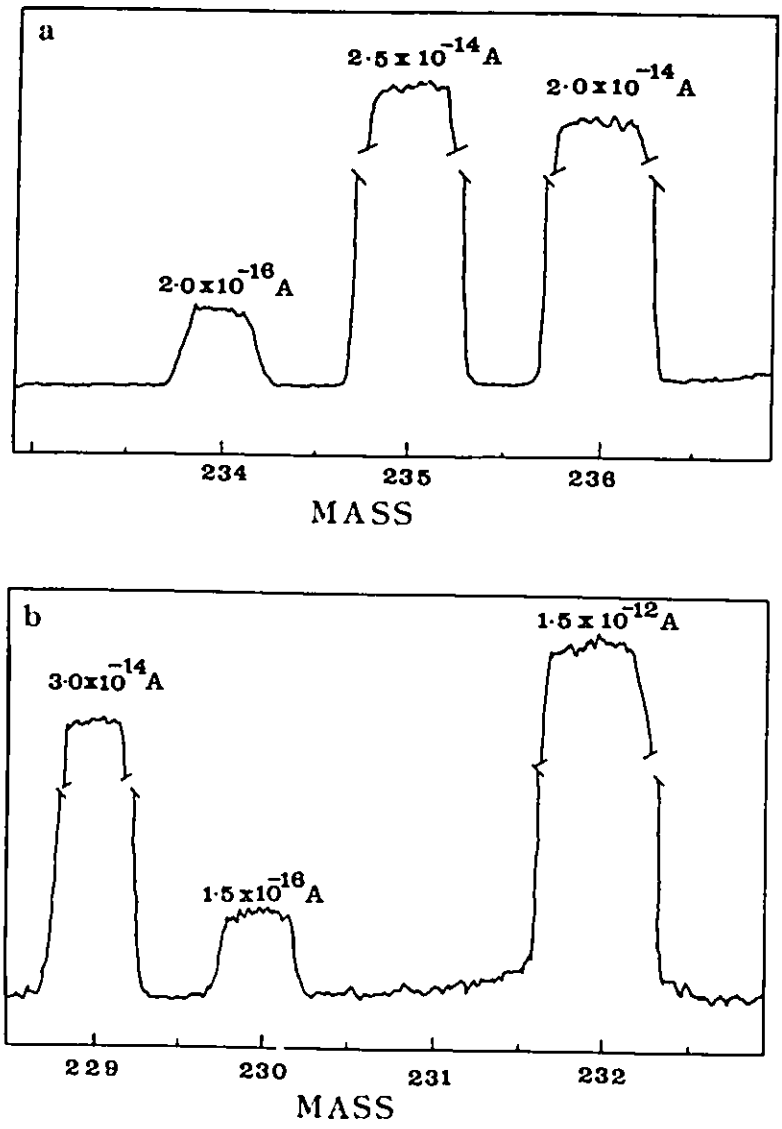

Figure 2.1: MASS SPECTRA FOR SPIKED SAMPLE. Note the changes in scale. (a) shows a typical uranium spectrum for the second stage of the uranium run. (b) shows a typical thorium spectrum. The tail from ^{235}U does not impinge onto the ^{234}U spectrum. The tail from ^{232}Th is greater but the effect on the ^{230}Th peak is only of the same order of magnitude as the variability on the peak count.

Chapter 3

CHEMISTRY

Thermal ionization mass spectrometry is successful only if the matrix has been removed and the elements of interest rigorously purified: otherwise the danger of isobaric interference is great and ionization efficiency is reduced by matrix interference. Consequently, U and Th must be concentrated and purified by chemical processing.

The chemistry of separation of U and Th from a carbonate matrix by nitrate form anion exchange is relatively simple. Two options are available: anion exchange alone or preliminary co-precipitation of U and Th with iron followed by anion exchange. Uranium ionizes at a lower temperature than thorium. While it is therefore possible to load the purified U-Th mixture and run the analyses sequentially, separation of U and Th for independent analysis is preferred. This separation is effected by chloride form anion exchange[9].

3.1.1 Separation of U and Th from carbonate matrix:

Faris and Buchanan (1964) published graphs of adsorption of all the elements onto strongly basic anion exchange resin at various nitric acid strengths. These indicate that both U and Th behave in a similar fashion with low adsorption at low acid strengths and maximum adsorption between 7 and 9 N HNO_3. Some of the rare earths, Bi, Pa and Pu will also be adsorbed but their levels in speleothem are insignificant and they do not interfere with mass spectrometry. The common ions making up a carbonate matrix (Ca^{2+}, Mg^{2+} and CO_3^{2-}) show no adsorption in any acid strength. This difference in distribution coefficients provides a method for the separation of U and Th ions from the matrix ions. The sample, dissolved in strong

[9] Potts (1987) gives an excellent account of ion exchange pre-concentration procedures. These are used (i) for concentrating an element to reduce the signal to noise ratio and (ii) to separate elements of interest from the matrix.

nitric acid, flows through the column where U and Th ions are adsorbed onto the resin while the unwanted ions are eluted and discarded. Later the U and Th are recovered by reducing the acid strength of the washing liquid. The distribution coefficient of Th is high. However, that of U is relatively low (Faris and Buchanan 1964, Arden and Gale 1974) so it is important to wash with the minimum acid volume required to effect purification.

3.1.2 Separation of Th from U:

Most of the literature indicates that thorium can most effectively be separated from uranium by anion exchange in hydrochloric acid medium (Kraus et al 1956, Jeffrey and Hutchison 1981, Korkisch and Dimitriadis 1973).

Thorium shows no adsorption onto resin in 0.1 N up to 12 N HCl. U shows negligible adsorption below 5.5 N HCl but increasing adsorption at higher concentrations. Thus, at HCl strengths of 5.5 N or higher U can be held on the resin while Th is eluted and collected; U can then be recovered by weak acid elution. Thorium elution is at its maximum at ~0.4 column volumes of effluent (Kraus et al 1956) so it is important to collect the first drop. Unlike the chemical procedure for alpha counting this separation does not have to be very rigorous. The thorium fraction runs best with little uranium contaminant, so the aim of the separation procedure is simply to concentrate as much of the thorium as possible into one fraction with only a small proportion of uranium. The uranium fraction will run successfully with any amount of thorium contaminant.

For thermal ionization mass spectrometry reagent blank must be kept to a minimum so the columns used are as small as possible with concomitant reduction in eluent volumes.

3.1.3 Sample preparation:

At all stages of preparation the emphasis is on protecting the sample from contamination. All work surfaces for drilling are washed before and after work and

cleaned of dust between sampling each layer. Each layer is collected on a fresh sheet of plastic and transferred to a sample jar. Drilling is done inside a fume hood to minimise dust dispersal.

The carbonate sample (usually speleothem) is cleaned on the outside with acid and water. Ideally speleothem is sampled along very thin growth bands. In practice the thickness obtainable depends on the friability of the sample and the quality of the sawing disc. With a fine dentistry drill, and a new disc, layers of about 0.5 cm for a friable sample and about 0.15 cm for a compact sample are possible. The cuts must follow the growth layers as far as possible but on highly convoluted surfaces sampling of non-contemporaneous calcite may be unavoidable. Before the next layer is cut the surface of the speleothem should be cleaned of dust with a jet of air and the work surface cleaned. Cleaning of each layer with acid is not recommended, to avoid any preferential leaching of the more soluble isotopes.

Each layer is now reduced to a mixture of pieces of crystal and powder. If there is enough sample then only the clean crystals should be used. These should not be ground to a powder because the chance of contamination from grinding instruments is high.

All further procedures take place in the clean laboratory. At every stage containers are covered except for the brief moment when a reagent is being added. Again every effort is made to avoid contamination of both the reagents and the samples. Reagents are added either directly from wash bottles or by Eppendorf pipettes. Only quadruply distilled water (MilliQ) is used and all acids have been distilled by sub-boiling in quartz glass apparatus. All labware is cleaned by (a) simmering in 20% Nitric acid for 24 hours, (b) simmering in MilliQ for 24 hours and (c) rinsing in MilliQ.

3.1.4 Sample Size:

The sample size required depends on the ^{230}Th content (the ^{232}Th content is irrelevant). ^{230}Th levels vary with the U concentration and age of the sample; the

sample size is assessed using estimates of these parameters. U content is obtained cheaply and rapidly by Neutron Activation Analysis, but for these low U samples the estimates are always about 20% higher than those obtained from alpha counting or mass spectrometry. Usually about 1 μg U is required: so, if a speleothem has ~0.5 ppm U then ~2 g of sample is required. The table of U required against approximate age (below) can be used as a guide to sample size.

Age class	μg U required
0 - 100 kyr	1.20
100 - 200 kyr	0.95
200 - 300 kyr	0.70
300 - 500 kyr	0.50

All of the thorium fraction should be loaded for the mass spectrometry run. The amount of U in the sample does not change with age, and only about 0.3 μg of U is needed for the mass spectrometry run, so the proportion of the uranium fraction used depends on the sample size: for larger (younger) samples only half of the uranium fraction is loaded.

3.2 DETAILS OF CHEMICAL PROCEDURES

The normal chemical procedures are outlined below. A list of reagents and materials is presented in the appendix. The step by step instructions set out below, for a standard sample, using the anion exchange only technique, are followed by instructions for the alternative co-precipitation method, and comments on some of the possible problems.

3.2.1 Preparation of anion exchange columns:

1. Small columns (0.25 ml capacity, 2.5 cm length) and medium sized columns (2.5 ml capacity, 6.0 cm length) must be plugged with a small wad of cotton wool and filled with 200 - 400 grade resin. The large columns (10 ml capacity, 18 cm length) are already filled with resin. The resin from the small and medium columns is

discarded after each use. The resin in the large columns is re-used.

2. The resin is cleaned by eluting with H_2O, 2.5 N HNO_3, 0.5 N HCl and H_2O in succession. The volume required depends on the size of the column. The sequence of reagents and volumes is shown in Table 3.1. The drip rate for water and dilute acids is approximately 0.5 ml / minute.

3. The resin is preconditioned with 7.5 N HNO_3 (Table 3.1). It is now ready for sample loading.

3.2.2 Preparation of sample for loading on column:

1. Weigh sample in 50 ml capacity Teflon beakers.

2. Dissolve sample in 7.5 N HNO_3. To minimise effervescence the acid is added in small volumes over the course of an hour. The volume required depends on the size of the sample. If precise U and Th concentrations are required then care must be taken to avoid any loss of sample by splashing.

3. Add ~0.25 g ST96 ^{236}U-^{229}Th spike. To avoid any problems with weighing an evaporating liquid the weight of spike is read as the loss in weight of the spike bottle. The spike is transferred directly from the spike dropping bottle: about 5 drops is usually sufficient. The exact quantity of spike depends on the sample. This is discussed below.

4. Dry under the heat lamps. Redissolve in 7.5 N HNO_3. The volume required depends on the original sample size:

Sample size	Volume of acid required
0 - 3 g	5 ml
3 - 5 g	10 ml
5 - 8 g	15 ml

Any samples of more than 8 g should be prepared with the ferric chloride co-precipitation method.

The sample is now ready for loading onto the large anion exchange column.

3.2.3 Anion exchange elution:

1. Load the 5, 10 or 15 ml of sample in acid into the column reservoir. The columns have no taps so the eluate begins to drip through immediately. It contains the unwanted ions and may be discarded. The Teflon beakers in which the samples were dissolved are filled with 2.5 N HNO_3 acid (to clean them) and left on the hot plate. When required again the acid is discarded and they are rinsed in MilliQ.

2. Wash the walls of the reservoir with 5 ml 7.5 N HNO_3 and allow it to drain fully. This ensures that the sample is completely washed into the resin.

3. The rest of the unwanted ions are washed out with 7.5 N HNO_3. The total volume of 7.5 N acid to go through the columns should not exceed 35 ml. If the sample was loaded in 5 ml and washed with 5 ml then another 25 ml is required to complete the washing process. The samples dissolved in 10 ml require an additional 20 ml and those dissolved in 15 ml need another 15 ml. The drip rate varies with the eluting liquid: 20 ml pure 7.5 N HNO_3 drips through in about 1 hour but if sample is dissolved in the acid then it may take 2 - 3 hours. The resin now holds U, Th, Pa, Pu, and, if they were present in the sample, some Au, Pd, Hg, Bi and some rare earths.

4. The U and Th are eluted from the resin first with 10 ml H_2O, and then 40 ml 1 N HBr. The eluate from each sample is collected in the appropriate Teflon beaker. The H_2O step is required to remove the nitrate ions before addition of the bromide ions. Otherwise an orange coloured nitrate-bromide complex forms which may block the columns. The H_2O removes about half of the U and a quarter of the Th. The dilute HBr removes the remainder.

5. The sample must now be put through the small columns for further cleaning and separation of U from Th. The 50 ml of eluate collected from the large columns is dried under the heat lamps.

6. The dried eluate is converted to the nitrate form by: (i) dissolving in 2 ml 7.5 N HNO_3, (ii) drying, (iii) dissolving in 1 ml 7.5 N HNO_3 and (iv) drying.

7. It is dissolved in 0.2 ml 7.5 N HNO_3 ready for loading onto the small columns.

8. The sample is loaded, and then washed in with 0.3 ml 7.5 N HNO_3.
9. Any remaining unwanted ions are washed out with 0.3 ml 7.5 N HNO_3 and the eluate discarded.
10. The Th fraction is eluted with 4 ml 6 N HCl which is collected in 5 ml capacity Teflon jars.
11. The U fraction is eluted in 4 ml 1 N HBr and collected in another set of Teflon jars.
12. Both fractions are dried under the heat lamps. The final dried residue should be yellow-brown in colour and look almost like a stain on the Teflon. If it looks too large or is white then it may be necessary to clean it again through a small column.
13. Completely dry samples are hard to load onto the filaments for the mass spectrometer runs. To keep the samples slightly moist a drop of 0.1 N HNO_3 and 0.3 N HPO_3 mixture is added. This is dried down to the last μl. The sample is then ready for loading onto the filaments. This procedure has already been described in the section on mass spectrometry.

3.2.4 Ferric chloride co-precipitation:

Prepare medium and small anion exchange columns as directed above.
Prepare the sample for loading on columns up to, and including, step 3. Continue as follows:
4. The sample is now dissolved in acid and spiked. Add a drop or two of ferric chloride solution. This forms a complex with U and Th which is soluble in acid conditions (pH must be less than 4.3).
5. Heat the sample under the hot lamps for about 20 minutes until it is just boiling. Boiling expels dissolved CO_2 which would otherwise form a soluble $UO_2(CO_3)_2$ complex and reduce yield.
6. Remove from heat and add concentrated ammonia, drop by drop, swirling the solution between each drop. When the pH rises to 4.3 a red-brown precipitate of $Fe(OH)_3$ forms. Do not add more ammonia than is necessary.

7. Leave solution to cool for at least 3 hours. The flocculate should settle out. The clear solution contains unwanted ions such as Ca^{2+}, Mg^{2+} and NO_3^- and NH_4OH.
8. Much of the clear solution can be aspirated off with an Eppendorf pipette, and discarded. The remainder must be centrifuged and the supernate discarded. The excess ammonia is washed off by shaking the flocculate in water and centrifuging it again. This step is then repeated twice more.
9. The flocculate is dissolved in ~2 ml 6 N HCl.
10. It must then be converted to the nitrate form by (i) drying under the heat lamps, (ii) dissolving in ~3 ml 7.5 N HNO_3, (iii) drying, (iv) dissolving in ~2 ml 7.5 N HNO_3, and (v) drying.
11. It is dissolved in 1 ml 7.5 N HNO_3 ready for loading onto the medium sized columns.
12. The procedure for the large columns is followed using smaller eluting volumes (Table 3.1). The total volume of 7.5 N HNO_3 should not exceed 4 ml so the sample is washed in with 1 ml and the rest of the unwanted ions washed out with 2 ml acid. The washing also removes the excess Fe from the precipitate; the yellow colour can be seen passing into the eluate. The U and Th is collected together in the Teflon beakers by elution with 2 ml H_2O and 6 ml 1 N HBr.
13. The final cleaning and separation in the small columns is the same as indicated for the normal chemical procedure.

Table 3.1: Quantities used in the ion exchange procedure.

	Large columns	Medium columns	Small columns
Length	15cm	5.5cm	2.2cm
Capacity	10ml	2ml	0.25ml
Resin Grade	100-200	200-400	200-400
CLEANING:			
H_2O	40ml	4ml	3ml
2 N HNO_3	40ml	4ml	3ml
0.5 N HCl	40ml	4ml	3ml
H_2O	40ml	4ml	3ml
If leaving for longer than 24 hours columns must be brought to this stage and left in water.			
CONDITIONING:			
7.5 N HNO_3	30ml	4ml	3ml
LOADING: Sample is dissolved in the following volumes of 7.5 N HNO_3	5ml	1ml	0.2ml
WASHING:			
7.5 N HNO_3	10ml	1ml	0.3ml
7.5 N HNO_3	20ml	2ml	0.5ml
ELUTION: (Collect both in same container)			
H_2O	10ml	2ml	
1 N HBr	40ml	6ml	
ELUTION: (Collect Th first and Ur second in separate containers)			
6 N HCl			4ml (Th)
1 N HBr			4ml (Ur)

3.3 NOTES ON SOME OF THE STEPS

3.3.1 Sample Dissolution:

If the sample is powdery then wetting it slightly with MilliQ helps to reduce splashing. 7.5 N HNO_3 is dribbled down the side of the beaker in 0.5 ml measures with the lid raised to a minimum, waiting between additions until all effervescence has stopped. A sample of 1.5 g requires about 5 ml acid added over about an hour.

3.3.2 Oxidation of organics:

If organics are present (detectable as foam or a film on the surface or as a yellow colour in the solution) these should be oxidised until the solution is virtually colourless and completely clear. Normally organics are oxidized effectively by putting the sample through about six cycles of dissolution in 7.5 N HNO_3 and drying under the heat lamps. For high organic content higher acid strength and/or more cycles may be required. If necessary the samples can be dissolved in acid (or aqua regia if required) and heated with lids on for several hours. Another option is to use a Teflon bomb which can be securely closed and heat the sample in the oven for a couple of days. Oxidization with H_2O_2 (Latham 1981) has not yet been implemented because of the danger of loss of sample and the possibility of reagent contamination.

3.3.3 Spiking:

The spike introduces known quantities of the artificial isotopes ^{236}U and ^{229}Th against which the unknown quantities of naturally occurring isotopes can be measured.

The spike concentration and composition is discussed fully in chapter 5. The amount of spike added is crucial: all isotopic ratios to be measured should ideally be close to 1.00 for maximum precision. This would avoid any problems of non-linearity in the detection system (see chapter 4). However, this is impossible for U and Th analyses because the abundance of the different isotopes in nature varies by orders of magnitude. Spiking helps to reduce extremes in the ratios measured when the spike isotopic abundance is intermediate between the naturally occurring isotopes. A value of around 1.00 for the sample ^{235}U to spike ^{236}U ratio usually gives suitable values for all the other ratios. If a sample has a high ^{232}Th content the level of spiking should not be increased in an attempt to balance the ratios. The date is calculated on the $^{229}Th/^{230}Th$ ratio, which can be measured directly. Spiking should aim to maximize precision on this ratio. The $^{229}Th/^{232}Th$ ratio simply gives a measure of detrital content and a low precision on this ratio is acceptable.

The old $^{229}Th/^{236}U$ spike, called WL96, has ~0.0045 μg ^{236}U per g solution (1.14×10^{11} atoms ^{236}U / g). A sample of ~1 μg U contains ~0.007 μg ^{235}U (0.72%) and thus needs ~1.5 g spike. However this spike has a higher ^{229}Th content than is optimum for speleothem samples: the ^{229}Th concentration is 0.002 μg / g (5.47×10^{10} atoms ^{229}Th / g) and the $^{229}Th/^{236}U$ ratio is 0.48. As a compromise ~0.8g (20 drops) is used. Very little of this spike is left.

The new spike, ST96, has 3.5×10^{11} atoms ^{236}U / g, 1.02×10^{11} atoms ^{229}Th / g and has a $^{229}Th/^{236}U$ ratio of 0.27. Approximately 0.25 g (5 drops) is adequate for most samples.

3.3.4 Insoluble matter:

No trace of solid matter should be loaded onto the columns. If any insoluble residue remains then it must be removed by centrifuging; the supernate is loaded onto the columns. In general the centrifuge step is performed as a precaution even where insolubles are not apparent. In some cases the insolubles float and are not easily separated by centrifuging. These may be organic particles and should be treated thus. If they still remain then they can be carefully pipetted out and discarded.

3.3.5 Anion exchange without preliminary co-precipitation:

Towards the end of the first drying, boiling of the very viscous solution may result in spattering. This may damage the lamps, reduce the size of the sample or contaminate neighbouring samples. It may be avoided by moving samples away from lamps for the final stage of drying. The problem is greater for large samples; they should be well segregated from other samples while drying. The lamps should be cooled and cleaned before further use.

Large samples may block the columns if they are dissolved in an inadequate volume of acid. When this occurs the column changes from the normal lemon yellow colour to a brown-orange colour. Addition of a little more acid may relieve the

problem. The only way to unblock a completely impermeable column is to physically break the resin up. In this case the eluate should be collected, diluted with a little more 7.5 N HNO_3 and sent through the column again before proceeding as normal. Samples which get blocked on the columns often fail to run well. As a precaution the resin should be discarded.

3.3.6 Co-precipitation of U and Th with Ferric Chloride:

The ammonia must be added carefully, drop by drop, down the side of the container. This should be done far away from any other sample because a cloud of ammonia is released from the hot liquid and splashing may occur.

The $Fe(OH)_3$ precipitate should be in the form of a loose flocculate. If a jelly-like brown precipitate forms instead, acid should be added until it disappears, the solution reheated and ammonia added again.

Sometimes problems are encountered in the nitration of the precipitate. If it will not dissolve in HNO_3 at any step (usually because it is overdried) then it can be dissolved in HCl again but all nitration steps must be repeated.

3.4 NOTES ON ANION EXCHANGE

3.4.1 Choice of resin grade:

Resin grade is indicative of the surface area of resin and thus the number of exchange sites. Grade 100 - 200, the coarser resin, has less surface area than Grade 200 - 400. Grade also affects the speed at which reagents are transmitted, the smaller grains, being more tightly packed, inhibit flow. The finer grade is usually preferable but the coarser grade resin was chosen for the big columns because the faster flow-through rate minimises the time in contact with strong acid (which eventually breaks down the resin).

3.4.2 Preparation of the columns:

The large columns of 10 ml capacity are made of quartz glass (in the glass

blowing workshop at McMaster University). These are cleaned with 7N HNO_3 and MilliQ before being plugged with a small wad of quartz wool. They are filled with 100 - 200 mesh (coarse) resin which, after settling, should reach just to the neck. The columns are housed in a rotating carousel made of Plexiglass (Perspex). Each carousel holds 8 large columns.

The medium and small columns are made from polyethylene pipettes which are cut to size. These are similarly cleaned, plugged with cotton wool (quartz wool will not compress sufficiently in these small bore tubes to give a good bed to hold the resin) and filled with 200 - 400 (fine) mesh resin. This resin is discarded after each use and the columns recleaned and refilled.

3.4.3 Resin contamination:

The resin ideally ought to be discarded after each use to avoid any problems of intersample contamination. However, in view of the high cost of the resin, and in view of the extra preparation time which refilling of the columns would entail in an already lengthy procedure, it was decided to re-use the resin in the large columns. The resin is cleaned both after use and before the next use. Tests of blanks show insignificant procedural contamination levels. As an added precaution against intersample contamination one carousel of columns is reserved for low U samples (generally 1 ppm or less) and the other for high U samples. After very high U samples such as corals (3 ppm) the columns are cleaned three times. If high and low U samples have to be processed at the same time then they should be kept apart as far as possible; this is especially important during the evaporation stages.

The large columns are used repeatedly for about a year. They are cleaned after each preparation to the second water stage and then left in a test tube of water. Each couple of weeks thereafter they should be flushed with water if not used.

3.4.4 Calibration of the columns:

Column calibration traces the elution history of ions of interest under different conditions and thus allows the user to minimize the volume of reagents while maximizing the desired effect of the column. Calibration of the removal of Ca^{2+} ions indicated that 99.95% was eluted after 3 column volumes. The size of the column had little effect. Cleaning with slightly less than 4 column volumes ensures removal of the majority of the unwanted ions while avoiding any breakthrough of U ions.

Rigorous calibration of U and Th ion elution from large, medium and small sized columns, by Li (1989), provided the basis for the choice of volumes of reagent used. U has a lower distribution coefficient than Th and is therefore released more easily: thus, U has a clearly defined peak to its elution curve while Th always has a tail. Most of the U and Th is eluted after 6 column volumes.

3.5 ADVANTAGES AND DISADVANTAGES OF ANION EXCHANGE ALONE compared to preliminary co-precipitation followed by anion exchange:

In 1988 the two methods were compared by running the same homogenised samples through both methods: results are presented below in Table 3.2. It is important to note that the $FeCl_3$ used was the normal lab reagent of 98.2% purity grade.

The co-precipitation method returns ages higher by ~17% for JC1 and ~10% for 76001. The principal cause is thorium contamination as indicated by the higher Th concentration values.

The result of this test is important for alpha counting studies because the ferric chloride must be used in chemical preparation for alpha counting. It suggests that alpha counted dates are likely to be slightly high.

In 1989, higher purity $FeCl_3$ (99.8%) was acquired. This showed less contamination and is now used for co-precipitation where a sample is > 8 g. A reagent blank correction factor was calculated (see below) and used to correct these

analyses. However, in view of the higher reagent blank of the co-precipitation method, the column only method is the preferred one.

Table 3.2: Comparison of the two methods of purification

Sample	$^{234}U/^{238}U$ (x 10^5)	$^{230}Th/^{234}U$ (x10)	U ppm	Th ppb	Age kyr
JC1 by columns only					
A	5.51	3.02	0.76	0.95	403
B	5.51	3.00	0.74	0.76	356
JC1 by co-precipitation					
K	5.53	3.05	0.76	0.75	459
H	5.57	3.05	0.77	1.47	431
	($x10^4$)				
76001 by columns only					
C	1.05	1.08	0.78	7.45	45.4
D	1.05	1.02	0.78	7.10	42.3
76001 by co-precipitation					
E	1.05	1.12	0.80	8.26	47.3
F	1.05	1.15	0.79	8.14	48.9
G	1.05	1.15	0.79	8.30	48.6

3.6 YIELD

Yield is of little importance to mass spectrometry providing the yield is high enough to sustain an adequate beam. However it is of interest to measure as a check on the chemical procedure.

To test for yield, two aliquots of the same sample are prepared (identical as far as possible). One (called "N") is spiked before chemistry, as normal. The second (called "T") is spiked after it has been processed through the large columns. Both samples must be put through the small columns to separate the U and Th fractions. Both sample and spike isotopes will be lost in N; only sample isotopes will be lost in T. The differences in the isotopic ratios between N and T are a measure of the yield.

The results for N are considered to indicate the true values. Based on the relative weights of the samples and weights of spike added, the expected results for

T are calculated as if that sample had been treated in the same way as N. The difference between the expected results for A and the actual results is a measure of the yield.

Table 3.3: Yield on column chemistry.

Sample	Sample Weight	Spike Weight	$^{230}Th/^{229}Th$	$^{234}U/^{236}U$
N (normal)	1.394	0.2913	$1.1504x10^{-2}$	$2.7944x10^{-2}$
T	1.396	0.2957	$0.4554x10^{-2}$	$2.7846x10^{-2}$

Expected $^{230}Th/^{229}Th$	Actual $^{230}Th/^{229}Th$	Thorium Yield	Expected $^{234}U/^{236}U$	Actual $^{234}U/^{236}U$	Uranium Yield
$1.1348x10^{-2}$	$0.4554x10^{-2}$	40.13%	$2.7566x10^{-2}$	$2.7846x10^{-2}$	101%

Yield on Ferric Chloride Co-precipitation Method:

Sample	Sample Weight	Spike Weight	$^{230}Th/^{229}Th$	$^{234}U/^{236}U$
N (normal)	2.5232	0.2625	$2.325x10^{-2}$	$5.765x10^{-2}$
T	2.5251	0.2833	$0.810x10^{-2}$	$4.344x10^{-2}$

Expected $^{230}Th/^{229}Th$	Actual $^{230}Th/^{229}Th$	Thorium Yield	Expected $^{234}U/^{236}U$	Actual $^{234}U/^{236}U$	Uranium Yield
$2.1559x10^{-2}$	$0.8102x10^{-2}$	37.58%	$5.3457x10^{-2}$	$4.344x10^{-2}$	81%

The McMaster speleothem standard, 76001, was used to test the yield. Results are shown in Table 3.3.

These results indicate that column chemistry alone is slightly superior to the co-precipitation method in terms of yield.

3.6 REAGENT/PROCEDURE BLANK CORRECTION

Contributions of U and/or Th from reagents are generally extremely small and have very little effect on the age calculations. Contamination will contribute ^{238}U, ^{235}U, ^{234}U, ^{232}Th and ^{230}Th. For these very low levels of contamination only the ^{238}U and ^{232}Th contributions were detectable. The ^{238}U correction will affect $^{234}U/^{238}U$ ratios which are in turn used to calculate age. However, for the majority

of samples variations in $^{234}U/^{238}U$ ratios have little effect on age (see Figure 1.2, variations of age with $^{234}U/^{238}U$ ratios and $^{230}Th/^{234}U$ ratios). The ^{232}Th contamination will affect the $^{230}Th/^{232}Th$ ratios only, and therefore has no effect on the age calculations unless the detrital correction is used; in this case the levels of sample ^{232}Th are so high that the small contribution from reagents is negligible. The normal age calculations use the $^{230}Th/^{229}Th$ ratio. This can be taken directly from the measured $^{229}Th/^{230}Th$ ratio or it can be taken from the measured $^{230}Th/^{232}Th$ and $^{229}Th/^{232}Th$ ratios. In this case the ^{232}Th in each ratio (from whatever source) cancels out. Thus, however it is measured, the $^{230}Th/^{229}Th$ ratio needs no correction.

The reagent blanks were measured using spike as a sample. The isotopic ratios of the spike are known. These were measured on samples which had been loaded directly onto filaments with no chemical processing. Reagent contamination was evaluated by passing spike through (i) the column only procedure and (ii) the ferric chloride co-precipitation procedure. The levels of contamination are very low (see details in appendix). For example, a sample of 0.5 μg U has $\sim 1.3 \times 10^{+15}$ atoms ^{238}U. The $1.9 \times 10^{+9}$ atoms ^{238}U from reagent contamination is therefore 0.00015% of the total ^{238}U. Table 3.4 shows values (1) from this study, (2) from Li (1989), (3) from Edwards (1988) and (4) Chen and Wasserburg (1981). The level of purity of the ferric chloride used for (3) and (4) is not known: it is assumed to be relatively impure from the contamination figures.

Table 3.4: Values for reagent contamination

	Columns only	$FeCl_3$ (98.8% pure)	$FeCl_3$ (standard purity)
No. atoms ^{238}U (1)	1.89×10^{9}	(1) 9.23×10^{9}	
(2)	2.53×10^{11}		(2) 5.82×10^{11}
			(3) 1.2×10^{10}
			(4) 2.5×10^{10}
No. atoms ^{235}U		(1) 6.26×10^{7}	
No. atoms ^{234}U			(3) $< 9.0 \times 10^{6}$
No. atoms ^{232}Th (1)	2.19×10^{9}	(1) 3.61×10^{9}	
(2)	2.73×10^{11}		(2) 1.3×10^{12}
			(3) 1.0×10^{10}
			(4) 8.0×10^{9}
No. atoms ^{230}Th			(3) $< 6.0 \times 10^{6}$

The reagent blanks from this study compare favourably with those from the other studies. The purified ferric chloride shows considerably less contamination than the less pure reagent.

The columns-only procedure is the most frequently used; the correction for it is small. The ferric chloride co-precipitation procedure has larger correction factors but is rarely used. If no chemical treatment is used then no correction is necessary.

Chapter 4

MINIMIZATION OF SOURCES OF UNCERTAINTY AND TREATMENT OF ERRORS

Odin (1982) notes that the apparent age is the analytical ratio between radioactive producer and radiogenic product, but the probable age is the interpretation of this ratio taking into account all the sources of uncertainty. Mass spectrometry has now opened the way to a new era of high precision U-series dating. The danger of accepting a single value without much consideration of its true meaning is real: the literature is plagued with poorly reported and poorly interpreted dates which are then used as a basis for erroneous conclusions. It is now very important that all sources of variation be clearly understood so that this very precise data can be fairly judged and correctly interpreted.

4.1 INHERENT VARIATION

4.1.1 Stratigraphic uncertainties:

Stratigraphic uncertainties relate to stratigraphy, continuity of units, correlation of units, etc. These are relevant for the comparison of dated sequences from different parts of a deposit: what may appear to be a single growth layer may in fact be diachronous. If possible, all samples should be from a vertical section. Stratigraphic uncertainty may be important for isochron dating of speleothem with high detrital content which involves dating different parts of the same growth layer. If the sampling is not actually of contemporaneous layers then this method of dating is erroneous.

4.1.2 Genetic uncertainties:

Genetic uncertainties relate to the isotope geology at the time of formation. The isotopic composition at the time of deposition must be known; otherwise, U-series disequilibrium dating assumes complete separation of U from Th at time of

deposition. Carbonates are comparatively simple in that Th is relatively insoluble in water and the crystal lattice is unlikely to contain any initial thorium. However, there is a possibility of inheritance of radiogenic ^{230}Th where detrital levels are high because Th is easily adsorbed onto detrital particles. For each date, ^{232}Th is measured to give an indication of possible inheritance and a rather crude correction factor is applied to the apparent age using an estimate of initial $^{230}Th/^{232}Th$ activity ratio of 1.7 (see section in chapter 1 on correction for detrital contamination). High levels of detritus occurred in only a few of the samples dated for this thesis. In no case did the simple correction give logical ages, but the problem was circumvented because in every case alternative, uncontaminated samples were available. Isochron dating has not yet been attempted.

4.1.3 Historical uncertainties:

Historical uncertainties relate to the history of the deposit after its formation. Reliable dating requires either (a) that the sample remain closed to isotopic migration since the time of origin, or (b) that the pattern of isotope migration be accurately modelled (Gale 1982). A major issue in the dating of carbonates such as shells and bones is uranium uptake subsequent to deposition, the effect of weathering, burial, etc. Open system behaviour was apparent in some of the corals dated in this study and in the ostrich eggshells. In the case of the shells, the system appears to have become closed soon after deposition and thus the dates are reasonably reliable. In the case of the corals, post-depositional migration of isotopes gives excessively high ages.

These three sources of uncertainty are independent of operator error. They affect the interpretation of a date but not its precision.

4.2 OPERATOR ERROR

Operator error gives variability during sampling, chemical preparation and instrument operation (Wainerdi and Uken 1971). These types of error are insidious

in that they may not affect the quoted precision of the result. If no replicate analysis is performed then the magnitude of these errors cannot be ascertained.

4.2.1 Sampling Error:

Sampling error may be inherent to the sample, and therefore unavoidable, or may be introduced by the sampling technique. For whole rock analysis it is customary to minimise the effect of inherent variation by using finely-ground, homogenized samples. For mass spectrometric dating even a sample from within a single growth layer should not be homogenized by grinding because the grinding apparatus may introduce contamination. The sample is left as crystal fragments. It is assumed that the sample is homogeneous within a growth layer but note that, because the sample is not ground and homogenized, any "replicate" analysis can never be a true replicate.

The second source of variation in sampling comes from drilling. Each sample should be taken strictly within a single growth layer but this can be difficult if the growth surfaces are uneven. The dates on "bumpy" or botryoidal speleothem are less reliable than those on smooth planar samples (although the error quoted may be comparable) because of this cutting problem. For α-counting this source of variation is more acute than for mass spectrometry because a very much larger sample size is required. None of the samples dated in this study were particularly difficult to sample.

4.2.2 Chemical preparation:

Variation from chemical preparation is minimized by operating in a clean lab with filtered air supply to reduce dust to a minimum. Reagents are ultra pure. All labware is thoroughly cleaned and stored in dust-free conditions. Glass is never used because it often has U or Th contamination and because Th can so easily adsorb to it. Instead, the exchange columns are made of quartz and plugged with quartz

wool. All the other labware in use is of Teflon or polyethylene.

The sample and spike are weighed to an accuracy of ± 0.00001g. These measures are used in the calculation of U and Th concentrations but do not affect the age calculations. Loss of sample by effervescence during dissolution, which may also cause variation in concentration values, is minimised by very slow addition of acid over about an hour, by keeping the reaction chamber covered and by careful washing of the lid. During drying some of the sample may be lost. Evaporation should be slowed as the sample approaches dryness to avoid loss by spitting. This source of variation will be minor since sample and spike should be well equilibrated by this stage and any loss is of both in equal proportions. An important source of contamination could be splashing from one reaction beaker to the next during evaporation. This can be avoided by using protective glass chimneys around each vessel and only one vessel under each heat lamp.

Reagent contamination contributes mainly ^{238}U and ^{232}Th which will lead to an overestimate of the age. For mass spectrometric dating this has been reduced to almost undetectable levels and thus has no significant effect on dates (see reagent contamination section above).

In spite of the care taken, sampling error and chemical variation are probably still the greatest sources of unexplained error in mass spectrometric dating.

4.2.3 Instrumental operation:

Variations from instrumental operation can be introduced during (i) filament construction and loading and (ii) the analytical procedure.

Filament geometry is an integral part of effective ion beam production. Filaments should be creaseless, at right angles to, close to and parallel to the neighbouring filament. This puts the sample vapour in intimate contact with the high temperature of the ionizing filament and the stream of Re^+ ions. The crimp to hold the thorium sample should be positioned midway between the posts with the "V" facing squarely opposite the third filament. The bead posts should be arranged so

that the filaments will be exactly aligned with the exit slit of the source. This ensures that the ion beam is not deflected off the shield plate.

Chemical variations and U/Th contamination within the filament metals are minimised by using zone-refined metals only. Variations in filament thickness cannot be controlled. This can cause error because: (i) a centre filament of irregular thickness may cause an irregular Re^+ ion beam, which in turn may affect the ionization of U or Th; and (ii) variations in thickness of the sample filament affect the current at which the sample runs and thus the temperature. Since temperature cannot be directly measured, and since fractionation is not reliably constant except in a narrow temperature band, the runs are kept within this band by controlling the current. The limits have been ascertained by experience but may not apply to an abnormally thick or thin filament.

Loading error is minimised by always loading samples of comparable size, aiming for a narrow plate-out in the centre of the filament. Usually the sample forms a thin, black deposit. However, variations in sample chemistry often cause loading problems: for example, samples with organic contamination may bubble when heated. During mass spectrometric runs a bubble of sample may contaminate the hot centre filament. If this happens the counts will rise dramatically but the ratios will change: abnormal fractionation will render those counts useless. Samples with clastic detrital contamination may form a very thick source which will not evaporate regularly during the mass spectrometric run. Any loading abnormalities should be reported.

Error during the mass spectrometric run can be considerable if the run is not supervised. The principal danger is that high side filament current may cause irregular fractionation (see discussion below). Side filament current limits have been established by experience but each run differs. The side filament should be kept between 2.0 A and 2.3 A for U runs and between 2.0 A and 2.6 A for Th runs. Above these limits fractionation quite noticeably accelerates. Below the limits the ion beam may contain other ion species as isobars (e.g. organics) If the sample is

too big then the required ion beam is produced at low current but is usually rather unstable. This has only happened for U runs: if the run is supervised then the aiming current can be raised during the run. However, for the first stage of the U analysis it cannot be set any higher than the Daly maximum of 5×10^{-13} A. Samples with high detrital levels are sometimes unusual in that the thorium run requires a high current (e.g. 2.6 A - 2.8 A) but fractionation appears to be constant. Operator flexibility is required in such situations. If the run has any abnormal characteristics then these should be recorded along with the final data output and if possible the sample measurement should be repeated.

Background zero (measured at mass 227.3) should be less than 10 counts. At the beginning of runs background may be above ~10 counts but the organics which usually cause it rapidly burn off. Nevertheless, on some thorium runs, for some samples, the background remains high for longer than the usual 10 minutes. In these cases the program is paused to let the background burn off. On rare occasions background remains high for the whole run. This should be reported in the final output: the dates from such a run are suspect.

Interpeak counts (measured at 0.5 mass units below and above each peak) should be close to zero. High interpeak counts may indicate drifting of the beam's focal point. The set should be aborted in order to allow the program to refocus the beam. The data from the abnormal set should not be included in the final grand means.

The counts on the smallest peak should be greater than 20 and at least six times the background count. However, if the peak is "ragged", if it has high variability, then the average count may need to be higher. Potts (1987) suggests that the "limit of quantification" (i.e. the minimum level at which measurement can begin) is 10σ above background.

The rate of ion beam change (growth or decay) should be linear and slow. At the start of each set, before isotopic ratio measurements begin, the program checks that the rate of change is between limits specified in the procedure file (e.g.

± 4.5% in 10 seconds), but during each set of 10 scanning cycles it has no control over the rate of beam change. It can accommodate regular, moderate change but it does not recognize an excessive rate of change. Such a set should be aborted and the data discarded. Similarly, if the beam has been unstable during a set the data must be regarded as suspect. Any abnormal beam behaviour should be reported along with the final date.

Variation in machine operation is still a cause of non-reproducibility in dating by mass spectrometry and requires skilled operation to control. In the presentation of a date these sources of error are rarely mentioned. If all of these parameters are kept to a similar level during each run then the results are reproducible to within ± 1%. If any of the parameters are outside the acceptable limits the results are questionable and must be treated with discretion.

4.3 PRECISION AND ACCURACY

Precision is the uncertainty associated with the reproducibility of an isotope ratio measurement. The precision quoted on a date is the result of the propagation of the precision for each isotopic ratio measurement through the dating equation.

Accuracy is the appraisal of how close the measured ratio (which has been corrected for fractionation and mass discrimination) is to the 'absolute' or 'true' value. The 'true' ratio is usually taken as the published value for established laboratory standards such as those produced by the U.S. National Bureau of Standards. NBS standards are available for uranium but not for thorium. For this reason McMaster University set up a standard speleothem, called 76001, which has been used for interlaboratory calibrations for U-series dating.

Precision is expressed as the standard error, σ_m, or standard deviation of the mean of many measurements of a ratio (usually 60 to 100) over the course of a run. Bièvre (1978) refers to this as the internal standard error, where the ratio is measured many times in a single run. The external standard error, is from one

sample measured in many separate analyses. As the number of replicates increases, the external error approaches the internal error. External error is rarely quoted. In the following chapters most of the errors reported are internal standard errors. The only analyses which were repeated more than two times were of standards and some of the corals.

Typical internal precision on U ratio measurement (e.g. $^{234}U/^{235}U$) is ~0.1% ($2\sigma_m$). External precision on repeat analyses of U standards is ~0.5% (e.g. on 6 repeats) but on samples only ~2% (e.g. on 3 repeats). However, note that "repeats" on samples are of a comparable but different sample.

Precision on Th ratios depends on ^{232}Th levels: for normal speleothem of moderate detrital content (e.g. with $^{230}Th/^{232}Th$ activity ratio in the range 100 to 2000) internal precision is ~0.3% ($2\sigma_m$). The best precision obtained to date is 0.16%. External precision on the natural thorium standard is ~0.8% (20 runs). For speleothem samples, even those which have been ground and homogenized, ^{232}Th levels are highly variable so that an external precision on $^{230}Th/^{232}Th$ ratios is not meaningful: for example the measured $^{230}Th/^{232}Th$ activity ratio on 76001 using WL96 spike varies from 360 to 426; 2σ is 12.7% of the mean.

To estimate precision on dates the errors on each ratio are propagated through the dating calculations (see account below). In addition the error on the spike calibration (see chapter 5) must be included. The following example shows a sample spiked with ST96. $2\sigma_m$ errors for each ratio are:

Ratio	Error
$^{230}Th/^{229}Th$	0.26%
$^{229}Th/^{232}Th$	0.15%
$^{230}Th/^{232}Th$	0.30%
$^{236}U/^{238}U$	0.19%
$^{234}U/^{236}U$	0.26%
$^{230}Th/^{234}U$	0.48%
$^{234}U/^{238}U$	0.32%

On propagation these errors lead to an internal precision on the age of 1.0% ($2\sigma_m$). Precision on dates (using the well calibrated spike, ST96) varies from ~0.8% up to ~2%. External reproducibility of dates for McMaster speleothem standard 76001 is 2.2% (16 runs using WL96 spike).

The factors which contribute to the accuracy of the isotopic ratio measurements are discussed below. Tests for accuracy are discussed in the section on standards.

For U-series dating the $^{235}U/^{238}U$ ratio is constant and its measurement in each sample serves as a check on accuracy. Any abnormal measured $^{235}U/^{238}U$ ratio is reported. In addition the standard speleothem 76001 is dated regularly.

4.4 MEASURED VS. TRUE ISOTOPIC RATIOS

The measurement of isotopic ratios by mass spectrometry requires that:-

1. the ratio of the number of ions be accurately expressed by the ratio of ion currents,
2. a small peak have no tail effects from a big peak or from memory effects, and
3. amplification be linear.

4.4.1. Standards:

The use of standards for calibration allows 'absolute' measurements of ratios. Calibration of the system involves comparing a true ratio with an observed ratio at different ratio magnitudes. Uranium standards are available where the $^{235}U/^{238}U$ ratio varies from 0.00017 up to 186.78. System calibration has been done in this research (see chapter 6, tests of standards) and by Li (1989) for the VG354. Measurement of U ratios on standards NBS 005a (this research) and NBS 500 (Li) yielded results within the certified errors. It is therefore assumed that the ratio of the number of ions is accurately expressed by the ratio of ion currents. Unfortunately, no thorium standards are available to test the accuracy of thorium

ratio measurement. The only test available is to date the speleothem standard 76001. Mass spectrometric dating yielded results clearly within the alpha counted error margin (details in chapter 6).

Table 4.1: Average counts over the thorium spectrum to show memory effects and tailing from ^{232}Th peaks.

Sample	227.5	228.5	229.5	230.0	230.5	232.0	A02	C230
RN Gbase	0.89	0.44	-0.22	22.33	0.44	2,225	1,870	0.11
RN D	1.09	0.73	-1.00	11.1	-0.55	2,984	724	-0.78
DWBAH Q	1.1	-0.4	0.4	18.54	0.10	4,147	36	0.25
Eggshell	1.9	-0.3	0.18	11.45	-0.55	7,762	285	-0.19
RN Etop	1.11	0.33	-0.62	72.2	-0.4	20,223	690	-0.51
D3	-2.00	-0.63	-1.86	244.3	-1.0	21,442	21,175	-1.4
RN G2	-0.44	-2.11	-2.44	142.7	-3.2	23,586	1,158	-2.8
DWBAH T4	2.4	1.3	0.7	31.4	0.17	24,532	228	0.44
RN C	4.22	1.89	0.78	97.3	0.41	32,728	548	0.60
DWBAH B2	2.33	0.22	-0.22	46.44	-0.78	45,070	187	-0.5
DWBAH 12	4.2	1.2	1.1	85.0	-0.11	198,530	80	0.50

A02 indicates the $^{230}Th/^{232}Th$ activity ratio.
C230 indicates the correction for the ^{230}Th peak assuming a linear background. It is the average of the counts at masses 229.5 and 230.5. Where this correction is positive the interpeak background is higher than the general random noise background.

4.4.2 Memory effects and tailing:

Memory effects on the VG354 are minor and are accounted for in the counting procedure. A 'dummy' peak is measured after any big peak, as a delay so that memory effects can be cleared before counting the small peak: mass 227.5 is measured immediately after mass 232, mass 229.3 immediately after 229, 233.5 after 238 and 232.5 after 236. The memory effect is small: for a 232 count of 2500 the memory effect during counting of mass 227.5 was 0.7 counts; for a 232 count of 200,000 the memory effect was 4 counts and, by the time 228.5 was measured, it had decayed to 1 count. Table 4.1 shows the memory effect on 227.5 and 228.5 of various 232.0 peaks.

Tailing, even for ^{232}Th, is insignificant and its effect on smaller peaks is

indistinguishable. Figure 2.1, a and b shows scans for (a) a uranium run and (b) a thorium run on a spiked sample (note the changes in scale for the larger peaks): neither of the two smallest peaks, ^{234}U and ^{230}Th, have significant interference from the large peaks nearby. Table 4.1 shows some average counts over the thorium mass spectrum for a variety of samples, a variety of ^{232}Th counts and a variety of $^{230}Th/^{232}Th$ activity ratios. The table is arranged in order of increasing ^{232}Th counts.

The principal concern is the effect of tailing from the ^{232}Th peak on the much smaller ^{230}Th peak. Several points are apparent from Table 4.1:-

(i) The counts on 230.5 do not increase with increasing 232.0 counts.

(ii) The background to either side of ^{230}Th, at masses 229.5 and 230.5 does not always increase towards the ^{232}Th side; for 50% of these samples it decreased.

(iii) There is no significant difference between the average 229.5 counts (-0.2 ± 2.0) and the average 230.5 counts (-0.4 ± 2.0).

(iv) Many of the counts to either side of 230.0 are lower than the background count measured at 227.3 and attributable to random electrical noise.

(v) Where the counts to either side of 230.0 are positive (i.e. greater than the general background noise) then the increase may not be towards mass 232.0. The positive corrections are, on average, 0.87% of the ^{230}Th peaks.

(vi) For two cases where background does increase towards mass 232 the linear correction was compared to an exponential correction: the difference in the two correction procedures introduced < 0.2% error.

Sample	Linear correction	Exponential correction	Difference as % of ^{230}Th peak
Coral D3	-1.43	-1.65	0.09%
RN Gb2	0.74	0.70	0.14%

Li (1989) examined tail shapes on very high ^{232}Th peaks from granitic samples. He reports that the linear correction was as good as the hyperbolic correction within the counting error.

All of these observations suggest that the background to either side of the ^{230}Th peak is not related to any tail effects from the ^{232}Th peak. The sampies dated in this study were of relatively low ^{232}Th content: Table 4.1 includes samples with

the highest levels of ^{232}Th. Tailing from the ^{232}Th peak was insignificant and, in any case, is accounted for in the interpeak interference correction.

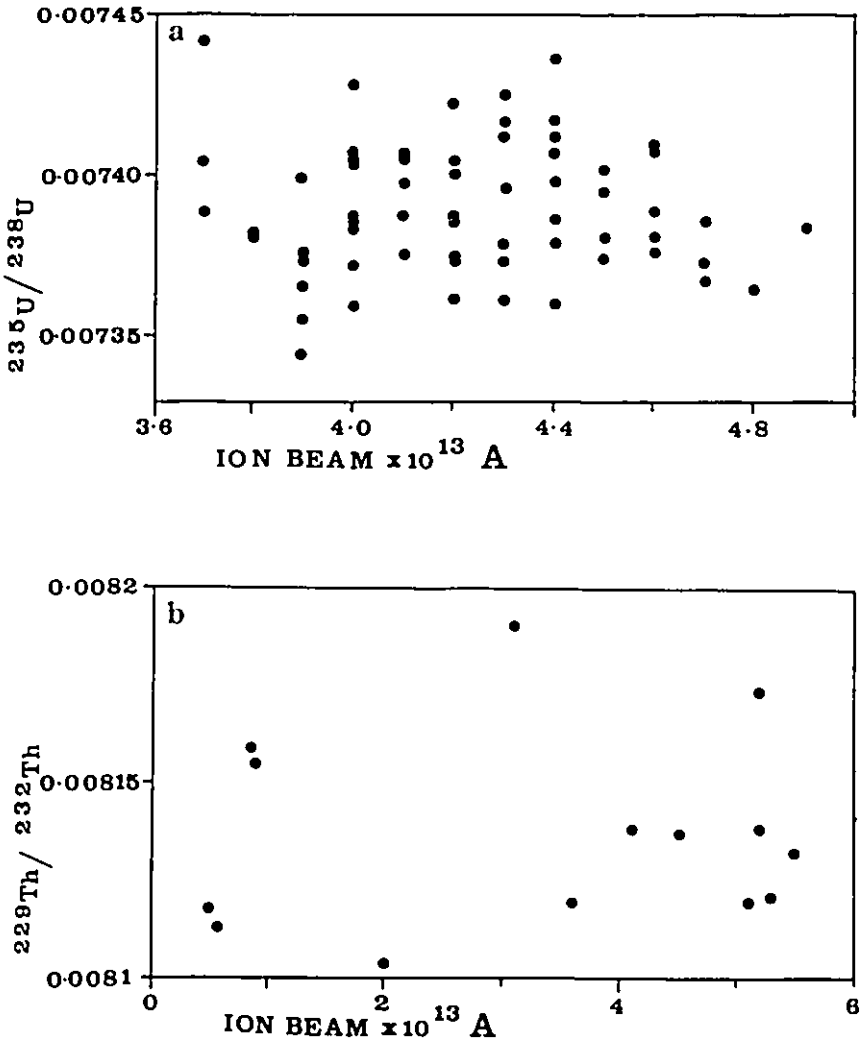

Figure 4.1: NON-LINEARITY IN THE DALY DETECTION SYSTEM. (a) shows variations in $^{235}U/^{238}U$ measured atomic ratio over a range of ion beam current values, taken from a number of analyses. $^{235}U/^{238}U$ is constant in nature. If the Daly showed any linearity or bias, then the measured constant ratio might be expected to show a correlation with ion beam current. Clearly, there is no relationship. (b) shows the variation in $^{229}Th/^{232}Th$ ratios for a single sample as ion beam current was raised. Again there is no apparent relationship, confirming non-linearity in the Daly detector.

4.4.3 Non-linearity in the detection system:

Chen and Wasserburg (1980) observed, on one of their mass spectrometers only, a decrease of measured ratio with increasing signal: i.e. as the detector became saturated it showed bias or linearity. This was not a problem for the McMaster Daly detector which was shown to be linear for signals up to 500,000 counts per second (Li 1989). Non-linearity would be revealed as a change in measured ratio with increasing ion beam current: figure 4.1 shows that, for both U and Th ratios, there is no correlation. The $^{235}U/^{238}U$ ratio is constant: these values are taken from several analyses. The $^{229}Th/^{232}Th$ ratio is constant only within a single sample: the Th ratio values are taken from one run where the ion beam current was raised throughout the run.

4.5 FRACTIONATION AND MASS DISCRIMINATION

Fractionation is the preferential evaporation of lighter isotopes (Fassett and Kelly 1984). It causes a difference between the isotope ratio in the sample and that in the ion beam. Fractionation occurs because the lighter isotope requires a slightly lower activation energy and is more likely to take part in a chemical or physical reaction than the heavier isotope. The ion beam will tend to have a higher proportion of the lighter isotope at the start of evaporation; towards the end of the run, as the lighter isotope is used up, the proportion decreases until only the heavier isotope is left. This process is called Rayleigh Distillation and is illustrated in Figure 4.2, A. The reaction may be divided into two parts: (i) the initial stage where isotope ratios remain constant over time, and (ii) the stage of rapidly accelerating change. In the first stage fractionation is almost constant: the reaction proceeds as if the sample were infinite. The duration of this stage depends on the speed of the reaction and on the supply of reactants: it should last for at least 2 to 3 hours. If the sample is too small or is run at too high a current then it burns off too quickly and the ratios change rapidly. Fractionation is apparent during a mass spectrometric run when the measured ratios change over time: initially the measured ratios (of light

to heavy isotopes) are slightly higher than the 'true' ratio. After about 1 hour, for small thorium samples, 3 hours for a good thorium sample, or 5 hours, for a normal uranium sample, the measured ratios become progressively lower as the light isotope becomes exhausted. In this first stage because fractionation is constant it can be corrected for (see below). The second stage results cannot be used because the changing rate of fractionation cannot easily be modelled. The time of the changeover from first to second stage can be seen in the run print out where the errors on the grand means begin to increase as more data are added. Data quality is also reflected in the number of rejected scans: high rates of change cause excessive levels of rejection.

Mass discrimination is "the difference in relative measurement efficiency of one isotope vs. another" (Fassett and Kelly 1984). It is the difference between the isotope ratios in the ion beam and the ratios as measured by the Daly detector. The Daly discriminates slightly in favour of the lighter isotope. This bias is constant for impinging ions of constant kinetic energy; it relates simply to the mass difference of the isotope pair.

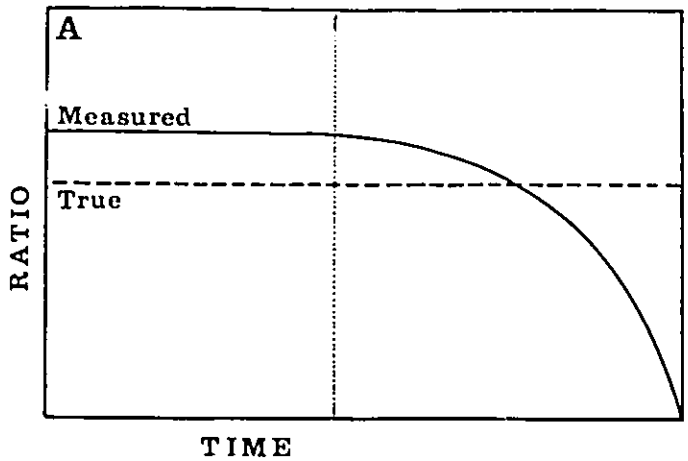

Figure 4.2, A: FRACTIONATION OR RAYLEIGH DISTILLATION. Where a sample is of finite size then at the start of a reaction the measured ratio (of light to heavy isotope) of the products is slightly higher than the true starting ratio of the reactants; in time, as the lighter isotope is used up the measured ratio becomes lower (shown as the solid line). The dotted line separates the first stage of the reaction, when ratios remain relatively constant over time, and the second stage, when ratios are rapidly changing.

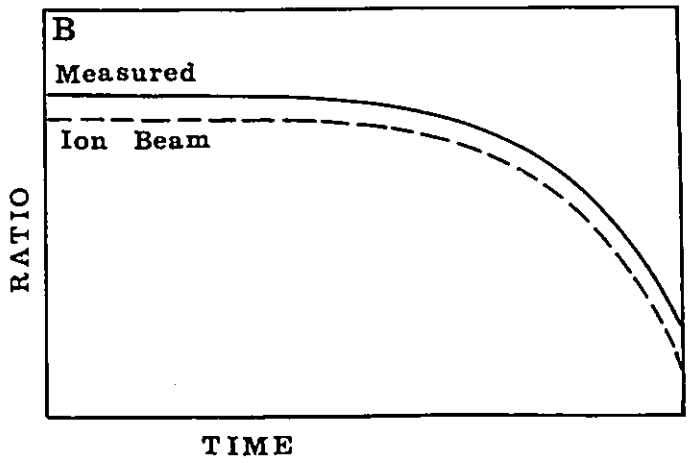

Figure 4.2, B: FRACTIONATION PLUS MASS DISCRIMINATION. The ratios in the ion beam differ from the true ratio because fractionation at the source causes Rayleigh distillation. The measured ratio is slightly higher than the ion beam ratio due to mass discrimination at the Daly detector. Most mass spectrometric runs conform to this pattern. The time scale varies according to the size of the sample.

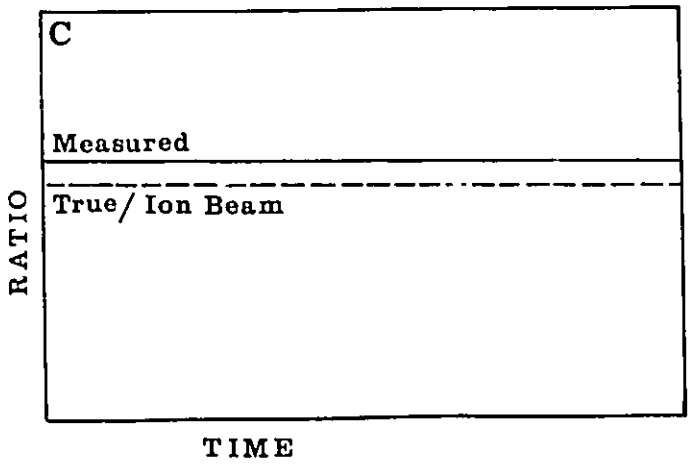

Figure 4.2, C: MASS DISCRIMINATION ALONE. If no fractionation at the source occurs then the isotopic ratios in the ion beam are the true ratios; the measured ratio is slightly higher because of mass discrimination but it does not change over time.

During a mass spectrometric run both fractionation at the source and mass discrimination at the detector affect the measured ratios. Figure 4.2, B illustrates how the isotopic ratios in the ion beam (dashed line) vary over time, caused by fractionation at the source. The measured ratio (solid line) is higher than this by a constant proportion, caused by mass discrimination at the detector. Most mass spectrometric runs confrom to this pattern. The time scale varies with the size of the sample.

A constant mass related discrimination (see Figure 4.2, C) is easy to correct for, but fractionation is not, because it is rather variable and depends on the size of the sample, the temperature, the loading techniques, etc.

4.5.1 Methods of correction for mass discrimination and fractionation:

Mass discrimination alone is corrected using only the relative mass difference of the isotopes:

Corrected ratio = Measured ratio x $\sqrt{(m_1/m_2)}$

Fractionation correction is a much more controversial procedure. The correction is actually of mass discrimination at the detector in addition to fractionation at the source. At least one of the measured isotope pairs must have a constant, known, true value. Then the proportion of the true value over the measured value gives a gauge of the degree of fractionation. This is used to correct the other ratios. However, the details of the correction procedure vary with different publications. The measured ratio is a function of the true ratio modified by a fractionation factor, α. The formulae may be expressed in different ways but only three basic fractionation laws have been proposed (Russell et al 1978, Wasserburg et al 1981): linear, power and exponential. Fractionation per mass unit, α, is given as:

Linear: $[R_T a,b/R_M a,b - 1] / \Delta_m a,b$

Power: $[R_T a,b/R_M a,b]^{(1/\Delta m a,b)} - 1$

Exponential: $(\ln[R_T a,b/R_M a,b]) / (m_b \cdot \ln[m_a/m_b])$

where R_T is the true ratio of the isotopes a and b, R_M is the measured ratio, Δ_m is the mass difference. The correction factor is then applied to calculate the true value of the ratio (c/d):

Linear: $R_Tc,d = R_Mc,d \times (1 + \alpha)^{\Delta mc,d}$

Power: $R_Tc,d = R_Mc,d \times (1 + \alpha)^{\Delta mc,d}$

Exponential: $R_Tc,d = R_Mc,d \times (m_c/m_d)^{\alpha md}$

The Rayleigh distillation law has also been proposed but Rees (1969) observed that fractionation cannot accurately be explained by Rayleigh distillation which occurs only where the sample is liquid and completely mixes as evaporation occurs. Kanno (1971) also showed that Rayleigh distillation does not apply to a multiple filament source.

Wasserburg et al (1981) note that for small fractionation the three laws give the same corrected values. The differences become apparent only for fractionation larger than commonly observed. Choice of the best fractionation law requires many tests with standards of known isotopic composition under different fractionation conditions. The appropriate law will give the same corrected ratio regardless of fractionation. Inappropriate correction will give a correlation of the ratio with fractionation. No law works on highly fractionated runs i.e. the "laws" are only semi-empirical approximations to the true fractionation behaviour (Russell et al 1978). All of these correction factor tests assume that the sample will be fractionated to the same extent as the standard: while this is generally true, samples are often very much more variable than standards.

The known, true ratio may occur naturally or may be provided by adding a spike to the sample. Dietz et al (1962), Chen and Wasserburg (1981) and Edwards et al (1986/87) used a double spike, ^{233}U-^{236}U, to correct for fractionation in U runs. The McMaster lab uses the naturally occurring constant $^{235}U/^{238}U$ ratio. No comparable standard exists for thorium because there is no sample with a well defined $^{230}Th/^{232}Th$ ratio.

4.5.2 Importance of fractionation vs. discrimination:

Fassett and Kelly (1984), reporting on interlaboratory tests, conclude that isotopic fractionation is the major source of imprecision and that the degree to which it can be calibrated limits the measurement accuracy; it is more important than contamination, background determination or instrumental discrimination. However, Li (1989) notes that, for analyses of U standards on the VG354, the deviations between the measured isotopic ratios and their true values are caused by a small amount of mass fractionation at the source, and a large amount of mass discrimination at the detector. Li measured these effects by comparing the ratios of NBS 500 U standard measured on the Daly and on the Faraday. The Faraday does not discriminate according to mass so the measured ratios reflect only fractionation at the source. This was 0.007% per mass unit (measured on the $^{235}U/^{238}U$ ratio). The ratio was misrepresented by 0.5% per mass unit on the Daly. If fractionation causes 0.007% per mass unit then the remaining 0.493% per mass unit caused by the Daly mass discrimination represents 98.6% of the bias. Li concludes that the ratios can be corrected as if only mass discrimination happens.

However, this model does not apply when samples are being run: Li notes that in U runs variation was found to be sporadic and relatively large so that correction by means of the simple discrimination factor $\sqrt{(m_1/m_2)}$ would be unreliable. Instead, correction requires the use of a normalizing ratio: i.e. the fractionation correction factor is calculated by normalizing a measured ratio to its known true value. For uranium ratio correction the ratio $^{235}U/^{238}U$ is constant in nature and known to be 0.0072526 ± 0.0000188 (Arden 1977).

4.6 CORRECTION FOR URANIUM RATIOS

This study, in choosing the power law for U ratio correction, follows the procedure used by Li (1989) which in turn follows that used by Wasserburg et al (1981) and Edwards et al (1986/87). Wasserburg et al note that the exact mathematical form of the fractionation law which describes instrumental mass

fractionation during thermal ionization is not well known; the power law may not be the optimum choice but it introduces no significant error where fractionation is small.

The correction factor per mass unit for the ratio $^{235}U/^{238}U$ (CF1) is given by:

$$CF1 = [R_T{}^{235}U/^{238}U/R_M{}^{235}U/^{238}U]^{(1/4m235,238)}$$
$$= [(0.0072526/R_M{}^{235}U/^{238}U]^{(1/3)}$$

where R_T and R_M are the true and the measured ratios. This correction factor is used to calculate the correct $^{236}U/^{238}U$ ratio and hence the correct $^{235}U/^{236}U$ ratio:

$$C68 = R_M{}^{236}U/^{238}U \times CF1^2$$
$$C56 = .0072526/C68$$

where C68 is the corrected $^{236}U/^{238}U$ ratio and 2 is the mass difference between ^{236}U and ^{238}U.

On the assumption that fractionation remains constant over the course of the run, the second stage of the uranium analysis is then corrected: the corrected $^{235}U/^{236}U$ for the first stage is used as normalization for the measured $^{235}U/^{236}U$ and $^{234}U/^{235}U$ of second stage. The second correction factor (CF2) is given by:

$$CF2 = C56 / R_M{}^{235}U/^{236}U$$
$$C46 = R_M{}^{234}U/^{236}U \times CF2^2$$

where C46 is the corrected $^{234}U/^{236}U$ ratio. From these the corrected $^{234}U/^{238}U$ (C48) is calculated:

$$C48 = (C46 \times C68).$$

In practice the correction of the ratio $^{236}U/^{238}U$ is done as part of the mass spectrometric analysis because the true $^{235}U/^{238}U$ is an input to the sequence type (see appendix) as a normalization ratio. All the other corrections are done in the dating program documented below.

4.7 CORRECTION FOR THORIUM RATIOS

The correction procedure described above is applicable only for uranium ratio correction: it cannot be used for thorium ratio correction because no normalization ratio is available. Li (1989) argues that mass fractionation in thorium runs is relatively small because during the course of a run the mean of each group (of 10 scans) deviates from the grand mean by less than 2 permil per mass unit. This deviation (D) is calculated thus:

$$D = \{[R29_{group} / R29_{grand\ mean}]^{1/3} - 1\} \times 100$$

where R29 is the measured $^{232}Th/^{229}Th$ ratio. The logic behind this assertion is presumably that if fractionation at the source were more significant, then variability would be greater. However, it could be argued that this stability simply indicates stable, but not necessarily small, fractionation characteristic of the first part of Rayleigh distillation when the sample is effectively infinite.

It is important to note that Li's data were from standards. During the current research Th runs on standards also gave a steady, invariant beam, some varying by as little as ± 1 permil per mass unit over the course of the run. However, Th runs on uraninite gave more inconstant patterns indicating less stable fractionation at the source: good uraninite runs varied by only ± 2 permil but some varied by ± 20 permil. Carbonate samples showed even higher variability, from ± 7 permil to ± 60 permil.

Li does not indicate the variability over the course of uranium runs, but implies that it is greater than over thorium runs. He also implies (i) that this variability is caused by fractionation at the source; (ii) that this is why uranium runs are corrected for fractionation as well as mass discrimination; and (iii) that thorium runs do not show this added fractionation effect and therefore need only be corrected for mass discrimination. He corrects the thorium ratios with the mass discrimination factor $\sqrt{(m_1/m_2)}$. Chen et al (1986), Edwards et al (1986/87) and Edwards et al (1987) also correct Th ratios only by mass discrimination but offer

no explanation or justification.

Li's arguments to justify his method of thorium ratio correction are not strictly valid. A comparison of uranium and thorium beam instability (Table 4.2) shows that: (i) U runs usually are less variable than Th runs suggesting that Th runs are more likely to show irregularities which may be attributable to source fractionation than are U runs; (ii) variation increases from standards runs to uraninite runs to sample runs. Variation is smaller for large samples with a good steady beam than for small samples. This variability must come from fractionation at the source caused by complexities in the carbonate samples which are not apparent in the pure standard solutions and the relatively pure uraninite solutions. Stability is also reflected in the error values, which are always higher for thorium runs. The assertion that thorium runs are not fractionated at the source has little basis. It is clear that mass discrimination correction alone is not adequate for uranium ratio correction (see Table 4,3) one might therefore expect it to be inadequate for thorium ratio correction. It then remains to decide how to correct the thorium ratios.

For much of this research the poorly calibrated, high ^{230}Th spike, WL96, was used: the error on the age was dominated by the error on the spike calibration and the error on the ^{230}Th contribution from the spike. The error introduced by the method of thorium ratio correction was insignificant compared to the error introduced by the spike. Now that the new spike, ST96, is available and has been very well calibrated, the error for the thorium ratio correction method is more significant in relation to the total error on the age.

The question of the optimum thorium ratio correction procedure remains open. Meadows et al (1980) averaged the fractionation corrections for all the uranium analyses on the same run and used that to correct the thorium runs. However, since fractionation is controlled by chemistry and the chemistry of uranium and thorium is different, it was concluded that the use of the mass discrimination correction alone is less likely to introduce error than is the use of a fractionation factor from a separate run, for a different element, which is almost certainly

not applicable. Until further elucidation of this problem, all ages presented are calculated using the mass discrimination factor for thorium ratios.

Table 4.2: Comparison of uranium and thorium beam instability for standards, uraninite and samples.

Maximum deviations (D) of mean of 10 scans from final grand mean (expressed in permil per mass unit):

$$D = \{[RATIO_{group} / RATIO_{grand\ mean}]^{1/3} - 1\} \times 100$$

	U run $^{236}U/^{238}U$	Th run $^{229}Th/^{232}Th$
Standard		
D (range)	-2.2 to +1.2	-0.6 to +0.6
Uraninite	$^{235}U/^{236}U$	$^{229}Th/^{230}Th$
D (range)	-1.8 to +3.5	-2 to +2
D (range)	-1.5 to +2.5	-17 to +18
Samples	$^{235}U/^{236}U$	$^{229}Th/^{230}Th$
D (range)	-2.5 to +1.5	-8 to +7
D (Range)	-3.0 to +5.0	-85 to +85

Table 4.3: Comparison of fractionation correction with mass discrimination correction for coral samples; MD is the mass discrimination factor, CF58 and CF56 are the fractionation correction factors for $^{235}U/^{238}U$ and $^{235}U/^{236}U$.

$MD\sqrt{(235/238)}$	$MD\sqrt{(235/236)}$	$MD\sqrt{(229/232)}$	$MD\sqrt{(230/232)}$
.9936774	.997891	.9935134	.9956803
Correction permil			
6.3	2.1	6.5	4.3
Permil per mass unit			
2.1	2.1	2.1	2.1
$(CF\ 58)^3$	$CF\ 56$	$(CF\ 56)^3$	$(CF\ 56)^2$
Mean and 2σ			
0.9869465	.9964542	.9894072	.9929233
0.0026283	.0032393	.0096714	.0064631
Correction permil			
13.1	3.5	10.6	7.1
Permil per mass unit			
4.4	3.5	3.5	3.5

If a measured $^{235}U/^{238}U$ ratio is 0.00735, then mass discrimination correction returns a value of 0.007304 which is 0.7% less than the true value of 0.0072526. In general, correction by mass discrimination will undercorrect by 1.4 permil per mass unit.

Table 4.4 Propagation of errors.

The errors are propagated as recommended in Bevington (1969) and Barry (1978):

For addition or subtraction (of A and B):

$$E_{sum} = \sqrt{(E_A^2 + E_B^2)}$$

For multiplication (of A and B):

$$E_{product} = A*B \sqrt{[(EA/A)^2 + (EB/B)^2]}$$

For division (of A by B):

$$E_{quotient} = A/B \sqrt{[(EA/A)_2 + (EB/B)^2]}$$

where E is the error and A and B are the variables. These steps assume that A and B are independent.

4.8 THE DATING PROGRAM

The dating program, called AGE.BAS, is documented in the appendix. It (i) corrects the measured ratios for fractionation, mass discrimination and contributions of isotopes from spike and reagent; (ii) propagates the errors on the ratios (see Table 4,4); (iii) calculates the activity ratios from the atomic ratios using the decay constants of the isotopes (see Table 4.5); (iv) calculates U and Th concentration of the sample; (v) calculates the age and its error either by the Newton-Raphson method of iteration or, where convergence does not occur, by the repeated bisection method (Bittinger and Morrel 1984, Pearson 1986); (vi) corrects the age for non-radiogenic ^{230}Th if necessary; (vii) calculates initial $^{234}U/^{238}U$ activity ratio and (viii) records the results onto disc if required. The age dating equation and the initial $^{234}U/^{238}U$ ratio equation are exactiy as used in most of the alpha counting programs (Schwarcz and Gascoyne 1984, for example). The error on the age includes the error on the spike ratio and on both $^{230}Th/^{234}U$ and $^{234}U/^{238}U$ activity ratios. All the errors are $2\sigma_m$ internal precision estimates. Errors on the decay constants and the error on true $^{235}U/^{238}U$ ratio are not included.

This program uses the observed standard errors from replicate measurements of the isotope ratio. In this it differs greatly from the α-dating program used in the McMaster laboratory, which assumes an error from Poisson statistics. This program also differs from the α-dating program (and from that of Li 1989) in that it includes errors on $^{234}U/^{238}U$ ratio in the age calculation. This contributes significantly to the

Table 4.5. Decay constants for isotopes: these are updated from those used in the McMaster alpha counting program.

Isotope	Decay constant	Reference
^{238}U	1.55125e-10 a^{-1} ± 0.045%	Jaffey et al 1971
^{235}U	9.8485E-10 a^{-1}	Steiger and Jager 1977
^{234}U	2.835e-06 a^{-1}	Li 1989
^{232}Th	4.9475e-11 a^{-1} ± 0.6%	Le Roux and Glendenin 1963
^{230}Th	9.195e-06 a^{-1} ± 0.78%	Meadows et al 1980
^{229}Th	9.443E-5 a^{-1}	Li 1989

age error towards the limit of dating and has a lesser effect on all dates.

An important difference between AGE.BAS and Li's program is that Li uses the ^{232}Th content in the age calculation. This is highly suspect because it depends on the presumption that the initial $^{230}Th/^{232}Th$ ratio is 1.7. This value is simply the modern $^{230}Th/^{232}Th$ ratio of one type of detritus: Kaufman and Broecker (1965) used this value as a correction factor only for similar types of material in the same area but of an older genesis. There is no justification for applying it to all U-series dates. Many labs use a different value but all should quote the uncorrected age, the corrected age and the assumed initial $^{230}Th/^{232}Th$ ratio. It is then up to the reader to assess the validity of the two dates.

It is possible, in certain circumstances, to test the validity of the detrital correction. Where a series of dates is available on clean parts of the speleothem it may be possible to calculate the growth rate. This can then be propagated to get an expected date for the more contaminated layer. If the correction factor on the observed date is correct then the two dates would coincide. For the flowstone sample called DWBAH, which is documented in chapter 7, the correction using an initial $^{230}Th/^{232}Th$ ratio of 1.7 did not correct the date sufficiently: i.e. the corrected dates were still too old. However, for the Rat's Nest Cave sample the detrital layers apparently need no correction at all.

The program AGE.BAS calculates the age. Then, if the $^{230}Th/^{232}Th$ ratio is < 500, it calculates the radiogenic $^{230}Th/^{234}U$ with the assumed initial $^{230}Th/^{232}Th$

of 1.7 and re-calculates the age using the radiogenic $^{230}Th/^{234}U$. The cut-off point of 500, though very much broader than the normal cut-off of 20 for α-counting dating, is chosen because beyond 500 the correction has no effect on the date. This broad range allows the worker more leeway in assessing dates. However, it must be stressed that the corrected date is significantly less reliable than its precision suggests because of the assumed initial $^{230}Th/^{232}Th$ ratio.

Li does not calculate the age if $^{230}Th/^{234}U$ activity ratio is greater than 1.0 but simply returns the message "Th230 age > 400,000 years". This is true only if the $^{234}U/^{238}U$ ratio is < 1.2. He also limits the age calculation to $^{230}Th/^{234}U$ ratios of greater than 0.1 This includes ages up to 10,000 years. AGE.BAS has neither limitation. The calculated date is printed and it is left up to the judgement of the worker to interpret the figures. Note that if $^{230}Th/^{234}U$ activity ratio is greater than 1.1 then the program should not calculate an age: the sample must either be leached or contaminated.

Chapter 5

CALIBRATING THE SPIKE

The spike is used to find both the isotopic ratios and the concentration of the sample, so the spike isotopic composition and concentration must be accurately calibrated.

The spike in use before 1989, which I have called WL96, was made up by Wangxing Li from (a) Ros 2, the ^{236}U - ^{229}Th spike used in the McMaster alpha counting lab and (b) ^{229}Th supplied in solid form by J. Harvey (McMaster University, Dept. of Health Physics) to W.L. in 1988. The Ros 2 spike was used as a source of ^{236}U: it was cleaned of thorium with anion exchange columns. The ^{229}Th was dissolved in HNO_3/HCl and the two mixed to make up WL96. A new spike, called ST96, was made up (by J.L.) in 1989 when WL96 was running low.

To calibrate a spike we must know (i) the isotopic composition of the Uranium and Thorium in the spike solution, (ii) the $^{229}Th/^{236}U$ ratio and (iii) the concentration of U and Th in the spike.

The isotopic composition: Ideally the spike should consist of only ^{236}U and ^{229}Th, two isotopes which do not occur in the sample. However, small quantities of the more common isotopes occur almost inevitably. Hence the spike isotopic composition must be determined in order to correct for contributions of common isotopes from the spike. The isotopic ratios are measured directly by the mass spectrometer and are corrected as follows:

(i) The uranium ratios are corrected for fractionation and mass discrimination using the average correction factor from samples of normal $^{235}U/^{238}U$ ratio (.0072526). The fractionation correction factor has varied slightly in the last two years: it was lower and more variable before January 1989 when adjustments to improve the peak shape were made. The average was 0.9939616 when WL96 was being calibrated, 0.9941656 when ST96 was being calibrated and is currently 0.995664.

(2) The thorium ratios are corrected for mass discrimination using $\sqrt{(m_1/m_2)}$.

The $^{229}Th/^{236}U$ ratio: The $^{229}Th/^{236}U$ ratio cannot be measured directly by mass spectrometry but must be measured indirectly: i.e. the spike must itself be spiked. This can be done in two ways: (a) the unknown concentrations of spike U and Th are measured against standards of known concentration or (b) the unknown spike ratio is calibrated against the known ratios of uraninite in secular equilibrium. Details of these methods are given below.

U and Th concentration: The spike U and Th concentrations are used to estimate how much spike to add to samples and to calculate the concentration of the sample. The ratio of Sample ^{234}U to Spike ^{236}U and Sample ^{230}Th to Spike ^{229}Th should be of the order of 0.1. The concentration values are taken from the analyses of spiked standards described above.

5.1 CALIBRATION OF WL96 SPIKE

This spike, made up by Wangxing Li for use with granites, has more thorium than appropriate for speleothem samples, contains nearly 57% ^{232}Th and significant ^{230}Th (0.4%). Its use was necessary for all of the DWBAH flowstone analyses pending arrival of fresh supplies of isotopes to make up a new spike.

5.2.1 Isotopic composition of WL96 spike:

The isotopic composition of the spike is measured by mass spectrometry. The measured ratios are corrected for fractionation and mass discrimination using the average fractionation correction factor.

These analyses were done in addition to those already done by Li (1989) as a test of the effect of the filament metal in use. The analyses by Li used the normal, slightly impure, metals. The analyses of spike samples below were done with high purity rhenium and tantalum bought especially for U-Th work.

8/12/88: ~2 g WL96 spike was loaded directly onto Re-Ta double filaments or Re-Re-Re triple filaments, without any preliminary separation into U and Th fractions. Uranium and, later, thorium isotopic ratios were measured for all samples. In general, the U analyses ran better on the tantalum filament and Th on the rhenium filaments.

Results:

A. Isotopic ratios - (this study):

Sample	$^{235}U/^{236}U$	$^{238}U/^{236}U$	$^{230}Th/^{229}Th$	$^{232}Th/^{229}Th$
1			9.009×10^{-3}	1.3219
2			8.984×10^{-3}	1.3211
B	4.69×10^{-5}	2.36×10^{-3}	9.135×10^{-3}	1.3119
D			9.134×10^{-3}	1.3146
E,F	4.80×10^{-5}	2.37×10^{-3}	9.147×10^{-3}	1.3252

Average and 2σ range:

$^{235}U/^{236}U$ on 2 samples: 4.74×10^{-5}

$^{238}U/^{236}U$ on 2 samples: 2.37×10^{-3}

$^{230}Th/^{229}Th$ on 5 samples: 9.08×10^{-3} (8.93×10^{-3} to 9.24×10^{-3})

$^{232}Th/^{229}Th$ on 5 samples: 1.3189 (1.3079 to 1.3299)

B. Isotopic ratios - (Li 1989):

Average and 2σ range -

$^{235}U/^{236}U$ on 8 samples: 7.4×10^{-5} (6.1×10^{-5} to 8.7×10^{-5})

$^{238}U/^{236}U$ on 8 samples: 2.24×10^{-3} (2.23×10^{-3} to 2.25×10^{-3})

$^{230}Th/^{229}Th$ on 4 samples: 9.05×10^{-3} (8.90×10^{-3} to 9.11×10^{-3})

$^{232}Th/^{229}Th$ on 3 samples: 1.3114 (1.3091 to 1.3137)

Comparison of the two sets of analyses:

The 2σ errors on the thorium ratios overlap but the uranium ratios are not within the error of Li's figures. The ^{235}U and ^{238}U content of the spike is so low in relation to that of the sample that any error in its measurement will have very little effect on the isotopic ratios measured. However, an accurate measurement of thorium ratios is important because the proportion of ^{232}Th is high and the ^{230}Th from the spike may be a significant part of the whole ^{230}Th count. The thorium ratios from the two sets of analyses are close enough to obviate the need for further tests.

The results suggest that the impure metals have little effect on the analyses, so the figures from Li were used to correct for spike ^{230}Th, ^{232}Th, ^{235}U and ^{238}U in the BASIC program called FRACT.BAS which is used for dating with WL96 spike.

C. Isotopic fractions - (this study):

	^{235}U	^{236}U	^{238}U	^{229}Th	^{230}Th	^{232}Th
1			0.429	$3.87x10^{-3}$	0.567	
2			0.429	$3.86x10^{-3}$	0.567	
B	$4.67x10^{-5}$	0.9976	$2.35x10^{-3}$	0.431	$3.94x10^{-3}$	0.565
D				0.430	$3.93x10^{-3}$	0.566
E,F	$4.78x10^{-5}$	0.9976	$2.36x10^{-3}$	0.428	$3.92x10^{-3}$	0.568
Average and 2σ:						
	$4.76x10^{-5}$	0.9976	$2.36x10^{-3}$	0.429	$3.90x10^{-3}$	0.567
				0.002	$0.07x10^{-3}$	0.002

D. Isotopic fractions - (Li 1989):

^{235}U	^{236}U	^{238}U	^{229}Th	^{230}Th	^{232}Th
$7.38x10^{-5}$	0.9977	$2.24x10^{-3}$	0.431	$3.90x10^{-3}$	0.565

5.1.2 Spike ratio calibration using standards:

In this method of calibration the concentration of ^{229}Th is measured against a thorium standard and that of ^{236}U against a uranium standard. Only the standard concentration is given; its isotopic composition must first be measured by mass spectrometry. The spike isotopic composition has already been measured.

For the spike calibration runs the isotopic ratios of a spike-standard mixture are measured by mass spectrometry. These are corrected for input of common isotopes from the spike and for ^{236}U from the standard. The concentrations of ^{236}U and ^{229}Th in the spike can then be calculated to yield the ratio.

The standards, "SPEX Industries Standards for Plasma Emission Spectroscopy", 1000 μg/ml in HNO_3, correct to 0.5%, were diluted by Li. The U standard is 0.99312 μg/ml. The Th standard is 1.06209 μg/ml.

5.1.3 Isotopic composition of SPEX standards

2/8/88: ~1 g of U standard was loaded onto Re-Ta double filaments and ~1 g of Th standard onto Re-Re-Re triple filaments and the isotopic ratios measured.

Results:
The thorium standard showed no trace of any thorium isotope other than ^{232}Th.

A. Uranium isotopic ratios - (this study):
Mean and 2σ of 2 samples:

$^{234}U/^{238}U$:	1.945×10^{-5} (0.052×10^{-5})
$^{235}U/^{238}U$:	3.216×10^{-3} (0.020×10^{-5})
$^{236}U/^{238}U$:	1.443×10^{-4} (0.124×10^{-4})

B. Uranium isotopic ratios - (Li 1989):
Mean and 2σ range:

$^{234}U/^{238}U$ (16 samples):	2.28×10^{-5} (1.98×10^{-5} to 2.58×10^{-5})
$^{235}U/^{238}U$ (23 samples):	3.20×10^{-3} (3.19×10^{-3} to 3.22×10^{-3})
$^{236}U/^{238}U$ (6 samples):	1.51×10^{-4} (1.45×10^{-4} to 1.56×10^{-4})

Note that the $^{235}U/^{238}U$ ratio is not the natural ratio (7.253×10^{-3}).

C. Isotopic fractions - (this study):

^{234}U	^{235}U	^{236}U	^{238}U	^{232}Th
1.938×10^{-5}	3.206×10^{-3}	1.438×10^{-4}	0.9966	1.000

D. Isotopic fractions - (Li 1989):

^{234}U	^{235}U	^{236}U	^{238}U	^{232}Th
2.272×10^{-5}	3.190×10^{-3}	1.505×10^{-4}	0.9967	1.000

Comparison of the two sets of analyses:

For this study the standards were analyzed using high purity Rh and Ta to test the effect of the small amount of contamination in the metals used for the original analyses by Li. The $^{235}U/^{238}U$ ratio is within the 2σ range of the 23 analyses done by Li on the slightly less pure metals. The other ratios are not sufficiently far out of the range to warrant further investigation.

5.1.4 Calibration of WL96 by SPEX U and Th standards:

The concentrations of the standards are guaranteed by the supplier; the isotopic composition has been established by mass spectrometric analysis. The isotopic composition of the spike has also been established by mass spectrometric analysis but the concentrations of U and Th are not yet known. If a known quantity of spike is mixed with known quantities of standards and the isotopic ratios of the mixture analyzed, then concentrations of the spike can be calculated.

The BASIC programs called ST96UCON.BAS and ST96THCONC.BAS, which are listed in the appendix, calculate the concentrations. The number of atoms ^{236}U and ^{238}U from the standard is known. The number of atoms of ^{236}U from the spike is calculated from the $^{235}U/^{238}U$ ratio, taking into account the contribution of ^{238}U from the spike. Similarly, the number of atoms of ^{232}Th from the standard is known. The number of atoms of ^{229}Th from the spike is calculated from the $^{229}Th/^{232}Th$ ratio, taking into account the contribution of ^{232}Th from the spike. These programs now contain information relevant to the new spike, ST96 (see below). They can be modified as required for different spikes and different standards.

The spike calibration is then the number of atoms of ^{229}Th (per g of spike solution) divided by the number of atoms of ^{236}U.

1/8/88: ~0.3 g U standard, ~0.4 g Th standard and ~2 g spike were homogenized, separated into U and Th fractions with small anion exchange columns, and analyzed by mass spectrometry.

Results: (raw data are presented in the appendix)

Sample	U ppb	Th ppb	$^{229}Th/^{236}U$
B1	4.4839	4.8714	0.4797
B2	4.4796	4.8643	0.4795
B3	4.4822	4.8755	0.4853
9	4.4758	4.8864	0.4803
10	4.4772	4.8904	0.4806

Average, 2σ and range:
U conc. from 5 samples: 4.4797 ± 0.0067 ppb (4.4730 - 4.4864)
Th conc. from 5 samples: 4.8776 ± 0.0215 ppb (4.8561 - 4.8991)
$^{229}Th/^{236}U$ ratio: 0.48108 ± 0.00482 (0.47626 - 0.48590)

Data from Li (1989): average, 2σ and range -
U conc. from 5 samples: 4.4710 ± 0.0036 ppb (4.4674 - 4.4746)
Th conc. from 5 samples: 4.8486 ± 0.0143 ppb (4.8343 - 4.8629)
$^{229}Th/^{236}U$ ratio: 0.47993 ± 0.00147 (0.47846 - 0.48140)

Comparing the two calibrations:

The 2σ range of both sets of data overlap for U and Th concentrations and for the $^{229}Th/^{236}U$ spike ratio.

As a further check WL96 was then calibrated against uraninite in secular equilibrium. This method is conventional in alpha counting labs. It is based on the assumption that the uraninite $^{234}U/^{238}U$ and $^{230}Th/^{234}U$ isotopic ratios are known, against which the unknown spike ratio can be measured.

5.1.5 Calibration of WL96 by uraninite:

This uraninite was obtained from the McMaster alpha counting lab. It was made up by Gascoyne (1977a) from the solid uraninite supplied by J.N. Rosholt, USGS (Dilution No. 3, ~0.1 g / l, dissolved in HF first and then brought up in HNO_3). It was diluted to ~2.8 μg / ml (1.419 g uraninite solution made up to 29.764 g in 2 N HNO_3) for mass spectrometric runs.

The uraninite has been dated (in USGS) by Th/U radiometric techniques and by U/Pb. It was found to be of infinite U-series age (i.e. > 2 million years) and to give concordant ages by $^{235}U/^{207}Pb$ and $^{238}U/^{206}Pb$ dating. It is therefore assumed to have been closed to isotopic migration since its formation. Thus both the $^{234}U/^{238}U$ and the $^{230}Th/^{234}U$ activity ratios must be 1.00.

A mixture of spike and uraninite is analyzed on the mass spectrometer for uranium and thorium isotopic ratios. The uraninite and spike mixture may be loaded directly onto a filament and analyzed sequentially for U and then Th. However, the runs are more successful if the mixture is dried, dissolved in 7 N HNO_3 and separated into U and Th fractions on small columns. Each fraction is then loaded and analyzed separately.

The measured U and Th ratios are corrected for fractionation and spike ^{238}U, ^{230}Th and ^{232}Th (with the BASIC program FRACT.BAS). The $^{235}U/^{238}U$ ratio of uraninite is normal (0.0072526), so the measured ratios can be corrected using this as the normalizing ratio. The uraninite $^{230}Th/^{234}U$ activity ratio is assumed to be 1.000; i.e. the atomic ratio is 0.3083198. The spike has no ^{234}U and the uraninite no ^{236}U or ^{229}Th. Thus the spike $^{229}Th/^{236}U$ ratio can be calculated from the $^{230}Th/^{229}Th$ ratio and the $^{234}U/^{236}U$ ratio of the mixture thus:

$$\text{Spike } {}^{229}Th/{}^{236}U = {}^{234}U/{}^{236}U \times {}^{230}Th/{}^{234}U + {}^{230}Th/{}^{229}Th$$

25/7/88: ~0.8 g WL96 spike was mixed with ~0.35 g uraninite solution and the isotopic ratios measured.

Results: (raw data are presented in the appendix)

A. Isotopic activity ratios:

Sample	$^{234}U/^{238}U$	$^{229}Th/^{236}U$
S	1.0002	
T	0.9979	0.4620
U	1.0010	
6	1.0008	0.4524
7	0.9995	0.4476
8	1.0040	0.4500
G	1.0040	
H	0.9984	0.4515
J	1.0000	0.4506
L	1.0022	0.4505
P	1.0022	0.4530

1st. Average and 2σ:
$^{234}U/^{238}U$: 1.0011 ± 0.0042 Range: 0.9969 - 1.0053

$^{229}Th/^{236}U$: 0.4522 ± 0.0086 Range: 0.4436 - 0.4608
Sample T is outside the 2σ range. Sample T was rejected and the mean and sigma recalculated:

$^{229}Th/^{236}U$: 0.45079 ± 0.00356 Range: 0.44724 - 0.45436

All values are within this new range. This mean and error are used in FRACT.BAS, the dating program for use with WL96 spike.

Table 5.1 Summary of WL96 $^{229}Th/^{236}U$ ratio calibrations:

By SPEX standards:	
(1) Li (1989):	0.47993 ± 0.00147 (0.47846 - 0.48140)
(2) This study:	0.481078 ± 0.004818 (0.476262 - 0.485896)
By Uraninite:	0.45079 ± 0.00356 (0.44724 - 0.454360)

The calibration from uraninite is used in the dating program. The reasons for doing so are discussed below in the section on calibration of ST96 spike.

5.2 ST96 SPIKE

The spike in use for speleothem analysis, "ST96" (Stalagmite 229/236), was made up (by J.L.) in December 1988. Stock solutions of ^{236}U and ^{229}Th were made up separately and their concentrations measured. The spike solution was then mixed and calibrated.

5.2.1 Making up ST96:

1. The Thorium-229 stock solution: ^{229}Th was supplied by Oak Ridge National Laboratories as 10 μg ^{229}Th in 0.27 ml 0.5 N HNO_3. About 30 μl of this solution was added to 100 ml 2 N HNO_3 (distilled) using the glove box in the Health Physics department, NRB, McMaster University. The remainder is stored inside this glove box. The remainder of the 100 ml of ^{229}Th stock solution is stored in the clean lab ANB407. Its concentration is 3.42×10^{11} atoms ^{229}Th per gram. There is also a little ^{229}Th solution of unknown concentration in GS404. This was made by A. G. Latham in 1978 and was left over after he made up the Ros2 spike.

The isotopic composition of the stock solution was measured by mass spectrometry to make sure that ^{232}Th levels were low. The atomic fractions were 0.997 for ^{229}Th and 0.003 for ^{232}Th. ^{230}Th was not detectable. The solution was also tested for uranium contamination: an initial small beam at mass 238.0 burned off rapidly and no peak registered.

The concentration of the stock solution was measured on the mass spectrometer by loading a mixture of ~0.03 g solution with ~0.3 g of the 1.109 ppm SPEX Thorium standard. The concentration was 3.4×10^{11} atoms ^{229}Th per gram.

2. The Uranium-236 stock solution: The remainder of the ^{236}U stock solution made by A. G. Latham for the Ros2 spike, which had been in GS404, has been moved to the clean lab ANB407.

The isotopic composition of the stock solution was tested before mixing: the atomic fraction of ^{236}U is 0.9995, ^{238}U 0.0004, and ^{235}U not detectable. It was also

tested for thorium contamination: counts could not be distinguished from background.

The concentration of the stock solution was measured by loading 0.066 g solution with 0.1691 g of the 1.0211 ppm SPEX Uranium standard. The concentration was 2.5×10^{12} atoms ^{236}U per gram.

3. A test mix of 0.08986 g U stock and 0.07700 g Th stock solution gave an isotopic composition (expressed as atomic fractions) of:- 0.00094 of ^{238}U, 0.99898 of ^{236}U and 0.00008 of ^{235}U; 0.00333 of ^{232}Th, 0.99667 of ^{229}Th. ^{234}U and ^{230}Th were not detectable.

4. The spike mixture should contain in the order of 1.5×10^{11} atoms ^{236}U and 5×10^{10} atoms ^{229}Th per gram and have a $^{229}Th/^{236}U$ ratio of approximately 0.3. A test batch of 0.5913 g Th stock and 0.3783 g U stock made up to 5.048 g solution in 2 N HNO_3 was prepared. The concentration of U and Th was measured against the SPEX standards.

Sample	U std	Th std	Test spike
H	0.1706		1.5959
K	0.1665		1.5377
J		0.2836	1.7299
L		0.2020	1.1412

The measured ratios were corrected with the average fractionation correction factor.

Results:
U concentration (atoms ^{236}U / g): H 1.85×10^{11}, K 1.86×10^{11}
Th concentration (atoms ^{229}Th / g): J 4.06×10^{10}, L 4.05×10^{10}
229/236 ratio: 0.22

These concentrations are suitable but a little more Th might be used to balance the typical U and Th concentrations found in speleothem. The ideal balance of sample and spike ratio is discussed in the section on running samples.

5. In order to make up 500 g spike, additional ^{229}Th stock was needed. A second

stock solution was made up of ~30 μl of ^{229}Th from the original Oak Ridge supply stored in the glove box in NRB made up to ~100 ml in 2 N HNO_3. The concentration of this ^{229}Th stock was tested against the SPEX thorium standard (0.027 g Th stock and 0.291 g Th std). It was 4.53×10^{11} atoms ^{229}Th per gram.

6. Mixing the spike (30/12/1988): 60.94 g of ^{236}U stock solution was mixed with 113.96 g ^{229}Th stock solution (7.65 g of the first stock and 106.31 g of the second stock) and made up to 500 g with 2 N HNO_3. All of the second ^{229}Th stock was used; some of the first remains in the clean lab. The stock spike bottle is of Teflon to avoid problems of (i) isotope adsorption to surfaces, and (ii) disintegration of plastic in the presence of acid. The cap is well sealed with plastic film ("Clingfilm") and electrical tape to avoid evaporation of its contents. The spike is transferred to a small dropping bottle for use. This is also sealed with plastic film and kept in a plastic bag.

5.3 CALIBRATION OF ST96 SPIKE

The new spike was calibrated just as WL96 had been, by standards and by uraninite.

5.3.1 Dilution of SPEX standards:

New dilutions of SPEX standards were made up for this calibration. The standards are supplied as 1000 μg / ml in 2% HNO_3.

A solution of **1.0211334 μg / g uranium standard** was prepared by diluting 1.00904 g of the 1000 μg / ml solution in 99.51436 g 2 N HNO_3, and further diluting 5.26335 g of this in 46.47600 g acid.

A solution of **1.1090232 μg / gm thorium standard** was prepared by diluting 1.04532 g of the 1000 μg / ml solution in 96.58155 g acid, and further diluting 5.20955 g of this in 45.08715 g acid. The isotopic composition is given above under the calibration of WL96 section.

5.3.2 Isotopic composition of ST96 spike:

30/12/88: ~2 g ST96 was separated into U and Th fractions. The fractionation factor used to correct the measured ratios was 0.9941656, the average at that date.

Results: (Raw data are presented in the appendix)

A. Isotopic ratios

Sample	$^{235}U/^{236}U$	$^{238}U/^{236}U$	$^{229}Th/^{232}Th$
1			1094.250
2	8.669×10^{-5}	3.658×10^{-4}	
3	8.375×10^{-5}	2.634×10^{-4}	1165.928
5			1131.980
6	8.550×10^{-5}	2.787×10^{-4}	1076.477
Average and $2\sigma_m$:			
	8.532×10^{-5}	3.026×10^{-4}	1117.159
	0.170×10^{-5}	0.638×10^{-4}	39.908

B. Isotopic fractions: ^{235}U barely detectable (<0.01%), ^{230}Th not distinguishable from background at 229 counts of 20000.

Sample	^{235}U	^{236}U	^{238}U	^{229}Th	^{232}Th
1				0.99909	9.130×10^{-4}
2	8.665×10^{-5}	0.99955	3.656×10^{-4}		
3	8.372×10^{-5}	0.99965	2.633×10^{-4}	0.99914	8.570×10^{-4}
5				0.99912	8.826×10^{-4}
6	8.547×10^{-5}	0.99964	2.786×10^{-4}	0.99907	9.281×10^{-4}
Average and $2\sigma_m$:					
	8.528×10^{-5}	0.99961	3.025×10^{-4}	0.99911	8.952×10^{-4}
	0.180×10^{-5}	0.00006	6.371×10^{-5}	0.00003	0.327×10^{-4}

These values are used in AGE.BAS, the dating program for use with ST96 spike.

5.3.3 Calibration of ST96 by SPEX U and Th standards:

U or Th standard is added to spike, dried, loaded and analyzed. The ratios can be corrected in two ways: (i) by assuming the average fractionation factor to date (.9941656) or (ii) by using the iterative procedure in the BASIC program ST96UCON.BAS (see appendix) which optimises the fractionation correction. Both corrections are presented but the differences are minor.

30/12/88: ~0.3 g U standard was added to ~1 g ST96 and ~0.4 g Th standard to ~1 g ST96 in order to measure the concentrations of U and Th in the spike.

Results: (Raw data are presented in the appendix)

Average of 3 samples and 2σ:
(i) Corrected with the average fractionation factor of .9941656:
Atoms ^{236}U / g: $3.5338 \times 10^{11} \pm 0.00328 \times 10^{11}$
(ii) Corrected by iterative procedure:
Atoms ^{236}U / g: $3.5388 \times 10^{11} \pm 0.00687 \times 10^{11}$

Atoms ^{229}Th / g: $1.0209 \times 10^{11} \pm 0.01059 \times 10^{11}$

Average $^{229}Th/^{236}U$ ratio and $2\sigma_m$[10]: .288693 ± .001016

5.3.4 Calibration of ST96 by old uraninite:

The uraninite is termed "old" from here on to distinguish it from the recently acquired, new uraninite, Ros89.

30/12/88: ~0.5 g uraninite solution and ~0.3 g ST96 spike were mixed, separated into U and Th fractions and their isotopic ratios measured.

Results: (Raw data presented in appendix)

Isotopic activity ratios:

Sample	$^{234}U/^{238}U$	$^{229}Th/^{236}U$
14	1.0026	0.2781
15	1.0016	0.2768
16	0.9975	0.2759
SU4	0.9963	0.2719
SU5	1.0016	
SU6	1.0004	0.2734
J	0.9968	0.2724
K	0.9991	0.2738

Average $^{234}U/^{238}U$, $2\sigma_m$ and 2σ range:
0.9997 ± 0.00177 (0.9950 - 1.0044)

Average $^{229}Th/^{236}U$, $2\sigma_m$ and 2σ range:
0.274633 ± 0.001766 (0.2700 - 0.2791)

---

[10] Standard deviation (σ) measures variability in a population or the spread of a distribution around its mean. Standard error (σ_m) measures how far from the 'true' mean the sample mean is likely to be. Thus, in this case standard error is preferable to standard deviation.

Table 5.2: Summary of first ST96 $^{229}Th/^{236}U$ ratio calibrations:

Average, $2\sigma_m$ and 2σ range:	
By SPEX standards:	0.288693 ± 0.001016 (0.284434 - 0.292952)
By Uraninite:	0.274633 ± 0.001766 (0.269605 - 0.279661)

5.4 EFFECT OF SPIKE CALIBRATION ON AGE

The choice of spike calibration makes a significant difference in the age calculation: if a sample is dated using the two spike calibrations then the derived estimates of age are not within a 2σ error margin (which is typically ~1.5%).

Example:			
Spike $^{229}Th/^{236}U$ ratio:	0.2887	Age:	209,168 y ± 3,000
Spike $^{229}Th/^{236}U$ ratio:	0.2746	Age:	185,617 y ± 3,000
Difference: 23,551 y	(11.3%)		

5.4.1 Which method is preferable?:

The discrepancy between the $^{229}Th/^{236}U$ spike ratios obtained by calibration against SPEX standards and against uraninite gives cause for concern. Three possible explanations come to mind: (i) the uraninite may have experienced isotope migration before it was collected, (ii) the uraninite solution may have experienced some loss of thorium through plating out on the container walls during the years of storage, (iii) the standards may have been incorrectly calibrated or diluted.

(i) The uraninite calibration stands on the assumption that no migration of daughter products has occurred in the deposit since its formation. This uraninite has been in use to calibrate spikes in the alpha counting lab since the '70s. It was originally supplied in solid form by John Rosholt (formerly of the United States Geological Survey). The source of this uraninite is not recorded. It was tested for secular equilibrium by Pb/U ratio measurement. The $^{207}Pb/^{235}U$ ratio and $^{206}Pb/^{238}U$ ratios were concordant so it was assumed that there had been no loss of intermediate daughter products.

If migration of daughter products occurs then the most soluble of the isotopes is the most likely to migrate. Uranium is more soluble under most conditions than thorium and ^{234}U is more soluble than ^{238}U. Thus, isotope migration is most likely to be expressed as a change in ^{234}U: the $^{234}U/^{238}U$ activity ratio would no longer be 1.00. On the mass spectrometer this measurement is affected by the fractionation and mass discrimination correction. All the $^{235}U/^{238}U$ measurements on the uraninite indicated that it did not differ significantly from the normal 0.0072526. The U ratios were corrected using 0.0072526 as the normalizing ratio. All the $^{234}U/^{238}U$ ratios are close to 1.00: the average of 20 analyses is 1.0004 ± 0.0010. Further, numerous α-counts on this uraninite over the last two decades have invariably shown ratios of unity. Alpha counting avoids any problems with mass discrimination and fractionation correction. These figures strongly suggest that U isotope migration has not occurred and it is therefore highly unlikely that Th isotopes have migrated.

(ii) The possibility that some of the thorium in solution may have plated out on the container walls must always be borne in mind. However, alpha counting spectrometric calibration of spike continues to give the same results as in the '70s. This suggests that no plating out has occurred. If the uraninite were depleted in ^{230}Th then the $^{230}Th/^{234}U$ ratio would be lower than 1.00 and the use of the value of 1.00 in the calculations would give a falsely high spike $^{229}Th/^{236}U$ ratio. The calibration with standards should give a lower $^{229}Th/^{236}U$ ratio. The one done by Li (1989) is lower but mine is not.

(iii) The standards may have evaporated slightly since preparation so that the concentration is higher now than it was when first measured. Measurement of the spike concentration against the standards would then give too low a value. The effect on the $^{229}Th/^{236}U$ ratio would depend on which standard had changed the most.

There were no clear reasons why the calibrations differed and no clear indication of which was the more correct while WL96 was being used for analysis

of DWBAH. At that time the uraninite calibration was accepted for the following reasons:

(i) All alpha counting dating laboratories use uraninite to calibrate spike, and

(ii) Calibration by standards depends on prior calibration of the isotopic composition of the standards by mass spectrometry which in turn depends on the fractionation correction factor. Because no information is available on the isotopic ratios of these standards no normalizing ratio is available (the $^{235}U/^{238}U$ ratio is not normal). The correction has to use the average fractionation factor from analyses of samples of normal $^{235}U/^{238}U$ ratio. Uraninite, on the other hand, has a normal $^{235}U/^{238}U$ ratio so that fractionation during each run can be corrected accurately. (This would affect the U calibration only. The Th ratios of the standard cannot be measured because it contains no ^{230}Th.)

In view of the discrepancies between the methods of calibration ST96 was again calibrated against (i) uranium and thorium standards from a different source, and (ii) a freshly supplied and dissolved sample of the Harwell Uraninite from J. Rosholt of the USGS. Full details of these calibrations are given below.

5.5 FURTHER CALIBRATION OF ST96 SPIKE

5.5.1 Calibration of ST96 by AESAR U and Th standards:

AESAR standards are supplied by Johnson Matthey (AESAR group).

Uranium standard: 1.0022 g of 1000 μg / ml standard was made up to 100.9388 g with 2 N HNO_3.
10.5835 g of this solution was made up to 109.7617 g with 2 N HNO_3. This gave a standard of 0.9574 ppm U.

Thorium standard: 0.9941 g of 1000 μg / ml standard was made up to 100.7970 g with 2 N HNO_3.
10.5835 g of this solution was made up to 102.2116 g with 2 N HNO^3. This gave a standard of 1.0212 ppm thorium.

20/9/89: ~0.3 g U standard was mixed with ~0.8 g ST96 spike, and ~0.4 g Th standard with ~0.8 g spike. The isotopic ratios were measured in order to calculate the concentrations of U and Th in the spike.

Results: (Raw data are presented in the appendix)

Average, $2\sigma_m$:
U conc. (atoms ^{236}U / g): $3.646 \times 10^{11} \pm 0.00156 \times 10^{11}$
Th conc. (atoms ^{229}Th / g): $1.006 \times 10^{11} \pm 0.00285 \times 10^{11}$

$^{229}Th/^{236}U$ ratio, $2\sigma_m$ and 2σ range:
0.27587 ± 0.00079 (0.27449 - 0.27724)

5.5.2 Calibration of ST96 by new uraninite (ROS89):

The new Harwell Uraninite was supplied by Rosholt as a powder. I have called it "Ros89". It was taken from the glass vial in 7 N HNO_3 and 6 N HCl, dried and put through the complete HF dissolution treatment to make sure that the whole sample went into solution:-

1. Sample + ~5 ml HF in bomb, tightly closed, placed inside jacket, left in oven at moderate setting for 48 hours.
2. Evaporated on hot plate with no glass chimneys. At final 0.5 ml added a few drops conc. HNO_3. Dried.
3. Added ~5 ml conc. HNO_3. Dried.
4. Added ~ 5ml 6 N HCl, closed bomb, placed in jacket in oven for 24 hours.
5. Dried. Then brought up in ~20 ml 7 N HNO_3 ready for use. This is called DILUTION A.

The concentration of Dilution A was 109 ppm U and 11.3 ppm Th.

DILUTION B: 3.339 g of Dilution A was made up to 30 g with MilliQ. It was used for a test calibration of ST96. ~0.3 g of Ros89 Dilution B was mixed with ~0.3 g ST96 and the isotopic ratios measured. Because the $^{235}U/^{238}U$ ratio of uraninite is normal, 0.0072526 was used as a normalizing ratio.

Results: (Raw data are presented in the appendix, A5.2, Samples P, Q and R.)

U conc.: 13.9 ppm
Th conc.: 1.245 ppb

At ~14 ppm U this dilution is still far too concentrated. It should be about 3 ppm so that an accurately weighable quantity (~.5 g) can be used in calibration tests. Samples P, Q and R were too large so that the side filament current did not get

high enough for consistent ionization of uranium. It was also appreciated later that acid should have been used rather than MilliQ in the preparation of Dilution B. A new dilution was prepared from the stock, Dilution A.

DILUTION C: 1.1 g of Dilution A was brought up to 50 .6 g in 2 N HNO_3. This was used to calibrate ST96. ~0.8 g Ros89, Dilution C, was mixed with ~0.3 g ST96. These were dried but not separated chemically and loaded onto separate beads, one third onto the uranium bead and two thirds onto the thorium bead.

Results:

Sample	$^{234}U/^{238}U$ Activity ratio	$^{229}Th/^{236}U$ Atomic ratio
P	0.98072	0.27052
Q	0.99376	0.27444
R	0.99658	0.27620
R3J	0.99658	
R3K	0.99887	0.27720
R3L	0.99899	0.27710
R3M	0.99901	0.27665
R3N	1.00875	0.27873
R3P	1.00533	0.27710

Average $^{234}U/^{238}U$ activity ratio, $2\sigma_m$ and 2σ range:
0.99758 ± 0.00310 (0.98829 - 1.00687)

Average $^{229}Th/^{236}U$ atomic ratio, $2\sigma_m$ and 2σ range:
0.275993 ± 0.001778 (0.27097 - 0.28102)

Table 5.3: Summary of ST96 $^{229}Th/^{236}U$ ratio calibrations:

Average, $2\sigma_m$ and range
(a) By SPEX standards: 0.288693 ± 0.001016 (0.287677 - 0.289709)
(b) By Old Uraninite: 0.274633 ± 0.001766 (0.272867 - 0.276399)

(c) By AESAR standards: 0.27587 ± 0.0008 (.275076 - .276658)
(d) By Ros89 Uraninite: 0.27599 ± 0.00178 (.274215 - .277771)

Grand Mean of (b), (c) and (d) and $2\sigma_m$:
0.275497 ± 0.000867

5.6 DISCUSSION

ST96 has now been calibrated in four ways: three of these (the old uraninite, the new Ros89 uraninite and the AESAR standards) give the same $^{229}Th/^{236}U$ spike

ratio within $2\sigma_m$; the 95% confidence intervals for the estimates of all three means overlap. The calibration by SPEX standards is clearly outside the range of the other calibrations. The conclusion is that the SPEX standards calibrations are not accurate and the use of the uraninite calibration for WL96 was justified. The calibration adopted for ST96 is the grand mean of the old uraninite, the AESAR standards and the Ros89 uraninite calibrations.

Chapter 6

URANIUM AND THORIUM STANDARDS

Uranium isotopic standards are available as a test for accuracy of uranium measurements and correction procedure. (i) "Natural Uranium" from C. E. Reese (late of Dept. of Geology, McMaster University) has a $^{235}U/^{238}U$ ratio of 0.0072526. This was analyzed in order to establish the fractionation correction for U runs. (ii) NBS 005a, a National Bureau of Standards Uranium isotopic standard was then analyzed using the average correction factor.

No thorium isotopic standard is available because no suitable long-lived isotope exists other than ^{232}Th. "Natural Thorium" from Reese contains some ^{230}Th as well as ^{232}Th but the ratios are not known. An attempt was made to establish the isotopic ratio by alpha counting but the low precision of the results offers no test for mass spectrometry. The only test for thorium ratio measurements and correction procedure is to date a well dated speleothem standard. 76001 McMaster standard speleothem was used.

6.1 "NATURAL URANIUM"

This standard has a normal $^{235}U/^{238}U$ ratio of .0072526. Uranium ratios of the pure standard were measured on the mass spectrometer. The fractionation and mass discrimination correction required to correct the measured $^{235}U/^{238}U$ ratio to 0.0072526 was calculated. Then the correction factors for many analyses were averaged. This provided a correction factor for samples which do not have the normal $^{235}U/^{238}U$ ratio and thus cannot be corrected using a normalizing ratio.

Results:

Sample	Measured 235/238	Correction Factor
B5U	.007351	0.9866
1NAT	.007351	0.9866
NAT	.007335	0.9888
UNAT1	.007360	0.9854
UNAT2	.007375	0.9834
B13NAT	.007362	0.9851

Average correction factor for $^{235}U/^{238}U$: 0.9860
Correction factor per mass unit: 0.9953
The average correction factor per mass unit from all analyses of natural uranium done at McMaster was 0.993616.

6.2 NBS 005a

This is a National Bureau of Standards uranium isotopic standard. The procedure for U analysis of this standard includes the NBS published $^{235}U/^{238}U$ ratio (.00509) as the normalization ratio.

1/11/88: ~1 g of standard was mixed with ~1 g WL96 spike and the isotopic ratios measured.

Certified ratios (NBS)	$^{235}U/^{238}U$	$^{234}U/^{238}U$
	0.00509	$3.417 \pm 0.070 \times 10^{-5}$

Results: (Raw data are presented in the appendix)

Sample	Measured $^{235}U/^{238}U$	Corrected $^{234}U/^{238}U$	U conc ppm
M	0.0051970	3.414×10^{-5}	2.2833
N	0.0051835	3.418×10^{-5}	2.2759
O	0.0051869	3.416×10^{-5}	2.2856
Average:		3.416×10^{-5}	2.2816
2σ:		0.004×10^{-5}	0.0101

The values for $^{234}U/^{238}U$ atomic ratio are within the 2σ error of the NBS values. The results of these analyses of uranium standards indicate that the uranium runs and the correction procedure are reliable.

6.3 NATURAL THORIUM STANDARD

The isotopic composition of this standard is not precisely known. It was measured by alpha counting but the uncertainties are high (see account below). Therefore the mass spectrometric runs serve only as a test of the reproducibility of thorium runs. The ratios were corrected with the mass discrimination factor $\sqrt{(m_1/m_2)}$.

2/8/87 Note: Run as ThO^+ ions m/e = 146, 148.

Sample	Measured 146/148	Corrected 146/148
XThNat	7.70×10^{-5}	7.65×10^{-5}
1ThNat	7.66×10^{-5}	7.61×10^{-5}
5ThNat	7.35×10^{-5}	7.30×10^{-5}

8/5/88 Run as Th^+ ions.

Sample	Measured $^{230}Th/^{232}Th$	Corrected $^{230}Th/^{232}Th$
ThNAT3	7.506×10^{-5}	7.473×10^{-5}
ThNAT2	7.425×10^{-5}	7.393×10^{-5}

Average $^{230}Th/^{232}Th$ and 2σ range:
This study, 5 runs: 7.528×10^{-5} (7.229×10^{-5} to 7.828×10^{-5})
Li (1989), 20 runs: 7.557×10^{-5} (7.497×10^{-5} to 7.617×10^{-5}).

Calibration by alpha counting:

An aliquot of the standard was counted for 14 days in the McMaster alpha counting lab. This count time is longer than usual in an attempt to improve counting statistics. However, over such a long time the tail from the ^{230}Th peak contributes significantly to the ^{232}Th peak. The counts were corrected as follows:

(a) Background was measured before the ^{232}Th peak and after the ^{230}Th peak (before the ^{228}Th tail begins). Average background count was 16.9 (per channel) with a relative error of 0.041%.

(b) All the counts were corrected for background.

(c) An exponential equation was fitted to the ^{230}Th tail:

$$y = 0.017\ e^{(0.156719\ x)}$$

where y is [count minus 17] and x is [channel minus 109].

(d) The tail was extrapolated back under the ^{232}Th peak.

(e) The ^{232}Th counts were corrected for the ^{230}Th tail.

(f) The activity ratio is the ratio of the corrected count for each peak. The standard deviation is the square root of the count; the relative error is the standard deviation divided by the count. The error from each is propagated to give the final error of the ratio.

Isotope	Total count	2σ	Rel. Error
^{232}Th	8374.3	183	.0218
^{230}Th	119339	691	.0058

$^{230}Th/^{232}Th$ Activity Ratio: 14.251
Atomic Ratio: $7.71x10^{-5}$ ($7.53x10^{-5}$ - $7.89x10^{-5}$)

$^{230}Th/^{232}Th$ atomic ratio measured on the mass spectrometer:

This study: $7.528x10^{-5}$ ($7.229x10^{-5}$ - $7.828x10^{-5}$)
Li (1898): $7.557x10^{-5}$ ($7.497x10^{-5}$ - $7.617x10^{-5}$).

The mass spectrometric results from this study are just within the 2σ range of the alpha counted figures. The mass spectrometric figures are likely to be the more correct in view of the lack of precision of the alpha counted figures and the tail correction procedure.

6.4 SPELEOTHEM STANDARDS

6.4.1 JC1:

This was prepared from a sample of Jewel Cave wall crust as practice material. The sample was ground with a steel pestle and mortar and then passed through a fine sieve to ensure a relatively homogeneous grain size. Afterwards it was shaken and stirred well to homogenize the grains.

Two samples (from the intact flowstone before homogenization) were dated by alpha counting.

	Top	Base
U conc. ppm	0.358 ± 0.007	0.447 ± 0.007
Th conc.ppb	7 ± 2	7 ± 2
$^{234}U/^{238}U$	0.922 ± 0.046	1.001 ± 0.032
$^{230}Th/^{234}U$	1.085 ± 0.060	1.001 ± 0.068
$^{230}Th/^{232}Th$	158.7 ± 107.8	185.9 ± 104.4
Age (y)	>350,000	263,500 +59,600 -46,800

Samples of JC1 were dissolved, spiked, purified, separated into U and Th fractions and analyzed by mass spectrometry.

The mass spectrometrically measured $^{230}Th/^{234}U$ and $^{234}U/^{238}U$ ratios are within the 2σ range of alpha counted ratios. Mass spectrometry always returns higher

$^{230}Th/^{232}Th$ ratios than alpha counting (also observed by Edwards 1988). Perhaps the low activity of ^{232}Th reduces the sensitivity of alpha counters to this isotope.

25/7/88: ~1.3 g JC1 sample was mixed with ~0.8 g WL96 spike; Samples A and B were processed with anion exchange columns only. Samples H, J and K were processed by $FeCl_3$ co-precipitation.

Results: (Raw data are presented in the appendix)

Sample	$^{234}U/^{238}U$ Activity	$^{230}Th/^{234}U$ Activity	$^{230}Th/^{232}Th$ Activity	Age years	U ppm	Th ppb
JC1A	1.0067	0.9781	1616	403,125	0.759	0.952
JC1B	1.0067	0.9643	1776	356,250	0.744	0.759
JC1J	1.0054				0.741	
JC1K	1.0112	0.9898	1984	459,375	0.763	0.753
JC1H	1.0186	0.9887	1416	431,250	0.768	1.474
Mean:	1.0098	0.9802	1698	412,500	0.755	0.985
2σ:	0.0109	0.0237	482	87,945	0.024	0.678

6.4.2 76001 McMaster speleothem standard:

This standard was made up by Thompson in the early '70s and re-homogenized by Gascoyne in 1982. It has been used as the standard in the alpha counting lab at McMaster and as one of the standards in the interlaboratory tests reported in Harmon et al (1979). The data for alpha counting comes from Gascoyne (1979) and the McMaster alpha counting laboratory records.

1/11/88: ~1.3 g 76001 standard was mixed with ~0.8 g WL96 spike. Samples C and D were processed using only anion exchange columns. Samples E, F and G used $FeCl_3$ co-precipitation.

16/4/89: ~1.5 g 76001 standard was mixed with ~0.2 g ST96 spike and processed with columns only.

Results from analyses using WL96 spike:

Sample	Age	2σ range	$^{230}Th/^{234}U$ Activity	$^{234}U/^{238}U$ Activity	U ppm	Th ppb
C	45,411	44,093-46,803	0.3518	1.925	0.781	7.45
D	42,335	41,236-43,507	0.3317	1.921	0.783	7.10
E	47,315	45,923-48,780	0.3638	1.918	0.795	8.26
F	48,927	46,657-51,271	0.3739	1.923	0.792	8.14
G	48,634	47,609-49,586	0.3719	1.920	0.792	8.30

Mean age from 5 runs: 46,524 ± 5,444 (41,080 - 51,968)

Results from analyses using ST96 spike:

Sample	Age	2σ range	$^{230}Th/^{234}U$ Activity	$^{234}U/^{238}U$ Activity	U ppm	Th ppb
X	47,120	46,387-47,858	0.3625	1.910	0.779	7.764
Z	46,226	44,888-47,579	0.3568	1.926	0.779	8.057

Mean of 7 runs, 2σ and range: 46,567 ± 4,477 (42,090 - 51,044)

Mean of 16 runs, 2σ and range (including data from Li 1989[11]):
46,813 ± 4,111 (42,702 - 50,923)

Two values are outside the 2σ range. If these are rejected and the mean recalculated the results are:

Mean of 14 runs, 2σ and range: 47,447 ± 2,372 (45,075 - 49,819)
$2\sigma_m$ and range: 634 (46,813 - 48,081)

Data from alpha counting:-
Mean age from 36 runs: 47,480 ± 6,720 (40,760 - 54,200)
Mean age from 33 runs (omitting extreme values):
47,760 ± 4,480 (43,280 - 52,240)
$2\sigma_m$ and range: 780 (46,980 - 48,540)

The $2\sigma_m$ range (95% confidence interval for the location of the mean) of the mass spectrometry results is virtually coincident with that of the alpha counted results. The conclusion is that thorium ratio measurement by mass spectrometry is accurate. (This conclusion is, of course, circumscribed by the assumption that alpha spectrometry is not subject to bias.)

The early tests, with WL96 spike, show greater variability than the later ones with ST96 spike. This relates to the properties of the spike (in addition to variation

---

[11] The data from Li (1989) were recalculated from his raw data using the spike calibration with uraninite. The ages shown in his thesis (Li 1989), with a mean of 51.98 kyr, were calculated using the SPEX standard calibration which I have since shown to be incorrect.

Data from Li recalculated with the uraninite WL96 calibration:-
Individual dates from 9 analyses:
46,436 48,047 47,754 47,957 45,557 42,408
47,315 48,926 48,633

Average, 2σ and range: 47,004 ± 4,034 (42,970 - 51,037)
$2\sigma_m$ and range: 1,345 (45,660 - 48,348)

in the chemical procedures). WL96 will always give a higher error than ST96 because (i) it has not been calibrated as rigorously and (ii) the high levels of ^{230}Th contribute significantly to the total ^{230}Th count.

The early 76001 analyses used either the normal column chemistry for sample preparation or the $Fe(OH)_3$ co-precipitation method with the relatively impure ferric chloride. This has since been shown to contribute high levels of contamination. The samples prepared with the normal 98.2% purity $FeCl_3$ (samples E, F and G) gave higher U and Th concentrations, $^{234}U/^{238}U$ activity ratios and thus higher ages than the samples prepared with columns only. For this comparison with the alpha counted results it is very important to note that the alpha counted samples are also prepared with this impure Ferric Chloride and therefore the dates can be expected to be slightly older than the ages actually are. Future analyses of 76001 by mass spectrometry, after preparation with columns only or with high purity $FeCl_3$, may bring the average somewhat below the alpha counted average.

Chapter 7

USING MASS SPECTROMETRIC DATING TO ELUCIDATE LATE PLEISTOCENE SEA LEVEL CHANGE IN THE BAHAMAS

Pleistocene sea level fluctuated in response to continental glaciation, which in turn fluctuated in response to climatic changes. The oxygen isotopic composition of foraminifera in deep sea cores reflects the isotopic variations of ocean water. These are predominantly caused by variations in the ocean volume as a result of the storage of fresh water on land as ice during the glaciations. The changes in foraminiferal isotopic composition should therefore mirror sea level change. However, the ocean cores are not well dated for the late Pleistocene. On the assumption that climatic change is directly linked to the orbital geometry of the earth (see Berger et al 1984), Imbrie et al (1984) published a curve of the oxygen isotopic variations of ocean foraminifera fitted to an orbitally tuned timescale. A shorter curve of higher resolution was then published by Martinson et al (1987). An independently and accurately dated sea level curve would provide a test for the orbital theory of climatic change.

The timing and elevation of high sea stands over the last 300,000 years can be obtained by dating now emergent fossil coral reefs (see Veeh and Chappell 1970, for example). Submerged speleothem can provide information on timing and position of low sea stands. Speleothem are deposited only in air-filled caves, so their presence in a now drowned cave indicates a former low sea stand. If sea level rises again deposition ceases, and some solution or bioerosion of the speleothem may occur. On subsequent sea level fall calcite deposition resumes on top of the hiatus. Dates on the layers immediately below and above the hiatus give limits on the timing of the high sea stand. Alpha-spectrometric studies have shown how dates on drowned speleothem can set limits on times of high sea stands on Bermuda and the Bahamas (Harmon et al 1978, Gascoyne et al 1979, Harmon et al 1981 and Harmon et al 1983). Mass spectrometric dating promises to provide a much more precise record.

7.1 DWBAH: LUCAYAN CAVERNS, GRAND BAHAMA ISLAND

DWBAH is a flowstone collected by the very experienced cave diver, Dennis Williams, from 15m below modern sea level[12] in Lucayan Caverns, Grand Bahama Island (Figure 7.1). This long, narrow island (about 10 km wide) is made up of carbonate eolianite in which are carved numerous caverns. As in all oceanic islands, a lens of freshwater overlies the salt water (see Back et al, 1984). As sea level varied the depth of the fresh water lens under the Lucayan Caverns region varied and for much of the last 300,000 years the cave was air filled. While it was above water level calcite flowstone was deposited over large areas of the cave floor. While it was fresh- or salt-water filled, deposition stopped and some erosion of the calcite layers occurred.

DWBAH represents several phases of drainage and inundation. Williams describes it as typical of the flowstone deposits which are abundant in submerged caves of the islands of the Bahama Banks. The sample has two clearly defined hiatuses (Hiatuses 2 and 3 on Figure 7.3) separating three layers of clean, white calcite. This "Pattern of three" periods of deposition is common in Bahamian caves to depths of 20 m; deeper than that the patterns become more complex (Williams 1988, pers. comm.). No samples from the deeper levels are available as yet.

Alpha spectrometric dating of DWBAH confirmed that the hiatuses represent periods of high sea level during interglacials, but the very low uranium levels resulted in dates of low precision and reproducibility. This sample was chosen for the first test of the mass spectrometric dating technique because: (i) the potential information about eustatic sea level change in the Late Pleistocene gave it great significance as a contribution to the current debate over the timing of sea level events and climatic change, (ii) the large amount of sample would allow for many trials if necessary, (iii) the calcite was clearly not re-crystallised and very clean so that problems of detrital thorium were unlikely to be encountered (except close to

---

[12] Depth was measured on commercial diving gauges accurate to ± 0.75m (Williams, pers. comm.).

the hiatuses), (iv) it had already been dated by alpha spectrometry so that mass spectrometric results could be compared. The low uranium levels, approximately 0.15 ppm, served as an additional test of the method.

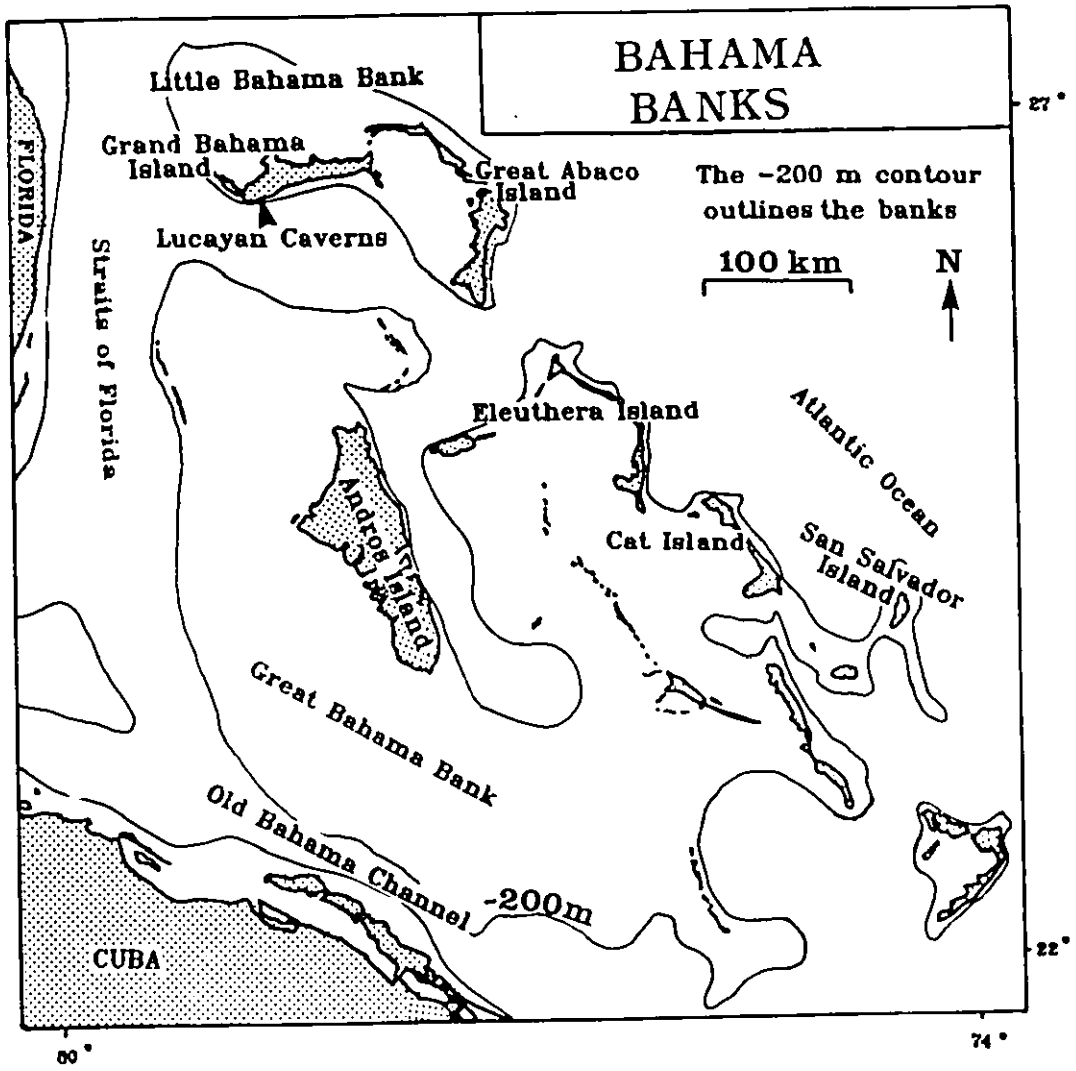

Figure 7.1: LOCATION MAP FOR DWBAH. DWBAH was collected from -15 m beneath modern sea level in the drowned Lucayan Caverns, Grand Bahama Island, Little Bahama Bank.

Figure 7.2: PHOTOGRAPHS OF DWBAH FLOWSTONE. The top photograph shows the complete sequence from the substrate of marine encrustations up to the modern erosional surface. The "Pattern of three" growth layers is clearly visible, separated by mud-lined hiatuses. Here, the thin layers of flowstone between hiatuses 1 and 2, and 3 and 4, are not apparent. The two mud-lined hiatuses, 3 and 4, are clearly demonstrated in the lower photograph. This piece had broken off at Hiatus 2, the mud-stained underside of which is visible. The faint horizontal line just above Hiatus 2 is not continuous and it is not mud-lined. It is not given the status of a true hiatus and is marked only as a "delineation". These pieces are illustrated in diagrammatic form in Figure 7.3.

PIECE 2

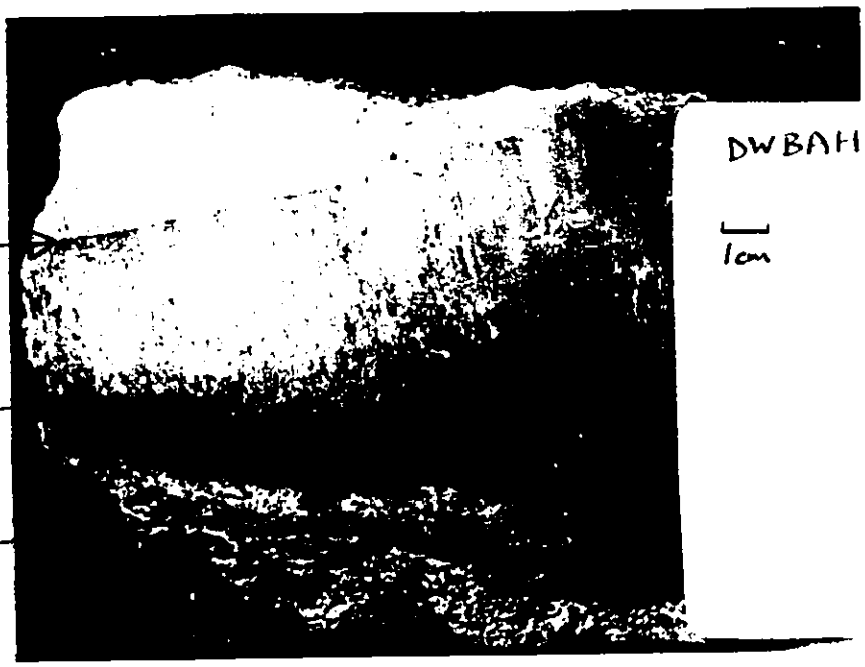

PIECE 1

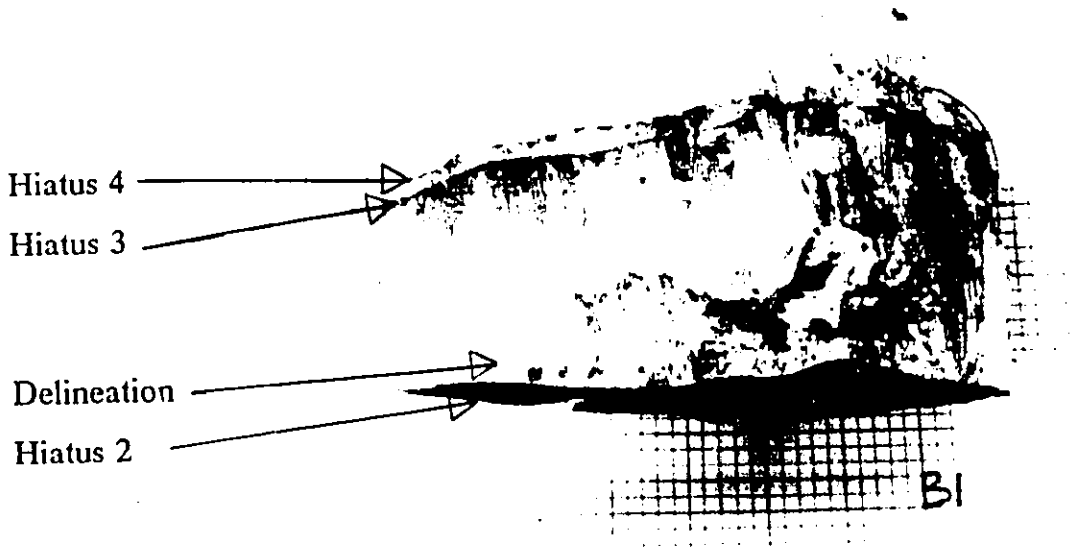

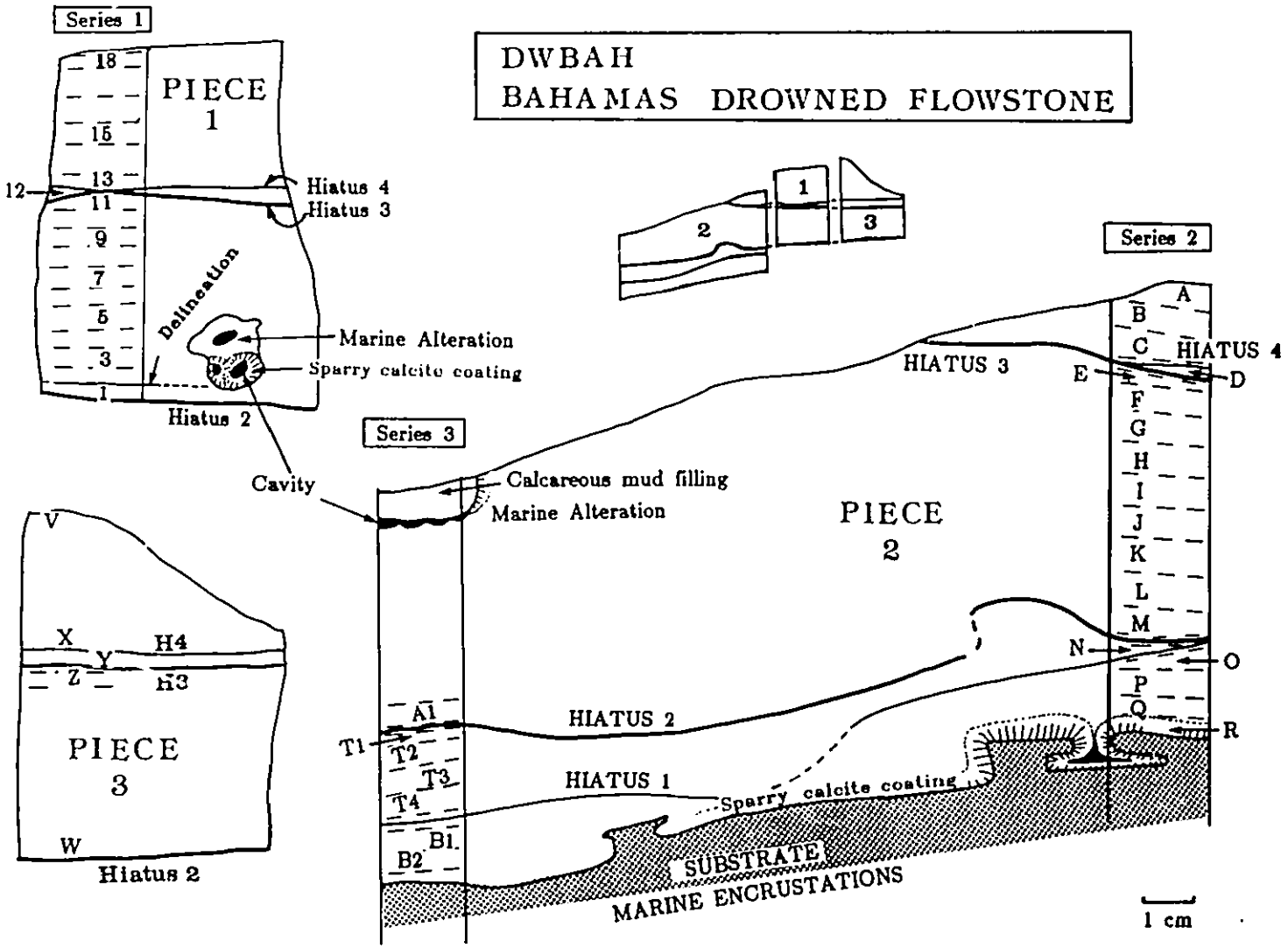

Figure 7.3: DWBAH: SAMPLE FEATURES AND SAMPLING DIAGRAM. This figure is fully discussed in the text.

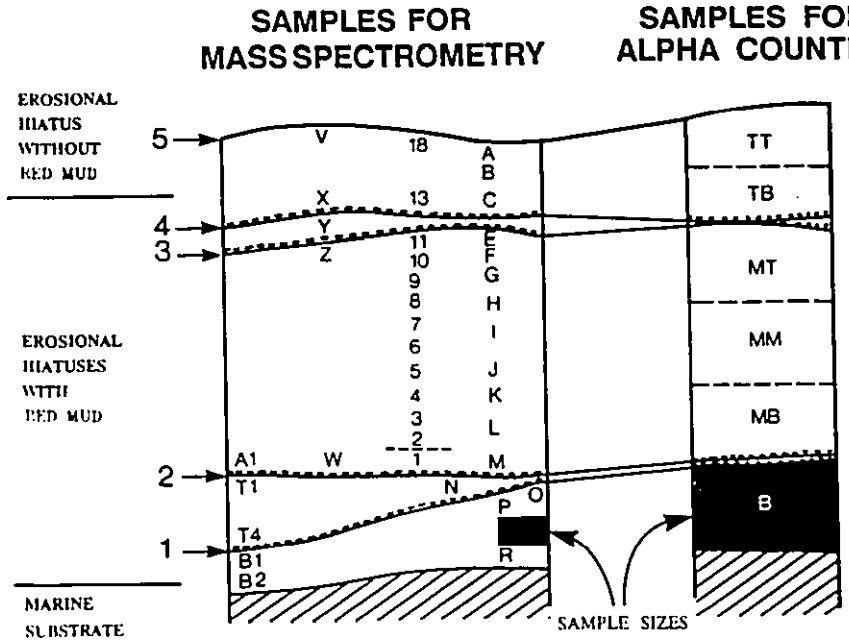

Figure 7.4: SIMPLIFIED SAMPLING DIAGRAM FOR DWBAH. The bold, dotted lines show the four erosional hiatuses with red mud. The uppermost erosional surface has no mud; sea level remains above it. The discontinuous delineation between samples 1 and 2 is shown as a short dashed line. Shaded areas compare sample sizes for the two dating methods. Samples required for alpha counting, on the right, are larger and thus fewer than those for mass spectrometry, on the left.

7.1.1 Sample description:

The specimen was supplied in several pieces representing the same stratigraphic sequence, three of which were sampled (pieces 1, 2 and 3). Figures 7.2 and 7.3 show the flowstone features and sample locations. Figure 7.4 presents a simplified diagrammatic version to allow for easier comparison of samples. It also shows the sample location for the alpha counted dates and the size of sample required for mass spectrometry in comparison to that needed for alpha counting.

DWBAH shows three prominent, and two lesser, growth layers of generally simple planar form. These lie above a substrate of marine encrustations deposited on the floor of the cave, mainly vermetid worm tubes and calcite sand grains. The

first calcite layer, of clear dogtooth spar, coats the encrustations, filling in depressions and cavities (shown as "sparry calcite coating" on Figure 7.3). Subsequent deposition is of typical speleothem calcite: clear to whitish, columnar (or "length fast") crystals with some horizons of fluid inclusions indicating growth lines. Each layer of flowstone is terminated by an erosional hiatus which cuts across growth layers, and, in some areas, cuts down to the previous hiatus or underlying flowstone layers. These hiatuses are taken to represent periods of flooding of the cave at times of high sea level (see discussion of evidence below).

Each of the hiatuses is clearly defined. However, there is an additional delineation just above hiatus 2, visible only in Piece 1, between samples 1 and 2. This is apparent in the lower photograph of Figure 7.2. It is a horizontal line which appears to represent a break in deposition at this point. It is not continuous throughout Piece 1 and is not apparent in the other pieces. It has not been given the status of an hiatus.

Upon each hiatus, except the final one, is a thin layer of yellow to red coloured mud. The hiatuses clearly separate the sample into layers. In addition, an occasional very faint and discontinuous "streak" of red-brown colour marks some of the growth lines within the zones of continuous growth. These stains probably do not indicate water levels. They occur close to some projection which was coated with older mud and represent redeposition of older mud from an exposed surface.

7.1.2 Analysis of hiatus mud:

Qualitative chemical analysis by surface X-ray fluorescence scan of the hiatus surface (by J. Hudak, Materials Research Laboratory, McMaster University) showed that, in addition to calcium, it consists primarily of iron with a very small components of aluminium, silicon, sulphur and phosphorus. Quantitative analysis by neutron activation (kindly provided by Dr. B. Blackwell, Dept. of Geology, McMaster University) of two samples gave the following results:

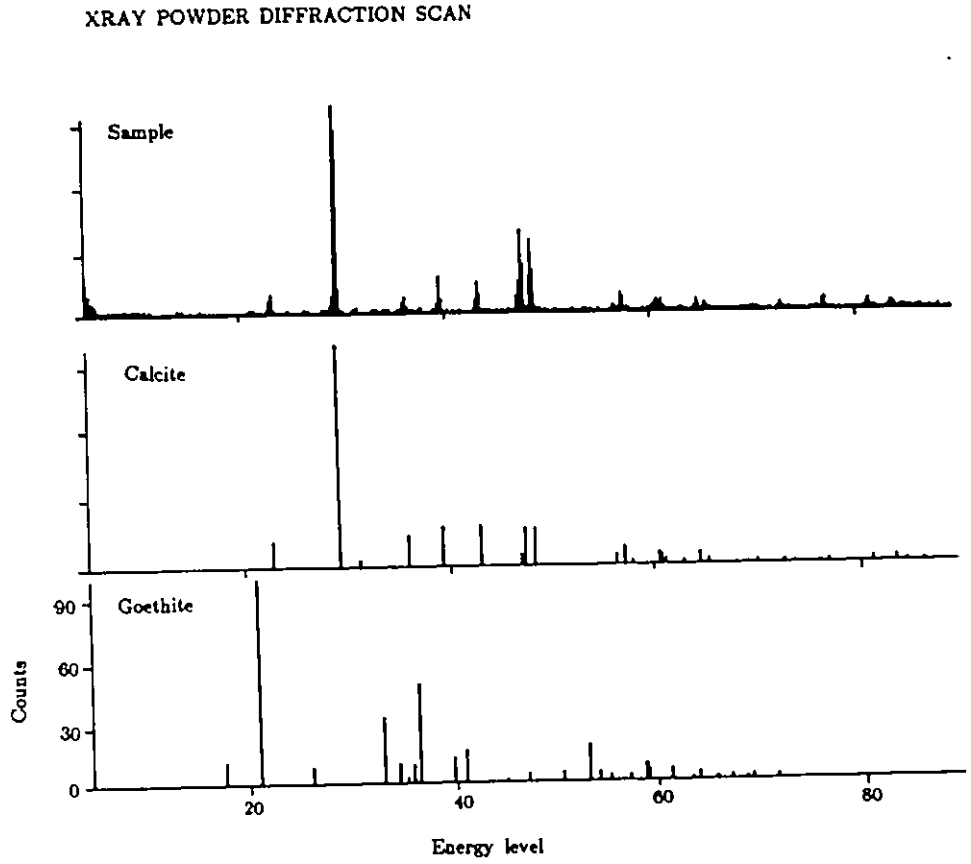

Figure 7.5: X-RAY POWDER DIFFRACTION SCAN OF HIATUS MUD. The sample is shown at the top. It clearly contains a large component of calcite (middle scan) but virtually no goethite (bottom scan). The sample was also compared with other iron compounds (not included here) but showed no correlation with any.

Element	Sample 1	Sample 2
Ca ppm	375,000 ± 17,000	274,000 ± 14,000 (27.4%)
Fe ppm	23,700 ± 600	170,000 ± 3,700 (17%)

Analysis of hiatus scrapings by X-ray powder diffraction (Materials Research Lab, McMaster University) indicated that it contains calcite but only a barely-detectable trace amount of goethite (FeO(OH)). The sample scan is shown together with scans for calcite, which makes up most of the sample, and goethite, in Figure 7.5. However, repeat analyses failed to detect any goethite or any other crystalline

iron mineral such as lepidocrosite (FeO(OH)), haematite (Fe_2O_3) or siderite ($FeCO_3$).

Some kind of amorphous iron oxide or hydroxide from the weathering of limestones or iron-containing minerals is indicated. This could be deposited either from (i) leaching or suspension of weathering products from the regolith above the cave, (ii) the flocculation of iron compounds which had been held in solution in acidic ground water when this water met the more basic salt water at the salt-fresh water interface, or (iii) precipitation of iron hydroxides by bacteria. Each possibility is discussed below.

(i) The leaching of weathering products is quite feasible. The mud resembles terra rossa both in its appearance and its chemical composition, although the level of silica is low. Terra rossa is a reddish clay-like soil, rich in iron hydroxides, the insoluble residue of weathering, which accumulates in depressions in limestone (Olson et al 1980). It is a type of pedogenic red bed (Pye 1983) common in tropical and Mediterranean regions. During periods of emergence of the cave any mud which is washed down to the cave does not remain on the flowstone surface because it is washed off by the dripping waters. During periods of inundation the terra rossa forms a suspension in the water and settles over all surfaces. The redeposited terra rossa would then be classified as a type of detrital red bed. Examples of red soils on marine limestones and eolianites in Bermuda and the Bahamas are numerous (e.g. Ruhe et al 1961, Mylroie and Carew 1988) but, unlike the mud on DWBAH, they contain a significant proportion of silica. The yellow, brown and red colours are caused by the presence of ferric forms of iron in a finely divided form. Haematite (Fe_2O_3) in very fine or poorly crystalline form (which is difficult to identify by X-ray methods) is usually the chief red pigment. Goethite (FeO(OH)), also common in red soils, is yellow to yellow-brown in colour.

(ii) Salt-water floccuiation of iron compounds to form lepidocrosite was suggested by D. Williams (Pers. Comm. 1987): lepidocrosite (FeO(OH)) is orange or reddish-brown and forms under hydromorphic conditions (Pye 1983).

(iii) R. Palmer, a cave diver with considerable experience in drowned caves of the Bahamas, suggested that the brown-red hiatus coating may represent the remains of bacterial colonies common on the walls of water-filled caves in the tropics (Pers. comm. 1989). This is often encountered by cave divers as a brownish slime on the walls. When the water levels fell the slime would have been sloughed off and deposited on the flowstone covered floor. Other samples similar to DWBAH show the red deposit coating highly convoluted surfaces such as emergent broken-off straw stalactites which fell from the roof.

Bacterial deposition of iron hydroxides is common (Harder 1919, Peck 1986). Microscopic examination of such sediments usually reveals bacterial coat remains in the form of short, spiral filaments. The particles of iron hydroxide appear as rounded grains. Microscopic examination of the DWBAH mud showed grains which closely resemble those of bacterially deposited sediment, but no evidence of bacterial sheaths. Bacterial deposition might account for the small quantities of phosphorus and sulphur detected. However, bacterial deposits typically have high levels of manganese in addition to iron.

The origin of the hiatus mud is not clear, but, for all of the possible cases, deposition at times of flooding is indicated. It is clear that the hiatuses do represent periods of non-deposition and erosion when the caves must have been inundated but the salinity of the water is not indicated.

7.1.3 Evidence for former sea level highs:

Zones of marine alteration occur throughout DWBAH in isolated pockets: these appear to be boreholes (probably of molluscs) which have been filled with a calcareous mud (probably a marine deposit) or with clear calcite crystals (possibly a fresh water deposit). The pattern of growth lines in the flowstone above the boring gives some indication of the time of alteration: if the growth lines follow the line of the boring or encrustation then the alteration happened before deposition of that layer; if the growth lines are cut by the borehole then the boring occurred

subsequent to the flowstone deposition. The borehole just above hiatus 2 in Piece 1 probably occurred during hiatus 3. This is confirmed by another part of the sample where hiatus 4 and the subsequent flowstone growth lines follow the curvature of the hiatus 3 borings and encrustations. This is clear evidence that sea water filled the cave during Hiatus 3. However, there is no evidence for boring activity during hiatus 1, 2 or 4.

Two interpretations are possible:

All hiatuses are similar in appearance. We know that the cave was filled with salt water before the deposition of the mud during Hiatus 3. It is reasonable to presume that the same conditions applied in each case, that each hiatus represents a period of salt water inundation of the cave, but the duration of high sea level may have been too short during Hiatuses 1, 2 and 4 to allow for appreciable marine alteration. This implies that sea level rose significantly higher than -15 m on five occasions since the beginning of deposition of this flowstone; the rise had to be sufficient that the cave was below the fresh water lens.

The second interpretation is that, while it is clear that the cave must have been full of water during these hiatuses, it may not have been salt water on each occasion. This implies that sea level rose on these five occasions but not necessarily to much higher than -15 m; the cave may have remained within the fresh water lens for all hiatuses other than Hiatus 3.

We know from dates and elevations on fossil corals that sea level rose to a maximum of ~ +5 m during the isotope stage 5e (Sangamon) interglacial (Hiatus 3). At this time Lucayan Caverns were filled with salt water. Therefore the fresh water lens was a maximum of 20 m thick. Its top would have been close to sea level. If a fresh water lens of similar thickness is presumed during the other high sea level events during Hiatuses 1, 2 and 4, sea level must have been between - 16 m and +4 m relative to current sea level.

Whichever interpretation is chosen the evidence is clear that sea level rose to close to -15 m or higher on five occasions in the last 300 kyr. The delineation just

above Hiatus 2 may represent a short break in deposition but it is not marked by a film of mud like the other hiatuses; it is not clear if sea level rose at this time.

7.1.4 Sequence of events interpreted from physical form of flowstone:

Host rock formation probably occurred some time after 730 kyr B.P. (evidence for this date is presented later.) Cave excavation may have been quite rapid: Mylroie and Carew (1988) give evidence, from a similar environment in San Salvador Island, Bahamas, of significant cave system excavation in about 3 thousand years. Cave excavation may have occurred by the normal processes of acidification of soil water by soil bacterial CO_2 during low sea stands; or it may have been formed through salt/fresh water mixing enhancement of solution (Sanford and Konikow 1989, Stoessell et al 1989) during high sea stands. Deposition of the marine encrustation substrate for DWBAH indicates sea water flooding the cave. The coating of dogtooth spar was probably deposited in fresh water. Deposition of the flowstone required fully air-filled conditions, so sea level must have been below -10 to -15 m during flowstone deposition (this estimate accounts for the rate of platform subsidence, see discussion below).

The hiatuses show solution of the calcite layers and subsequent coating of these solution surfaces with red-brown mud. The solution surfaces are smooth and do not have the fretted appearance typically formed from halocline (salt/fresh interface) solution (Back et al 1984). It was therefore concluded that most of the solution took place in fresh water while the fresh water lens was migrating as the sea level rose and then fell. The iron-rich mud layer is interpreted as a deposit from quiet backwater ponding as water level fell to below the level of the cave.

Thus the sequence of (i) flowstone deposition, (ii) dissolution of its surface, (iii) mud deposition and (iv) resumption of flowstone deposition represents (a) calcite deposition in the vadose zone, (b) subaqueous solution, (c) subaqueous deposition of mud and (d) return to vadose conditions.

Because the hiatuses are products of sea level rise, dating of the flowstone

immediately above each mud layer dates sea level fall through -15m; however, the date of each sea level rise cannot be pinpointed so confidently because an unknown amount of flowstone is lost by dissolution during each inundation and submergence of the cave.

7.2 ANALYTICAL PROCEDURES

7.2.1 Sampling:

Samples were taken parallel to growth lines where these could be seen, or parallel to the lower hiatus line. None were taken close to mollusc borings. Sampling of the flowstone below Hiatus 1, between Hiatuses 2 and 3 and above Hiatus 4 was straightforward. However, there was very little material available for sampling in the thinner layers between Hiatuses 1 and 2, and 3 and 4. These samples were assembled from many small remnants throughout the specimen piece (for example sample 12, series 1).

Sampling also required consideration of the removal of flowstone by erosion during hiatuses. In order to date sea level rise as closely as possible the youngest layer beneath the hiatus had to be sampled. Since this could not be clearly identified from a physical examination (because the growth layers were not apparent) the youngest was found by dating several samples of the erosional surface from different areas of the three specimen pieces.

For the first set of analyses samples were taken from immediately beneath the hiatuses. It became apparent that these dates did not follow the trend established for the rest of the flowstone in that growth period: they were too old. It was suspected that uranium leaching on the solution surface interfered with the isotopic ratios. Repeat samples were taken but the solution surface was cleaned of the top millimetre of calcite. These samples gave results consistent with the rest of the dates.

The first set of samples taken from immediately above each hiatus gave very high detrital thorium levels and thus dates of low precision (caused by low ^{230}Th counts) and low accuracy (caused by non-radiogenic ^{230}Th included at time of

deposition). Subsequent samples did not include the millimetre immediately above the hiatus.

The sample taken from immediately above the marine substrate also gave extraordinarily old ages. This was presumed to have occurred through slight contamination of the sample by marine deposits or through isotopic exchange of the dogtooth spar coating with the encrustations. Sampling just above the dogtooth spar layer gave consistent dates.

7.2.2 Chemistry

(a) Sample size and spiking: The low levels of uranium necessitated a large sample size. For the first set of analyses approximately 3 g was used. Subsequent analyses used 5 to 6 g for the younger layers and 3 to 4 g for the older layers. The only spike available was WL96, which has high ^{232}Th and ^{230}Th contamination. Approximately 0.8 g of spike was added to each sample after dissolution in 7 N HNO_3.

(b) Removal of detritus: Most of the samples were very clean and required no treatment to remove dirt. Samples from the vicinity of the hiatuses required more care: centrifuging after dissolution was required.

(c) Column chemistry: Samples of this size loaded unto the columns in the usual 5 ml of acid were found to frequently block the columns. When they were loaded in 10 ml acid the problem rarely occurred. It was especially important to make sure that these samples were at 7 N strength: the large amount of material slowed down the drying process and obscured any remaining liquid which would then dilute the acid. This problem was overcome by repeating the drying and dissolution in the 7 N HNO_3 step. If the initial loading was successful then the rest of the column chemistry was uneventful.

7.2.3 Filament loading and mass spectrometry:

All of the thorium fraction was loaded for all samples. The proportion of uranium loaded varied with the age (sample size): for old samples of 3 g nearly all

the uranium was loaded; for young samples of 6 g only half was loaded.

The uranium runs were generally uneventful. Thorium runs were highly variable and required constant attention. The extreme variability of ^{232}Th in the vicinity of the hiatuses (and these were the more common samples because the greatest interest lay in the dates of the hiatuses) required that each sample be controlled in a different manner. The best runs were done when similar samples were run sequentially so that the thorium behaviour was a little more predictable.

These samples were the first to be dated for this thesis. The precision is lower than would now be obtainable (December 1989) for the following reasons: (i) Control of the thorium runs requires a high level of skill. This was developed during the course of the DWBAH study: later runs have a higher precision than earlier ones. (ii) The levels of ^{230}Th are very low: the ^{230}Th count was usually only ~10 - 40. The lowest error was achieved by keeping the counts low and running for as long as possible. (iii) The precision was eventually limited by the high spike ^{230}Th levels.

The following criteria were used to evaluate the data: (i) A $1\sigma_m$ error on the $^{230}Th/^{232}Th$ atomic ratio of < 1% was required. (ii) A 1σ error on the age of < 5% was required unless the date was clearly consistent with several other dates from adjacent samples; for example, samples 17 and A1 have high error but appear to be consistent with the adjacent dates.

7.3 RESULTS

7.3.1 Dates:

Table 7.1 compares a selection of the alpha counted dates with mass spectrometric dates from the same region of DWBAH. It is impossible to directly compare alpha counted with mass spectrometrically counted dates because the larger samples needed for α-spectrometry necessitated analyzing a longer stratigraphic interval. However, it is clear that the results from the two dating techniques are not in conflict. This table illustrates (i) the higher precision, (ii) the higher reproducibility and (iii) the better resolution of older dates obtainable by mass

spectrometry.

The errors shown here are only 1σ because this is customary for alpha counted dates. This indicates the 68% confidence interval that the true date is located between ± 1σ. However, there is obviously a 32% probability that the true value lies outside of these limits. With the higher precision of mass spectrometry all age quotations should henceforth conform to the general principle in absolute dating work of quoting all errors as 2σ (95% confidence interval) unless otherwise stated.

Table 7.1: A comparison of alpha counted ages and some mass spectrometric ages for equivalent samples of the DWBAH speleothem. (Age shown in kyr B.P.)

α-counted dates				Mass spectrometric dates			
Sample	Age	1σ error		Sample	Age	1σ error	
BHB	>350			Q	270	+13.0	-11.5
B	>350			P	241	+3.5	-3.5
----------	Hiatuses 1 & 2	----------					
MBR	307	+119	-64	A1	209	+14.0	-11.0
MB	170	+69	-42	1	197	+3.5	-3.5
MM	203	+121	-55	6	168	+2.0	-2.0
MT	139	+54	-39	10	144	+5.2	-4.6
----------	Hiatuses 3 & 4	----------					
TB	66	+11	-10	14	71	+2.0	-2.0
TBR	60	+6	-6	15	64	+0.5	-0.5
TT	76	+8	-7	18	39	+0.7	-0.7

Figure 7.6 shows mass spectrometric dates with the 1σ range as a solid line and 2σ range as dashed lines. Table 7.2 shows some of the data. The full table of data is presented in the appendix. The dates are generally in chronological order within 2σ error. Some of the exceptions (bracketed in Figure 7.6) are explainable: (i) Samples 11, 12 and T1 are from the erosional surfaces of hiatuses and probably experienced U leaching during the dissolution events discussed above. An alternative reason for the unexpectedly old age could be detrital contamination. The possibility of leaching or contamination on the hiatuses was first suspected when sample 11 was run and clearly did not fit the sequence established for samples 1 to 10. If the regression line through samples 1 to 10 is propagated to the relative position of sample 11, then its age would be 138 kyr B.P.. After this, all samples taken from the

Table 7.2: DWBAH data

Sample	Age kyr	-2σ	+2σ	$^{234}U/^{238}U$ Act.	$^{230}Th/^{234}U$ Act.	$^{230}Th/^{232}Th$ Act.	Initial $^{234}U/^{238}U$	U conc (ppm)
1	196.9	7.0	7.0	1.07	0.85	200	1.12	0.14
2	177.0	9.4	11.1	1.07	0.82	362	1.11	0.13
4	164.1	10.0	11.7	1.06	0.79	1499	1.10	0.12
5	177.0	10.0	10.5	1.06	0.81	682	1.10	0.13
6	168.2	4.1	4.1	1.06	0.80	562	1.10	0.14
7	94.3	8.2	8.8	1.06	0.58	849	1.08	0.15
8/9	129.5	4.4	4.4	1.06	0.70	2202	1.08	0.13
10	144.1	9.4	10.5	1.06	0.74	1466	1.08	0.13
10	138.9	10.0	10.5	1.06	0.73	1635	1.08	0.13
11	188.7	5.3	4.7	1.07	0.84	67	1.13	0.21
12	133.6	2.3	2.3	1.07	0.72	64	1.10	0.28
13	92.6	2.6	2.3	1.06	0.58	196	1.08	0.16
14	70.6	3.8	4.1	1.06	0.48	1459	1.07	0.15
14	64.5	4.4	4.4	1.06	0.45	1395	1.07	0.15
15	64.2	1.2	1.2	1.06	0.45	1250	1.07	0.19
16	64.0	5.3	5.6	1.06	0.45	1236	1.07	0.15
17	51.0	5.0	5.1	1.02	0.38	799	1.04	0.08
18	39.1	1.4	1.4	1.05	0.30	237	1.06	0.12
F	143.0	3.5	2.9	1.06	0.74	1864	1.09	0.16
G	145.9	4.7	4.7	1.06	0.75	2484	1.09	0.18
H	149.0	4.1	4.7	1.06	0.75	2642	1.09	0.20
I	140.0	5.9	5.3	1.06	0.73	2461	1.09	0.20
N	226.2	8.2	8.2	1.06	0.89	228	1.11	0.21
P	241.4	7.0	7.0	1.05	0.90	1567	1.11	0.26
Q	236.7	11.7	14.1	1.06	0.90	854	1.11	0.34
Q	269.5	21.1	25.8	1.05	0.93	963	1.11	0.34
R	328.1	18.8	23.4	1.05	0.97	133	1.13	0.38
A1	208.6	22.3	28.1	1.05	0.86	1285	1.08	0.09
T1	239.1	19.9	23.4	1.06	0.90	1573	1.11	0.14
T2	225.0	11.7	15.2	1.06	0.89	1215	1.11	0.14
T4	225.0	7.0	5.9	1.06	0.89	173	1.11	0.22
T4	222.7	9.4	8.2	1.06	0.88	223	1.11	0.21
B1	240.2	9.3	10.5	1.06	0.90	769	1.11	0.22
B2	274.2	9.4	9.4	1.05	0.93	186	1.11	0.16
Y	108.4	2.9	3.2	1.04	0.64	278	1.06	0.25

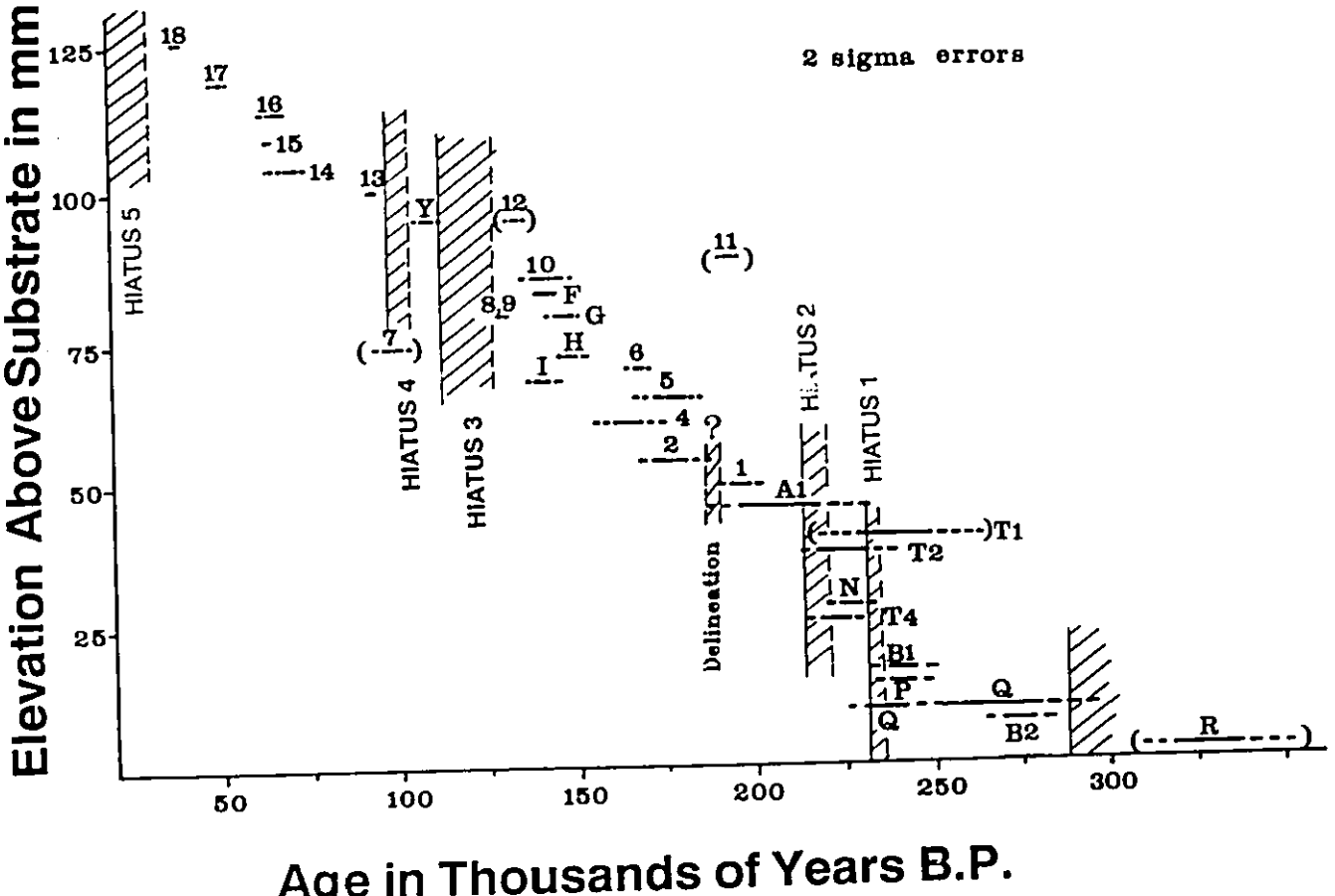

Figure 7.6: MASS SPECTROMETRIC DATES FOR DWBAH. The 1σ range is shown as a solid line and 2σ as dotted lines to either side. Brackets indicate (i) samples on hiatuses that show unexpectedly high ages as a result of U leaching or detrital contamination, and (ii) samples which do not fit the general trend for no obvious reason. Vertical solid lines show the date of sea level fall. Vertical dashed lines show the approximate date of sea level rise. The cross-hatched areas show periods of non-deposition during high sea stands. The question mark at ~188 kyr B.P. marks the delineation between samples 1 and 2 which possibly indicates a short hiatus.

vicinity of the hiatuses were carefully cleaned of all traces of detrital contamination or leached surfaces. Sample Y was taken to replace 12: the younger date is the more reliable. (ii) Sample R was replaced by B2 when marine substrate contamination was suspected in view of the large gap between the dates for samples Q and R.

Some of the exceptions are not explainable: Samples 8/9, I and the repeat on Q appear to be a little too young to fit the general trend of the adjacent dates while sample 7 is clearly outside of the range of adjacent samples. For these analyses the errors were low and there is no obvious reason for the erroneous ages.

The visible hiatuses indicate periods of high sea level. Except for Hiatus 3 there is no clear break in the dates. It is salutary to note that if the hiatuses were not visible then it would be difficult to appreciate them by dating alone even at this high density of sampling. The delineation between Samples 1 and 2 may represent an hiatus but it does not necessarily indicate a period of high sea level.

7.3.2 Dating the hiatuses: The locating of sea level events (rises and falls) is somewhat arbitrary in that flowstone only contains a record of the times when sea level was low and, in addition, deposition of calcite occurred that was not removed by erosion. The periods of high sea level are represented by an absence of information. In Figure 7.6 the dates of sea level fall are shown as solid vertical lines. At the end of each hiatus sea level must have fallen a short while before the deposition of the first layer of flowstone immediately above the hiatus. These lines are placed with reasonable confidence. However, when sea level rose again, an unknown quantity of flowstone was lost to re-solution, so some information is lost. Sea level rose some time after the deposition of the last remaining layer of flowstone beneath the hiatus. Sea level rise is shown as vertical dashed lines to indicate that these lines are not so confidently placed.

The lines to indicate sea level fall were placed several kyr before the date of the following flowstone layer (to account for the millimetre or so of flowstone above the hiatus which could not be sampled): for example, the end of Hiatus 4 was

placed at 97 kyr B.P., which is 4 kyr older than the date on sample 13 (92.6 kyr B.P., 90 - 95 2σ range). Similarly the end of Hiatus 3 is placed at 115 kyr B.P., which is 7 kyr older than the date on sample Y (108 kyr B.P., 105 - 112 2σ range). The end of Hiatus 2 is placed at 212 kyr B.P., 3 kyr older than sample A1 (209 kyr B.P.).

The placing of the beginning of Hiatus 3 was slightly more difficult. Sea level rose some time after the deposition of sample 11 but before sample Y. However, sample 11 showed detrital contamination or U leaching. The growth line for the well dated samples 1 to 10 ($r = 0.94$, omitting samples 8,9 and I) was propagated to the position of Hiatus 3 and the date calculated as 130 kyr B.P..

The dates for the initial fall in sea level and for Hiatus 1 are not so reliable as the others. The initial fall must have occurred some time before B2 was deposited but the 2σ range on these older dates is high (B2 is 265 - 284 kyr).

The close juxtapositions of the dates on samples N and T4 (above the hiatus) and B1 and P (below the hiatus) severely constrain the placing of limits on Hiatus 1. Its end was placed at 232 kyr B.P., which is 6 kyr before N (226 kyr, 218 - 234 range). Its start was placed at 235 kyr B.P., 5 kyr after B1 (240 kyr, 231 - 251 range).

The placing of sea level rise for Hiatus 2 was similarly constrained by the closeness and imprecision of the dates on samples T1, T2 and N (below the hiatus). It was placed at 217 kyr B.P., 8 kyr after T2 (allowing for the deposition of T1).

The possible break in deposition above Hiatus 2 was placed at 188 kyr B.P., midway between the dates on samples 1 and 2.

In summary, the hiatuses indicate periods of sea higher than -10 to -15 m at > 284 kyr, 235 - 232 kyr, 217 - 212 kyr, 130 - 115 kyr, 103 - 97 kyr and < 38 kyr B.P.. The delineation above Hiatus 2 indicates a possible sea level rise at ~188 kyr B.P.. The dates of these rather short-lived sea level peaks (at around 233, 215, (188?), 125 and 100 kyr B.P.) is generally in agreement with the high sea stand chronology inferred from oxygen isotope stratigraphy of oceanic foraminiferal cores (Imbrie et al 1984, Martinson et al 1987). The timing of sea level events indicated

by the dating of DWBAH and from other sources in the literature is further discussed below.

7.3.3 Growth Rates:

The line of best fit through the dates for each of the three major periods of flowstone growth gives a measure of the growth rate. Growth rate gives only limited information on paleoenvironment because it varies in complex ways, with amount of precipitation, amount of percolation, level of saturation of the drip waters (which in turn reflects the CO_2 levels of the regolith and the complexity of the flow lines) and CO_2 levels of the cave air.

From ~280 kyr to 235 kyr B.P., isotope stage 8, growth was rather slow, at approximately 0.3 mm / kyr. The growth rate in the short period between Hiatuses 1 and 2, from 230 kyr to 220 kyr, isotope stage 7.4 (Martinson et al 1987), appears to have been quite fast at approximately 1.5 mm / kyr. This growth rate is measured from samples T1 to T4. These may represent only a locally high growth rate because elsewhere in the master sample this growth layer is rather thin. The second major period of growth, from 212 kyr to 133 kyr B.P., isotope stages 7.2 to 6.0, was relatively fast at ~0.6 mm / kyr. The last period of growth, between 97 kyr and 30 kyr, was slightly slower, at ~0.45 mm / kyr.

7.3.4 Initial $^{234}U/^{238}U$ Activity ratio and U concentration over time[13]:

The initial $^{234}U/^{238}U$ ratio shows a clear, and accelerating, decrease with time (Figure 7.7, A). The relationship is described by the equation:

$$\text{Initial } ^{234}U/^{238}U = 0.032 * \ln(\text{Age}) + 0.709$$

The relationship is strong with a correlation coefficient (r) of 0.89 and a coefficient of determination (R^2) of 0.78.

---

[13] For these comparisons the five questionable dates (11, 12, 7, T1 and R) have been omitted.

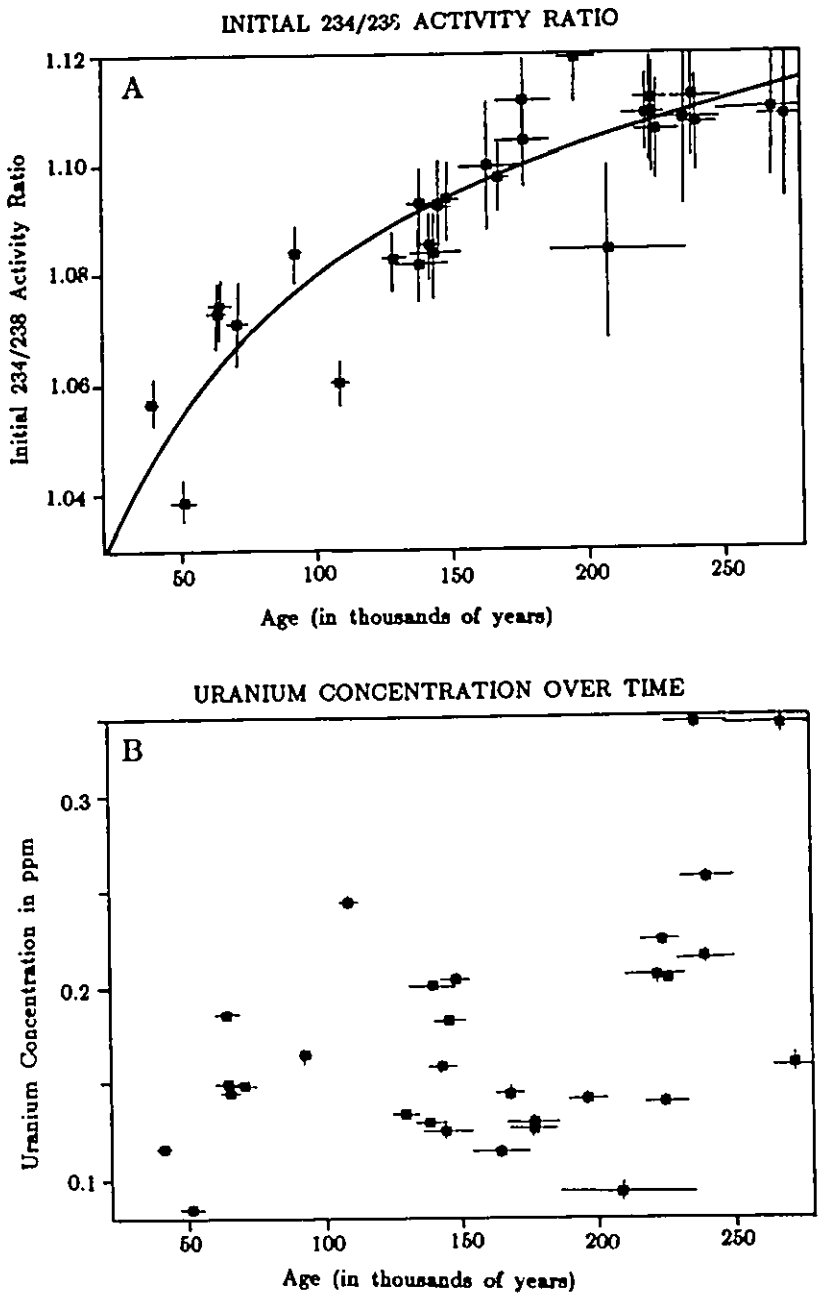

Figure 7.7: A. CHANGE IN INITIAL $^{234}U/^{238}U$ ACTIVITY RATIO OVER TIME. The error bars are 2σ. Note that the error on initial $^{234}U/^{238}U$ is more a function of the error on the age than the error on the ratio measurement. The initial $^{234}U/^{238}U$ activity ratio decreases towards the present. The solid line is the curve of best fit. It indicates strongly accelerating preferential leaching of the more soluble ^{234}U from the host rock.
B. CHANGE IN URANIUM CONCENTRATION OVER TIME. There is a slight indication of a decrease in U concentration over time as it is leached out of the host rock.

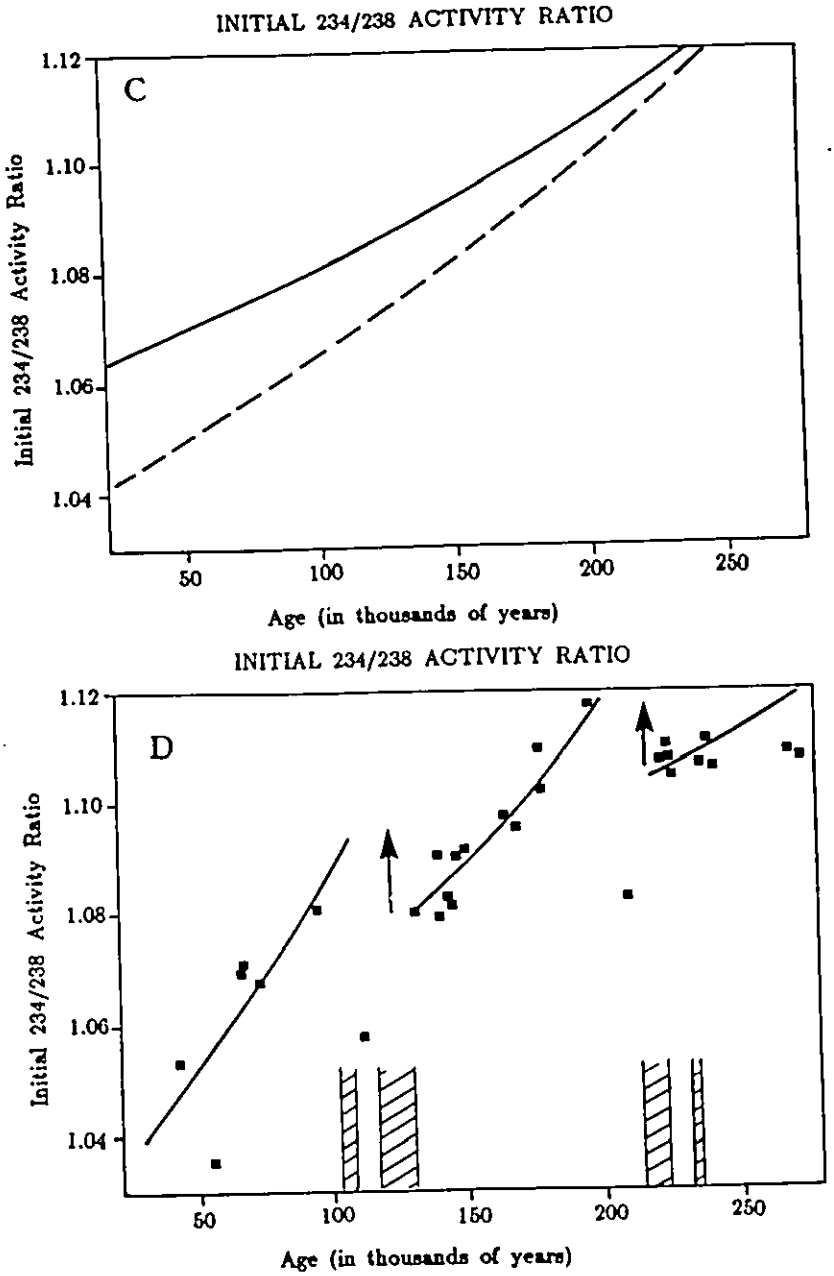

C. MODELS FOR CHANGE IN INITIAL $^{234}U/^{238}U$. The solid line shows the change in initial $^{234}U/^{238}U$ caused by normal decay from the initial value of 1.144 at ~300 kyr B.P. towards 1.00. The dashed line indicates the effect of preferential leaching of ^{234}U at a constant rate.

D. ALTERNATIVE MODEL FOR CHANGING INITIAL $^{234}U/^{238}U$ ACTIVITY. This model envisages normal decay and leaching of ^{234}U with the inclusion of a step wise re-adjustment of the starting value at each major sea level rise as a new bed of eolianite is deposited. The solid lines show $^{234}U/^{238}U$ decreasing by decay and through leaching; the arrows indicate the periodic augmentation of the ratio; the cross hatched zones are the periods of sea level high as indicated by the hiatuses on DWBAH; the original points data are included.

If this trend is propagated back to the $^{234}U/^{238}U$ activity ratio of seawater (1.144) then a date of 731 kyr B.P. is calculated. It is likely that the original material, of which the host rock is made, was deposited with a $^{234}U/^{238}U$ ratio in equilibrium with seawater. Ball (1967) indicates that much of Grand Bahama Island is made up of an eolianite ridge. Garrett and Gould (1984) observe that the eolianites of the nearby New Providence Island did not occur before the late Pleistocene, 200 kyr B.P.. The DWBAH initial $^{234}U/^{238}U$ data suggests that the sand making up the eolianites is at least 731 kyr old; it may have been reworked several times.

There is a parallel, though weak, trend in the total uranium concentration over time. This is shown in Figure 7.7, B. Here the R^2 value is only 0.23.

The pattern of change in initial $^{234}U/^{238}U$ is difficult to explain. The normal decay of excess ^{234}U towards a $^{234}U/^{238}U$ ratio of 1.00 decelerates with time (Figure 7.7, C solid line). If a constant rate of leaching is added to the loss of ^{234}U by decay then the change is more rapid but still decelerating (Figure 7.7 C, dashed line). The rate of decay cannot change; thus the rate of leaching must accelerate. The volume of leachate (rainwater) is likely to have remained approximately constant, so its load of dissolved ^{234}U relative to ^{238}U must have increased over time. This is unlikely.

A much more complicated scenario provides an alternate explanation. Although the fit appears to be good, it may be that the logarithmic trend is not the best fit. If normal decay and constant leaching are accepted as the only means of changing initial $^{234}U/^{238}U$, then the change cannot accelerate over time. It must be presumed that the host marine eolianite was originally deposited with an initial $^{234}U/^{238}U$ of 1.144 (in equilibrium with sea water). After emergence of the land mass, the $^{234}U/^{238}U$ would begin to decay towards 1.00. However, a rise in sea level would interrupt the process, a new bed of eolianite might be deposited on top of the original (and now partly eroded away) eolianite. The new material would be of initial $^{234}U/^{238}U$ of 1.144. On subsequent sea level fall the dripwaters producing the flowstone would leach both the new eolianite and the old and would thus have a

"rejuvenated" initial $^{234}U/^{238}U$ ratio which would then begin to decay towards 1.00 as usual. This process is repeated whenever sea level rises sufficiently to produce a new deposit of eolianite. This speculative model is illustrated in Figure 7.7, D: the solid lines show $^{234}U/^{238}U$ decreasing by decay and through leaching; the arrows indicate the addition of fresh eolianite at $^{234}U/^{238}U$ of 1.144; the cross hatched zones are the periods of sea level high as indicated by the hiatuses on DWBAH; the original points data are included without error bars.

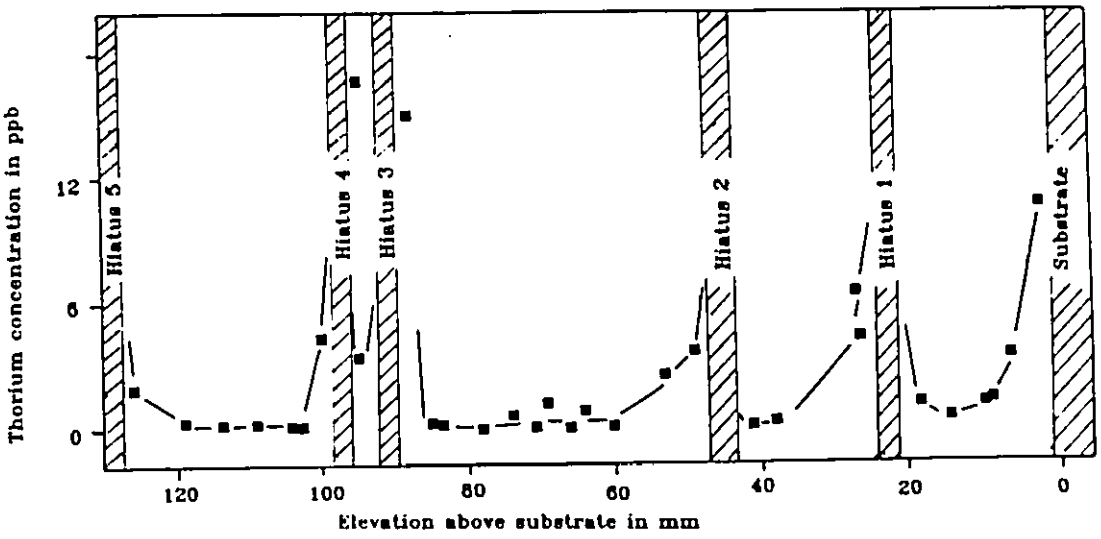

Figure 7.8: RELATIONSHIP OF THORIUM CONCENTRATION AND SEA LEVEL. Thorium concentration rises significantly in the vicinity of the hiatuses and can be viewed as a very rough indicator of sea level.

7.3.5 Variations in detrital thorium:

Thorium concentration varies greatly with detrital ^{232}Th content: close to the hiatuses it rises markedly. It can be taken almost as a proxy of sea level change. Figure 7.8 shows Th concentration plotted against position in the flowstone. Relative position was chosen for the x-axis rather than time in order to avoid any problems of interpretation of dates with detrital contamination or U leaching close to hiatuses.

7.4 DISCUSSION

7.4.1 Causes of sea level change:

This is a complex subject which touches on geophysics (rheology, isostasy, changes in the geoid), climatology (interrelationships of climate, ice volumes and sea level), geology (evidence for sea level change, tectonic activity), geochemistry (deep sea core stratigraphy) and geomorphology (evidence and timing of sea level events). The following is a very brief introduction in order to provide background to the interpretation of the dates on DWBAH. It is more thoroughly discussed in Tooley and Shennan (1987), Mörner (1980) and Peltier (1988).

Sea level is controlled at the present time (see Mörner 1987) by:
(i) gravity and the earth's rotation, causing ~180 m of relief in the surface of the ocean, (ii) the attraction of sun and moon, causing tidal variations of up to 20 m, and (iii) meterological, hydrological and oceanographic factors, such as winds and currents (e.g. the Gulf Stream), causing dynamic changes up to a maximum of 4 m.

Over the longer term, changes in sea level are caused by: (a) glacial eustasy (changes in ocean volume in response to changes in ice volume), (b) tectono-eustasy (changes in basin volume such as the gradual sinking of the ocean floor, or flow in the mantle caused by glacial loading of the mantle (Peltier 1988)), (c) geoidal eustasy (gravitational attraction of the water surface to a large mass such as a continent or an ice mass), and (d) dynamic sea level changes.

The term "Eustasy" loosely means "worldwide simultaneous changes in sea level": i.e. any kind of absolute and widespread ocean level change. This normally excludes changes caused by local factors. It was originally thought that eustatic changes were globally uniform in timing and amplitude. This led to the idea that information on sea level change from one area could be applied directly to another. However, more recent literature suggests that the amplitude of sea level changes may differ significantly in each region in response to global effects: i.e. there is a globally synchronous eustatic curve but a globally divergent history of geoidal height.

The current approach to sea level research in a region is to (i) determine

the sea level history for sample areas of it, and (ii) subtract crustal components to reveal regional eustatic changes. Then a comparison of different regions will give an indication of geoidal deformations with time.

The DWBAH sample can be used to test models of sea level change. It records glacial eustasy for the S.W. Atlantic ocean over the last 300 kyr and includes a small effect from ocean basin subsidence leading to subsidence of the Bahama Platform (Mullins and Lynts 1977). The DWBAH record is especially valuable as a history of the timing of sea level events in relation to (i) changes in foraminiferal oxygen isotope signals from deep sea cores and (ii) changes in insolation relating to the earth's orbital geometry or Milankovitch cycles (see discussion below.)

Glacial eustasy occurs because the water volume of the ocean changes in response to the glacial volume. However, both sea-level data and oxygen isotope records are influenced by other factors in addition to paleoglacial volume changes, e.g. geoidal changes and Arctic basin to Atlantic basin interchange of water as well as many other factors (Mörner 1987). Sea level changes follow the timing and general pattern of the foraminiferal isotopic variations but the magnitude of variations need not be directly comparable (Chappell and Shackleton 1986). For this reason, and because DWBAH does not provide complete information on the magnitude of sea level changes, the emphasis in this report is on their timing rather than their magnitude.

7.4.2 Choice of site:

Chappell (1987) observed that sea-level studies require sites where the evidence is accessible, is continuous through time and is dateable. DWBAH fulfills all these criteria. Bloom (1967) suggested studying pinnacle islands because they should act like dipsticks and show "true" eustatic changes. However, Mörner (1987) maintains that their mass causes local geoid rises of up to 4 m and thus are not reliable. The choice of the Bahama Banks avoids this problem.

The Bahama Platform is a particularly good area to study eustatic sea level change because tectonic activity has been restricted to subsidence, since the Early Jurassic (Garrett and Gould 1984), at an approximately known rate. Mullins and Lynts (1977) observe that drill data and geophysical data indicate that the northwestern Bahama Platform has subsided 6 to 10 km since Early Jurassic time. (Shallow water carbonate sedimentation kept pace with the subsidence to maintain the level of the banks.) They present several estimates for the rates of subsidence of the southeastern continental margin of the United States: on average the drop shown is ~500 m in the last 25 myr. Thus the rate of subsidence is about 0.02 m / kyr or 1 m in 50 kyr (see also Gascoyne et al 1979).

7.4.3 Summary of sea level history as indicated by DWBAH:

The hiatuses indicate periods of sea higher than -10 to -15 m at > 284 kyr, 235 - 232 kyr, 217 - 212 kyr, (?190 - 186 kyr ?), 130 - 115 kyr, 103 - 97 kyr and < 38 kyr B.P.: i.e. they show sea level peaks at around 233, 215, (188?), 125 and 100 kyr B.P. These are illustrated in Figure 7.9. The figure includes other, alpha counted, dates from speleothem and the oxygen isotope curves from Imbrie et al (1984), the solid line, and Martinson et al (1987), the dotted line. The DWBAH data are plotted on a slope of 1 m in 50 kyr to reflect the tectonic subsidence of the Bahamas Banks.

7.4.4 Comparison with Oxygen isotope stratigraphy:

The record of sea level change inferred from DWBAH is in excellent agreement with the high sea stand chronology inferred from oxygen isotope stratigraphy of oceanic foraminiferal cores (Imbrie et al 1984, Martinson et al 1987). The initial fall at > 284 kyr corresponds with the fall in isotope stage 8 which begins at ~286 kyr B.P. Hiatus 1, at 235 - 232 kyr B.P., occurs just after the isotope stage 7.5 peak (~240 - 236 kyr B.P.), but its position is rather poorly fixed: it could, almost equally probably, coincide with the peak. Hiatus 2, at 217 - 212 kyr B.P., coincides precisely with isotope stage 7.3 peak, at 218 - 213 kyr B.P.. The delineation

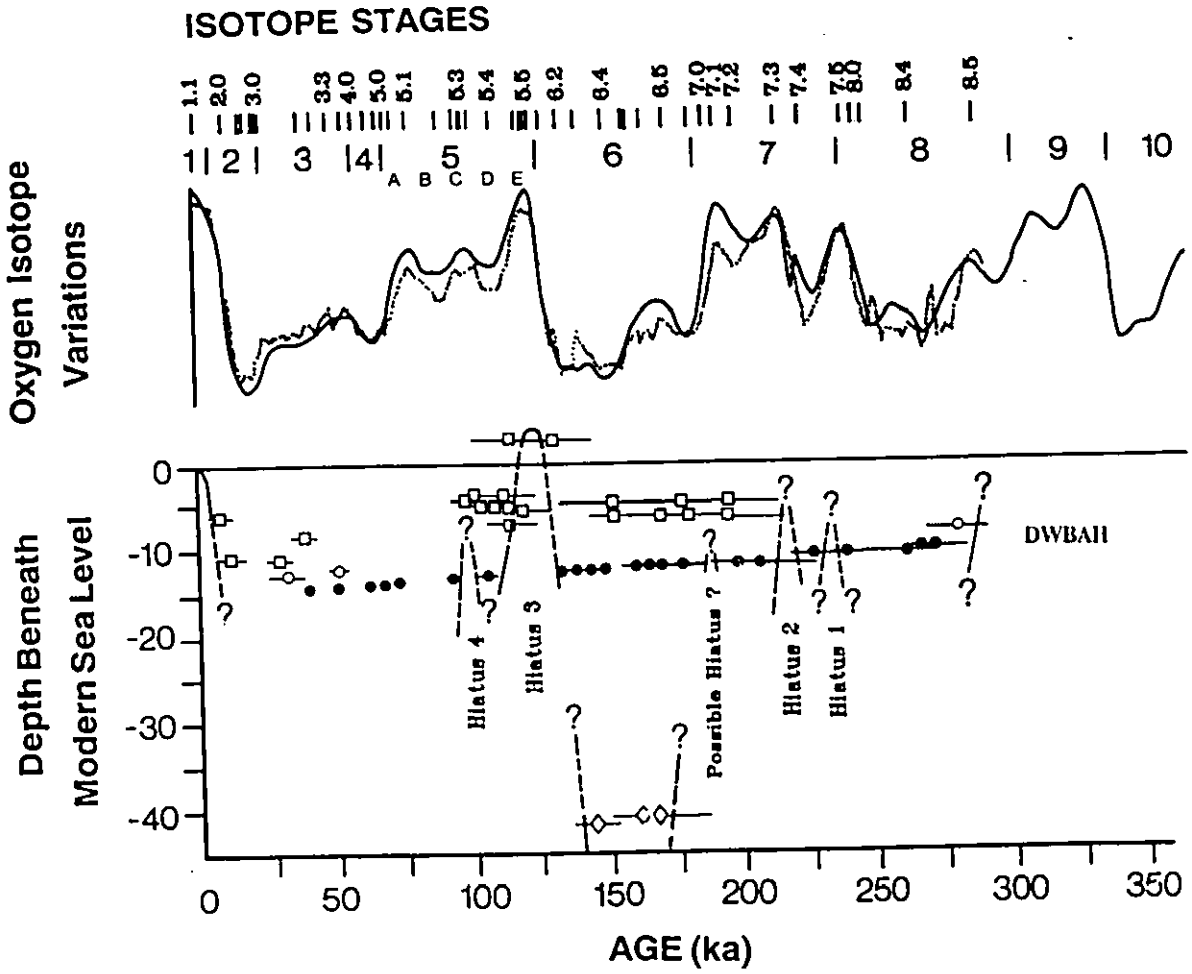

Figure 7.9: PLEISTOCENE SEA LEVEL CURVE FOR BAHAMAS. This sea level curve is assembled from dates on DWBAH and other speleothem dates. It is correlated with the oxygen isotope record from Imbrie et al (1984), the solid line, and Martinson et al (1987), the dotted line. The slope on which the speleothem dates are plotted is the maximum estimated tectonic subsidence rate of 1m / 50 kyr. The mass spectrometric dates from DWBAH are shown as solid circles, alpha counted dates from Gascoyne et al (1979) by open diamonds and from Harmon et al (1978, 1981 and 1983) by open squares. The open circles mark three mass spectrometric dates on another sample from the Lucayan area but from several metres higher elevation than DWBAH.

above Hiatus 2 correlates roughly with the stage 7.1 high at ~195 kyr B.P. but it does not clearly indicate a sea level rise. Sea level may not have risen as high as -10 to -15 m at this time; but it could have risen to within a couple of metres of this without a noticeable effect on the sample. Hiatus 3, at 130 - 115 kyr B.P., corresponds exactly with the rise at isotope stage 5.5 (125 - 116 kyr B.P.) and Hiatus 4, at 103 - 97 kyr B.P., with 5.3 (102 - 96 kyr B.P.). There is no record of the expected rise at stage 5.1. Hiatus 5 then correlates with the stage 1 rise to modern levels.

In order to appreciate the significance of these correlations it is important to understand the method of dating the isotopic record. The isotope data from Imbrie et al (1984) are taken from five deep-sea cores, measured on shallow-dwelling planktonic foraminifera, at widely distributed, open ocean sites in low- and mid-latitudes. Three of them penetrate what is presumed to be the Brunhes-Matuyama magnetic reversal dated, by the K-Ar method, at 730 ± 11 kyr B.P. This point is therefore fixed. Other points used as fixed controls are U/Th radiometric dating of corals associated with the isotope stage 5e at 127 ± 6 kyr B.P. and two radiocarbon dates, 21.4 ± 2 kyr B.P. and 17.8 ± 1.5 kyr B.P. for deep sea sediment. The data for the curve in Martinson et al (1987) are taken from a single core from the southwestern sub-polar Indian Ocean. This core provided five climatically-sensitive data sets and was sampled at a high frequency.

The timescale for the rest of the data, which cannot be absolutely dated, is fixed by orbital tuning: i.e. by assuming that variations in orbital precession and obliquity cause changes in global climate. The isotopic variations displayed at this time scale are strongly correlated with orbital variations. This implies that orbital variations are the main external cause of the succession of late Pleistocene ice ages (Imbrie et al 1984). The close correlation of the absolutely dated hiatuses of DWBAH with the isotope data gives further credence to this implication. The use of obliquity and precession curves rather than an insolation curve avoids problems of deciding which latitude and season to use. Since climate will take some time to

show a response to orbital forcing a lag factor has been built in to the timescale. Martinson et al (1987) observe that the tuned result is fairly insensitive to the actual tuning technique and climatic indicator used. The timescale is estimated to be accurate within 5 kyr for the Imbrie et al curve, and within 3.5 kyr for the Martinson et al curve.

This close fit of the DWBAH data with the isotopic record does not support the recent suggestion, by Winograd et al (1988), that the chronology of the marine foraminiferal record is faulty. They obtained a continuous record of $\delta^{18}O$ variations during the middle- to late-Pleistocene from a calcite vein in the southern Great Basin, Nevada. The $\delta^{18}O$ curve closely resembles the marine foraminiferal $\delta^{18}O$ curve but the U/Th dates on the calcite suggest a discrepancy in the timing of key climatic events: for example, their dates imply that the last interglacial began at least 17 kyr earlier than indicated by the marine record.

7.4.5 Comparison with other estimates of sea level change[14]:

In general the evidence from DWBAH agrees with other estimates of sea level with some minor differences in detail. The other estimates are based principally on alpha counted U-series dating of fossil corals and speleothem, coupled with the deep sea foraminiferal oxygen isotope stratigraphy.

Moore (1982) presents an excellent summary of the Late Pleistocene sea-level history that is indicated by dating fossil corals. The coral record appears to be even more complex than that inferred from the isotope record. Moore's summary diagram, using a synthesis of fossil coral ages from many parts of the world, is reproduced in a slightly modified form in Figure 7.10. The highs at ~28 kyr and ~50 kyr are shown as dashed lines because they are not well dated. The record is extended to include sea level changes older than 150 kyr as reported from coral and speleothem dates in Harmon et al (1983), Bender et al (1979) and Radtke et al

[14] For the following discussion the possible hiatus above Hiatus 2 has been ignored because there is little evidence for sea level rise at this time.

(1988). Both the dates and the elevations of the rises earlier than ~200 kyr B.P. are tentative. The parallel dotted lines, at -10 to -15 m, correspond to the elevation of DWBAH: any rises above this should be recorded in DWBAH if they were worldwide events. Any oscillations above the line would not be recorded in DWBAH. The cross hatched zones within the dotted lines show the location of hiatuses on DWBAH. The areas where the cross hatched zones do not coincide with the sea level rises indicate points where the DWBAH data apparently conflict with the literature. The similarities and discrepancies are discussed below. This figure can be compared with the record of sea level rise from DWBAH depicted in Figure 7.9.

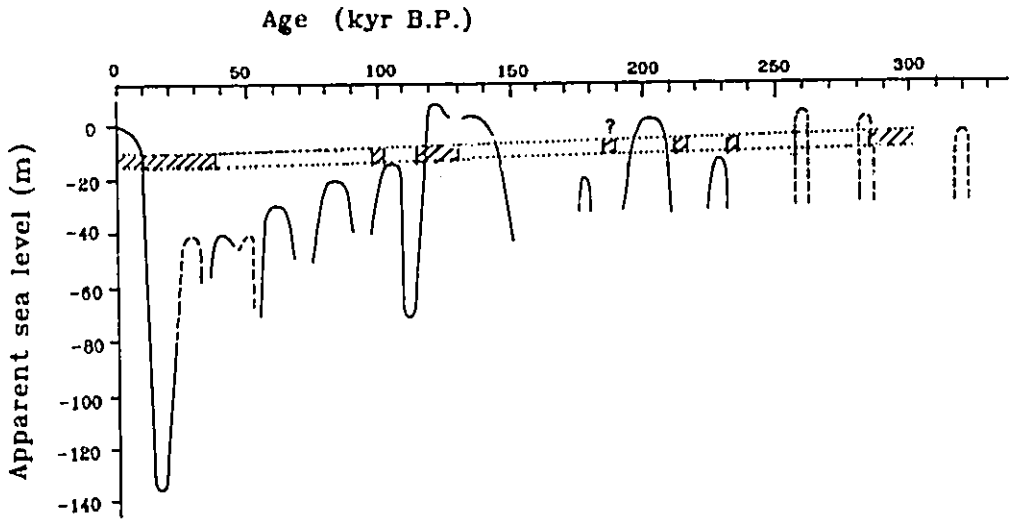

Figure 7.10: LATE-PLEISTOCENE SEA LEVEL CURVE. This figure is an amalgam of the sea level synopsis shown in Moore (1982) and that in Harmon et al (1983) combined with information from Bender et al (1979) and Radtke et al (1988). Both the dates and the elevations of the rises earlier than ~200 kyr B.P. are tentative. The high at ~50 kyr is shown as a dashed line because it is not well dated. The parallel dotted lines correspond to the elevation of DWBAH: any rises above them should be recorded in DWBAH if they were worldwide events, but oscillations above the line would not be recorded. The cross hatched zones within the dotted lines show the location of hiatuses on DWBAH. The question mark indicates the poorly substantiated hiatus or delineation at ~188 kyr B.P..

The DWBAH hiatuses do not correspond exactly with any of the sea level rises shown in Figure 7.10. In general where conflicts exist DWBAH corresponds more closely with the isotopic record than the U-series dated coral record. Some of the conflicts are minor: for example, rises in DWBAH might be expected at ~145 - 118 kyr and at ~108 - 102 kyr. They occur instead at 130 - 115 kyr and 103 - 97 kyr B.P. None of the younger rises might be expected to be recorded in DWBAH and they are not.

The number and ages of high sea level stands during isotope stages 7 and 5.5 as recorded by DWBAH are in conflict with some of the reports in the literature. In all these reports the alpha counted dates are quoted with only 1σ error (the 68% confidence interval); it is more prudent to quote the 2σ error (95% confidence interval). When the α-counted dates are viewed thus (Figure 7.11) many apparent conflicts with the DWBAH data disappear. Figure 7.11 displays dates not as a single point (as they are usually quoted in the literature) but, more correctly, as the 1 and 2σ ranges. It is also important to note that, although little confidence should be placed in single, random U-series ages (Moore 1982), many publications are based on single (e.g. Szabo and Halley 1988), and perhaps dubious (e.g. Muhs and Bush 1987), dates.

Harmon et al (1983) suggest that sea level rose to about +2 m between 210 and 190 kyr B.P. Hiatus 2 from DWBAH puts the sea level peak at 217 - 212 kyr B.P. The four coral dates in Harmon et al (Group 5) range from 282 to 168 kyr thus completely overlapping the two hiatuses resolved by mass spectrometric dating of DWBAH. The coral dates average 214 kyr. This would place the high sea stand exactly coincident with the DWBAH record. The four dates overlap each other considerably (see Figure 7.11) and there is no indication that they can be separated into two groups. However, Harmon et al present two sea level rises at this time: the first at ~230 kyr B.P. and the second at ~210 - 190 kyr B.P. It would appear that the conflict comes not from the raw data but from the interpretation. There is no real conflict of DWBAH dates and the coral dates in Harmon et al (1983). Similarly

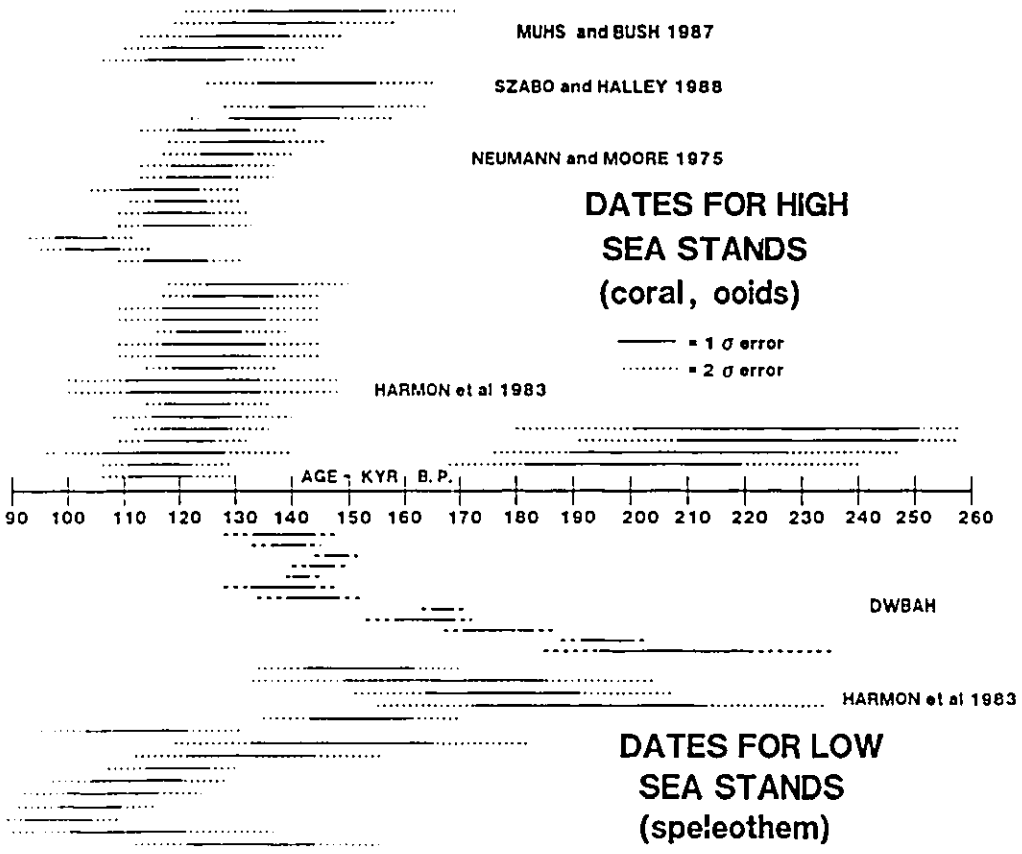

Figure 7.11: SUMMARY DIAGRAM OF ALPHA COUNTED DATES ON CORALS, OOIDS AND SPELEOTHEM AND MASS SPECTROMETRIC DATES ON DWBAH SPELEOTHEM. The 68% confidence interval is shown as a solid line, 95% as dashed lines. Dates on corals and ooids indicate high sea stands; those on drowned speleothem indicate low sea stands.

This diagram shows: (i) considerable overlap in alpha-counted speleothem dates for different low sea stands. Physical hiatuses may indicate sea level rise but the timing cannot be clearly resolved from these dates. (ii) the dates from DWBAH on flowstone deposited just before the 5e sea level rise (~135 kyr B.P.) strengthen the argument that there is no evidence of a sea level high at ~145 kyr B.P.. (iii) The populations of dates on 5e corals cannot be separated into two groups. (iv) The coral dates for the stage 7 rise(s) cover all of stage 7 and allow no resolution into separate events.

there is no conflict with the speleothem data. For example, in DWBAH the first date after the isotope stage 7.2 recession (sample A1) is 237-186 kyr B.P.; the equivalent stalagmite date in Harmon et al is 235-155 kyr.

Part of the reason for different interpretations of raw data is that many workers try to make the data fit the marine isotope record. For example, Chappell and Shackleton (1986) modified their sea level curve by orbital tuning to fit the expected rises indicated by the isotopic record. It is of interest that their original (pre-tuned) dates at approximately 220 and 235 kyr B.P. (as taken from their diagram) coincide closely with Hiatuses 2 and 1 (217-212 and 235-232 kyr) from DWBAH. This type of data "tuning" is a logical step but perhaps somewhat premature. Alpha counted dates are simply not precise enough beyond 150 kyr B.P. to decide which isotope peak to choose to tune to.

The behaviour of sea level during the period around isotope stage 5.5 (5e) is the most controversial: some records clearly show a single rise in sea level at around 125 kyr B.P. (see below); some show what appears to be a double rise (at around 122 and 135 kyr B.P.) both on morphological and dating evidence; some simply show a wide spread in the age data from ~120 to 140 kyr B.P. The marine isotope record gives no reason to suspect a rise at ~135 kyr although it is possible that the double peak was smoothed by bioturbation (Chappell and Veeh 1978a). Kaufman (1986) performed statistical tests on the 80 most reliable analyses and concluded that (i) if there was only one rise in sea level then it probably lasted no more than 12 kyr; and (ii) if there were two rises then the gap between them must have been less than 7.5 kyr.

Apart from the delineation visible in a small part of Piece 1, DWBAH shows continuous deposition between Hiatus 2 and Hiatus 3 (~212 - 130 kyr): i.e. at approximately 12 m below modern sea level, deposition occurred until approximately 134 kyr B.P. or later and did not resume until around 110 kyr B.P.. Any oscillations that may have occurred above -10 m (as shown in Moore 1982 and Chappell and Shackleton 1986) thus would not be recorded in DWBAH. However,

the problem is an important one and is therefore discussed briefly below.

Many difficulties are removed when alpha counted dates are considered in their context, rather than in isolation (Figure 7.11). DWBAH shows that the sea rose to ~-15 m after 149-129 kyr B.P. (sample 10). Harmon et al (1983) place cessation of stalagmite growth at 156-112, 171-135 and 182-118 kyr B.P.. Their coral dates for the stage 5e high range from 150 to 106 kyr B.P.; those of Neumann and Moore (1975), from 164 to 93 kyr B.P., Szabo and Halley (1988), 165 to 125 kyr B.P.. Dates on ooids and peloids (Muhs and Bush 1987) range from 169 to 105 kyr B.P.. Ku et al (1974) show a wide range of dates from Oahu, Hawaii but conclude that all the ages are centred on 122 ± 7 kyr B.P. Data from the Bahamas show a spread from 145 to 100 kyr B.P. (Neumann and Moore 1975) with no clear division into groups. Fairbanks and Matthews (1978) show one rise at 125 kyr B.P. in Barbados. Unquestionably these ages cannot be resolved into two populations.

There is greater difficulty in explaining data from areas where dates, stratigraphy and other evidence suggest a double sea level peak. Recurring dates at ~135 kyr B.P. are problematic because, according to Milankovitch cycle theory, the climate should be cold at that time. Veeh and Chappell (1970) and Chappell (1974) report that stratigraphic evidence on the New Guinea terraces shows a slight retreat and readvance of the strand line between samples NG616 (120 - 160, 113 - 153 kyr B.P) and NG 618 (102 - 130, 105 - 133 kyr B.P.). The smaller reef VIIb disconformably overlies reef VIIa. Beneath the disconformity are broken and rolled corals with debris and carbonate sand; above are corals in growth position. Bloom et al (1974) suggest that the reef complex was built up over the period 140 - 120 kyr B.P.; that temporary cessation and a "possible minor regression" during this period is suggested by stratigraphy; and that the 20 kyr difference in dates "may reflect experimental or diagenetic error". Fossil reefs from Timor and Alauro shows a similar pattern of growth: the major reef grew at ~130 kyr B.P. and the minor reef at ~120 kyr B.P. (Chappell and Veeh 1978). Evidence from Jamaica (reported in Moore 1982) shows two units separated by an unconformity at 134 ± 4 and 123 ± 5

kyr B.P..

Other evidence also suggests a double peak. Aharon, Chappell and Compston (1980) and Aharon and Chappell (1986) report that isotopic variations in giant clams, Tridacna, show a double rise at this time. Boardman et al (1984) examined aragonitic cycles from a rather poorly dated Bahamian platform core. They found sea level rises to at least 2 or 3 m below modern levels (if their model of lagoonal aragonitic production is correct) at 141 and 133 kyr B.P.. Duplessy et al (1970) present a diagram of oxygen isotope variations in the Orgnac stalagmite from southern France. This shows a slight double peak, at 130 and 125 kyr B.P.

The number of reports of double reefs is too great to ignore; it must be concluded that there was indeed a sea-level oscillation during the last interglacial. However, the timing of this oscillation is by no means clear. Edwards et al (1986/87) reanalyzed the New Guinea samples and showed that all the ages lie within 122 - 130 kyr B.P. If other examples of double reefs are also re-dated and shown to be of a similar age then the problem of a sea level high during the cold period around 135 kyr B.P. is solved: the double rise was simply an oscillation within the 5e Milankovitch cycle (see also Ku et al 1990).

A source of slight controversy is the height to which sea level rose at ~40 kyr B.P. Mylroie and Carew (1988) dated a rise to close to modern levels on San Salvador Island, Bahamas, at ~40 kyr B.P.. Other dates on corals from this period suggest a rise to only ~-40 m (e.g. Chappell and Veeh 1970 and Chappell and Veeh 1978). If the rise was indeed to modern levels then DWBAH should indicate that but it shows no evidence of a rise at this time. However, the youngest layer dated is 39 kyr old (38 - 41 range). All younger parts have been lost to erosion and thus any rise which may have occurred after 38 kyr B.P. is not recorded. Boardman et al (1984) used aragonitic cycles in sea cores to establish a chronology of sea level rises and found no evidence for such a rise. Furthermore, the isotopic record gives no reason to suspect a rise approaching modern levels at this time. It is unlikely that San Salvador Island experienced a purely local rise to modern levels; it is more likely

that the stalagmite dating or its interpretation was at fault.

7.4.6 Milankovitch cycles: The astronomical theory of climatic change formulated by Milankovitch (see Berger et al 1984) states that the fluctuations in Pleistocene climate are caused by changes in the distribution of solar energy received by the earth due to changes in (i) the obliquity of the ecliptic, (ii) the eccentricity of the earth's orbit, and (iii) precession of the earth's axis of rotation. The summer insolation received at 65° N is considered to be the most likely forcing function controlling climate. Low values of summer insolation should cause glacials and high values deglaciation. The proportion of water trapped on land as ice affects sea level. Therefore in a very simplistic model sea level should reflect variations in summer insolation at 65° N.

Figure 7.12 shows variations in solar insolation at 65° N in terms of deviations from the value in 1950. The cross hatched zones show periods when sea level was high (i) according to the dates of hiatuses on DWBAH and (ii) according to mass spectrometric dates on corals in Edwards et al (1987). All three indices agree at only one period: the ~125 kyr B.P. interglacial high sea level is shown by the coral dates, Hiatus 3 in DWBAH and a peak of insolation.

The correlation of Milankovitch cycles and sea level as indicated by DWBAH is reasonable. Hiatus 1 may be placed a little too late and so may in fact correlate with the insolation high at ~240 kyr B.P.. Hiatus 2 appears just after the 217 kyr B.P. insolation high. Hiatus 4 slightly postdates the 104 kyr B.P. insolation high. Sea level, as indicated by DWBAH, lags the insolation signature by a few kyr. However the relationship is not simple: there are many insolation highs not matched by a sea level rise to the elevation of DWBAH.

It has already been shown that the hiatuses in DWBAH correlate well with the marine foraminiferal oxygen isotope record which has a lag built in. The table below shows the dates of the insolation highs, the isotope highs, the DWBAH highs and the coral dates. The dates which may not be correct are in brackets.

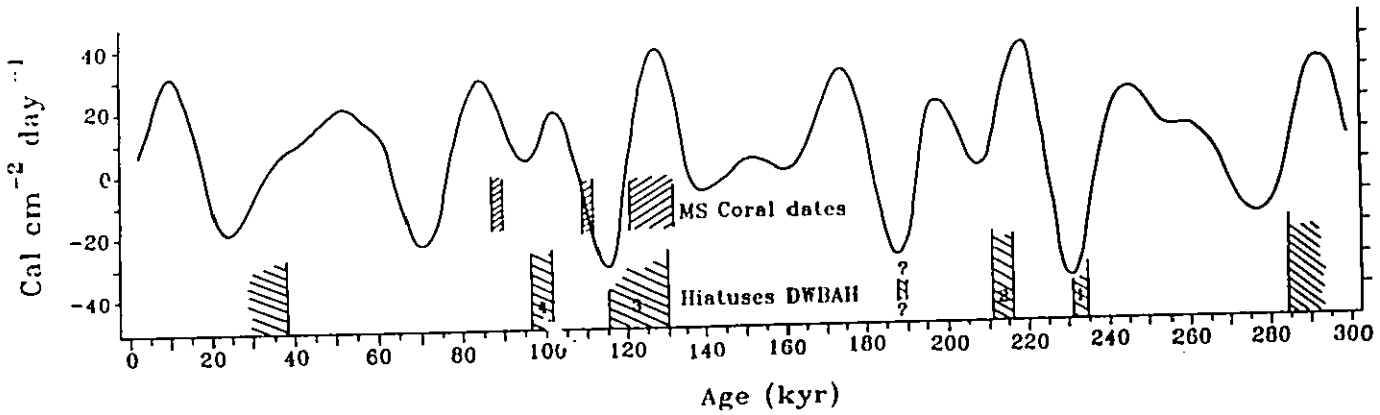

Figure 7.12: MILANKOVITCH CYCLES AND SEA LEVEL. The vertical axis shows the average solar insolation received at the top of the atmosphere at 65 N for the summer half year expressed as deviations from the 1950 value (Berger 1978). The cross hatched zones show periods when sea level was high (i) according to the dates of hiatuses on DWBAH and (ii) according to mass spectrometric dates on corals in Edwards et al (1987). The question marks show the very approximate position of the possible hiatus between Hiatuses 2 and 3.

Milankovitch high	Isotope high	DWBAH high	Corals high
292	287	> 284	
245	238	(235-232)	
218	216	217-212	
197	195	?188?	
173			
128	122	130-115	130-122 114-110
102	100	103-97	
84	80		86-88
53			
12	0	< 38	

The close correlation of both DWBAH data and coral dates with the ~128 kyr insolation high supports the idea that Pleistocene sea level highs can be the result of orbital forcing. Edwards et al (1987) suggest that, according to their model of reef growth in relation to tectonic uplift and changing sea level, the corals dated should represent times when sea level was close to a maximum but still rising. This might explain why the coral dates around 88 kyr B.P. slightly predate the 84 kyr insolation high. However, the other coral dates at ~112 kyr do not correlate with the insolation data or with DWBAH. Edwards (1988) concluded that Milankovitch forcing does not explain all the variations in climate. It is possible that the 112 kyr coral did not grow at maximum sea level. If sea level rises at a faster rate than coral growth rate then the coral will die before the sea level maximum is reached.

7.4.7 Future research in this area:

Mass spectrometric dating of submerged speleothem from various depths in the Bahamas and elsewhere should permit construction of paleo-sea level curves of much greater precision than any that exist currently. At present the paucity of data from other depths precludes the modelling of sea level change, temperature change, ice volume change and marine foraminiferal isotopic change.

Chapter 8

WIND CAVE SUBAQUEOUS WALL CRUST

Wind and Jewel Caves are dense, multi-story, rectilinear maze caves located in the southern edge of the Black Hills, South Dakota and developed in the Pahasapa limestone. Figure 8.1 shows their location and the geology of the area (from Bakalowicz et al 1987). Jewel Cave, with 118 km of mapped passage is the fourth longest known cave in the world and Wind Cave, with 80 km of passage, is the tenth longest. There is a major filled paleokarst in the rock which the modern caves intercept (Deal 1962, Bakalowicz et al 1987). The fillings are chiefly of indurated terra rossa, a typical residue from tropical weathering of limestones.

Wind Cave (Figure 8.2) extends between 1,120 and 1,265 m above sea level. At its lowest levels the passages terminate in lakes which mark the water table. Over the Quaternary the water table has gradually fallen and it is still retreating. In the lower two thirds of the cave the walls and ceilings are covered with thin encrustations of calcite which formed subaqueously. These tend to thicker with depth in the cave but in most places are < 1 cm thick. A few rock projections into the centres of passages in the lower maze have accumulations of up to 3 cm. In addition, in the lower half of the cave there are (i) "shelfstones" at some levels that grew precisely at past water lines, either at the paleo-water table or at pools stranded above it, and (ii) calcite raft debris which sank from the site of formation on water surfaces when they became too thick to continue floating, or were stranded by descending water levels.

8.1.1 The caves:

The extraordinary character of the caves has attracted attention over the years (e.g. Davis 1930, Deal 1962, Palmer 1975). The most recent model for their origin is that of Bakalowicz et al (1987) who studied erosional morphology, mineralogy of the secondary crusts and ^{13}C and ^{18}O characteristics of the secondary crusts and of

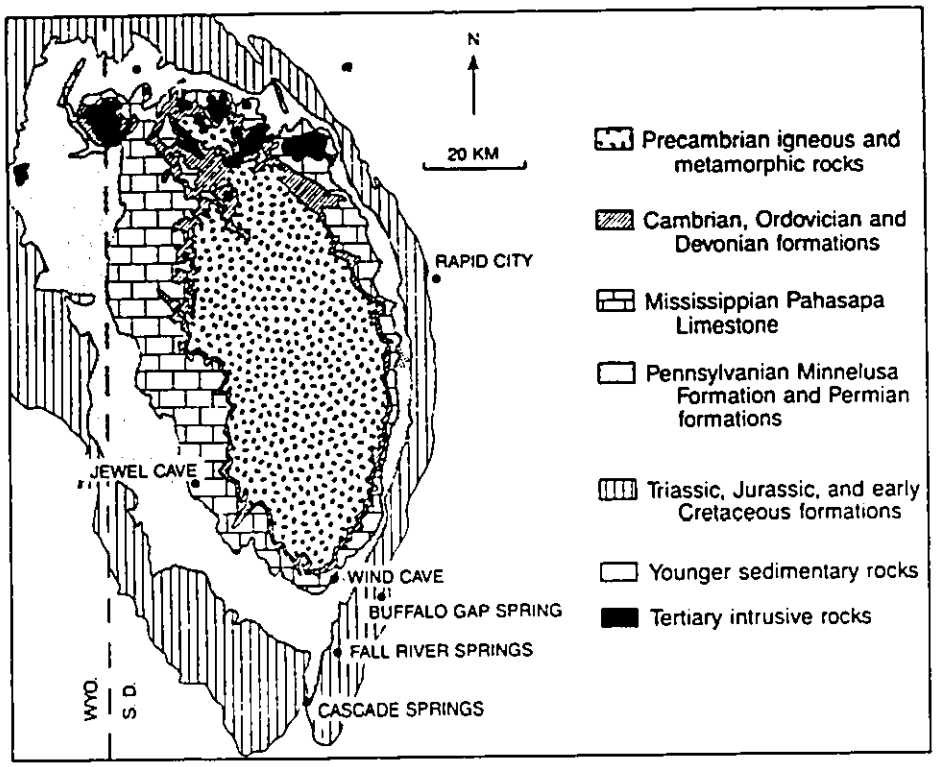

Figure 8.1: GEOLOGIC MAP OF BLACK HILLS showing location of Wind Cave (from Bakalowicz et al 1987).

altered and unaltered wall rocks. They concluded that Wind and Jewel Caves were created by ascending thermal waters focusing on paleospring outlets in overlying sandstones.

The caves are morphologically similar to thermal caves in Europe: they have a three-dimensional, one-phase maze form with convectional erosion features. A thermal anomaly at the regional hot springs extends beneath Wind Cave and the waters of its basal lake have thermal and isotopic similarities to thermal waters elsewhere. Isotopic studies of $\delta^{13}C$ and $\delta^{18}O$ of the suspected thermal sub-aqueous calcite deposits place them in the same domain as modern hot spring deposits. The pattern of deposition and petrography of precipitates support a model of cooling waters followed by degassing waters. Bakalowicz et al's U-series dates on calcite raft material show that dewatering of Wind Cave is quite recent (the deposits are all

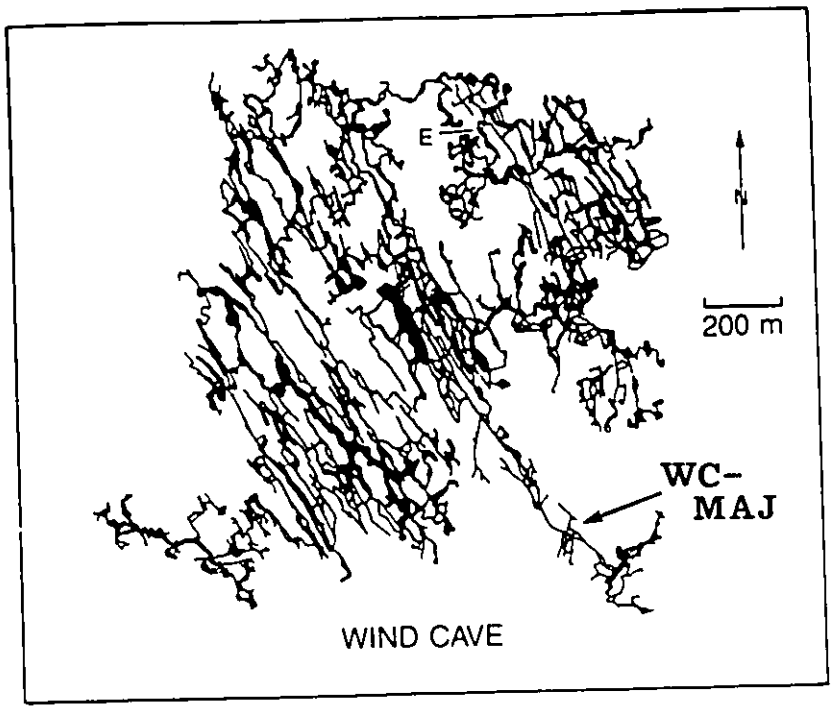

Figure 8.2: MAP OF WIND CAVE (from Bakalowicz et al 1987) showing location of WC-MAJ sub aqueous wall crust.

Quaternary) and that the cave is still draining. They suggest that the dissolution and mineralization of the caves are both the product of rising thermal waters. The evidence is fully discussed in their paper and will not be further considered here. Their thesis is also supported by the evidence of Millen and Dickey (1987).

Ford (unpublished) returned to the lower cave to collect further samples in an attempt to date the dewatering more precisely. All samples except the one discussed below, WC-MAJ, were too thin to permit more than one alpha counting date. The $^{234}U/^{238}U$ ratios were sufficiently uniform that Ford used the R.U.B.E. dating technique (Gascoyne, Ford and Schwarcz, 1983) to extend age estimates to ~ 500 kyr B.P. and to deduce that the entire cave has dewatered in the past ~600 kyr. Earlier, water flowed upwards through it to discharge at higher springs. During dewatering, water in the cave was exchanging very slowly (it was semi-static) in what was a backwater region of the Pahasapa aquifer. This implies that the wall crusts

Figure 8.3: WC-MAJ SUB-ACQUEOUS WALL CRUST, cut section, showing the laminated nature of the crust and the thin "skin" on the outer surface. Scale is in centimetres.

were deposited from cooling, degassing, very slowly exchanging phreatic water of thermal origin, with perhaps some local meteoric water mixed in.

8.1.2 Wall crusts:

The calcites of this cave have been well dated by alpha counting. The sample analyzed here, WC-MAJ, is the thickest of the wall encrustations. It grew on a rock projection at approximately 1,170 m above sea level or 50 ± 5 m above the modern lake water level. Dates on the crust indicate the growth rate of the crust and the time of drainage of that portion of the cave. It was analyzed as a test of mass spectrometric dating; the analysis was not expected to contribute much new information on the calcites of Wind Cave or on the origin of the cave. However, as well as confirming the alpha counting, some striking new data emerged.

8.1.3 Alpha-counted data

Table 8.1 gives alpha counted data on wall crusts similar to WC-MAJ (from Bakalowicz et al (1987) and Ford (unpublished, in prep)).

Table 8.1: Alpha counted dates on Wind Cave wall crusts.

Sample	Elevation a.s.l.	Uppm	$^{234}U/^{238}U$ Current	234U/238U Initial	$^{230}Th/^{234}U$	Age (kyr) ± 1σ
WC 7	1180m	2.17	1.587	2.157	0.982	242 ± 16
WC 10	1155	2.67	1.670	2.284	0.974	230 ± 20
WC 20	1145	2.62	1.585	2.101	0.957	225 ± 15
WC 14	1135	1.71	1.736	2.421	0.984	234 ± 20
WC 19	1130	1.51	1.514	1.922	0.931	208 ± 23

These samples indicate that between approximately 200 and 250 kyr B.P. this lower region of the cave was water filled and experienced slow deposition everywhere. Other dates from the lowest parts of the cave indicate that crust formation continued until ~150 kyr. Dates on calcite raft material indicate that between ~200 and 150 kyr B.P. the water table stood close to an elevation of ~1,180 m. From these dates, and many others, Ford (unpubiished, in prep.) estimated a rate of water table fall of 0.375 m per thousand years but water levels have fluctuated within the overall lowering. The drawdown is not caused by changes in local base level, which has been close to its modern level since the Eocene (Bakalowicz et al 1987), but rather by an increase in porosity of the local sandstones through which the water flows en route to its outlet at the Buffalo Gap Spring, 8 km east of the lakes in Wind Cave.

WC-MAJ grew at an elevation of ~1,170 m, between WC7 and WC 10. Four alpha counted dates were measured on this specimen and seventeen mass spectrometric dates. Table 8.2 gives the ranges of values for the two techniques.

Table 8.2: Data from alpha counting and mass spectrometry of WC-MAJ wall crust.

	Alpha counting	Mass spectrometry
U conc., ppm:	2.72 - 3.35	3.34 - 4.59
234/238 activity:	1.46 - 1.66	1.45 - 1.68
Initial 234/238:	1.88 - 2.13	1.94 - 2.16
230Th/234U activity:	0.83 - 0.95	0.75 - 1.04
Age, kyr B.P.:	160 - 232	131 - 311

The mass spectrometric data clearly duplicate the alpha counted data while providing greater resolution and precision. Details are given below.

8.2 WIND CAVE SUBAQUEOUS CALCITE WALL LINING: WC-MAJ

8.2.1 Sample Description

This sample was collected in 1987 from the lower part of the cave (see Figure 8.2) where calcite crust covers all surfaces. It is a finely laminated calcite overgrowth on a substrate of old cave fill made up of pink/brown clasts, yellow silty matrix and "fins" or "boxwork". Figures 8.3 and 8.4 show general views of the sample and a breakdown of the visible laminations. Laminations are made up of cycles of dense, opaque white horizons grading to more brittle, translucent pale brown layers. If sectioned through the upward facing part of the crust (i.e. facing the water surface) the sample is clearly divided by a thin layer of pink coloured calcite (marked "pd" on Figure 8.4). The U-series analysis of this layer failed but it is presumed to contain significant detritus because sample D1, of similar appearance and the only successful analysis on Series D, showed elevated ^{232}Th levels. The pink layers within the crust and on its surface are evident only on the upward facing parts. They indicate some kind of rain-out, in the near-static water, of particles from above which were probably released from poorly-indurated or non-indurated terra rossa from the paleokarst fills exposed in the cave walls above the crust sample site.

The outermost pink layer is deposited on top of a thin "skin" which covers the whole surface. For sampling series A and B, this was cleaned off first so that A1 and B1 were taken from 1 mm beneath the top surface. Samples Ca and D1 included the "skin". Analytical results, discussed in detail below, show that these two samples are anomalous in many respects.

The calcite is unusually hard. To sample a layer a slot was cut with the small disc drill and the piece knocked off with a hammer. The U concentration had already been determined by alpha counting to be 3.3 - 4.5 ppm so that only 0.3 g was required for mass spectrometric analysis.

8.2.2 The analysis:

A total of four runs were made. Unfortunately, during the summer of 1989

the vacuum pump to the detector unit was turned off accidentally. The effect was generally deleterious but also somewhat random; most thorium runs were poor but the occasional one was excellent, thus the error was not quickly detected. Runs A (10 April 1989) and C (10 May 1989 and 12 Dec 1989) gave acceptable results but runs B and D (June 1989) were generally unacceptable.

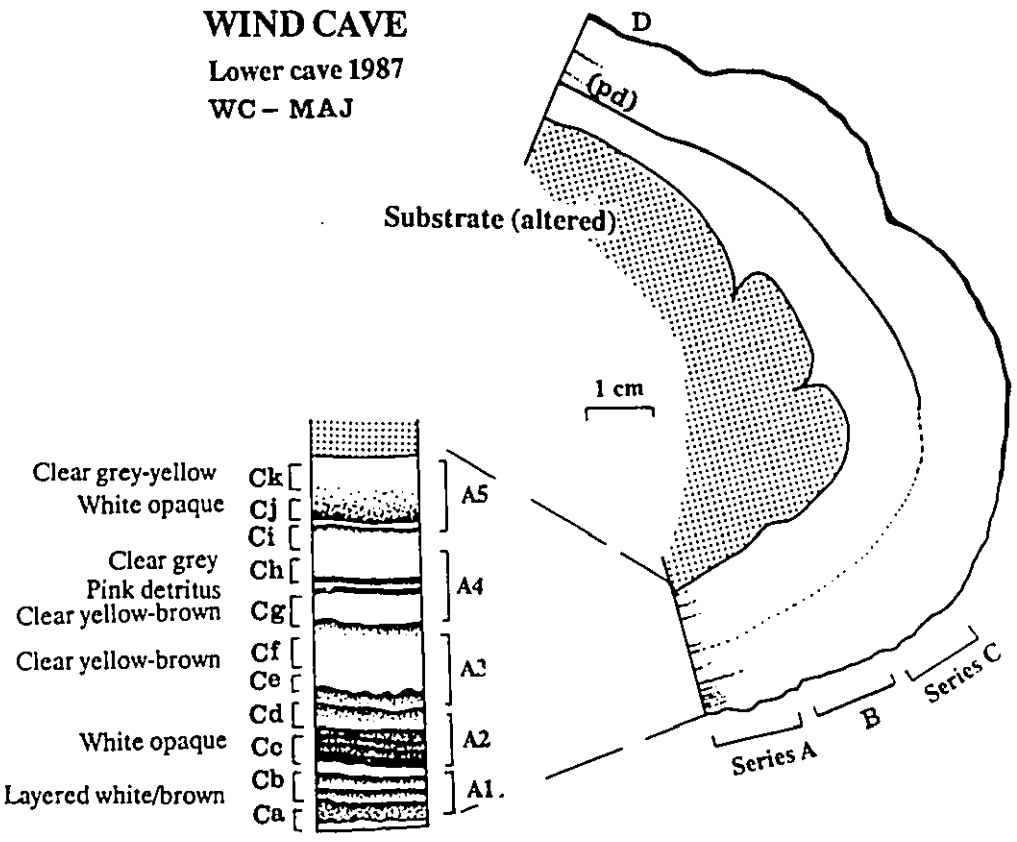

Figure 8.4: DIAGRAM OF SECTION OF WC-MAJ SHOWING SAMPLING SITES. The sample is shown in the correct orientation with respect to the vertical. Sampling series D was taken from the top side, the other three series from the cleaner underside. The layer of pink coloured detritus (which is the same colour as the altered substrate) is marked as (pd); it is not so obvious on the underside. The stratigraphic section shows the visible layering and colour changes. Note that, because this is a section of the underside, the oldest layers are towards the top of the diagram. Details of the sampling series A and C are shown to either side of the stratigraphic section. The section is only 20 mm in thickness: Series A was sampled every 4 mm, and Series C every 2 mm.

Table 8.3: WC-MAJ analytical data

Sample	Uppm	$^{234}U/^{238}U$ Current	$234U/^{238}U$ Initial	$^{230}Th/^{234}U$	Age (kyr)	-2σ	$+2\sigma$
Run A							
A1	4.27	1.66	2.07	0.859	171	-2.0	+2.1
A2	4.11	1.67	2.11	0.872	177	-3.8	3.9
A3	3.69	1.64	2.11	0.909	195	-3.4	+3.5
A4	4.23	1.55	2.07	0.966	232	-8.2	+8.7
A5	4.53	1.45	2.02	1.019	289	-14	+15
Run C							
Ca	4.30	1.66	1.96	0.747	131	-2.7	+2.8
Cb	4.21	1.68	2.08	0.840	163	-3.7	+3.8
Ce	4.14	1.65	2.08	0.871	177	-2.1	+2.1
Cf	3.34	1.64	2.16	0.934	208	-5.2	+5.5
Cg	3.97	1.59	2.12	0.958	225	-3.7	+3.8
Cg,h	4.23	1.54	2.06	0.969	236	-3.5	+3.6
Ci,j	4.48	1.47	2.05	1.019	286	-16	+19
Ck	4.27	1.46	2.10	1.037	311	-12	+13
B1	4.26	1.68	2.07	0.835	161	-2.1	+2.1
D1	3.93	1.64	1.97	0.797	148	-1.9	+1.9

The sampling sites are shown on Figure 8.4, and the analytical data in Table 8.3. The full table of results is given in the appendix. Series A, sampled every 4 mm, gave a general growth trend. Series C was then sampled at a higher density, every 2 mm, as a check to see if the trend for A could be replicated and to see if the visible stratigraphy was mirrored in variations in growth rate or some other characteristic. Series B and D were sampled to see if samples from the same growth layer, determined visually, would give the same date.

One important, general point emerges from the data: samples which appear to be in the same stratigraphic growth layer show a clear difference in age (because this sample grew so slowly). Samples A1 and B1 were taken side by side but the dates differ by 10,000 years (~6%). Similarly Ca and D1 differ by 17,000 years (~12%). These differences do not reflect analytical non-reproducibility: a repeat analysis on a separate sample of Cf reproduced the date to within 0.6%. This illustrates the need for very careful sampling and scrupulous recording of precise

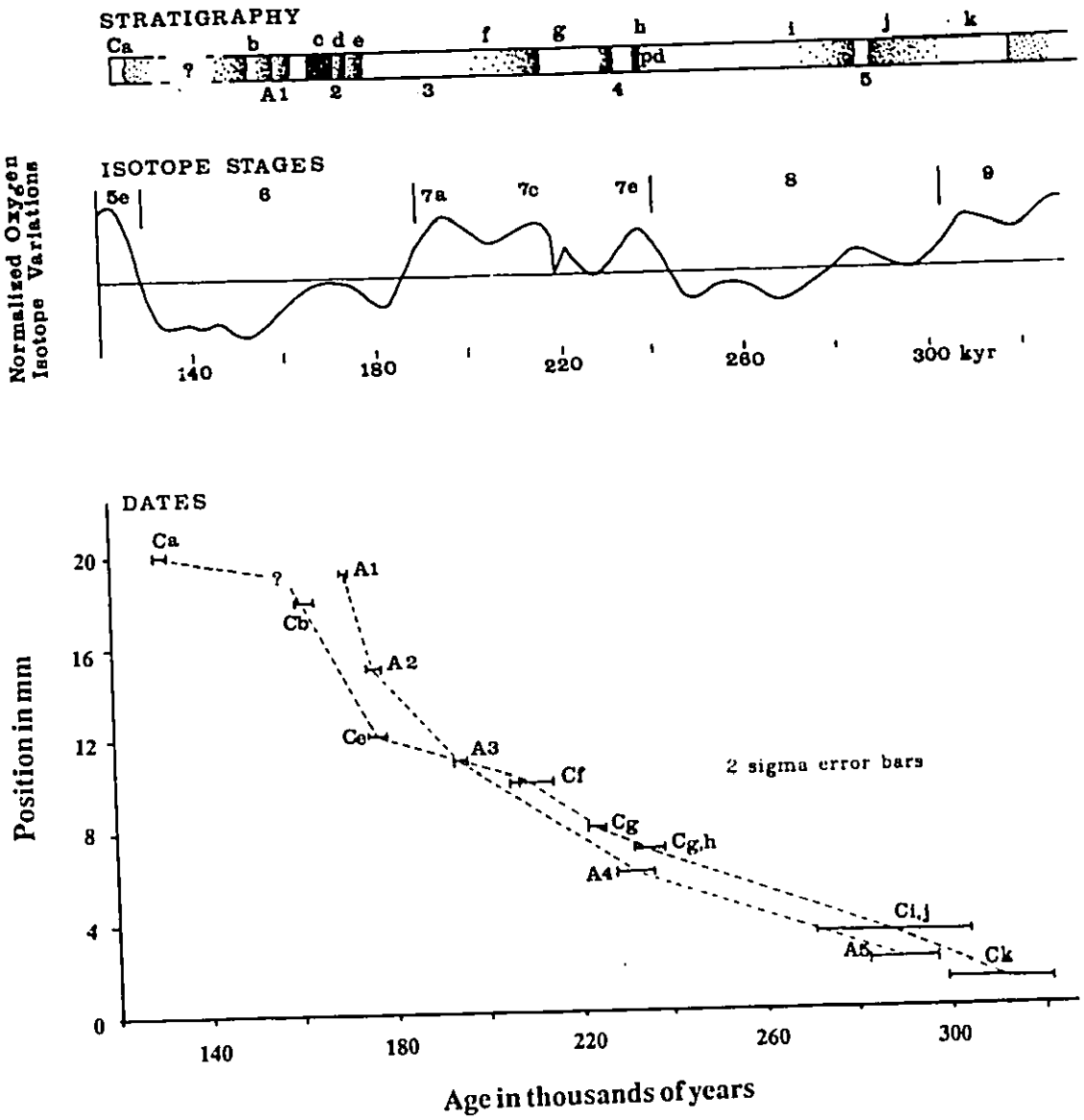

Figure 8.5: DATES FROM SERIES A AND C, AND FORAMINIFERAL OXYGEN ISOTOPE VARIATIONS. Dates are shown (with 2σ error bars) in relation to position in the stratigraphic sequence above the substrate. Dashed lines connect the samples in each series to show continuous deposition. The break and question mark between Ca and Cb marks a possible break in deposition. The oxygen isotope curve (from Imbrie et al 1984) shows variations in $\delta^{18}O$ of ocean foraminifera, around a mean normalized to zero. The stratigraphic section of WC-MAJ is plotted against time: the denser layers are associated with the period of rapid deposition around samples A1 to A2 and Cb to Ce.

sample location, particularly in slow growing samples and if other types of analyses such as oxygen isotopic analyses are to be correlated with the dated samples. Furthermore, it has implications for the technique of isochron dating where several samples from the same growth layer are analyzed to correct for detrital contamination. In an extremely slow growing sample such as this it may not be possible to sample correctly along a single growth layer.

8.2.3 Growth Rates:

The dates for the top and base give a measure of the growth rate. The dates in between should all be in chronological order and should show a sensible pattern of growth. Figure 8.5 shows the dates for runs A and C. These present a closely parallel pattern, with all the ages in chronological order. Sample Ca appeared to be anomalous (see below) and so was not used to estimate the general growth rate. This part of the wall crust grew to about 20 mm thickness in approximately 150,000 years i.e. 1 mm in ~7500 years or 0.133 mm / kyr. This is consistent with the alpha counted estimate of growth rates for other samples of wall crust of 0.15 mm / kyr (Bakalowicz et al 1987, Ford unpublished results).

8.2.4 Drainage of the aquifer:

The date on the youngest layer indicates the earliest possible time for drainage of that part of the cave which is currently 50 ± 5 m above the modern lake level. The youngest layer is sample Ca at 131 kyr B.P. This estimate agrees well with the mean trend of the paleo-water table determined from numerous alpha counted dates (the dashed line in Figure 8.6): at an elevation of 45 - 55 m, drainage occurred at ~110 - 140 kyr B.P. However, because samples Ca and D1 appear to be anomalous, it might be more appropriate to choose Cb, 160 kyr B.P., as the more accurate indicator of the date of draining. This is older than the mean trend but within the range of oscillatory behaviour during the Penultimate glaciation (Ford, unpublished results in prep.).

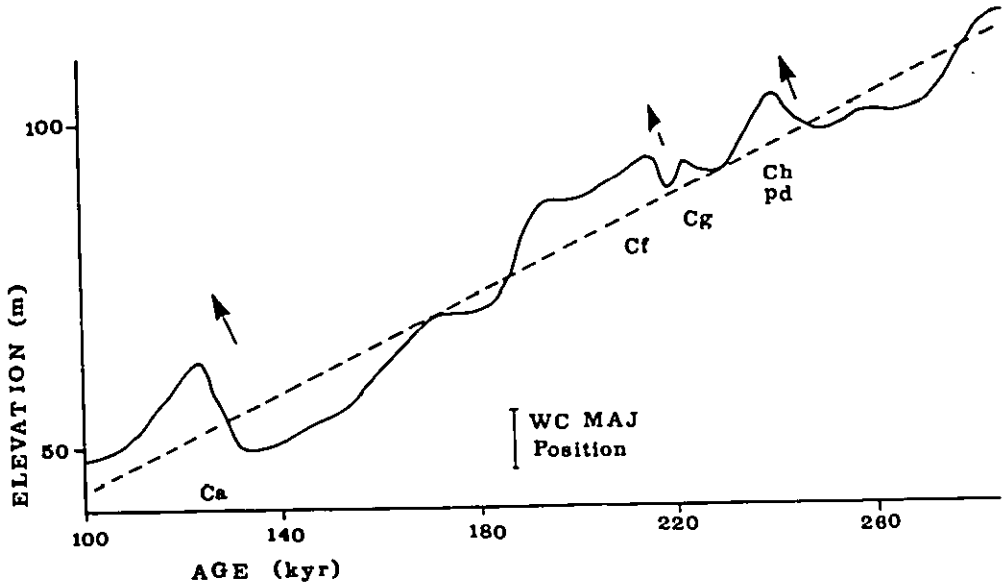

Figure 8.6: POSSIBLE BEHAVIOUR OF LAKE LEVEL. The general slope of the water level drawdown (dashed line) is taken from Ford (1989 unpublished, in prep.). The alpha counted dates from numerous deposits throughout the cave indicate that water level oscillated as it was retreating, although the extent of oscillation is not known. During glaciations this area is likely to have been cold and dry so the water level is likely to have been low. During interglacials it rose again. The oxygen isotope data are taken as an indication of glacial and interglacial conditions. These have been superimposed on the general drawdown line to give the solid line which shows how the cave water level may have changed. The arrows highlight periods of possibly rapid rise. The rise at ~240 kyr B.P. may have caused the release of the detritus associated with sample Ch (the "pd" layer).

8.2.5 Model for growth:

Bakalowicz et al (1987) point out that in most sites of hydrothermal deposition through degassing in Budapest thermal caves precipitation is intense down to 2 m below the paleowater tables but reduced to zero at depths greater than ~10 m. These caves are well ventilated and thus the degassing is very rapid. Wind Cave degassing rate would have been considerably slower so that the precipitates are not so clearly zoned. WC-MAJ shows continuous deposition over a range of 140 kyr. Using the general rate of paleowater level retreat reported by Ford (unpublished, in prep), this range of ages suggests that precipitation in Wind Cave began about 70 m below the water surface.

The pattern of accelerating growth and sudden cessation fits a degassing model admirably. A possible interpretation of WC-MAJ is as follows:

1. During Isotope stage 9 (pre-300 kyr B.P.) this part of the cave was beneath the zone of calcite deposition: i.e. it was too far from the water surface for any degassing to produce supersaturation. At this depth the water was probably causing alteration of the substrate material instead.
2. During the isotope stage 8 glacial the water level fell so that deposition of sub-aqueous crust began, although at the very slow rate of approximately 1 mm in 15 kyr.
3. Continued decline of the water surface during the isotope stage 7 interglacial brought this elevation closer to the surface zone of rapid degassing. The rate of deposition of wall crust accelerated to approximately 1 mm in 7 kyr.
4. The penultimate glaciation which started in isotope stage 6 coincided with the final very rapid lowering of the water table. This produced a thick layer of wall crust at a rate of approx 1 mm in 5 kyr.
5. The water table remained below WC-MAJ level until the end of the penultimate glaciation. At the start of the Sangamon interglacial the water rose briefly and deposited the final skin.

8.2.6 Stratigraphy:

The layered character of this crust is clear (Fig. 8.4 - the density of stippling indicates density of layer) but very fine, so that it was impossible to sample cleanly within a single layer. Thus the relationship between the visible layers and the sample analyses is not clear cut: only a little information can be gleaned from the stratigraphy. Samples Cb to Ce and A1 to A2, the more dense opaque white layers, correlate with the more rapid deposition. If the rate of deposition is always related to depth of water (and if deposition is controlled only by degassing then this will be true) then the gradations in density may represent minor changes in water level, the more dense layers reflecting slightly lower water. The general trend of water level

retreat, 0.375 m per thousand years, shown as the dashed line in Figure 8.6, is clear from numerous alpha counted dates (Ford, unpublished data, in prep.). This relates to changes in hydraulic gradient caused by increase in the porosity and permeability of the sandstones and to the lowering of the outflow spring position (Bakalowicz et al 1987). However, the alpha dates also indicate that the water level oscillated as it retreated. During glaciations this area is likely to have been cold and dry. Thus the water level would have dropped. The opposite would have occurred during the interglacials. Variations in ocean foraminiferal oxygen isotopes can be taken as a gauge of climatic change. A rough indication of the behaviour of the water surface can be estimated by superimposing the isotopic variations onto the general rate of water level retreat. This yields periods of rising water, stable water and falling water (the solid line on Figure 8.6). There is some slight indication that the stratigraphy and water level may be rather tenuously interrelated. The layer of pink detritus corresponds to the first period of water level rise after a long period of stable or falling levels. Similarly the pink coating on the outermost skin may be caused by the change to rising water levels at isotope stage 5e after a long period of stable or falling levels.

8.2.7 Anomalous samples, Ca and D1:

Samples Ca and D1 were taken from the outermost, surface "skin" of WC-MAJ. In almost all respects these two samples show anomalous behaviour (see Figure 8.7). They both have ^{232}Th levels significantly higher than the rest of the sample and closer to the ^{232}Th levels normally found in meteoric water speleothem. Figure 8.7, D clearly shows how samples D1 and Ca are offset from the main trend of the data: their uranium concentration is lower than would be expected from their initial $^{234}U/^{238}U$ activity. Their current $^{234}U/^{238}U$ activity (Figure 8.7, E) is lower than might be expected from the trend of the rest of the data. This abnormal behaviour points to either a marked change in the chemistry of the waters causing the deposition of the outermost "skin" or a change in the chemistry of the calcite

during the years after deposition. The second option is the more likely: the reduced total U concentration and ^{234}U activity suggest uranium leaching. These samples from the exposed outer layer could easily have been leached over the ~125 kyr since their exposure. If this is true then the ages calculated may be slightly too old.

8.3 CURRENT $^{234}U/^{238}U$ ACTIVITY, INITIAL $^{234}U/^{238}U$ ACTIVITY AND URANIUM CONCENTRATION

Initial $^{234}U/^{238}U$ activity and uranium concentration vary over time in a complex, and complementary, fashion (Figure 8.7, A and C) with initial $^{234}U/^{238}U$ activity inversely related to U concentration. They display roughly sine wave forms. The plot of initial $^{234}U/^{238}U$ against U concentration (Figure 8.7, D) shows a clear inverse relationship (with the exception of two anomalous surface samples D1 and Ca). Neither appear to relate in any way to the rate of deposition of calcite. When these variations are set against the foraminiferal oxygen isotopic variations (Figure 8.7, B) it becomes apparent that the patterns of change for uranium activity and concentration appear to be related to isotopic stages: glacial periods (250 -300 kyr B.P. and 130 - 180 kyr B.P.) correspond with periods of high U content but low ^{234}U activity, while the interglacial (180 - 240 kyr B.P.) coincides with the period of low concentration and high ^{234}U activity.

8.4 MODELS OF AQUIFER BEHAVIOUR

In order to explain or model this behaviour the general geography has to be discussed. Figure 8.8 shows the cave in relation to the local base level (the outlet springs) and the recharge area (the Black Hills). The waters in the cave are recharged from meteoric waters which circulate at much greater depth through granitic rocks before emerging at the outlet springs. The granitic rocks are probably the source of the uranium. The model(s) proposed below postulates that the local hydrology has a significant effect on the chemistry of the ground waters.

Figure 8.7: VARIATIONS OF URANIUM CONCENTRATION AND $^{234}U/^{238}U$ ACTIVITIES. 2σ error bars are included for both axes. Note that the high error on the initial $^{234}U/^{238}U$ activity is a function of the error on the date more than the error on the ratio measurement.
Figure 8.7, A and C demonstrate the complementary changes of initial $^{234}U/^{238}U$ and U concentration over time.

Figure 8.7, B shows the oxygen isotope variations for ocean foraminifera (Imbrie et al 1984) over the same time scale. It is clear that the colder phases during isotope stages 6 and 8 are associated with higher U content and lower ^{234}U activity while the warmer interglacial phase at isotope stage 7 is associated with the lower U content and high ^{234}U activity. The curves for A and C are fitted by hand. The solid line in A (curve J) takes samples Ca and D1 into account. However, these are possibly anomalous so the more correct curve is represented by the dashed line (H). The curve in C is not constrained to pass through Ca and D1. The arrow shows the direction in which D1 may have been altered.

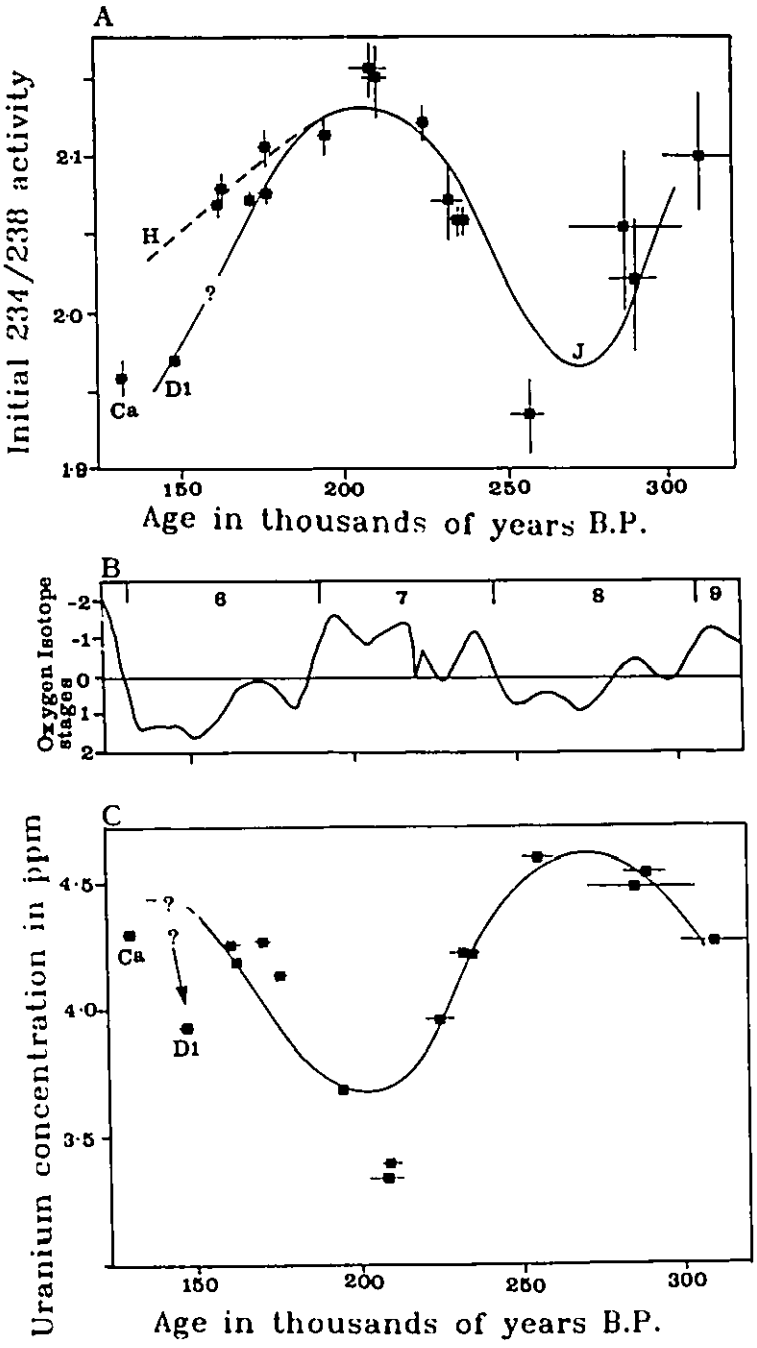
A
Initial 234/238 activity
2·1
2·0
1·9
H
?
Ca
D1
J
150
200
250
300
Age in thousands of years B.P.
B
Oxygen Isotope stages
-2
-1
0
1
2
6
7
8
9
C
Uranium concentration in ppm
4·5
4·0
3·5
?
Ca
D1
150
200
250
300
Age in thousands of years B.P.

Figure 8.7, D shows the negative relationship of initial $^{234}U/^{238}U$ and U concentration. Samples D1 and Ca are clearly offset from the general trend; arrows show the trend of possible alteration. The log relationship has a correlation coefficient of 0.92, a linear relationship would have an r value of 0.84.

Figure 8.7, E illustrates how the measured $^{234}U/^{238}U$ ratio changes with time. Here, Ca and D1 are not so clearly distinct from the remainder of the data. Dashed line K gives the theoretical change over time from an initial $^{234}U/^{238}U$ ratio of 2.06 (the average initial ratio for all the samples). The data do not fit this line well. Dotted line J shows the fit if the values for curve J from Figure 8.7, A are used - this includes Ca and D1. Solid line H fits the remaining data better.

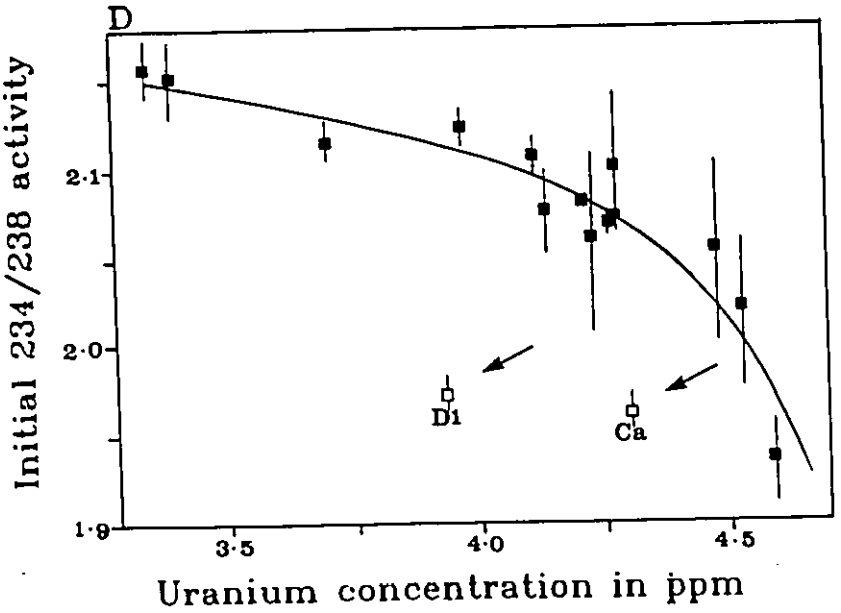
D
Initial 234/238 activity
2·1
2·0
1·9
3·5
4·0
4·5
D1
Ca
Uranium concentration in ppm

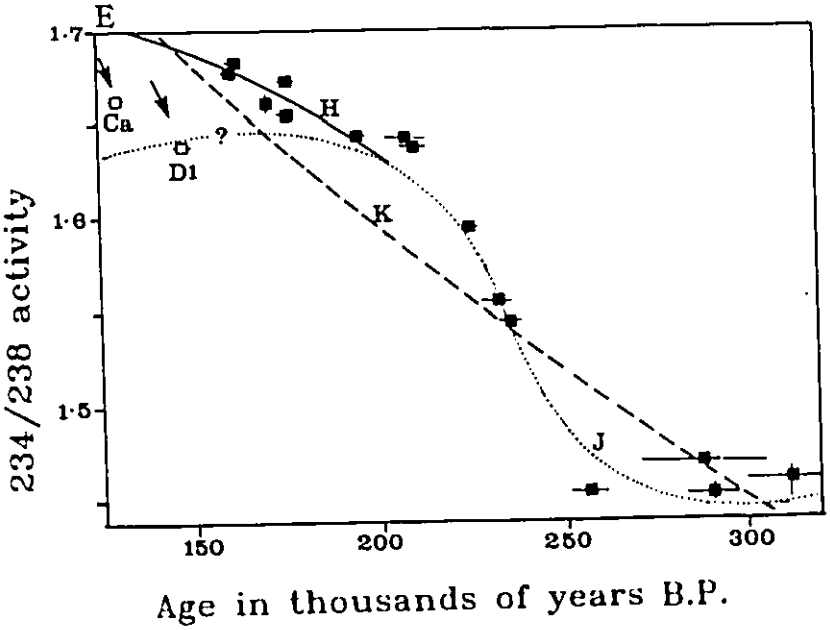
E
1·7
1·6
1·5
234/238 activity
Ca
D1
?
H
K
J
150
200
250
300
Age in thousands of years B.P.

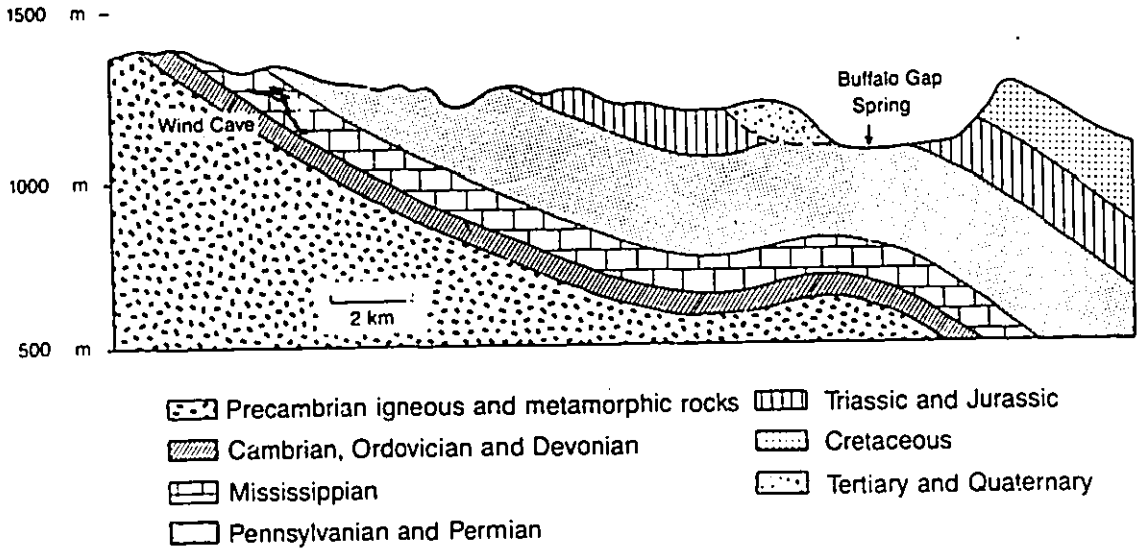

Figure 8.8, A: GEOLOGIC SECTION SHOWING WIND CAVE IN RELATION TO OUTFLOW POINT, BUFFALO GAP SPRING (from Bakalowicz et al 1987).

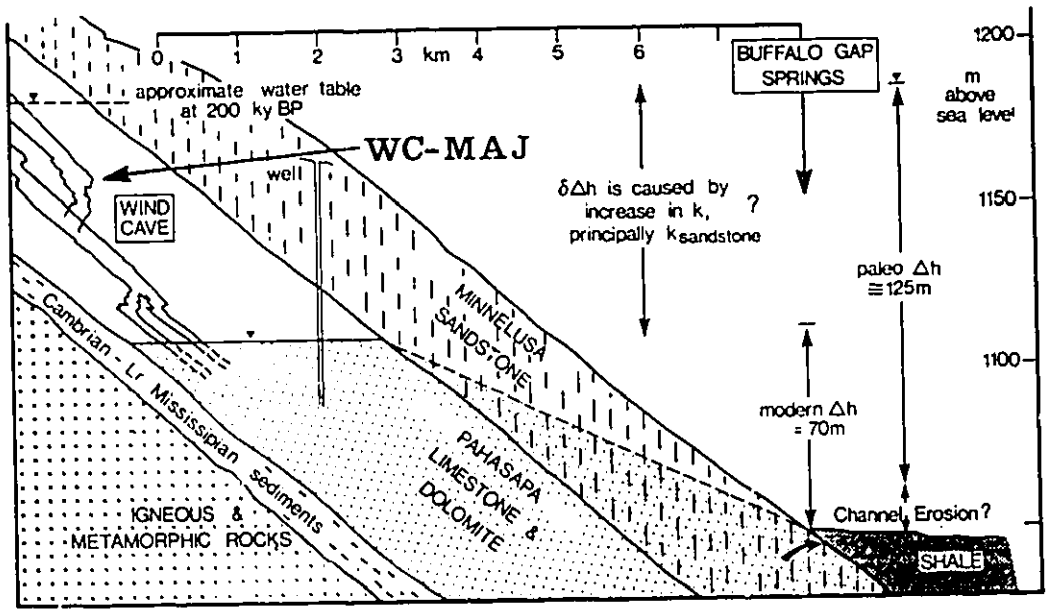

Figure 8.8, B: DIAGRAM OF WIND CAVE HYDROLOGY (from Ford, unpublished, in prep.). Location of WC-MAJ is included.

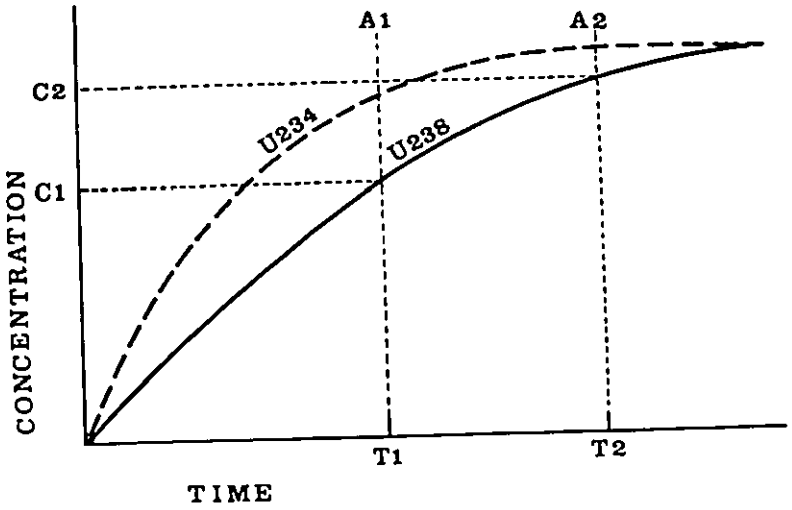

Figure 8.9: SCHEMATIC ILLUSTRATION OF RESIDENCE TIME AND SOLUTION KINETICS MODEL. The x-axis is residence time of ground water on its route through the source of uranium, the granitic rocks. For the purposes of this model, the water is assumed to have an initial U concentration of zero and an initial $^{234}U/^{238}U$ of 1.00. T1 shows the short residence time of the interglacial waters which are recharged relatively quickly and have a fast flow-through time; T2 indicates the longer residence time of the glacial waters. The concentration, on the y-axis, is not to the same scale for ^{234}U and ^{238}U: ^{238}U will be in much greater abundance. The solid curve shows the solution of ^{238}U, slowly reaching equilibrium. In time T1 the waters have reached a ^{238}U concentration of C1. Glacial waters of longer residence time continue to dissolve ^{238}U until at T2 they have reached concentration C2. The change in activity levels is caused by the faster solution kinetics of ^{234}U. The heavy dashed line shows the approach of ^{234}U towards its equilibrium concentration. At T1 the ratio of ^{234}U and ^{238}U is relatively high; at T2 it is low.

Varying conditions over the course of the glacial-interglacial cycle modified the local hydrology. The hydraulic gradient, and thus the local elevation of the water table in the cave, is a function of the elevation of the outlet spring, the porosity and permeability of the aquifer and the conditions of recharge. Over the relatively short term of one glacial-interglacial cycle the first two effects can be taken to be constant or changing in a steady manner, so that they cannot explain the oscillatory behaviour of the uranium concentration and ^{234}U activity. The conditions of recharge are the most likely to fluctuate rapidly. The resultant changing water levels will have no direct effect on the rate of deposition of the subaqueous crust since this was far

below the water surface for much of its period of growth. However, the changing recharge conditions may have a strong effect on the chemistry of the groundwaters from which the crust is precipitated.

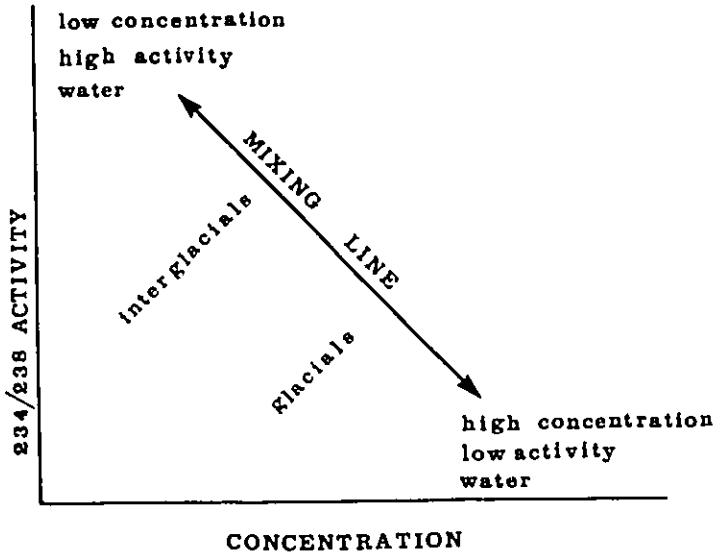

Figure 8.10: SCHEMATIC ILLUSTRATION OF MIXING MODEL. The upper left and the lower right of the graph represent the two end members of the mixture. The low concentration, high $^{234}U/^{238}U$ activity water on the upper left is the shallow, younger meteoric water which picks up excess ^{234}U from the weathered surficial zone through which it passes rapidly. The high concentration, low activity water on the lower right is the deep groundwater slowly circulating in contact with ^{234}U and ^{238}U from the granite. During interglacials the higher recharge rate causes a greater proportion of shallow water compared to deep water; the composition of the groundwater from which WC-MAJ was precipitated moves towards the left. The opposite happens during glacial periods.

The change in uranium concentration can be explained by a simple model of changing recharge in response to changing climate. The high concentrations during glacial stages reflect the low rate of recharge and ensuing longer residence time of the water on its flow paths. Increased recharge during the interglacials causes more rapid flowthrough and thus shorter residence time in contact with the source of uranium. This is shown diagramatically in Figure 8.9 and is more fully explained in the figure caption.

To explain the change in initial $^{234}U/^{238}U$ activity requires further development of the model. Differences in the residence times of the groundwater

will exploit differences in the kinetics of solution of ^{238}U (solid line in Figure 8.9) and ^{234}U (dashed line). Water of short residence time is more likely to pick up the more soluble isotope. Thus the residence time of the water controls the $^{234}U/^{238}U$ ratio: recharge waters of short residence time during interglacials have a higher proportion of ^{234}U, long residence time waters a lower $^{234}U/^{238}U$ ratio, closer to that of the source rock (~1.0).

This simple model does explain the pattern of variation but the changing residence time may be only one aspect of a larger, more complex story. For example, the hydrology may not be so simple. Instead of treating the water as a single unit it may be more correct to view it as a two component mixing system: the ground water body may consist of (i) deeply circulating, long resident waters of meteoric origin mixed with (ii) greater or lesser proportions of shallow meteoric waters of short residence time. The first water will have a high concentration of uranium of $^{234}U/^{238}U$ ratio close to that of the source granitic rocks, as discussed above. The shallow meteoric water will spend little time in contact with the granitic rocks. Instead its principal uranium source will be the surface weathered zone, which is an important source of ^{234}U excess (Osmond and Cowart 1982). Thus the second component of the ground water will have a high $^{234}U/^{238}U$ activity ratio although the total uranium concentration may be low. The varying patterns of U concentration and ^{234}U activity may then be explained by a mixing model: varying proportions of the two components contribute to the final mix from which the calcite crust is deposited. During wetter interglacials the proportion of shallow meteoric water increases, thus diluting the more concentrated deep waters but contributing high levels of ^{234}U. During drier glacial times the shallow meteoric waters form a much smaller proportion of the ground water mix so that the composition is closer to that of the deep waters alone.

Studies of changes in $\delta^{13}C$ and $\delta^{18}O$ of the calcite precipitates over time are being carried out at present and may support this mixing model: deep waters will have a composition averaging older meteoric waters while surface waters will reflect

shorter term recharge and may differ in $\delta^{18}O$. $\delta^{13}C$ values may differ due to glacial / interglacial shifts in plant cover.

Chapter 9

RAT'S NEST: 881010

881010 is a sample of stalactite from Rat's Nest Cave, Bow Valley, Rockies, Alberta which was collected by Dr. C.J. Yonge.

Rat's Nest Cave is located in a spur on the north side of the Bow Valley, Rocky Mountains, Canada (see Figure 9.1, the location map). Figure 9.2 is a diagrammatic section from south to north to show the cave in relation to the Bow Valley. It is the eighth longest cave in Canada and is developed in the Livingstone Formation limestones and controlled in part by a thrust fault and major bedding planes. The known passages hint at a much larger drainage complex related to the now extinct Bow Glacier (Yonge 1990). The cave is a relict phreatic system with little evidence of any vadose phase. It is richly decorated with a variety of speleothem many of which exhibit re-solution textures. The cave has many other deposits of great potential interest to geomorphologists, biologists, prehistorians, etc.

9.1.1 Significance of sample:

Sample 881010 shows repeating units of speleothem deposition and erosional hiatuses with some deposition of mud. The site of the cave is such that valley glaciers in the Bow valley may have obstructed drainage from the cave causing flooding (see Figure 9.2). This would explain the intermittent erosional hiatuses. It is postulated that the sample thus contains a record of the sequence of valley glaciation. The dating of this record would be an important contribution to the study of the glacial history of the Rockies. The site is very close to the margin of the ice-free corridor, the belt of land that may have been largely ice-free during maximum Pleistocene glaciations (Rutter 1984). It was hoped that the growth layers in Sample 881010 would record oscillations of the ice margin coincident with the waxing and waning of Rockies glaciers.

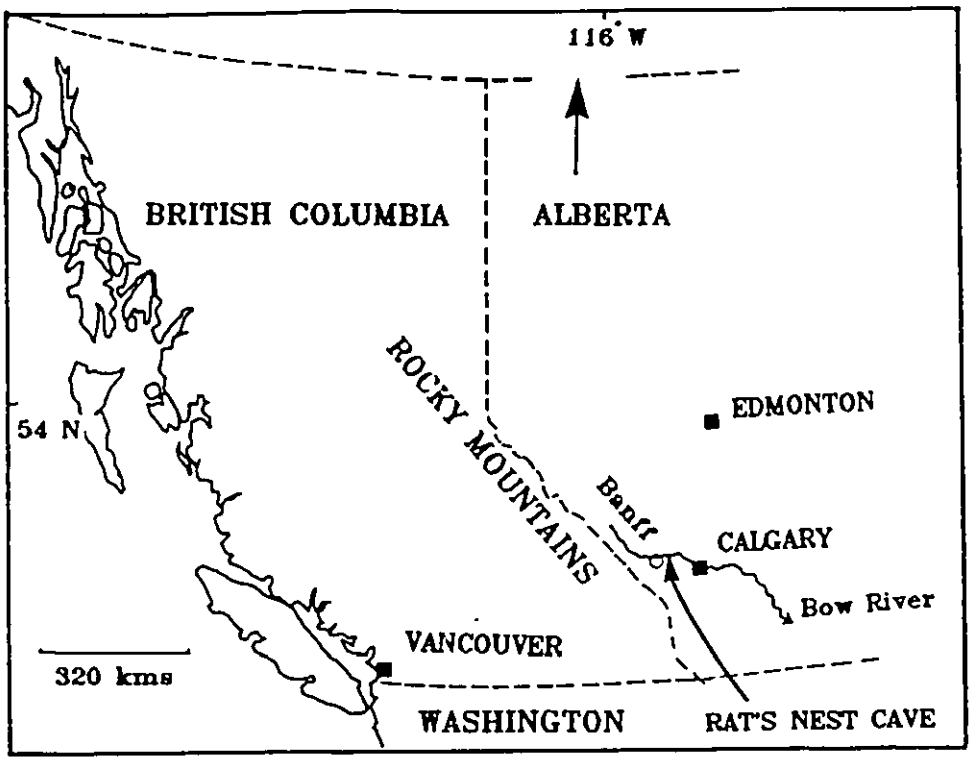

FIGURE 9.1: LOCATION MAP FOR RAT'S NEST CAVE.

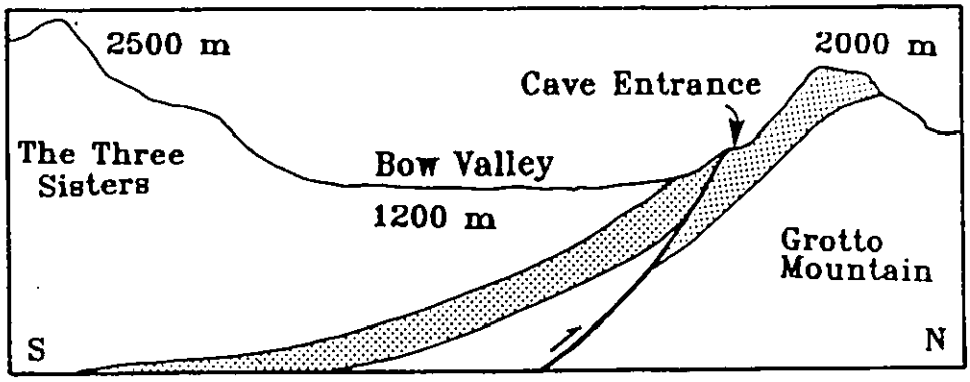

FIGURE 9.2: DIAGRAM OF THE CAVE IN RELATION TO THE BOW VALLEY. The cave is developed in the limestones of the Livingstone Formation of Mississippian age (shaded). Its form is guided by bedding planes and the thrust fault. The elevations are included to demonstrate how glacial advance in the Bow Valley may block drainage from the cave. The ensuing flooding events may have caused the hiatuses and re-solution apparent in many of the speleothem.

FIGURE 9.3A: PHOTOGRAPH OF 881010 (underside of piece IV).

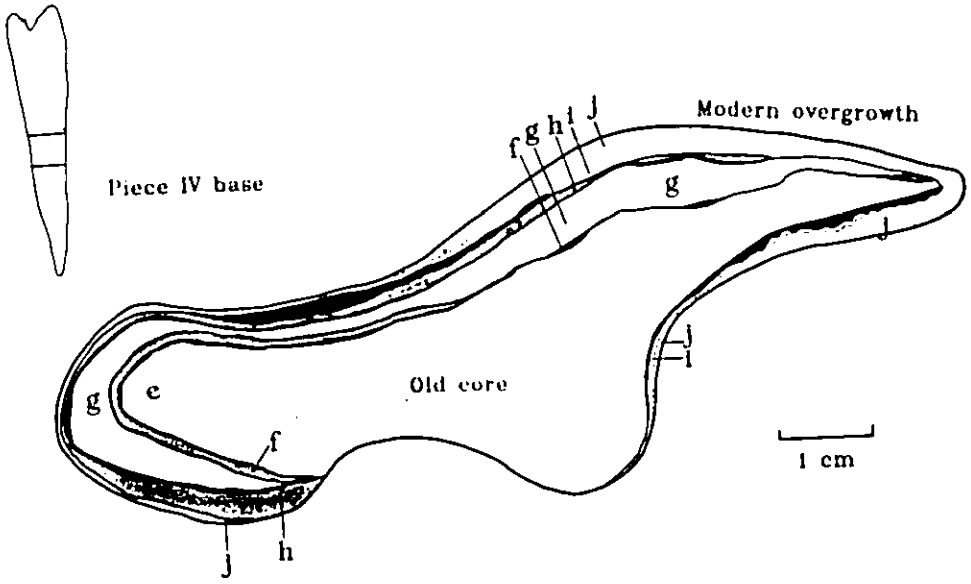

FIGURE 9.3B: DIAGRAM OF 881010 (underside of piece IV, as in photograph).

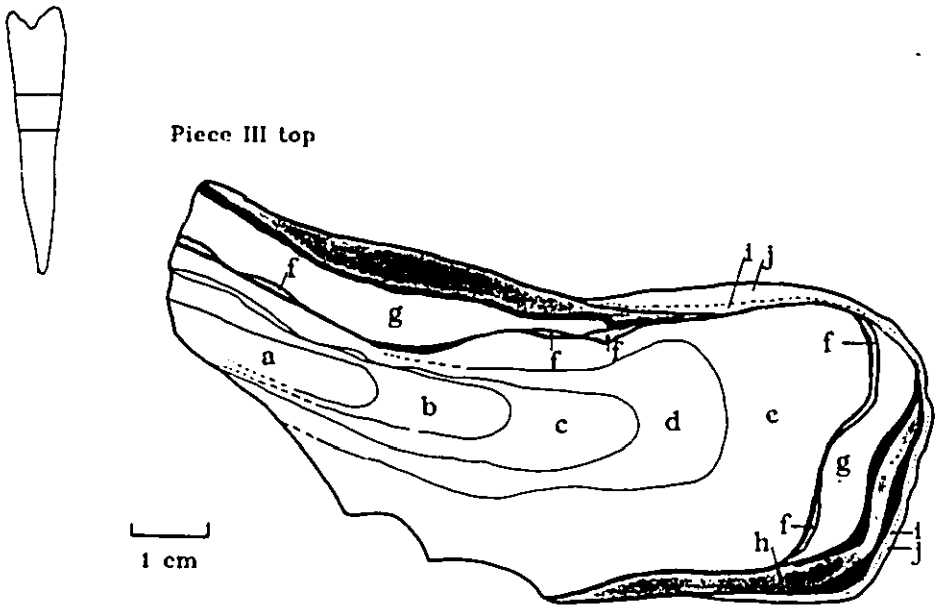

FIGURE 9.3C: DIAGRAM OF 881010 (top of piece III).
The hiatuses with mud are shown as solid black. Alternate growth layers are shaded in order to clarify the sequence of events. The letters refer to the growth layers.

9.1.2 Sample description:

This stalactite is made up of an old core showing some growth lines surrounded by three thin layers of calcite separated by erosional hiatuses. It had fallen from its growth position and suffered considerable erosion by runnels. Some parts were then covered with a modern overgrowth of calcite.

The sample was supplied in the form of slices: Piece I was at the presumed top of the stalactite, Piece V at the tip. Figures 9.3A, B and C show the visible features of Pieces III and IV. Alternate layers are shaded to clarify their relationships. The hiatuses and their mud fillings are shown in solid black.The stratigraphy of flood events is most clearly visible on the underside of Piece IV; the growth lines in the old core are most clearly visible on the topside of Piece III.

The "old core" is of clear dark brown calcite grading outward to yellowish, more opaque calcite. Four growth lines are discernible separating growth layers labelled "a" to "e". During the first hiatus much of the old core was removed. Three more hiatuses interrupt the growth of this sample. The final layer, "j", is a modern overgrowth of clean white calcite on top of the broken speleothem fragment.

9.1.3 Stratigraphy:

Dates are shown in Table 9.1.

1. Initial calcite growth was in four repeated sequences of dark brown clear calcite grading up into fawn coloured opaque calcite terminated by a white growth line: Layers A, B, C and D. The white growth lines are probably not weathering hiatuses because they are visible in only one part of the sample.

2. Substantial deposition of clear brown calcite: Layer E. This layer was dated at 385 kyr. B.P.

3. Erosional hiatus followed by detrital deposition.

4. Renewed stalactite growth of dark grey clear calcite, Layer F. Only a sliver is still intact. This layer was too small to date any of it.

5. Erosional hiatus marked by some detritus.

6. Growth of dark grey, clear calcite, Layer G. The oldest part was dated at 215 kyr B.P. and the youngest at 211 kyr B.P. (disregarding the questionable dates on the highly detrital samples G2 base* and G2 top*).

7. Erosional hiatus marked by some detritus.

8. Thin layer of dark grey, clear calcite, Layer H. No satisfactory date was obtained on this layer: the date on H1base* is questionable because of the high detrital content.

9. Erosional hiatus with substantial mud/sand detritus layer (some has been washed out to leave a void)

10. Thin outer crust of dull cream coloured calcite, Layer I. It is too thin to sample.

11. Breakage from roof.

12. Erosional hiatus.

13. Overgrowth of white calcite on uppermost surfaces, Layer J, dated at 3.8 kyr B.P.

Table 9.1. Rat's Nest Speleothem sample 881010.

Dates are given in kyr B.P. Ages are shown uncorrected for detrital contamination. The terms "base" and "top" in the sample names refer to the oldest and youngest part of the layer.

Sample	Th/U age and 2σ range	$^{234}U/^{238}U$ activity	U/U age and 2σ range
Ancient core			Initial U/U = 2.1
B		1.24	533 (499-565)
C	Infinite	1.23	556 (521-588)
D	Infinite	1.29	469 (434-502)
E base	371 (299-558)#	1.31	448 (413-480)
E mid		1.30	458 (424-490)
E top	385 (359-418)	1.37	
----------Hiatuses 1 and 2----------			
G2base*	212 (209-215)	1.88	
G2 b1	215 (209-220)	1.93	
G2 t1		1.94	
G2 top	211 (209-214)	1.93	
G2top*	116 (115-117)	2.29	
----------Hiatus 3----------			
			Initial U/U = 2.7
H1base*	157 (155-159)	1.91	220 (216-224)
H1 mid	1.90		223 (218-227)
Hiatus 4			
Jbase*	3.8 (3.7-3.9)	2.80	
J top		2.79	

high error
* sample with high detrital content. Detrital contamination seems to have an unexpected effect on the ages: the contaminated samples are younger than their less contaminated counterparts. This suggests that the detritus has contributed excess uranium which overrides the effect of any excess ^{230}Th.

9.2 RELATIONSHIP TO ISOTOPIC RECORD

Figure 9.4 shows the pattern of deposition and hiatuses in relation to the marine foraminiferal oxygen isotope record for the last 400 kyr. The solid line is the record from Imbrie et al (1984) and the dotted line the slightly shorter one from Martinson et al (1987).

In general the information obtained by dating the growth layers is rather unsatisfactory. Only the samples from the clean middle parts of layers gave good

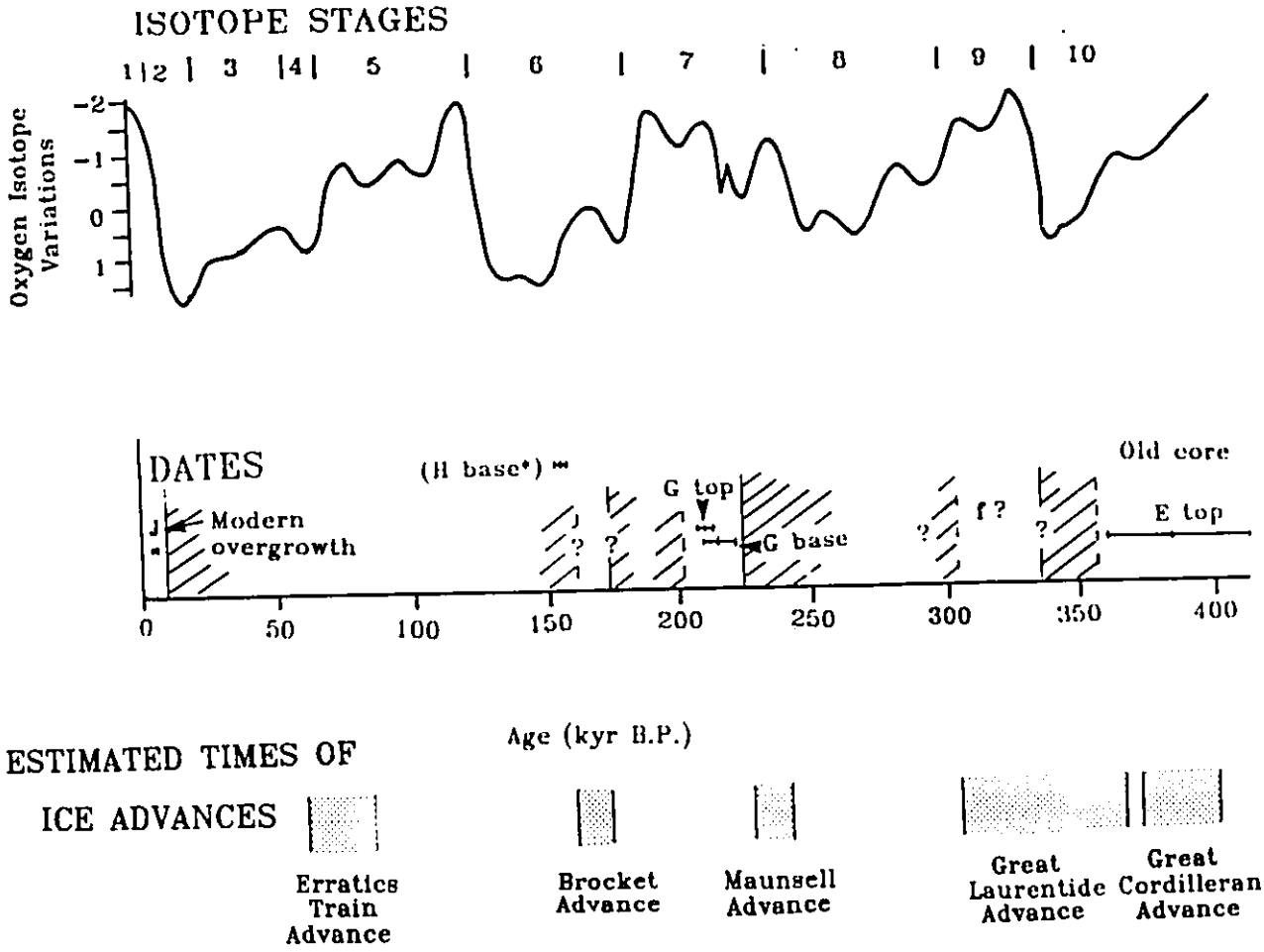

FIGURE 9.4: DATES ON 881010 IN RELATION TO THE ISOTOPE RECORD. The solid line shows variations in the oxygen isotopic signature from marine foraminifera from Imbrie et al (1984). The dotted line shows the shorter record of higher resolution from Martinson et al (1987).

The dates from 881010 are plotted with 2σ error bars. The cross-hatched zones are very tentative estimates of periods of non-deposition which may represent periods when glaciers filled the valley. The lower part of the diagram shows periods of ice advance (modified from Rutter 1984) which have been estimated from geomorphological evidence in the area.

dates. Those samples close to hiatuses showing detrital contamination gave unreliable dates.

The date on the youngest part of layer E is reliable. This indicates uninterrupted growth from an unknown starting date until the isotope low at the end of Stage 10. If we assume an initial $^{234}U/^{238}U$ ratio for this sample of 2.1 (from the good date on E top) then layer B can be dated at ~534 kyr B.P. on the basis of its present day $^{234}U/^{238}U$. The growth rate from this U/U dating would then give a date on the centre of the core around 650 kyr B.P..

The next reliable date is from the lower part of layer G which corresponds to the middle of interglacial isotope stage 7. Between these two dates are two hiatuses and one growth layer (F). These have been tentatively indicated on Figure 9.3. The placing of layer G during isotope stage 9 is based on a guess that growth was more likely during an interglacial period.

Two samples from the top of layer G were dated. The one was clean and the other showed detrital contamination. Surprisingly this one gave a younger date than the clean sample. If the initial $^{234}U/^{238}U$ ratio from the clean sample is used for U/U dating of the dirty sample then its age is 208 kyr B.P..

The only date obtained on layer H is unreliable because it shows detrital contamination. If this date follows the behaviour shown in sample G top then it is too young. For this reason it is shown in brackets in Figure 9.3 and the growth layer shown to correspond with the small isotope high at stage 6.5, nearest to the date on H. However, H may equally likely have been deposited at stage 7.1. If the initial $^{234}U/^{238}U$ ratio from sample G top is used then the U/U date on H base is 220 kyr and on H middle is 223 kyr B.P.. Since this would put H out of chronological order the estimate of initial U/U must be wrong. This indicates that the U/U ratio of the drip must have changed after the hiatus (as is quite common).

No further growth occurred (or if it did then all evidence has been eroded) until the final modern overgrowth, layer J.

9.3 RELATIONSHIP TO THE GEOMORPHOLOGICAL RECORD IN THE LITERATURE

Rutter (1972) recognised three, and possibly four, Wisconsinan glacial advances in the Bow valley. If any evidence for these existed in stalactite 881010 then it has been completely lost to re-solution. 881010 contributes nothing to the problem of dating the Wisconsinan advances. However, it does contribute some information about pre-Wisconsinan glaciations.

Bow Valley is now at an elevation of ~1200 m (4000 ft.). Rutter (1984) presents a diagram of glacial advances and retreats according to elevation set against an estimated time frame. The information relevant to the Rat's Nest Cave area has been plotted in Figure 9.4 underneath the record as indicated by 881010. There are three points worth noting:

1. According to Rutter's diagram the whole area was ice-free from earlier than 600 kyr B.P. up to ~400 kyr B.P.; it was then ice covered until ~300 kyr B.P. (first by the Cordilleran advance and then, after a very short break, by the Great Laurentide advance). The continued deposition of the core of 881010 until ~360 kyr B.P. suggests that this early ice-free time should be extended.
2. The dates from the oldest part of layer G of 881010 coincide with the ice-free time after the Maunsell Advance.
3. The uncorrected date on layer H coincides with the ice-free stage after the Brocket advance. Better dates on layer H are needed to fix this ice-free period.

9.4 CONCLUSION

The only firm conclusions which may be drawn are:

(i) that the old core grew until at least 359 - 418 kyr B.P.;

(ii) that layer G grew during the isotope stage 7 interglacial;

(iii) that the overgrowth is modern.

The surviving layers are too thin and the uranium concentration too low (at ~0.2 ppm) to permit more detailed resolution of the deposition events. Nevertheless,

these are unexpectedly good results from a small specimen that suffered many episodes of re-solution. The cave contains similar eroded deposits in some abundance (Dr. C. J. Yonge, pers. comm. 1989) and clearly has the potential to become a very important Quaternary site in the Rocky Mountains. Dating of other samples may elucidate the timing of the Wisconsinan advances for which evidence exists in the surface geomorphology. These cave calcites are particulary valuable as paleoenvironmental indicators because they contain information about earlier glaciations for which little clear evidence remains on the surface.

Chapter 10:

OTHER CARBONATES: CARLSBAD CAVE CALCITE RAFTS, OSTRICH EGGSHELLS, CORALS

10.1 CARLSBAD LAKE OF CLOUDS, CALCITE RAFT MATERIAL

(Samples 87 CLC / JRH -1.0 ft. and 87 CLC / JRH -2.0 ft.)

These samples, supplied by John Roth (staff geologist), are of calcite raft debris interspersed with lake deposits from the Lake of Clouds area, Carlsbad Caverns.

Calcite rafts are precipitates of $CaCO_3$ which float on the surfaces of pools. They form when the water becomes supersaturated with respect to $CaCO_3$ due to the loss of CO_2. Jones (1989) classified rafts according to form and crystal structure. Crystals nucleate on dust particles and then grow into thin films over the surface of the water. Rafts are commonly made up of a paper-thin micrite core onto which are rooted zoned spar calcite, on one or both sides of the core, making up a raft up to 0.5 mm thick. When the raft gets too heavy to float it sinks to the floor to form debris of white powdery material. The dust on which the crystals initially nucleate may be detrital or organic and may introduce some problems of initial ^{230}Th which may interfere with dating of calcite raft debris.

Figure 10.1 shows a diagrammatic view of the sample location. The rafts were collected from the wall of a 25 cm diameter corrosion shaft drilled through the raft debris by a persistent acidic condensate roof drip. Alpha counting on the lower layers had established a gradient of age versus depth but the two top layers (minus 0.30 m and minus 0.61 m) either would not run or gave an infinite age, although they were expected to be between 50 and 100 kyr old. A sample of calcite raft material from the surface of the nearby cones (10 m distant) gave a very good alpha counted date of 50 kyr B.P. (Table 10.1).

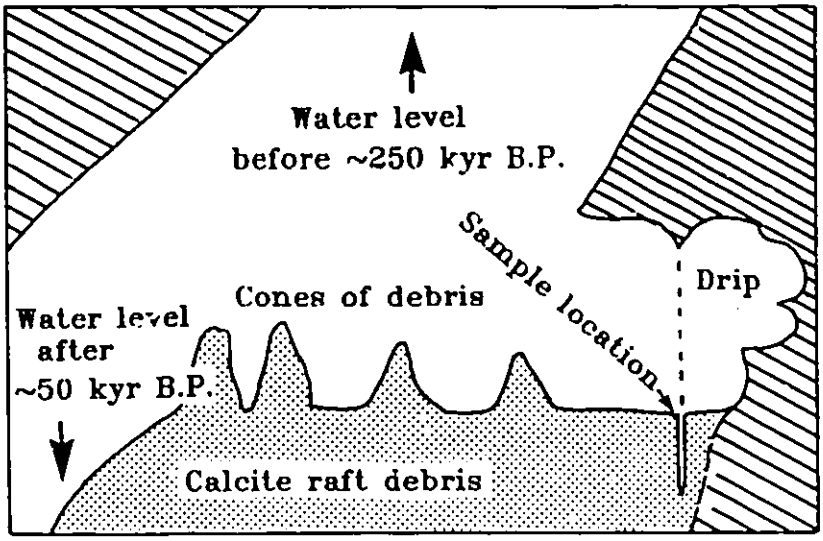

Figure 10.1: CALCITE RAFT DEBRIS, DIAGRAM OF SAMPLE SITE.

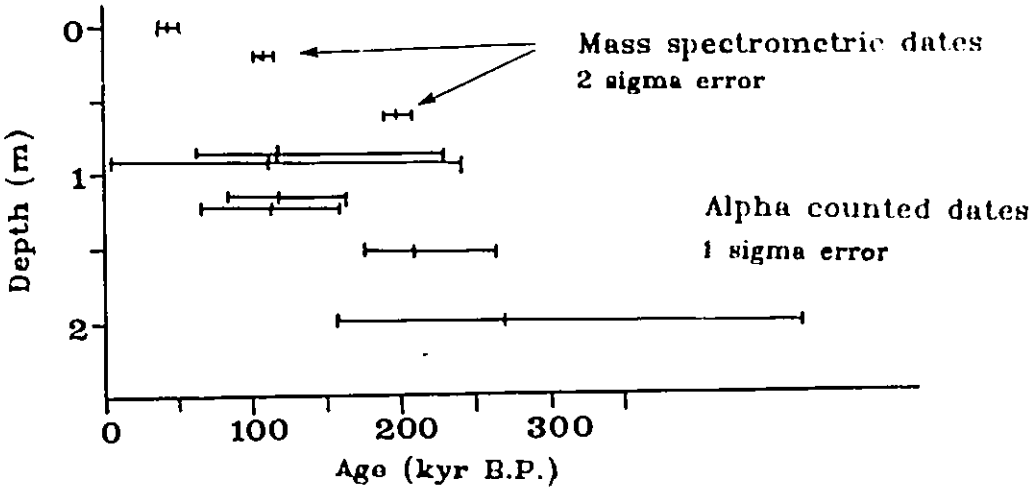

Figure 10.2: DATES ON CARLSBAD CALCITE RAFT MATERIAL. The two mass spectrometric dates are added to the alpha counted dates.

Conclusion:

Figure 10.2 shows both the alpha counted dates and the mass spectrometric rsults. The mass spectrometric dates do not fit into the expected pattern suggested by the trend of the lower samples dated by alpha counting: they are too old. These alpha counted dates could not be confirmed by MS because the samples were used up.

Two explanations are tenable. The position of the samples in relation to the local environment of the cave is shown in Figure 10.1. Calcite rafts form only on the surface of still waters. In order to become deposited underneath an overhanging roof (as is the case here) the water level must have been lower than the overhang to allow the rafts to float in. The alpha counted dates on the lower part of the sedimentary body suggest that water level was beneath the overhang by about 250 kyr BP, and that sedimentation continued at a steady rate until approximately 100 kyr B.P.. The water level must have remained close to this position until the upper layers of raft material had been deposited. If the date of 50 kyr on the youngest sample is correct then water level fell after this; i.e. water level was virtually stable for ~175 - 200 kyr. The line of best fit through the alpha counted dates (ignoring the error bars) yields a mean accumulation rate of 0.78 cm / kyr. The relationship has a correlation coefficient (r) of 0.92. If the error terms on the ages are ignored then the relationship is very strong. The simple model originally envisaged presumed that sedimentation would continue in the same straightforward manner and that the dates on the upper two samples would be younger than for the lower samples. Then the gradation in dates would give a rate of accumulation.

If this model is assumed then the mass spectrometric dates can be combined with the alpha counted dates in order to yield an accumulation rate. In this case the strength of the relationship decreases to an r value of 0.75 and the accumulation rate becomes 0.65 cm / kyr.

An alternative approach is to presume that the older dates on the topmost, mass spectrometrically dated, layers indicate a change in the process of deposition.

The most likely explanation is that older material was swept in by an underwater landslide. The nearby calcite raft cones indicate that local underwater relief was significant. After several thousand years of unequal deposition on the cones compared to under the overhang the slope angles on the cones may have increased to an unstable point. Landsliding then occurred and transferred the older materials from the buried layers of the cones to the topmost layers underneath the overhang.

Table 10.1 Dates on Carlsbad calcite raft material.

Alpha counting results (1σ error):

Depth	Date (kyr B.P.)
1.98 m	268 +202 -118
1.52 m	207 +48 -33
1.22 m	115 ±47
	122 +48 -33
0.91 m	114 ±123
	120 +112 -56
0.61 m	>350
0.30 m	>350
	302 +57 -90
0.15 m	>350

Mass Spectrometric dating results:

Sample 87 CLC / JRH, - 0.30 m:
Run 1 115,430 -1758 +1758 (2σ) 0.76% 1σ error

Sample 87 CLC / JRH, - 0.61 m:
Run 2 199,219 -8203 +10547 (2σ) 2.35% 1σ error

Comments:

The samples were of calcite raft debris in sand sized particles. They were dirty yellow/white in colour and appeared to contain a lot of detritus. In fact the insoluble content was minor, the ^{232}Th counts were not particularly high and the normal thorium procedure was used rather than the two stage detrital procedure. The high background is most likely to have been caused by soluble organics which were not fully oxidised during the acid dissolution stage. Large sample sizes (~8 g) were necessary because of the low uranium levels. The analyses cannot be repeated because the samples are exhausted.

It was later realised that these analyses were done when the VG354 was not running properly and that some of the variability may be attributable to machine error.

10.2 OSTRICH EGGSHELLS

Two groups of ostrich egg shell samples were supplied by H.P. Schwarcz: the first, for experimentation, were almost modern, the second were believed to be c.100 - 200 kyr old fragments from a sequence of lake deposits in Bir Tarfawi and Bir Sahara, Egypt. These analyses were a small part of a larger study on the carbonates of Bir Tarfawi and Bir Sahara which is reported in Schwarcz and Morawska (in prep., 1990). The complex of lake deposits in this now dry area indicates a time of wet conditions. It would be of interest to know which isotope stage corresponded to these conditions. It was hoped that the dating of the eggshells would indicate this.

In order to oxidize organics the samples were treated by repeated dissolution in acid and drying. Experiments with the modern shells indicated that uranium runs are more sensitive to the presence of organics than are thorium runs: the uranium is more easily lost during chemical preparation.

The old eggs have extremely high U concentrations when compared to the modern eggs, being around 5 ppm for the old, but only around 0.06 ppm for the young eggs. This suggests that U was taken up after death. However the dates agree with those measured on calcareous marl from the area. It is concluded that the U uptake was completed soon after death and the eggs remained as closed systems since then. The extreme aridity of the site greatly improves the chances of closed system behaviour in these highly porous media. Other shells in more vulnerable locations may not be datable. The thorium concentrations for the young and the old eggs were about the same at around 30 ppb.

The results, Table 10.2, are of rather low precision caused by low counts on ^{230}Th. Larger sample sizes would probably alleviate this. A full table of results is presented in Appendix 5.9.

The average age using corrected values for samples 41 and 44 is 130 ± 13. The range suggests that the eggs were deposited over the period 122 to 136 kyr B.P.. This straddles the boundary of isotope stages 6 and 5e, between the close of

the penultimate glaciation and the peak of the following interglacial.

Table 10.2: Dates on eggshell fragments from Bir Tarfawi and Bir Sahara. The numbers marked with an asterisk show the ages corrected by assuming an initial $^{230}Th/^{232}Th$ activity ratio of 1.7.

Sample	Age	-2σ	+2σ	234/238 Act.	Initial 234/238	U conc ppm	% error 1σ
41	129	8.1	8.9	0.74	0.63	0.48	3.3%
	126*	7.9	8.6		0.63		
42	136	6.2	6.7	0.74	0.61	6.94	2.4%
43	122	2.8	2.9	0.74	0.64	4.28	1.2%
44	135	4.1	4.4	0.74	0.62	5.28	1.6%
	134*	4.1	4.3		0.62		

However, using all the ages is not necessarily advisable because they are not equally reliable. Samples with detrital contamination usually give a falsely old date. The correction for detrital contamination is dubious because it relies on an assumption of an initial $^{230}Th/^{232}Th$ ratio. Thus the dates on samples 41 and 44 may not be trustworthy. Sample 42 had a high error on the thorium run (1.14%). Sample 43 is the most credible date because it did not have detrital contamination and the error on the thorium run was moderate, at 0.5%. This suggests that the deposits date from the middle of isotope stage 5e, the last interglacial.

The initial $^{234}U/^{238}U$ activity ratios show an average of 0.626 ± 0.021 using the corrected values. This provides an estimate of initial $^{234}U/^{238}U$ for U/U dating of other carbonates (see Schwarcz and Morawska). These ratios are extremely low. It is more common for ratios to be greater than unity (Osmond and Cowart 1982). Since all of the eggshells give a similar initial ratio it must be presumed that this low value existed for some time. Similar low values are observed in coeval marls of the enclosing lake deposits. The problem of low initial $^{234}U/^{238}U$ values is hard to explain. Schwarcz and Morawska suggest that these values may reflect a short-lived extreme departure from a normally higher ratio, such as might occur from a sudden flooding of a previously depleted aquifer. Another possible explanation relates to aquifer porosity. If an aquifer is old then its secondary porosity and permeability may

be high. ^{234}U is more soluble in groundwater than ^{238}U, so the ^{234}U is removed preferentially. This usually results in a high $^{234}U/^{238}U$ activity ratio in the groundwater. However, if the porosity is so high that each ^{234}U atom is removed as soon as it is made, then the activity of ^{234}U in the groundwater is limited by the rate of production rather than the solubility. This would result in groundwaters of low $^{234}U/^{238}U$ ratios.)

10.2.1 Conclusion:

These results, from very small samples of shell, are encouraging. They demonstrate that U-series dating of certain eggshells has potential if the diagenetic history of the samples is known. Further work on other samples from these sites may allow more definitive paleoenvironmental reconstruction.

10.3 CORALS

Coral dating was not a major part of this study; samples were dated simply to check its feasibility.

The first successful mass spectrometric U-series dating was carried out on corals by Edwards et al (1986/87, 1987 and 1988) and Edwards (1988) in the Cal Tech laboratory. The samples were prepared with great care; the results were clearly reproducible. Even very young corals (from the earlier parts of this century) could be accurately dated. Several points of interest in this work are discussed below.

The samples were broken up into little pieces, picked over by hand, ultrasonically cleaned, and the largest ones chosen for processing. This procedure is more rigorous than has been used in the current study. Much of the non-reproducibility of my dates can be attributed to contamination during sampling. A new sampling area is to be prepared for future work.

Edwards et al used separate samples and separate spikes for U and Th runs. The ratios are calculated from the concentrations of ^{230}Th, ^{234}U, etc. Errors on age were as low as 0.5% 2σ for 10 kyr old coral and < 1% for 50 - 500 kyr corals. They

note that corals older than 600 kyr are not distinguishable from infinity at the 2σ level. The separate preparation of U and Th samples seems to be of no particular benefit. Separate loading of different proportions of each fraction achieves the same object. Given normal running conditions, the errors in this thesis are of comparable size.

Edwards et al calculated the initial ^{230}Th in corals of known age (already dated by another means) and concluded that the assumption of initial of zero ^{230}Th was valid for them. They tested for closed system assumptions by (i) dating the same, young sample in several different ways (^{14}C, growth band counting); (ii) dating different parts of the same coral, for samples older than ~200 years, to check that all the ratios measured were the same; (iii) looking at the broken grains by eye and at polished etched surfaces by S.E.M. to check for the characteristic cleavage of calcite; (iv) measuring Mg and Sr levels by A.A.S. (calcite. with 120,000 ppm Sr, 800 ppm Mg and ~13 n moles U / g, has more Mg and less Sr than aragonite).

None of these measures have been taken in this study. For any future work they should be adopted where possible.

Edwards et al compared initial $^{234}U/^{238}U$ ratios of the dated corals with sea water to see if there is any evidence of alteration in the corals. The $^{234}U/^{238}U$ atomic ratio of sea water is $6.258 \pm 0.012 \times 10^{-5}$ (activity = 1.144 or $\delta^{234}U = 144$). In corals they found slightly higher ^{234}U activity than open water ($\delta^{234}U$ of 149 - 174) but not enough to prove alteration. They concluded that this range was consistent with closed system evolution.

Edwards et al investigated the possibility that $^{234}U/^{238}U$ of sea water has changed over the time elapsed since the older corals were formed. They concluded that shifts of the order of tens of δ-units (one δ-unit is 0.001 activity ratio units) over ~100 kyr might be possible. Any greater differences than this in old corals must therefore be diagenetic.

They also compared $^{232}Th/^{238}U$ of the corals with that of open water as a further check on diagenesis. The $^{232}Th/^{238}U$ atomic ratio should be $3.7 \pm 0.2 \times$

10^{-5} (i.e. an activity ratio of $1.18 \pm 0.06 \times 10^{-5}$). Any large shifts away from this would indicate Th or U addition during diagenesis. The range in corals is 0.35×10^{-5} to 17.2×10^{-5} (activity range of 1.116×10^{-6} to 5.486×10^{-5}); they suggest that any major shift greater than this indicates either that the coral did not form in normal open ocean water or it has experienced diagenesis.

10.3.1 Coral 75036:

This sample was run to practice chemical procedures and mass spectrometer runs. 75036 was the only large sample of coral available at McMaster. It was presumed to be of last interglacial age. It was not tested for alteration.

Samples 1b, 1d and 1f were taken from a series drilled from consecutive growth layers. They are probably only a few years apart in age and might be expected to yield the same dates. The suffix BA indicates that the sample was boiled in acid under reflux for 6 hours; NA means no special acid treatment.

Table 10.3: Dates on coral 75036. (The full table of data is in the appendix.)

Sample	Age (kyr)		U ppm	Th ppb	Initial	232/238 U Uage
		2σ range			234/238	Activity
1bBA	143	-2.0 +2.0	2.55	6.82	1.161	8.35E-4 155
1dBA	147	-2.1 +2.2	2.41	1.79	1.168	9.97E-5 145
1dNA	199	-2.1 +2.2	2.37	0.79	1.193	2.28E-4 146
1fBA	320	-10 +11	1.47	2.36	1.277	4.95E-4 140

Table 10.3 presents results. Samples 1bBA and 1dBA just overlap at the 2σ range. Samples 1dNA and 1fBA clearly have some contamination, acquired either during sampling or during chemical preparation. The U concentration is noticeably lower for 1fBA, which suggests some organic chelation of sample U (but not of spike U) and inadequate oxidation.

The initial $^{234}U/^{238}U$ ratios of samples 1dNA and 2fBA are extraordinarily high, which suggests significant diagenetic alteration (possibly U loss). If the U/U dating program is used with an assumed initial $^{234}U/^{238}U$ value of 1.1666 the dates on the last two samples are closer to the first two samples. The initial $^{234}U/^{238}U$ ratio of the first two samples is higher than that of normal seawater, 1.144, but close

enough to assume closed system evolution. Edwards et al (1986/87) found that their corals ranged from 1.149 to 1.174. The fact that corals have this range of initial $^{234}U/^{238}U$ ratios has implications for those studies where the initial $^{234}U/^{238}U$ ratio is assumed to be the same as seawater. In this example an assumption of 1.14 as the initial $^{234}U/^{238}U$ ratio gives ages of 94, 83, 85 and 79 kyr B.P. for the four samples (about 30% error).

The $^{232}Th/^{238}U$ ratios of all of these samples are higher than the range reported by Edwards.

The general pattern of the results suggests either considerable diagenesis of this particular coral specimen or else contamination during processing.

10.3.2 Sample 790513-2 from Harmon et al 1983:

This is a sample of Diploria coral quoted by Harmon et al 1983 as:-

Aragonite content:	100%
U content:	2.7 ppm
$^{234}U/^{238}U$ activity ratio:	1.06
$^{230}Th/^{234}U$ ratio:	0.70
$^{230}Th/^{232}Th$ ratio:	27
Age:	127 ± 18 (2σ) kyr BP.

Samples M1 to M7 were run on 23/7/89 during the time when the detector vacuum was faulty. Only three gave acceptable results. This series was intended to determine the optimum sample size for coral dating. The samples were treated for organics using the following sequence:- (i) dissolve in 7 N HNO_3, (ii) evaporate to dryness, (iii) dissolve in concentrated HNO_3, (iv) dry, (v) dissolve in aqua regia, (vi) dry, (vii) dissolve in 7 N HNO_3, and (viii) dry.

The results are shown in Table 10.4. The principal conclusions are:-

1. The effect of sample size is hard to determine in view of the failing detector vacuum. M3 is the best run so one might conclude that less than 1 g is the best sample size.

2. The poor runs may be partly explained by low ^{232}Th counts causing problems for focussing. A solution might be to add ^{232}Th in the form of thorium standard which

contains no ^{230}Th.

3. The reproducibility of the age is only 5%. This probably reflects a need for more meticulous care during sampling or during chemistry.

4. The initial $^{234}U/^{238}U$ ratio is very close to that of sea water and within the limits suggested by Edwards et al. This suggests closed system evolution. The $^{232}Th/^{238}U$ activity ratio of sample A is just outside the limits specified by Edwards et al, suggesting slight alteration of this sample. Its higher age tends to confirm this suspicion.

Table 10.4: Results for 790513-2 coral. (Full table of data in appendix.)

Sample	Weight (g)	Age kyr	Error -2σ	Error $+2\sigma$	U ppm	Th ppb	Initial $^{234}U/^{238}U$	$^{232}Th/^{238}U$
A	0.4	127	-2.9	+2.9	2.95	0.58	1.15	5.78E-5
M3	0.75	118	-0.9	+0.9	2.99	0.31	1.15	2.83E-5
M4*	1.09	121	-4.8	+5.0	3.02	0.40	1.15	3.77E-5
M6+	2.42	123	-7.5	+8.0	3.00	0.46	1.15	4.42E-5

Average age (excluding A): 120.7 ± 5.8 kyr B.P.

Average initial $^{234}U/^{238}U$: 1.149 ± 0.004
Average ppm U: 2.99 ± 0.05
Comparison with data from Harmon et al 1983:
Age 127 -18 +18
U ppm 2.7

* Abnormal $^{235}U/^{238}U$ ratio, high error.
+ High error.

10.3.3 Coral samples D3 and VI:

These samples are from an underwater reef on the north shore of Jamaica (supplied by Lynton Land to H. P. Schwarcz).

In order to test the idea that the low ^{232}Th levels may contribute to focussing problems, some pure ^{232}Th was added to samples D3A and V1A in the form of thorium standard solution. This explains the absence of data for Th ppb and $^{232}Th/^{238}U$ activity for these two samples. These two runs were quite successful, but

so were the runs where thorium standard had not been added. The conclusion was that the levels of ^{232}Th had little effect in this case and that the restoration of the

Table 10.5: Results for D3 and VI corals.

Sample	Age (kyr)	U ppm	Th ppb	Initial $^{234}U/^{238}U$	$^{232}Th/^{238}U$ Activity
18/11/89 D3A*	138 -2.7 +2.8	3.24	1.200		
21/11/89 D3B	133 -1.3 +1.3	3.20	0.44	1.189	3.84E-5
18/11/89 D3C	132 -1.5 +1.5	3.20	1.80	1.189	1.72E-4
Average age: 132.42 +/-1.72 (1.3% reproducibility)					
28/10/89 VIA	126 -1.8 +1.9	3.48		1.160	
18/11/89 VIC	125 -1.2 +1.2	3.48	0.26	1.175	1.90E-5
Average age:	125.28 +/-0.93 (0.7% reproducibility)				

* Sample D3A has a higher initial 234/238 activity ratio than the other two dates on D3, and its age is outside their range. The average is taken from D3B and D3C.

detector vacuum was more important to the run than ^{232}Th levels.

The initial $^{234}U/^{238}U$ of sample D3, at 1.19, is outside the limits recommended by Edwards, suggesting diagenesis. The $^{232}Th/^{238}U$ activity for sample D3B is also outside the range.

Sample VI is within the ranges for both initial $^{234}U/^{238}U$ (1.16) and $^{232}Th/^{238}U$. No diagenesis is presumed.

These samples were recovered during dredging of a channel through the submerged reef north of Discovery Bay, Jamaica, in water of < 10 m depth. They are believed to represent the last high sea stand, isotope stage 5e. The most reliable date, on sample VI, 125 kyr B.P., clearly corresponds to the stage 5e isotope peak at ~120 - 128 kyr B.P. The less reliable date, on the probably altered sample D3, 132 kyr B.P., slightly pre-dates the isotope peak. Altered samples will almost always yield a falsely old age: another early date on a completely reliable sample would be required before any conclusions can be drawn about the timing of the sea level rise.

Chapter 11

FUTURE RESEARCH AND CONCLUSION

11.1 FUTURE RESEARCH ON TECHNIQUES

11.1.1 Apportioning the error:

The final error of the age estimate is made up of the combined effect of errors on four ratios: the spike $^{229}Th/^{236}U$ ratio and the measured ratios $^{236}U/^{238}U$, $^{234}U/^{236}U$ and $^{229}Th/^{230}Th$. For table 11.1, the total error is calculated using typical 2σ error values for each of these ratios: 0.32% on $^{229}Th/^{236}U$, 0.08% on $^{236}U/^{238}U$, 0.30% on $^{234}U/^{236}U$ and 0.50 on $^{229}Th/^{230}Th$. If one of these errors is removed then its effect on the total can be gauged: the separate contribution from each of these is shown in Table 11.1 below.

Table 11.1 Apportioning the error.

Error on $^{236}U/^{238}U$	0.5%
Error on $^{229}Th/^{236}U$	17%
Error on $^{234}U/^{236}U$	29%
Error on $^{229}Th/^{230}Th$	53%

The greatest contribution comes from the error on the $^{229}Th/^{230}Th$ ratio. If this is halved (reduced to ~0.25%) then the contribution is reduced to ~25%. The error on the $^{229}Th/^{230}Th$ ratio decreases with increasing levels of ^{230}Th. If an accurate $^{230}Th/^{232}Th$ ratio is not required then the levels of ^{229}Th can be reduced slightly for samples of low ^{230}Th content, but the error cannot be much improved if the levels of ^{230}Th are only marginally above background. The only approach may be improve the chemical procedures and/or ionization of Th from the filament.

The error on the spike ratio $^{229}Th/^{236}U$ has now been significantly reduced by rigorous calibration. Further refinement at this stage would be relatively unproductive but might be undertaken in the future.

There is no need for any improvement in the measurement of $^{236}U/^{238}U$ ratio (i.e. the first stage of the U run).

If the error on $^{229}Th/^{230}Th$ is halved then the error on $^{234}U/^{236}U$ will be equally important; reduction of the $^{234}U/^{236}U$ error would be the next step. Decreasing the levels of spike ^{236}U would increase the error on the $^{236}U/^{238}U$ measurement. If this were done, then a balance would have to achieved to yield the minimum total error. Some improvements in the ionization of U from the filament would also reduce the error on $^{234}U/^{236}U$.

11.1.2 Chemistry:

Research into chemical procedures to improve thorium yield may further reduce the sample size requirement. The anion exchange technique currently in use probably cannot be refined much further. The only possibility is that HCl at a higher strength may improve yield. Berman et al (1960) separated trace amounts of Th from large amounts of U by anion-exchange in 9.6 N HCl, the concentration at which the distribution coefficient of U is at its maximum. They claim to have separated Th completely from U and recovered at least 99% of the Th. The U was then eluted with 0.1 N HCl. At present 6 N HCl is used in the McMaster lab because the undiluted, distilled acid is of this strength.

Significant improvement of the Th yield may require a different approach: for example, mixed solvent elution with anion exchange resin has been used for rare earth elements (Potts 1987) and occasionally for U or Th. Tera et al (1961) found that Th was more strongly adsorbed unto anion exchange resin if loaded in a solution of nitric acid and methanol than in simple nitric acid solution, and the strength of acid had little effect. U was not adsorbed in a medium of 9 parts methanol to 1 part 5 N nitric acid while Th was strongly adsorbed. Th was later eluted with 1 N HNO_3. The behaviour of common carbonate matrix ions was not reported and would need to be evaluated if such a system were to be adopted. Any deleterious effects of the introduction of an organic would also have to be investigated.

Williams (Pers. comm. 1989) and Lauritzen (Pers. comm. 1989) report very

high Th yields in their laboratories. Their methods will be considered when this information is available.

11.1.3 Thorium ionization:

To optimise ionization the sample should be in a strongly reducing environment: this is the reason for the high current on the rhenium centre filament. There is no possibility of raising this because at the present setting the centre filament usually lasts for only 2 - 3 hours before breaking.

Graphite has been used to improve the ionization efficiency of U (Arden 1977, Chen and Wasserburg 1980). Chen and Wasserburg loaded a suspension of graphite in water unto Re filament, evaporated it, loaded the U sample in 0.1 N HNO_3, dried it, and finally loaded another layer of graphite. In the McMaster lab initial attempts to load Th in a similar fashion failed: the sample simply flaked off the filament during heating. Another factor to be considered is the high levels of contamination in graphite. Further research into loading may improve the technique. If this is adopted then a clean source of graphite will be required.

Possible approaches to improving the ionization efficiency include:-

(i) Load the Th fraction after etching the side filament with phosphoric acid,

(ii) Load in phosphoric acid/ graphite mixture,

(iii) Load after etching in layers: graphite followed by the sample in phosphoric acid,

(iv) Compare these methods for crimped and uncrimped filaments,

(v) Load half the sample on each side filament,

(vi) Load another reducing agent such as graphite on the other side filament,

(v) Compare loading in various acids instead of phosphoric.

(vi) Change the filament geometry slightly by tilting the two side filaments to an acute angle with the centre filament to put the sample in slightly closer proximity to the source of Re^+ ions.

11.1.4 Isochron dating:

The next development for mass spectrometric dating will be isochron dating of dirty calcites. Where ^{232}Th levels are extremely high then the tail from ^{232}Th may cause some interference in the ^{230}Th peak. The form of the tail must be studied and an appropriate interference coreection applied. Then isochron dating, using the leachates alone method, can be used.

11.1.5 $^{231}Pa/^{235}U$ dating: Protactinium dating is possible by alpha counting where the levels of U are high enough (> 1 ppm) to provide adequate quantities of ^{231}Pa. The method is based on the decay of ^{235}U through a very short lived intermediary ^{231}Th ($t_{1/2}$ = 25.6 h) to ^{231}Pa. The relationship is :

$$^{231}Pa/^{235}U = 1 - e^{-\lambda 231 t}$$

If alpha counting is used, ^{235}U activity can be measured directly or from ^{238}U activity assuming the constant $^{235}U/^{238}U$ activity ratio of 1/21.7; ^{231}Pa is measured indirectly by assuming secular equilibrium with one of its daughters, ^{227}Ac or ^{227}Th.

It should be possible, in samples of high U content, to measure the isotopic ratio by mass spectrometry. However, ^{227}Th or ^{227}Ac cannot be measured because their abundance is so small, so ^{231}Pa would have to be measured directly. A special spike would have to be made up, of ^{236}U (or ^{233}U) and an isotope of Pa such as ^{233}Pa (see Ku 1965).

Although Pa behaves chemically in a similar fashion to Th the chemical preparation may have to be modified to improve the separation of Pa. Kraus et al (1956) show that Th can easily be separated from Pa and U in strong (>7 N) HCl from anion exchange resin: Th shows negligible adsortion onto the resin while Pa and U show strong adsorption. The Pa may then be removed at low HCl concentration, or, more effectively, with concentrated HCl containing small amounts of HF. The U remains adsorbed and may be eluted with weak HCl. They sequentially eluted Th in 10 N HCl, Pa in 9 N HCl + 1 N HF and U in 0.1 N HCl.

For the mass spectrometric analysis the optimum conditions for Pa

evaporation and ionization would have to be identified. The abundance of ^{231}Pa, even in samples of >1 ppm U content, is very low. All the problems of ^{230}Th analysis are likely to be encountered for ^{231}Pa measurement. The improvement from mass spectrometric measurement of the $^{231}Pa/^{235}U$ ratio is not likely to be so dramatic as that achieved for $^{230}Th/^{234}U$ ratios.

This $^{231}Pa/^{235}U$ system allows dating to about 200 kyr B.P. and probably longer if mass spectrometry is used. If the $^{231}Pa/^{230}Th$ ratio is used then the range is extended to about 300 kyr B.P. (or a little beyond).

11.2 ^{230}Th DECAY CONSTANT

The sources of error which can be controlled have been minimized so that the error on a date is now of the order of 1% (2σ) or less. However, the absolute accuracy of any date is limited by the accuracy of the constants used to calculate it. The best estimate available of the half life of ^{230}Th is of rather low precision: the decay constant used in the dating program is 9.195×10^{-6}. The error on this figure, $\pm$ 0.78%, is not included in the calculation of error on the age. Table 11.2 below shows how this error affects the age estimate.

Table 11.2: Effect on age of error on $\lambda^{230}Th$.

Age using standard $\lambda 230$	132,296 y
Age using low $\lambda 230$	131,344 y
Age using high $\lambda 230$	133,267 y

The difference caused by the error represents 0.73% of the age.

The error on the age caused by the error on $\lambda 230$ is ~0.8%. This is approaching the same order of magnitude as the error from statistics. This might suggest that further refinement of the mass spectrometric dating procedure should come second to an attempt to refine the estimate of the half-life of ^{230}Th.

11.3 CONCLUSION

Mass spectrometry has improved the precision of measurement of $^{230}Th/^{234}U$ and $^{234}U/^{238}U$ isotopic ratios, compared to alpha counting, by an order of magnitude. Uranium ratios are typically measured to a 2σ precision of 0.2% and thorium ratios to 0.5%. The high precision on the measured ratios combined with careful calibration of the $^{229}Th/^{236}U$ spike has reduced the final error on the age estimate to ~1% (2σ). The high precision $^{234}U/^{238}U$ ratio measurements has significantly improved the precision of U/U dating and R.U.B.E. dating.

The technique has been demonstrated to be effective for several types of relatively clean carbonates: sub-aerial flowstone and stalactite, sub-aqueous calcite crust and calcite raft debris, coral and ostrich eggshell.

Mass spectrometry is now the best option for measurement of the less active but more abundant isotopes of the U-series decay chains: e.g. ^{238}U, ^{234}U and ^{230}Th. The detection of the less abundant but more active isotopes such as ^{231}Pa, ^{226}Ra, is likely to remain in the realm of alpha counting.

REFERENCES

Aharon, P. and Chappell, J. 1986 Oxygen isotopes, sea level changes and the temperature history of a coral reef environment in New Guinea over the last 10^5 years. Palaeogeog., Palaeoclimat., Palaeoecol., 56: 337 - 379.

Arden, J.W. 1977 Isotopic composition of uranium in chondritic meteorites. Nature 269: 788 - 789.

Arden, J.W. and Gale, N.H. 1974 Separation of trace amounts of uranium and thorium and their determination by mass spectrometric isotope dilution. Anal. Chem., 46: 687 - 691.

Atkinson, T.C., Harmon, R.S., Smart, P.L. and Waltham, A.C. 1978 Palaeoclimate and geomorphic implications of $^{230}Th/^{234}U$ dates on speleothem from Britain. Nature 272: 24 - 28.

Atkinson, T.C., Lawson, T.J., Smart, P.L., Harmon, R.S. and Hess, J.W. 1986 New data on speleothem deposition and paleoclimate in Britain over the last forty thousand years. J. of Quaternary Science, 1: 67 - 72.

Back, W., Hanshaw, B.B. and van Driel, J.N. 1984 Role of groundwater in shaping the eastern coastline of the Yucatan peninsula, Mexico. In LaFleur, R.G. (ed) Groundwater as a geomorphic agent, Allen and Unwin, Boston: 281 - 293.

Bakalowicz, M. 1982 U-Th dating and the problem of organic matter in speleothem Dept. of Geology, McMaster University, Tech. Memo. 82-2.

Bakalowicz, M.J., Ford, D.C., Miller, T.E., Palmer, A.N. and Palmer, M.V. 1987 Thermal genesis of dissolution caves in the Black Hills, South Dakota, Geol. Soc. of America Bull. 99: 729 - 738.

Ball, M.M. 1967 Carbonate sand bodies of Florida and the Bahamas. J. of Sed. Pet., 37: 556 - 591.

Barnes, J.W., Lang, E.J. and Potratz, H.A. 1956 Ratio of ionium to uranium in coral limestone. Science 124:175 -176.

Barry, B.A. 1978 Errors in practical measurement in science, engineering and technology. Ed. Morris, M.D., Wiley-Interscience.

Bender, M.L., Fairbanks, R.G., Taylor, F.W., Matthews, R.K., Goddard, J.G. and Broecker, W.S. 1979 Uranium -series dating of the Pleistocene reef tracts of Barbados, West Indies. Geol. Soc. Am. Bull., 90: 577 - 594.

Berger, A., Imbrie, J., Hays, J, Kukla, G. and Saltzman, B. (eds) 1984 Milankovitch and Climate NATO ASI series Series C, 126 Parts 1 and 2, D.Riedel, 895pp.

Berman, S.S, McKinney, L.E. and Bednas, M.E., 1960 The separation of carrier-free 234 Thorium (UX_1) from uranium by anion-exchange. Talanta, 4: 153 - 157.

Bevington, P.R. 1969 Data reduction and error analysis for the physical sciences. McGraw-Hill New York, 336pp.

Bièvre, P. de 1978 Accurate isotope ratio mass spectrometry: some problems and possibilities. Adv. Mass Spectrometry, 7A: 395 - 447.

Bittinger, M. L. and Morrel, B. B. 1984 Applied Calculus. Addison-Wesley, 686pp.

Blackwell, B. and Schwarcz, H.P. 1986 U-series Analyses of the Lower Travertine at Ehringsdorf, DDR. Quaternary Research, 25: 215 - 222.

Bloom, A.L. 1967 Pleistocene shorelines: a new test of isostasy. Geol. Soc. of America Bull., 78: 1477 - 1494.

Bloom, A.L., Broecker, W.S., Chappell, J., Matthews, R.K. and Mesolella, K.J. 1974 Quaternary sea level fluctuations on a tectonic coast: New $^{230}Th/^{234}U$ dates from the Huon Peninsula, New Guinea. Quaternary Research, 4: 185 - 205.

Boardman, M.R., Dulin, L.A., Kenter, R.J. and Neumann, A.C. 1984 Episodes of banktop growth in periplatfrom sediments and the chronology of Late Quaternary fluctuations in sea level. In Teeter, J.W. (ed) Proc. 2nd. Symp. on the Geology of the Bahamas, College Centre ofthe Finger lakes Bahamian Field Station, Ft. Lauderdale, Florida: 129 - 152.

Broeker, W.S. 1963 A preliminary Evaluation of Uranium Series Inequilibrium as a tool for absolute age measurement on marine carbonates. J. of Geophysical Res., 68: 2817 - 2834.

Broecker, W.S. and van Donk, J. 1970 Insolation changes, ice volumes and the ^{18}O record in deep sea cores. Rev. Geophys. Space Phys. 8, 169 - 198.

Chappell, J. 1974 Geology of coral terraces, Huon Peninsula, New Guinea: a study of Quaternary tectonic movements and sea-level changes. Geol. Soc. of America Bull., 85: 553 - 570.

Chappell, J. 1987 Late Quaternary sea-level changes in the Australian region. In Tooley, M.J. and Shennan, I. (Eds.) Sea-level Changes, Blackwell, 399pp.

Chappell, J. and Shackleton, N.J. 1986 Oxygen isotopes and sea level. Nature, 324: 137-140

Chappell, J. and Veeh, H.H. 1978 $^{230}Th/^{234}U$ age support of an interstadial sea level of -40 m at 30,000 yr BP Nature, 276: 602 - 603.

Chen, J.H. and Wasserburg, G.J. 1980 A Search for isotopic anomalies in Uranium, Geophysical Research Letters 7: 275 - 278.

Chen, J.H. and Wasserburg, G.J. 1981 Isotopic determination of uranium in picomole and subpicomole quantities. Anal. Chem., 53: 2060 - 2067.

Chen, J.H., Edwards, R.L. and Wasserburg, G.J. 1986 ^{234}U, ^{238}U and ^{232}Th in sea water. Earth planet. Sci. Letters, 80: 241 - 151.

Cherdyntsev, V.V., Kazachevskiy, I.V. and Kuz'mina, Ye. A. 1965 Dating of Pleistocene carbonate formations by the thorium and uranium isotopes. Geochemistry International 2: 794 - 801.

Daly, N.R. 1960 Scintillation type mass spectrometer ion detector. Rev. Scientific Instruments, 31: 264 - 267.

Davis, W.M. 1930 Origin of limestone caverns. Geological Society of America Bulletin, 41: 475 - 648.

Deal, D.E. 1962 Geology of Jewel Cave National Monument, Custer County, South Dakota with special reference to cavern formation in the Black Hills. M.Sc. thesis, University of Wyoming, Laramie, Wyoming.

Dietz, L.A., Pachucki, C.F. and Land, G.A. 1962 Internal standard technique for precise isotopic abundance measurements in thermal ionization mass spectrometry. Anal. Chem., 34: 709 - 710.

Duplessey, J.C., Labeyrie, J., Lalou, C. and Nguyen, H.V. 1970 Continental climate variations between 130,000 and 90,000 years B.P.. Nature, 226: 631 - 633.

Edwards, R.L. 1988 High Precision Thorium-230 ages of corals and the timing of Sea level Fluctuations in the Late Quaternary. Unpublished Ph.D. thesis, California Institute of Technology, Pasadena, California.

Edwards, R. L., Chen, J.H. and Wasserburg, G.J. 1986/87 ^{238}U-^{234}U-^{230}Th-^{232}Th systematics and precise measurement of time over the past 500,000 years. Earth and Planetary Science Letters 81, 175-192.

Edwards, R.L., Chen, J.H., Ku, T.L. and Wasserburg, G.J. 1987 Precise timing of the last interglacial period from mass spectrometric determination of Thorium-230 in corals. Science, 236: 1547 - 1553.

Edwards, R.L., Taylor, F.W. and Wasserburg, G.J. 1988 Dating earthquakes with high-precision Thorium-230 ages of very young corals. Earth Planet. Sci. Letters, 90: 371 - 381.

Emiliani, C. J. 1955 Pleistocene temperatures. Geology 63, 538-578.

Fairbanks, R.G. and Matthews, R.K. 1978 THe marine oxygen isotope record in Pleistocene coral, Barbados, West Indies. Quaternary Research, 10: 181 - 196.

Faris, J.P. and Buchanan, R.F., 1964 Anion exchange characteristics of elements in nitric acid medium. Anal. Chem., 36: 1157 - 1158

Fassett, J.D. and Kelly, W.R. 1984 Interlaboratory isotopic ratio measurements of nanogram quantities of uranium and plutonium on resin beads by thermal ionization mass spectrometry. Anal. Chem., 56: 550 - 556.

Ford, D.C., Schwarcz, H.P., Drake, J., Gascoyne, M., Harmon, R.S. and Latham, A.G. 1981 Estimates of the age of the existing relief of the southern Canadian

Rockies. J. Arctic and Alpine Res., 13: 1 - 10.

Gale, N. H. 1982 The physical decay constants in Odin, G. S. (Ed) Numerical Dating in Stratigraphy, John Wiley UK

Gancarz, A.J. and Wasserburg, G.J. 1977 Initial Pb of the Amitsoq gneiss, West Greenland, and implications for the age of the earth. Geochim. et Chosmochim. Acta, 41: 1283 - 1301.

Garrett, P. and Gould, S.J. 1984 Geology of New Providence Island, Bahamas. Geol. Soc. of America Bull., 95: 209 - 220.

Gascoyne, M. 1977a Uranium series dating of speleothem: an investigation of technique, data processing and precision. Dept. of Geology, McMaster Univ., Tech. Memo., 77-4.

Gascoyne, M. 1977b Uranium Series Dating of Speleothem: Analytical Procedure Dept. of Geology, McMaster Univ., Tech. Memo. 77-5

Gascoyne, M. 1977c Trace element geochemistry of speleothems. Proc. 7th. Int. Spel. Cong., Sheffield, England: 205 - 208.

Gascoyne M. 1979 Pleistocene climates determined from stable isotope and geochronologic studies of speleothem. Unpublished Ph.D. thesis, McMaster University, Hamilton.

Gascoyne, M. 1981 A climate record of the Yorkshire Dales for the last 300,000 years. Proc. 8th. Int. Cong. Spel., Bowling Green, Kentucky: 96 - 98.

Gascoyne, M. 1984a Uranium-series ages of speleothem from Bahamian Blue Holes and their significance. Trans. Brit. Cave Res. Assoc., 11: 45 - 49.

Gascoyne, M. 1984b Twenty years of Uranium-series dating of cave calcites: a review of results, problems and new directions. Studies in Speleology, V: 15 - 30.

Gascoyne, M. and Ford, D.C. 1984 Uranium series dating of speleothem, Part II. Results from the Yorkshire Dales and implications for cave development and Quaternary climates. Cave Science, Trans. of the British Cave Res. Assoc.: 11(2): 65 - 85.

Gascoyne, M. and Schwarcz, H.P. 1982 Carbonate and Sulphate Precipitates. In Ivanovich, M. and Harmon, R.S., 1982 (eds.) Uranium Series Disequilibrium: Application to Environmental Problems. Clarendon Press, Oxford, 571pp.

Gascoyne, M., Ford, D.C. and Schwarcz, H.P. 1981 Late Pleistocene chronology and paleoclimate of Vancouver Island determined from cave deposits. Can. J. of Earth Sciences, 18: 1643 - 1652.

Gascoyne, M., Ford, D.C. and Schwarcz, H.P. 1983 Rates of cave and landform development in the Yorkshire Dales from speleothem age data. Earth Surface Processes and Landforms 8(6), 557-568

Gascoyne, M., Schwarcz, H.P. and Ford, D.C. 1980 A paleotemperature record for the mid-Wisconsin in Vancouver Island. Nature, 285: 474 - 476.

Gascoyne, M., Schwarcz, H.P. and Ford, D.C. 1983 Uranium-series ages of speleothem from Northwest England: Correlation with Quaternary climate. Phil. Trans. R. Soc. Lond., B 301: 143 - 164.

Gascoyne, M., Schwarcz, H.P. and Ford, D.C. 1978 Uranium Series dating and stable isotope studies of speleothem: Part 1 Theory and Techniques. Trans. British Cave Res. Assoc., 5: 91 - 111.

Gascoyne, M., Benjamin, G.J., Schwarcz, H.P. and Ford, D.C. 1979 Sea-level lowering during the Illinoian glaciation: Evidence from a Bahama 'Blue Hole'. Science, 205: 806-808

Gordon, D., Smart, P.L., Andrews, J.N., Atkinson, T.C., Rowe, P., Christopher, N.S.J. and Ford, D.C. 1989 Dating of United Kingdom interglacials and interstadials from speleothem growth frequency. Quat. Res., 31: 14 - 26.

Harder, E.C. 1919 Iron-depositing Bacteria and their geologic relations. U.S.G.S. Prof. Pap., 113, 89 pp.

Harmon, R.S. 1975 Late Pleistocene paleotemperatures in North America as inferred from isotopic variations in speleothem. Unpublished Ph.D. thesis, Dept. of Geology, McMaster University, Hamilton, Canada.

Harmon, R.S., Mitterer, R.M., Kriausakul, N., Land, L.S., Schwarcz, H.P., Garrett, P., Larson, G.J., Vacher, H.L. and Rowe, M. 1983 U-series and amino-acid racemization geochronology of Bermuda: implications for eustatic sea-level fluctuation over the past 250,000 years. Palaeogeog., Palaeoclimat., Palaeoecol. 44, 41-70.

Harmon, R.S., Ford, D.C. and Schwarcz, H.P. 1977 Interglacial chronology of the Rocky and Mackenzie Mountains based on $^{230}Th/^{234}U$ dating of calcite speleothem. Canadian Journal of Earth Sciences,14: 2543 - 2552.

Harmon, R. S., Schwarcz, H.P. and Ford, D.C. 1978 Late Pleistocene sea level history of Bermuda. Quaternary Research 9, 205-218.

Harmon, R. S., Ku, T.-L., Matthews, R.K. and Smart, P.L. 1979 Limits of U-series analyses: Phase I results of the Uranium-Series Intercomparison Project. Geology 7, 405-409.

Harmon, R.S., Thompson, P., Schwarcz, H.P. and Ford, D.C. 1975 Uranium-series dating of speleothems. Nat. Spel. Soc. Bull., 37: 21 - 33.

Harmon, R.S., Thompson, P., Schwarcz, H.P. and Ford, D.C. 1978 Late Pleistocene paleoclimates of North America as inferred from stable isotope studies of speleothem. Quat. Res., 9: 54 - 70.

Harmon, R.S., Land, L.S., Mitterer, R.M., Garrett, P., Schwarcz, H.P. and Larson, G.J. 1981 Bermuda sea level during the last interglacial. Nature 289, 481-483.

Imbrie, J., Hays, J.D., Martinson, D.G., McIntyre, A., Mix, A.C., Morley, J.J., Pisias, N.G., Prell, W.L. and Shackleton, N.J. 1984 The orbital theory of Pleistocene climate: support from a revised chronology of the marine $\delta^{18}O$ record. In A. L. Berger et al.(eds.) Milankovitch and Climate, 269-305 (Reidel, Dordrecht).

Inghram, M.G. and Chupka, W.A., 1953 Surface ionization source using mulitple filaments. Rev. Scientific Instruments, 24: 518 - 520.

Ivanovich, M. 1982 Uranium series disequilibria applications in geochronolgy. In Ivanovich, M. and Harmon, R.S., (eds.) Uranium Series Disequilibrium: Application to Environmental Problems. Clarendon Press, Oxford, 571pp.

Ivanovich, M. and Harmon, R.S., 1982 (eds.) Uranium Series Disequilibrium: Application to Environmental Problems. Clarendon Press, Oxford, 571pp.

Jaffey, A.M., Flynn, K.F., Glendenin, L.E., Bentley, W.C. and Essling, A.M. 1971 Precision measurements of half-lives and specific activities of ^{235}U and ^{238}U. Phys Rev. C4: 1889 - 1906.

Jeffery, P.G. and Hutchison, D., 1981 Chemical methods of rock analysis. Pergamon Press, 378 pp.

Jones, B. 1989 Calcite rafts, peloids, and micrite in cave deposits from Cayman Brac, British West Indies. Can. J. of Earth Sci., 26: 654 - 664.

Kanno, H. 1971 Isotopic fractionation in a thermal ion source. Bull. of the Chem. Soc. of Japan, 44: 1808 - 1812.

Kaufman, A. 1971 U-series dating of Dead Sea Basin carbonates Geochim. et Cosmochim. Acta, 35: 1269 - 1281.

Kaufman, A. 1986 The distribution of $^{230}Th/^{234}U$ ages in corals and the number of Last Interglacial high sea-stands. Quaternary Research, 25: 55 - 62.

Kaufman, A. and Broeker, W. 1965 Comparison of ^{230}Th and ^{14}C ages for carbonate materials from Lakes Lahontan and Bonneville. J. Geophys. Res. 70: 4039 - 4054

Kaufman, A., Broecker, W.S., Ku, T.-L. and Thurber, D.L. 1971 The status of U-series methods of mollusk dating. Geochim. et Cosmochim. Acta, 35: 1155 - 1183.

Korkisch, J. and Dimitriadis, D. 1973 Anion-exchange separation and spectrophotometric determination of thorium in geological samples. Talanta, 20: 1199 - 1205.

Kraus, K.A., Moore, G.E. and Nelson, F., 1956 Anion-exchange studies. XXI. Th(IV) and U(IV) in Hydrochloric Acid. Separation of Thorium, Protactinium and Uranium. J. Amer. Chem. Soc., 78: 2692 - 2694.

Ku, T.-L. 1965 An evaluation of the $^{234}U/^{238}U$ method as a tool for dating pelagic

sediments. J. of Geophysical Res., 70: 3457 - 3474.

Ku, T.-L. 1968 Protactinium 231 Method of dating coral from Barbados Island. J. of Geophysical Res., 73: 2271 - 2276.

Ku, T.L. 1976 The uranium-series methods of age determination. Ann. Rev. Earth Planet. Sci., 4: 347 - 380.

Ku, T.-L. and Liang, Z.-C. 1984 The dating of impure carbonates with decay-series isotopes. Nuclear Instruments and Methods in Physics Research, 223: 563 - 571.

Ku, T.-L., Ivanovich, M. and Luo, S. 1990 U-series dating of last interglacial high sea stands; Barbados revisited. Quat. Res., 33: 129 - 147.

Ku, T.-L., Bull, W.G., Freeman, S.T. and Knauss, K.G. 1979 Th^{230}/U^{234} dating of pedogenic carbonates in gravelly desert soils of Vidal Valley, South-eastern California. Bull. Geol. Soc. America, 90: 1063 - 1073.

Ku, T.-L., Kimmel, M.A., Easton, W.H. and O.Neil, T.J. 1974 Eustatic sea level 120,000 years ago on Oahu, Hawaii. Science, 183: 959 - 962.

Latham, A.G. 1981 Paleomagnetism, rock magnetism and U-Th dating of speleothem deposits. Unpublished Ph.D. thesis, Dept. of Geology, McMaster University, Hamilton.

Lauritzen, S.-E. 1983 Organic metter in Speleothem. Progress report, May 1983. Unpublished manuscript, Dept. of Geography, McMaster University.

Le Roux, R. J. and Glendenin, L. E. 1963 Half-life of ^{232}Th. Proc. Natl. Meet. on Nucl. Energy, Pretoria, 77 - 88.

Li, W.-X. 1989 Isotopic studies of the ground waters and their host rocks and minerals from the underground research laboratory (URL), Pinawa, Manitoba, Canada. Unpublished M.Sc. thesis, Dept. of Geology, McMaster Univ., Hamilton, Canada.

Lundberg, J. 1990 Dating of carbonates by mass spectrometry: a technical manual. In prep. Dept. of Geology, McMaster Univ., Hamilton, Canada.

Mahnes, G., Allegre, C.J. and Provost, A. 1984 U-Th-Pb systematics of the eucrite "Juvinas": Precise age determination and evidence for exotic lead. Geochim. et Chosmochim. Acta, 48: 2247 - 2264.

Martinson, D.G., Pisias, N.G., Hays, J.D., Imbrie, J., Moore, T.C. Jr. and Shackleton, N.J. 1987 Age dating and the orbital theory of the ice ages: Development of a high-resolution 0 to 300,000-year chronostratigraphy. Quat. Res., 27: 1 - 29.

Meadows, J.W., Armani, R.J., Callis, E.L. and Essling, A.M. 1980 Half life of 230-Th. Phys. Rev. C22: 750.

Millen, T.M. and Dickey, N.Jr. 1987 A stable isotopic investigation of waters and speleothems in Wind Cave, South Dakota: an application of isotope

paleothermometry. Nat. Spel. Soc. Bull. 49: 10 - 14.

Moore, W.S. 1982 Late Pleistocene sea-level history. In Ivanovich, M. and Harmon, R.S., 1982 (eds.) Uranium Series Disequilibrium: Application to Environmental Problems. Clarendon Press, Oxford, 571pp.

Mörner, N.-A. 1980 (ed) Earth Rheology, Isostasy and Eustasy. Wiley, 599 pp.

Mörner, N.-A. 1987 Models of global sea-level changes. In Tooley, M.J. and Shennan, I. (Eds.) Sea-level Changes Blackwell, 399pp.

Muhs, D.R. and Bush, C.A. 1987 Uranium-series age determinations of Quaternary Eolianites and implications for sea-level history, New Providence islands, Bahamas. Abst. with Prog., Geol. Soc. Amer., 19: 780

Mullins, H.T. and Lynts, G.W. 1977 Origin of the northwestern Bahama Platform: Review and reinterpretation. Geol. Soc. of America Bull., 88: 1447 - 1461.

Mylroie, J.E. and Carew, J.L. 1988 Solution conduits as indicators of Late Quaternary sea level position. Quat. Sci. Rev., 7: 55 - 64.

Neumann, A.C. and Moore, W.S. 1975 Sea level events and Pleistocene coral ages. Quat. Res., 5: 215-224

Odin, G.S. 1982 Introduction: uncertainties in evaluating the numerical time scale. In Odin, G. S. (Ed) Numerical Dating in Stratigraphy, John Wiley UK

Osmond, J.K., May, J. P. and Tanner, W.F. 1970 Age of the Cape Kenned barrier-and-lagoon complex. J. Geophys. Res., 75: 469 - 479.

Opdyke, N.D. 1972 Rev. Geophys. Space Phys. 10, 213 - 249.

Osmond, J.K. and Cowart, J.B. 1982 Ground water. In Ivanovich, M. and Harmon, R.S., 1982 (eds.) Uranium Series Disequilibrium: Application to Environmental Problems. Clarendon Press, Oxford, 571pp.

Osmond, J.K., Carpenter, J.R. and Windom, H.L. 1965 Th230/U234 age of the Pleistocene Corals and Oolites of Florida. J. of Geophysical Res., 70: 1843 - 1847.

Olson, C.G., Ruhe, R.V. and Mausbach, M.J. 1980 The terra rossa limestone contact phenomena in Karst, Southern Indiana. J. Soil Soc. Am., 44: 1075 - 1079.

Palmer, A. 1975 The origin of Maze Caves. National Speleological Society Bulletin, 37: 56 -0 76.

Pearson, C. E. 1986 Numerical methods in Engineering and Science. Van Nostrand Reinhold Company, New York, 214p.

Peck, S.B. 1986 Bacterial deposition of iron and manganese oxides in North American caves. Nat. Speleological Soc. Bull., 48: 26 - 30.

Peltier, W.R. 1988 Lithospheric thickness, Antarctic deglaciation history, and ocean basin discretization effects in a global model of postglacial sea level change: a summary of some sources of nonuniqueness. Quat. Res., 29: 93 - 112.

Potts, P.J. 1987 A handbook of silicate rock analysis Blackie, Glasgow and London, 622 pp.

Przyblowicz, W., Schwarcz, H.P. and Latham, A.G. 1990 Dirty calcites, 2: U-series dating of artificial calcite-detritus mixtures. In prep. Chem. Geol.

Pye, K. 1983 Red beds. In Goudie, A.S. and Pye, K. (eds) Chemical sediments and geomorphology, Academic press, London, New York: 227 - 263.

Radtke, U., Grün, R. and Schwarcz, H.P. 1988 Electron spin resonance dating of Pleistocene coral reef tracts of Barbados. Quat. Res., 29: 197 - 215.

Rec, J.R., Myers, W.G. and White, F.A., 1974 Diffusion controlled thermal ionization source for mass spectrometric analysis of trace metals. Anal. Chem., 46: 1243 - 1247.

Rees, C.E. 1969 Fractionation effects in the measurement of molybdenum isotope abundance ratios. Int. J. of Mass Spect. and Ion Phys., 3: 71 - 80.

Rokop, D.J., Perrin, R.E., Knobeloch, G.W., Armijo, V.M. and Shields, W.R., 1982 Thermal ionization mass spectrometry of urnanium with electrodeposition as a loading technique. Anal. Chem., 54: 957 - 960.

Rutter, N.W. 1972 Geomorphology and multiple glaciations in the area of Banff, Alberta. Geological Society of Canada Bull. 206: 31pp.

Rutter, N.W. 1984 Pleistocene history of the Western Canadian ice-free corridor. In Fulton, R.J. (ed.) Quaternary Stratigraphy of Canada - a Canadian contribution to IGCP project 24, Geological Survey of Canada Paper, 84-10: 50 - 56.

Ruhe, R.V., Cady, J.G. and Gomez, R.S. 1961 Paleosols of Bermuda. Geol. Soc. Am. Bull., 72: 1121 - 1142.

Sanford, W.E. and Konokow, L.F. 1989 Porosity development in coastal carbonate aquifers. Geology, 17: 249 - 252.

Schwarcz, H.P. 1979 Uranium-series dating of contaminated travertines: a two-component model. Tech. Memo., 79-1, Dept. of Geology, McMaster University, Hamilton, Ontario, Canada.

Schwarcz, H.P. 1980 Absolute age determination of archaeological sites by uranium series dating of travertines. Archaeometry, 22: 3 - 24.

Schwarcz, H. P. 1986, In Fritz, P. and Fontes, J.-C. (eds) Handbook of Environmental Geochemistry. The terrestrial Environment, Part B., 271-303 (Elsevier, Amsterdam)

Schwarcz, H.P. 1989 Uranium series dating of Quaternary deposits. Quaternary International, 1: 7 - 17.

Schwarcz, H. P. and Gascoyne, M. 1984 Uranium-series Dating of Quaternary Deposits. In Quaternary Dating Methods W. C. Mahaney (ed) Elsevier, Amsterdam: 33 - 51.

Schwarcz, H.P. and Latham, A.G. 1990 Dirty calcites, 1. Uranium-series dating of contaminated calcite using leachates alone. In Press. Chem. Geol.

Schwarcz, H.P and Morawska, L. 1990 Uranium series of carbonates from Bir Tarfawi and Bir Sahara. In prep.

Schwarcz, H.P. and Skoflek, I. 1982 New dates for the Tata, Hungary archaeological site. Nature, 295: 590 - 591.

Shackleton, N.J. and Matthews, R.K. 1977 Nature 268, 618 - 620.

Shennan, I. and Tooley, M.J. 1987 In Tooley, M.J. and Shennan, I. (Eds.) Sea-level Changes Blackwell, 399pp.

Snelling, N.J. 1987 Measurement of geological time and the geological time scale. Modern Geology, 11: 365 - 374.

Steiger, R.H. and Jager, E. 1977 Subcommission on Geochronology: Convention on the use of decay constants in geo- and cosmochronology. Earth and Planet. Sci. Lett., 36: 359 - 362.

Stoessell, R.K., Ward, W.C., Ford, B.H. and Schuffert, J.D. 1989 Water chemistry and $CaCO_3$ dissolution in the saline part of an open-flow mixing zone, coastal Yucatan Peninsula, Mexico. Geol. Soc. of America Bull., 101: 159 - 169.

Strelow, F. W. E. 1960 An ion exchange selectivity scale of cations based on equilibrium distribution coefficients. Analytical Chemistry 32 (9): 1185 - 1188.

Szabo, B.J. and Halley, R.B. 1988 $^{230}Th/^{234}U$ ages of aragonitic corals from the Key Largo Limestone of South Florida. Amer. Quat. Assoc., Prog. and Abstr., Tenth Biennial Mtg.: 154

Szabo, B.J. and Rosholt, J.N. 1969 Uranium-series dating of Pleistocene Molluscan shells from Southern California - An Open System Model. J. of Geogphysical Res., 74: 3253 - 3260.

Szabo, B.J. and Rosholt, J.N. 1982 Surfical Continental Sediments. In Ivanovich, M. and Harmon, R.S., 1982 (eds.) Uranium Series Disequilibrium: Application to Environmental Problems. Clarendon Press, Oxford, 571pp.

Szabo, B.J., Malde, H.E. and Irwin-Williams, C. 1969 Dilema posed by Uranium-series dates on archaeologically significant bones from Valsequillo, Puebla, Mexico. Earth and Plant. Sci. Letts., 6: 237 - 244.

Tera, F., Korkisch, J. and Hecht, F., 1961 Ion exchange in mixed solvents - IV. The

distribution of Thorium between alcohol-nitric acid solutions and the strongly-basic anion exchanger DOWEX-1. Separation of Thorium from Uranium. J. Inorg. Nucl. Chem., 16: 345 - 349.

Thirlwall, M.F. 1982 A triple filament method for rapid and precise analysis of rare-earth elements by isotope dilution. Chem. Geol., 35: 155 - 166.

Thompson, P. 1973 Speleochronology and Late Pleistocene climates inferred from O, C, H, U and Th abundances in speleothem. Unpublished Ph.D. thesis, McMaster University, Hamilton, Ontario, Canada.

Thompson, P., Ford, D.C. and Schwarcz, H.P. 1975 $^{234}U/^{238}U$ ratios in limestone cave seepage waters and speleothem from West Virginia. Geochim. Cosmochim. Acta, 39: 661 - 669.

Tooley, M.J. 1987 Sea level studies. In Tooley, M.J. and Shennan, I. (Eds.) Sea-level Changes Blackwell, 399pp.

Tooley, M.J. and Shennan, I. 1987 (Eds.) Sea-level Changes Blackwell, 399pp.

Veeh, H.H. and Chappell, J. 1970 Astronomical theory of climatic change: support from New Guinea. Science, 167: 862 - 865.

Veeh, H.H. 1966 Th^{230}/U^{238} and U^{234}/U^{238} ages of Pleistocene high sea level stand. J. Geophys. Res., 71: 3379 - 3386.

Wainerdi, R.E. and Uken, E.A. 1971 Modern Methods of Geochemical Analysis. Plenum Press.

Wasserburg, G.L., Papanastassiou, D.A., Nenow, E.V. and Bauman, C.A. 1969 A programmable magnetic field mass spectrometer with on-line data processing. The Review of Sci. Inst., 40: 288 - 295.

Wasserburg, G.J., Jacobsen, S.B., DePaolo, D.J. and McCulloch, M.T. 1981 Precise determination of Sm/Nd ratios, Sm and Nd isotopic abundances in standard solutions. Geochimica et Cosmochim. Acta, 45: 2311 - 2323.

Winograd, I.J., Szabo, B.J., Coplan, T.B., and Riggs, A.C. 1988 A 250,000-Year climatic record from Great Basin vein calcite: Implications for Milankovitch theory. Science, 242: 1275 - 1280

White, B., Kurkjy, K. and Curran, H.A. 1984 A shallowing-upward sequence in a Pleistocene coral reef and associated facies, San Salvador, Bahamas. In Teeter, J.W. (ed) Proc. 2nd. Symp. on the Geology of the Bahamas, College Centre ofthe Finger lakes Bahamian Field Station, Ft. Lauderdale, Florida: 53 - 68.

Yonge, C.J. 1990 Rats Nest Cave (Provincial Historic Resource, 1987). Unpublished report.

Appendix 1

A1.1 THE VG 354 MASS SPECTROMETER

The ion source of the VG 354 contains a rotating magazine on which are mounted up to 16 samples. The current supplied to each filament is controlled by the ion beam output through a feedback loop: the operator supplies an "aiming current" for both the Rhenium ion beam and the sample ion beam; the automatic control system adjusts the filament supply according to the output ion beam intensity.

The accelerating voltage on the flight tube plates is set at ~5836 V for U/Th runs.

The electromagnet has a 90° sector. The mass calibration (i.e. the magnet current at which each mass will be focussed) for the mass range 84 to 238, at an accelerating voltage of 5836 V, is entered into the Mass Calibration information file. The current mass calibration (December 1989) was input on January 17 1989:

Mass	Field
84	2.7500
88	2.8163
187	4.1514
232	4.6490
238	4.7124

The Daly voltage is adjusted regularly to optimize peak flatness: it was around -13.8 kV in 1988 and is currently around -11.6 kV (December 1989). The photomultiplier tube of the detector has a ~1.3 kV supply. This is also adjustable and has varied from 1.030 kV in 1988 to 1.137 kV by December 1989.

A1.2 URANIUM AND THORIUM RUNS

The General Peak Jumping System is used for uranium and thorium analyses.

The analysis program receives instructions for each run from the procedure file which contains information on the number of filaments in the bead, the number of collectors to be used, length of time to integrate counts, ratios to be measured, initial focus settings, filament current limits and aiming intensities, limits on rate of beam growth, number of cycles and runs, etc. An example is given below.

The procedure file calls a sequence type file for information on which ratios to measure, integration times for peak measurement, corrections to be made, etc. An example of a sequence type is given below.

A1.3 PROCEDURES

PROCEDURE FILE (Explanation of all the terms):

Procedure Name: U 234 TWO STAGE DOUBLE GPJ[a] Type: AXIAL Peak Jump[b]

	-----CENTER-----			-----SIDE-----			-----WARMUP TIMES[f] (mins)--		
Filament	P-heat[c]	Init[d]	Max[e]	P-heat	Init	Max	Preheat	Hold	Measure
Currents	0.00	4.50	5.50	0.00	1.50	2.80	00.0	00.0	05.0

Pyrometer[g]	Initial	Z-bias	Z-focus	Slit	D-focus	D-bias	Extract	Source
0000'C	values	400	500	500	600	500	900	050

Rhenium aiming current[h] 2.5E-12 Beam growth limit[i] -2.5 to +2.5% in 10sec.

Sequence[j]	1	2	3	4	5	6
Detector[k] (F/D)	D	D	D	D	D	D
Aiming current[l]	1.0E-13	3.0E-13	4.0E-13	8.0E-15	1.5E-14	2.5E-14
No. of runs[n]	01	02	04	01	02	08
No. of cycles[m]	02	05	10	02	03	10
Sequence type[o]	05	05	05	27	27	27

Daly bias[p] +0.000E+00 Faraday bias +0.000E+00

Start Grand Totals[q] at Seq. No. 6

(a) GPJ: General Peak Jumping Routine (always used for U and Th runs).

(b) AXIAL Peak Jump: the collector is the central or axial one; either the Faraday or Daly.

(c) P-heat: Preheat: with the VG354 preheating is done before running, so the P-heat current for both filaments is always at zero.

(d) Init: the current will be raised to this value initially because the relevant beam (i.e. rhenium for the centre filament and U or Th for the side filament) is expected to be large enough at this setting. If no beam is found then the program raises the current in stages.

(e) Max: the maximum current allowed: the system will not raise the filament any higher than this. Uranium does not need as strong a reducing environment as thorium so the centre Re current is lower for uranium.

(f) WARMUP TIMES: the filament current is raised slowly over this time: Preheat warmup and Hold are again zero, warmup times for Measuring are usually 5 minutes.

(g) The pyrometer is not used for these analyses. The Initial values for Z-bias, Z-focus, D-focus, D-bias, Extract and Source settings usually remain unchanged around the middle of their ranges; the system will automatically change these as it focusses on the beam.

(h) Rhenium aiming current: the program raises the current on the centre Re filament to produce a Re^+ ion beam close to this figure (within tolerance limits). The current will be higher if a stronger reducing environment is required, e.g. if the metal oxide beam is too high on a metal ion count. It is usually set to about $2.5x10^{-12}$ amps for U runs and $1.5x10^{-11}$ amps for Th runs. Once the correct current on the centre filament has been reached it is left at that setting for the rest of the analysis. The rhenium ion beam should remain close to the aiming current.

(i) Beam Growth limit: if the rate of beam change exceeds these values the filament current is adjusted and data are not collected until the beam stabilises. For uranium runs it is set as +/- 2.5% in 10 seconds, for thorium +/- 4.5% in 10 s.

(j) Sequence: The program is run in steps or sequences with different conditions or procedures. These are explained below.

(k) Detector: normally the Daly is used for U and Th runs.

(l) Aiming current: this is for the sample ion beam current. The system adjusts the side filament current to keep the beam at this level within tolerance limits. The aiming current normally is raised during the course of the analysis while the beam is becoming stable. It then may remain unchanged or rise slightly while data is being collected. It must be lower than the Daly limit ($5x10^{-13}$ A) but high enough to give a detectable count on the minor isotopes. For $^{235}U/^{238}U$ and $^{236}U/^{238}U$ ratios it must be reasonably high (e.g. 1.0 to $4.0x10^{-13}$ A) to ensure an adequate ^{236}U count amidst the abundant ^{238}U ions. For $^{234}U/^{235}U$ and $^{236}U/^{235}U$ ratios and for Thorium isotope ratios the current can be lower (e.g. 1.0x10-15 A to $4.5x10^{-14}$ A). This is the only parameter which can be changed while the program is running. It is input by typing AIMC = X.

(m) No. of cycles: each scan over all the masses (e.g. from 233.5 to 238) is one cycle. The system scans twice before calculating ratios from an average of two counts for each mass. The ratios are thus running means of two counts. While the beam is stabilizing only about two cycles are measured for one run. For data collection this may be increased to 10 or 20 cycles per run.

(n) No. of runs: a run is a group of cycles. Before the run the focus and deflection units are adjusted, the filament currents are adjusted and the background zero is measured. These values are readjusted between runs. At the start the runs are short because frequent adjustments are necessary until the beam is stable. A higher number of runs per sequence usually increases the precision of the grand mean until the sample begins to burn out and fractionation increases. In the thorium procedures the number of runs is set at 25: this gives flexibility to the operator; runs rarely last this long.

(o) Sequence type: a sequence is a group of runs. The sequence type is the suite of masses and ratios measured (e.g. $^{235}U/^{238}U$, $^{236}U/^{238}U$ etc.). Between sequences the aiming current may be changed, sequence type changed, etc.: e.g. TWO STAGE URANIUM analysis uses two sequence types. Details of the sequence types are given below.

(p) Daly bias and Faraday bias: If the amplifier had a simple constant bias its value would be entered here and the ratios modified accordingly.

(q) Start Grand Totals: The program allows only one set of grand totals in a procedure. Normally one would begin the grand means as soon as the beam was stable. However with TWO STAGE URANIUM analyses the first sequence type runs must be averaged by hand: only the last of the sequence types is automatically averaged.

A1.4 SEQUENCE TYPES

The sequence type indicates the ratios to be measured and integration times for each measurement. Below is an example of a sequence type with an explanation of terms.

(a) The ratios include the ones of interest, such as 229/232, and "dummy" ratios, such as 229.3/232, which are measured simply to give a delay while high peaks die before the next low peak is measured.

(b) If required, one of the ratios can be input as a normalising ratio: i.e. the true value is input. For U analyses the true 235/238 ratio is input as:

Ratio 1 235.0/238.0 = .0072526

(c) The "interference ratios" indicate (i) where the interpeak background and tail is to be measured and (ii) what weighting each interference is to be given. In this case the interpeak background is measured at 0.5 mass units to either side of the peak of interest and each side is presumed to have equal weight (both contribute 0.5 of

the interference). This linear interference correction is discussed at length in Li 1989. The interference line should be read as: " The first interference is on the 229 peak, is to be measured at 228.5 and is to be given a weighting of 0.5".

The weighting factors are decided by examining the shapes of peak tails by using the SCAN program or by running a special sequence type to measure the tails at close intervals. For U and Th scans tailing is insignificant and the interpeak background to either side can simply be averaged. If the tail were not linear then the curvature can be accounted for by changing the weighting. For example a linear correction for an exponential tail would overcorrect. In this case the lower side may be given a higher weighting.

(d) Channel z measures the background counts away from any peak. This is chosen to avoid any peaks or possible isobars.

Peak jumping TYPE Number 04

Ratio 1 229.0/232.0
Ratio 2 230.0/232.0
Ratio 3 227.5/232.0
Ratio 5 229.3/232

Intrf 1 229.0/228.5 = .5000
Intrf 2 229.0/229.5 = .5000
Intrf 3 230.0/229.5 = .5000
Intrf 4 230.0/230.5 = .5000

Channel	Mass	Integration time
z	221.500	
1	227.500	1
2	228.500	1
3	229.000	2
4	229.300	1
5	229.500	2
6	230.000	4
7	230.500	2
8	232.000	1

Note: Channel z is used to measure background zero.

(e) The Integration time for each channel varies from 1 to 4 seconds depends on the size and importance of the beam.

(f) The program automatically corrects the counts for background and for interpeak interference. If a normalising ratio has been entered then the ratios are also corrected for fractionation and mass discrimination.

A1.5 PROCEDURES AND SEQUENCES TYPES FOR U AND TH RUNS

The procedures and sequence types in use for U and Th analyses are presented below. These are the current settings (December 1989): they may be changed as required.

1. Uranium Analysis for Normal Samples:

This procedure is applicable for nearly all samples. The first stage measures masses 235, 236 and 238 with sequence type 3. The ratios are corrected for background and interpeak interference and for fractionation and mass discrimination by the $^{235}U/^{238}U$ normalizing ratio. The second stage measures masses 234, 235 and 236 with sequence type 26. These ratios are corrected only for background and interpeak interference.

2. Uranium Analysis for small samples:

The only time this was required was for the tiny samples of ostrich eggshell.

3. Uranium Analysis for non-normal samples:

This procedure does not correct for fractionation and mass discrimination by the $^{235}U/^{238}U$ normalizing ratio. This must be done by hand. It is normally used only for spiked standards.

1. URANIUM ANALYSIS FOR NORMAL SAMPLES

Procedure name: U 234 TWO STAGE NORMAL SAMPLES Type: AXIAL Peak Jump

	-----CENTER-----			-----SIDE-----			-----WARMUP TIMES (mins)--		
Filament Currents	P-heat 0.00	Init 4.50	Max 6.00	P-heat 0.00	Init 1.60	Max 2.60	Preheat 00.0	Hold 00.0	Measure 05.0

Pyrometer 0000'C	Initial values	Z-bias 400	Z-focus 500	Slit 500	D-focus 600	D-bias 500	Extract 900	Source 050

Rhenium aiming current 2.0E-12 Beam growth limit -3.0 to +3.0% in 10sec.

Sequence	1	2	3	4	5	6
Detector (F/D)	D	D	D	D	D	D
Aiming current	1.0E-13	3.0E-13	4.0E-13	5.0E-15	1.7E-14	2.5E-14
No. of runs	02	03	06	01	01	10
No. of cycles	02	02	10	02	02	10
Sequence type	03	03	03	26	26	26

Daly bias +0.000E+00 Faraday bias +0.000E+00

Start Grand Totals at Seq. No. 6

Peak jumping TYPE Number 3

Ratio 1 235.0/238.0 =.0072526
Ratio 2 236.0/238.0 =
Ratio 3 233.5/238.0 =

Intrf 1 235.0/234.5 = .5000
Intrf 2 235.0/235.5 = .5000
Intrf 3 236.0/235.5 = .5000
Intrf 4 236.0/236.5 = .5000

Channel	Mass	Integration time
z	221.500	
1	233.500	2
2	223.500	2
3	235.000	4
4	235.500	2
5	236.000	4
6	236.500	2
7	238.000	1

Peak jumping TYPE Number 26

Ratio 1 234.0/236.0 =
Ratio 2 235.0/236.0 =
Ratio 3 232.5/236.0 =

Intrf 1 234.0/233.5 = .5000
Intrf 2 234.0/234.5 = .5000
Intrf 3 235.0/234.5 = .5000
Intrf 4 235.0/235.5 = .5000
Intrf 5 236.0/235.5 = .5000
Intrf 6 236.0/236.5 = .5000

Channel	Mass	Int.time
z	227.3	
1	232.500	1
2	233.500	2
3	234.000	5
4	234.500	2
5	235.000	2
6	235.500	1
7	236.000	1
8	236.500	1

2. URANIUM ANALYSIS FOR SMALL SAMPLES:

Procedure name: U 234 GENTLE FOR SMALL SAMPLES Type: AXIAL Peak Jump

	-----CENTER-----			-----SIDE-----			-----WARMUP TIMES (mins)--		
Filament Currents	P-heat 0.00	Init 4.50	Max 6.00	P-heat 0.00	Init 1.60	Max 2.60	Preheat 00.0	Hold 00.0	Measure 05.0

Pyrometer 0000'C	Initial values	Z-bias 400	Z-focus 500	Slit 500	D-focus 600	D-bias 500	Extract 900	Source 050

Rhenium aiming current 2.0E-12 Beam growth limit -3.0 to +3.0% in 10sec.

Sequence	1	2	3	4	5	6
Detector (F/D)	D	D	D	D	D	D
Aiming current	1.0E-13	1.5E-13	2.0E-13	5.0E-15	1.0E-14	1.5E-14
No. of runs	02	03	06	01	01	10
No. of cycles	02	02	10	02	02	10
Sequence type	03	03	03	26	26	26

Daly bias +0.000E+00 Faraday bias +0.000E+00

Start Grand Totals at Seq. No. 6

3. URANIUM ANALYSIS FOR NON-NORMAL SAMPLES: e.g. Standards whose 235/238 ratio is not normal.

Procedure name: U 234 TWO STAGE DOUBLE (OLD) Type: AXIAL Peak Jump

	-----CENTER-----			-----SIDE-----			-----WARMUP TIMES (mins)--		
Filament Currents	P-heat 0.00	Init 4.50	Max 5.50	P-heat 0.00	Init 1.50	Max 2.80	Preheat 00.0	Hold 00.0	Measure 05.0

Pyrometer 0000'C	Initial values	Z-bias 400	Z-focus 500	Slit 500	D-focus 600	D-bias 500	Extract 900	Source 050

Rhenium aiming current 2.0E-12 Beam growth limit -4.5 to +4.5% in 10sec.

Sequence	1	2	3	4	5	6
Detector (F/D)	D	D	D	D	D	D
Aiming current	1.0E-13	3.0E-13	4.0E-13	5.0E-15	1.7E-14	2.5E-14
No. of runs	01	01	05	01	02	10
No. of cycles	02	02	10	02	02	10
Sequence type	05	05	05	26	26	26

Daly bias +0.000E+00 Faraday bias +0.000E+00

Start Grand Totals at Seq. No. 6

PROCEDURES USED FOR THORIUM ANALYSES

1. Thorium Analysis for normal samples:

This procedure is for samples with an average detrital thorium content. It measures $^{229}Th/^{232}Th$, $^{229}Th/^{230}Th$ and $^{230}Th/^{232}Th$ ratios. It corrects for interpeak and background interference but does not normalize any of the ratios. The thorium ion beam aiming current is just a guide: it normally has to changed during the run.

2. Thorium Analysis for High U, Clean samples:

When a sample has very low detrital thorium content then the thorium aiming current has to be quite low to give suitable counts on ^{230}Th and maintain a stable beam for a couple of hours.

3. Thorium Analysis for high detrital content:

If detrital ^{232}Th is high then it is impossible to get a high enough beam on ^{230}Th in the same stage as the ^{232}Th. These samples must be run in two stages: $^{229}Th/^{232}Th$ in the first and $^{230}Th/^{229}Th$ in the second.

1. THORIUM ANALYSIS FOR NORMAL SAMPLES:

Procedure name: TH 230 FOR NORMAL SAMPLES Type: AXIAL Peak Jump

	-----CENTER-----			-----SIDE-----			-----WARMUP TIMES (mins)--		
Filament Currents	P-heat 0.00	Init 4.50	Max 5.80	P-heat 0.00	Init 1.80	Max 3.50	Preheat 00.0	Hold 00.0	Measure 05.0

Pyrometer 0000'C	Initial values	Z-bias 400	Z-focus 500	Slit 500	D-focus 600	D-bias 500	Extract 900	Source 050

Rhenium aiming current 1.5E-11 Beam growth limit -4.5 to +4.5% in 10sec.

Sequence	1	2	3	4	5	6
Detector (F/D)	D	D	D	D	D	D
Aiming current	8.0E-16	2.0E-15	4.0E-15	6.0E-15	8.0E-15	0.0E-00
No. of runs	01	01	01	01	25	00
No. of cycles	02	02	02	02	10	00
Sequence type	04	04	04	04	04	00

Daly bias +0.000E+00 Faraday bias +0.000E+00

Start Grand Totals at Seq. No. 5

Peak jumping TYPE Number 4

Ratio 1 229.0/232.0 =
Ratio 2 229.0/230.0 =
Ratio 3 230.0/232.0 =
Ratio 4 227.5/232.0 =
Ratio 5 229.3/232.0 =

Intrf 1 229.0/228.5 = .5000
Intrf 2 229.0/229.5 = .5000
Intrf 3 230.0/229.5 = .5000
Intrf 4 230.0/230.5 = .5000

Channel	Mass	Integration time
z	221.400	
1	227.500	1
2	228.500	1
3	229.000	2
4	229.300	1
5	229.500	2
6	230.000	4
7	230.500	2
8	232.000	1

2. THORIUM ANALYSIS FOR HIGH U, CLEAN SAMPLES:

Procedure name: TH 230 FOR NORMAL SAMPLES Type: AXIAL Peak Jump

	-----CENTER-----			-----SIDE-----			-----WARMUP TIMES (mins)--		
Filament Currents	P-heat 0.00	Init 4.50	Max 5.80	P-heat 0.00	Init 1.80	Max 3.50	Preheat 00.0	Hold 00.0	Measure 05.0

Pyrometer 0000'C	Initial values	Z-bias 400	Z-focus 500	Slit 500	D-focus 600	D-bias 500	Extract 900	Source 050

Rhenium aiming current 1.5E-11 Beam growth limit -4.5 to +4.5% in 10sec.

Sequence	1	2	3	4	5	6
Detector (F/D)	D	D	D	D	D	D
Aiming current	6.0E-16	8.0E-16	1.0E-15	1.2E-15	1.4E-15	0.0E-00
No. of runs	01	01	01	01	25	00
No. of cycles	02	02	02	02	10	00
Sequence type	04	04	04	04	04	00

Daly bias +0.000E+00 Faraday bias +0.000E+00

Start Grand Totals at Seq. No. 5

3. THORIUM ANALYSIS FOR HIGH DETRITAL SAMPLES:

Procedure name: TH 230 TWO STAGE DETRITAL CARB Type: AXIAL Peak Jump

	-----CENTER-----			-----SIDE-----			-----WARMUP TIMES (mins)--		
Filament Currents	P-heat 0.00	Init 4.50	Max 5.80	P-heat 0.00	Init 1.80	Max 3.50	Preheat 00.0	Hold 00.0	Measure 05.0

Pyrometer 0000'C	Initial values	Z-bias 400	Z-focus 500	Slit 500	D-focus 600	D-bias 500	Extract 900	Source 050

Rhenium aiming current 1.5E-11 Beam growth limit -4.5 to +4.5% in 10sec.

Sequence	1	2	3	4	5	6
Detector (F/D)	D	D	D	D	D	D
Aiming current	1.0E-14	8.0E-14	1.0E-13	5.0E-16	1.0E-15	1.4E-15
No. of runs	01	02	12	01	02	25
No. of cycles	02	02	10	02	02	10
Sequence type	33	33	33	34	34	34

Daly bias +0.000E+00 Faraday bias +0.000E+00

Start Grand Totals at Seq. No. 6

Peak jumping TYPE Number 33

Ratio 1 229.0/232.0 =
Ratio 2 227.5/232.0 =

Intrf 1 229.0/228.5 = .5000
Intrf 2 229.0/229.5 = .5000

Channel z	Mass 221.400	Integration time
1	227.500	1
2	228.500	1
3	229.000	3
4	229.500	1
5	232.000	1

Peak jumping TYPE Number 34

Ratio 1 230.0/229.0 =
Ratio 2 229.3/229.0 =

Intrf 1 229.0/228.5 = .5000
Intrf 2 229.0/229.5 = .5000
Intrf 3 230.0/229.5 = .5000
Intrf 4 230.0/230.5 = .5000

Channel z	Mass 221.400	Int.time
1	228.500	1
2	229.000	2
3	229.300	1
4	229.500	2
5	230.000	4
6	230.500	2

A1.6 TEST OF RHENIUM QUALITY

Zone refined rhenium (99.995%) from H. Cross Company, 363 Park Ave., Weehawken, New Jersey 07087, was tested for levels of contamination.

The beads were preheated at 3 A for 1 minute. (Normally filaments would be preheated for about 10 minutes). The filament current was set at a higher amplitude than is normal during a run. All beads showed consistently low U and Th levels. The figures below are for one batch of metal. This test is done for every new batch of metal.

^{238}U count	Filament current	^{232}Th count	Filament current
28	5.3 A	38	5.3 A

A1.7TREATMENT OF SAMPLES WITH DETRITAL CONTAMINATION

Sampling of contaminated material:

If the detrital material is visible then as much as possible should be removed before dissolution. In flowstone or speleothem the line of darker coloured clay can be cleaned away with a sanding disc. Alternatively the sample may be broken up and only the pure white portions taken for analysis.

If isochron dating is required then several samples of the same growth layer, with varying quantities of detrital contamination, should be taken.

Dissolution and spiking:

The sample is dissolved as usual in 7 N nitric acid and spiked. It is then centrifuged, the supernate saved and the detritus discarded. If any soluble organics are present the supernate may be yellow or brown in colour. It should be treated for oxidation of organics and then processed as normal.

If several leachates are required then the sample should be only partly dissolved in the first step and should not be spiked before centrifuging. The residue from the first centrifuging step is saved. This is treated in the same manner: it is incompletely dissolved, centrifuged and the supernate spiked. The residue may again be saved until the required number of leachates has been produced.

Mass spectrometry:

Samples with high levels of ^{232}Th are usually easy to run because the supply of thorium is large; the thorium beam is easily produced and is stable. However the levels of ^{230}Th may be quite low; if the normal procedure for thorium analysis is used (which measures ^{229}Th, ^{230}Th and ^{232}Th in the one scan) then the aiming current may be raised as high as possible but the counts on ^{230}Th may still be too low. It is not advisable to set the aiming current higher than $3x10^{-13}$ A because Daly amplification is not reliably linear close to its limit. The run should be terminated and restarted using the two stage detrital procedure instead. In the first stage this measures the $^{229}Th/^{232}Th$ ratio only, at relatively low side filament currents. The second stage moves the focus to measure only ^{229}Th and ^{230}Th: the current can then

be raised sufficiently to achieve high ^{230}Th counts and the Daly is not swamped by ^{232}Th.

For detritus-rich samples the side filament current may need to rise higher than is normal (up to around 2.6 A). Fractionation should be carefully watched. If the beam is stable and the ratios do not change significantly over the course of the run then fractionation is probably insignificant in spite of the high current.

The dating program uses only the $^{230}Th/^{229}Th$ ratio. This is translated into the $^{230}Th/^{234}U$ ratio which enters the dating equation for iterative solution. The two-stage thorium analysis procedure measures $^{230}Th/^{229}Th$ directly. The normal single-stage procedure measures $^{230}Th/^{229}Th$ in two ways and the dating program AGE.BAS chooses the ratio with the lowest error: the ratio is measured directly or it may be calculated from the $^{230}Th/^{232}Th$ and $^{229}Th/^{232}Th$ ratios. The error for either method depends on the relative proportions of the three isotopes. The closer a ratio is to unity the lower will be the error. In general the direct $^{230}Th/^{229}Th$ ratio is the better one. However, if the levels of ^{232}Th are low then the indirect method may be applicable.

The number of scans required for the first stage of the two-stage analysis depends on the type of date needed. If only an uncorrected date is requested than the levels of ^{232}Th are not important to the dating procedure and only the second stage of the two stage procedure need be used.

If the date is to be corrected by the simple assumption of an initial $^{230}Th/^{232}Th$ ratio (see discussion of methods of correction for detrital contamination in Chapter 1) then the $^{230}Th/^{232}Th$ ratio must be known. However, it need not be measured very rigorously because this type of correction is quite imprecise. Ten to twenty scans for the first stage may be sufficient to get an adequate measure of ^{232}Th levels.

If an isochron graph is to be constructed then precision on the $^{229}Th/^{232}Th$ ratio is important: the first stage should scan 50 to 100 times.

A1.8 TREATMENT OF SAMPLES WITH VERY LOW ^{232}Th LEVELS

The success of the thorium run relates both to the levels of ^{230}Th and to the total quantity of thorium. There must be enough ^{230}Th to provide an adequate count significantly higher than background and interpeak counts. However, moderate levels of ^{232}Th make for a larger ion beam which is more easily focused, and is longer-lived.

For most speleothem samples much of the thorium beam is made up of ^{232}Th. However, Wind Cave sub-aqueous crust deposited from thermal waters has extremely low levels of ^{232}Th, of the same order of magnitude as ^{230}Th. For these very clean samples the thorium ion beam is made up primarily of spike ^{229}Th. The counts on ^{230}Th may be very high but often the beam does not last long.

For thorium runs on very clean samples two strategies are possible. The first is to aim for good counting statistics on a small number of scans by raising the ^{230}Th count to its maximum. In this case the beam usually does not last long. The second approach is to keep the ^{230}Th counts moderately high but scan for longer. This gives a more controlled beam and is generally preferable. The thorium runs should be extremely gentle using the procedure "TH230 FOR CLEAN, HIGH U SAMPLES". This provides for very low aiming currents but the runs still need to be monitored. The first step may need an aiming current as low as 3.0×10^{-16} A. The final aiming current may be only 8.0×10^{-16} A.

If thorium runs are consistently short-lived and/or unstable for a particular sample then they may be improved by the provision of artificially high ^{232}Th levels. The sample is "doped" with extra ^{232}Th atoms from a pure source. The AAS standards are virtually 100% ^{232}Th. Addition of ~0.1 g of 1 ppm Th standard to the sample (as well as the normal ~0.25 g spike) will not affect the age calculations; only the ^{230}Th/^{232}Th ratios will be wrong. The thorium beam will be augmented, more easily focused and longer-lived.

Appendix 2.1 REAGENTS AND MATERIALS

Spex U and Th Standards: SPEX Industries Standards for Plasma Emission Spectroscopy, 1000 μg/ml in HNO_3

Aesar U and Th Standards: Johnson Matthey, Aesar group, Toronto,
Uranium standard (Cat. No. 13873): Atomic Absorbtion Spectrometry Standard, 1000 +/- 3 μg/ml in 5% HNO_3
Thorium standard (Cat. No. 13820): Atomic Absorbtion Spectrometry Standard, 1000 +/_ 3 μg/ml in 5% HNO_3

NBS 005a uranium isotopic ratio standard: National Bureau of Standards
$^{234}U/^{238}U$: $3.417x10^{-5}$ +/-$0.07x10^{-5}$
$^{235}U/^{238}U$: $5.09x10^{-3}$
$^{236}U/^{238}U$: $1.19x10^{-5}$ +/-$0.01x10^{-5}$

Uraninite: (i) Solution from McMaster alpha counting lab, supplied at ~0.1 g/l in HNO_3, diluted to ~2.8 μg/ml (ii) Harwell Uraninite from U.S.G.S. in HNO_3

Spike Uranium: ^{236}U from (i) Ros 2 spike, McMaster alpha counting lab., (ii) ^{236}U solution made up by Dr. A. Latham.
Spike Thorium: 229Th from Oak Ridge National Laboratories, Oak Ridge, Tennessee.

WL96 spike

Concentration:
0.0045 μg ^{236}U per g or 1.14×10^{11} atoms ^{236}U per g
0.002 μg ^{229}Th per g or 5.47×10^{10} atoms ^{229}Th per g

Isotopic ratios:
Average and 2σ range -
$^{235}U/^{236}U$ on 8 samples: $7.4x10^{-5}$ ($6.1x10^{-5}$ to $8.7x10^{-5}$)
$^{238}U/^{236}U$ on 8 samples: $2.24x10^{-3}$ ($2.23x10^{-3}$ to $2.25x10^{-3}$)
$^{230}Th/^{229}Th$ on 4 samples: $9.05x10^{-3}$ ($8.90x10^{-3}$ to $9.11x10^{-3}$)
$^{232}Th/^{229}Th$ on 3 samples: 1.3114 (1.3091 to 1.3137)

Isotopic fractions:

$\frac{^{235}U}{}$	$\frac{^{236}U}{}$	$\frac{^{238}U}{}$	$\frac{^{229}Th}{}$	$\frac{^{230}Th}{}$	$\frac{^{232}Th}{}$
$7.38x10^{-5}$	0.9977	$2.24x10^{-3}$	0.431	$3.90x10^{-3}$	0.565

Calibration:
$^{229}Th/^{236}U$ ratio
Average and 2σ
By SPEX standards:
(1) by W.L. 0.47993 ± 0.00147 (0.47846 - 0.48140)
(2) by J.L. 0.48108 ± 0.00482 (0.47626 - 0.48590)
By Uraninite: 0.45079 ± 0.00356 (0.44724 - 0.45436)

ST96 spike

Concentration:
By SPEX standards:
Average and 2σ:
(i) Corrected with the average fractionation factor of .9941656:
U conc (atoms ^{236}U / g): $3.5338 \times 10^{11} \pm 0.00328 \times 10^{11}$
(ii) Corrected by iterative procedure:
U conc (atoms ^{236}U / g): $3.5388 \times 10^{11} \pm 0.00687 \times 10^{11}$
Th conc (atoms ^{229}Th / g): $1.0209 \times 10^{11} \pm 0.01059 \times 10^{11}$

By AESAR standards:
Average, $2\sigma_m$:
U conc. (atoms ^{236}U / g): $3.646 \times 10^{11} \pm 0.00156 \times 10^{11}$
Th conc. (atoms ^{229}Th / g): $1.006 \times 10^{11} \pm 0.00285 \times 10^{11}$

Isotopic ratios:

$^{235}U/^{236}U$	$^{238}U/^{236}U$	$^{229}Th/^{232}Th$
Average and $2\sigma_m$:		
8.532×10^{-5}	3.026×10^{-4}	1117.159
0.170×10^{-5}	0.638×10^{-4}	39.908

Isotopic fractions:

^{235}U	^{236}U	^{238}U	^{229}Th	^{232}Th
Average and $2\sigma_m$:				
8.528×10^{-5}	0.99961	3.025×10^{-4}	0.99911	8.952×10^{-4}
0.180×10^{-5}	0.00006	6.371×10^{-5}	0.00003	0.327×10^{-4}

Calibration:
ST96 $^{229}Th/^{236}U$ ratio
Average, $2\sigma_m$ and range
(a) By SPEX standards: 0.288693 ± 0.001016 (0.287677 - 0.289709)
(b) By Old Uraninite: 0.274633 ± 0.001766 (0.272867 - 0.276399)

(c) By AESAR standards:0.275867 ± 0.00079 (0.275076 - 0.276658)
(d) By Ros89 Uraninite:0.27599 ± 0.00178 (0.274215 - 0.277771)
Grand Mean of (b), (c) and (d) and $2\sigma_m$:
0.275497 ± 0.000867

MilliQ: quadrupally de-ionized distilled water.

Acids:
Nitric acid: HNO_3 16N, 7.5N, 2.5N
Hydrochloric acid: HCl 6N, 0.5N
Phosphoric acid: HPO_3 0.3N
Hydrobromic acid: HBr 1N

All acids are distilled from concentrated analytical grade reagents (ACS grade). The undiluted output from the still is 16N strength for HNO_3, 6N for HCl and 9N for HBr. Other concentrations required (7N, 2.5N) are diluted and the concentration of each batch confirmed by titration.

Ammonia: NH_4OH, 28 - 35%, analytical grade without further purification. An ammonia still is being set up for future work.

Ferric chloride: $FeCl_3$ in MilliQ slightly acidified with HCL, 0.4 g / ml, is made up from high purity (99.8% pure) grade reagent from Johnson-Matthey.

Quartz wool is cleaned by boiling in 2 N HNO_3 overnight and then MilliQ overnight. It is finally rinsed and stored in MilliQ.

Anion exchange resin: Bio-Rad anion exchange resin AG 1-X8, grades 100 - 200 (coarse) or 200 - 400 (fine) is supplied in moist condition. It is washed in a large beaker with a series of reagents: MilliQ, 2N HNO_3, MilliQ, 7N HNO_3, MilliQ, 6N HCl and MilliQ. Each time the slurry is well agitated, allowed to settle and the liquid decanted along with any floating resin particles. The resin is then stored in MilliQ.

Columns: The large quartz columns are made up in the glass blowing workshop. The medium and small columns are made up from polyethylene droppers cut to size; the tips are made by heating the tube and drawing it out to a point.

	Large columns	Medium columns	Small columns
Length	18 cm	6.0 cm	2.5 cm
Diameter	1.0 cm	0.8 cm	0.4 cm
inside diam.	~0.8 cm	~0.7 cm	~0.35 cm
Capacity	10 ml	2.5 ml	0.25 ml

Teflon beakers and jars: These are supplied by Savillex Corporation, 5325 Highway 101, Minnetonka, Minnesota 55343, USA.
Cat. No.: #02.25 R (T) Teflon Vials with round bottoms (in tray)

Filament metals: H. Cross Co., 363 Park Ave., Weehawken, N. J. 07087, USA.
High purity rhenium 0.001" x 0.030", in lengths of 6" or more (99.995% purity) ~$1.20 / inch
Zone refined, high purity tantalum 0.001" x 0.030", on spool.

A2.2 CONSTANTS

Isotope	Mass	Decay constant		Half life (y)
^{229}Th		229.0316	9.443×10^{-5}	7340
^{230}Th		230.0331	9.195×10^{-6}	±0.78%75383
^{232}Th		232.0382	4.9475×10^{-11}	±0.6%14.010x10^{+9}
^{234}U		234.0409	2.835×10^{-6}	$2.445 \times 10^{+5}$
^{235}U		235.0439	9.8485×10^{-10}	$0.7038 \times 10^{+9}$
^{236}U		236.0457	2.900×10^{-8}	$2.39 \times 10^{+7}$
^{238}U		238.0508	1.5513×10^{-10}	±0.045%4.468x10^{+9}

$^{235}U/^{238}U$ 0.0072526 ±0.0000188

A2.3 REAGENT CONTAMINATION CORRECTION

The isotopic ratios of the spike were measured from samples of spike loaded directly onto the filament with no chemical pretreatment. In order to calculate reagent blanks spike was processed (i) through columns only and (ii) by ferric chloride co-precipitation. The ratios observed were compared to the correct ratios of the untreated spike. If the measured ratios were outside the 2σ range for the spike ratios then a correction factor was calculated. For the columns-only method corrections were calculated for ^{238}U and ^{232}Th; for the ferric chloride method corrections were calculated for ^{238}U, ^{235}U and ^{232}Th.

The number of atoms of each isotope contributed from the reagent was calculated by comparing isotopic ratios of the spike alone with isotopic ratios from the spike plus contaminant mixture.

Example: 0.6 g of pure ST96 spike has a $^{238}U/^{236}U$ ratio of 0.003, made up of $6x10^{+8}$ atoms ^{238}U and $2x10^{+11}$ atoms ^{236}U. The spike plus contaminants had a $^{238}U/^{236}U$ ratio of 0.014, made up of $3x10^{+9}$ atoms of ^{238}U and $2x10^{+11}$ atoms of ^{236}U. This ^{238}U is made up of $6x10^{+8}$ atoms of ^{238}U from the spike and $2.2x10^{+9}$ atoms from the reagent.

The amount of reagent used is relatively constant so it can be presumed that the reagent will always contribute $2.2x10^{+9}$ atoms of ^{238}U. However, the number of atoms is not counted directly so the reagent blank cannot simply be subtracted from the total ^{238}U counts. Instead the $^{238}U/^{236}U$ ratio must be corrected. The number of ^{236}U atoms depends on the weight of spike added, so the ratio correction must take into account the weight of spike added. (Note that this correction is quite separate from the correction for contributions of 238U from the spike itself.)

Correction for ^{238}U contamination

ST96 $^{238}U/^{236}U = 0.00296$

1 g ST96 = $3.53x10^{+11}$ atoms ^{236}U, $1.05x10^{+9}$ atoms ^{238}U

WL96 = $1.14x10^{+11}$ atoms ^{236}U,

Columns only:

0.582 g ST96 = $2.05x10^{+11}$ atoms ^{236}U, $6.27x10^{+8}$ atoms ^{238}U

$^{238}U/^{236}U$ measured = 0.01383 = $2.84x10^{+9}$ atoms ^{238}U

Number of atoms ^{238}U in reagent = $2.2x10^{+9}$

Average number of atoms of ^{238}U in reagent (2 tests): $1.89x10^{+9}$

CORR86 for COLUMNS (Correction factor for $^{238}U/^{236}U$ ratio): $1.89x10^{+9}$ divided by the number of atoms of ^{236}U from the spike (which is calculated for each sample according to the weight of spike added).

A summary of the results is given below. The full table of data is shown in appendix 5.

	Columns	$FeCl_3$
No. atoms ^{238}U	$1.89x10^9$	$9.23x10^9$
No. atoms ^{235}U		$6.26x10^7$
No. atoms ^{232}Th	$2.19x10^9$	$3.61x10^9$

The relative importance of the correction factor which is subtracted from the measured ratio is calculated from typical values. The example shows the correction of the 238U/236U ratio in a sample treated by the ferric chloride co-precipitation method.

Example: Reagent contamination contributes $9.23x10^9$ atoms ^{238}U. A typical sample has $1.06x10^{11}$ atoms ^{236}U. The correction factor is thus ($9.23x10^9$ / $1.06x10^{11}$) or 0.087. A typical $^{238}U/^{236}U$ measured ratio is 300. The correction factor, 0.087, is only 0.03% of the ratio. The corrected ratio is 299.913.

The significance of the ^{232}Th correction is given as a range which depends on the ^{232}Th content of the sample. The value in brackets shows the highest range found for abnormally ^{232}Th-deficient samples.

Treatment	Relative importance of correction	
	$^{238}U/^{236}U$ ratio	$^{232}Th/^{229}Th$ ratio
$FeCl_3$	0.03%	0.01 - 1.2%
Columns	0.006%	0.007 - 1.2% (1.4%)

Appendix 3

A3.1 PROGRAM: AGE.BAS

"AGE.BAS" is a Basic program to correct for fractionation and mass discrimination, to calculate isotopic ratios, U and Th concentrations, and the sample age.

Variable names: The variable names for ratios follow a pattern:

M = Measured
A = Activity Ratio
H = High L = Low
FF = Fractionation factor
WT = Weight
TH = Total Thorium
SP or K = Spike
AMU = Atomic Mass Unit
INA = Initial Activity ratio
9 = ^{229}Th
2 = ^{232}Th
5 = ^{235}U
8 = ^{238}U

R = Atomic Ratio
E = Error, 2 sigma
D = Decay constant
NA = Number of Atoms
UR = Total uranium
SM or M = Sample
CORR = Correction factor

0 = ^{230}Th
4 = ^{234}U
6 = ^{236}U

Inputs:"AGE.BAS" is used for samples spiked with ST96. Information is input on request: if more than one number is requested then the inputs are separated by a comma.

(a) If required the data can be saved on a floppy in drive A. In this case remove the program disk and insert the data collection disk. This step is important to avoid contamination of the program with data. A filename is required - a shortened form of the sample name is suitable. If the program hangs while data is being recorded then enter CLOSE #1 after the control break step.

(b) Sample name can be many words long but cannot contain a comma.

(c) Sample weight and spike weight are used only to calculate U and Th concentrations; if these data are not available then estimates are input and the age and ratios will be correct but the concentrations will not be correct.

(d) The program provides for uranium ratios only or both uranium and thorium, but assumes that thorium ratios only never occur.

(e) The type of chemical extraction affects the correction factors used: the "small columns or no chemistry" category requires no correction and applies only to spike calibrations; the "large columns and small ones" category requires very minor correction and applies to most samples processed in the normal way; "Ferric Chloride co-precipitation" requires the largest correction and applies where the co-precipitation method has been used with the medium and small columns.

(f) If the values are already corrected for fractionation (but not for spike and reagent contributions) then these can be input directly along with the $2\sigma_m$ error for each ratio.

(g) If the sample has a high detrital content then the thorium analysis is done by the "Two stage detrital procedure". In this case the thorium ratios to be input and some of the calculations differ slightly from the normal one stage procedure.

(h) Measured uranium ratios are input in two sections: the mass spectrometric program "MEASURE" does not total the ratios from the first stage of the uranium run. AGE.BAS calculates the grand means and standard deviations for the first stage. The number of ratios is input: this is normally 6. However, if the beam exceeds the Daly capacity at any stage then the ratios for that run may be abnormal and should not be included.

(i) Each of the six $^{235}U/^{238}U$ ratios (taken from the "After Rejection" column on the mass spectrometry output) is entered.

(ii) Each of the six $^{235}U/^{236}U$ ratios is entered.

For both ratios the mean is calculated and the standard deviation. Then the ratios are checked for extreme values: only those within 1.8 sigma of the mean are accepted. A new mean and standard deviation are calculated using only the accepted ratios. These have already been corrected for fractionation against the $^{235}U/^{238}U$ normalizing ratio. The standard error is then calculated.

(iii) The grand mean (after rejection) and percentage error for $^{235}U/^{236}U$ ratio and the grand means and percentage error for the $^{234}U/^{236}U$ ratio are entered. These last two inputs are usually taken from the final result on the mass

spectrometry output. However, if the error has increased towards the end of the run, the result with the lowest error on the $^{234}U/^{236}U$ ratio is chosen. The $^{234}U/^{236}U$ ratio is corrected for fractionation.

(For special runs where the $^{235}U/^{238}U$ ratio is not normal then a special procedure is used for the mass spectrometry run, the correct $^{235}U/^{238}U$ ratio is entered onto the relevant line of this program and the U ratios have to be corrected for fractionation by hand before inputting.)

(i) Measured thorium ratios are input: normally $^{229}Th/^{232}Th$, $^{229}Th/^{230}Th$ and $^{230}Th/^{232}Th$ ratios and their relative errors are available. Again the result with the lowest error is chosen. These are corrected for mass discrimination. If the thorium was run as a two stage procedure then the first stage $^{229}Th/^{232}Th$ ratios must be entered from each run and the mean and standard deviation calculated as in the first stage uranium analysis.

(j) The number of cycles and the percentage error (1σ) contributing to the $^{230}Th/^{232}Th$ ratio are entered. These are simply printed on the results sheet in order to help in the evaluation of the result.

Outputs:

(a) The average $^{235}U/^{238}U$ ratio and error and the fractionation factor for this ratio are printed out to help in the evaluation of the result. The measured ratio should be between .00733 and .00736. These limits are +/- 1 standard deviations of the mean of the $^{235}U/^{238}U$ ratios measured since February 1989. (N = 39, Mean = .0073478, Standard deviation = .0000151). Fractionation factor should be between .9950 and .9963 (N = 39, Mean = .995664, Standard deviation = .000681).

(b) The "Corrected" ratios are corrected for fractionation only.

(c) The "Sample/ Spike" ratios are corrected for spike and reagant ^{235}U, ^{238}U and ^{232}Th contributions.

(d) Atomic ratios are calculated from the spike ratio and the corrected ratios.

(e) Activity ratios are calculated from the atomic ratios and decay constants:

Activity $^{230}Th/^{234}U$ = λTh230/ λU234 * Atomic ratio $^{230}Th/^{234}U$

(f) Age is calculated from the standard dating equation which is solved by the Newton-Raphson method of iteration (Bittinger and Morrel 1984) using a weighting or "relaxation" factor of 1/2 to facilitate convergence (Pearson 1986):

$$x_{n+1} = x_n - [f(x) / f'(x)] / 2$$

The initial time used to start the convergence series is 100,000 years. The iterations continue until the difference between the last and the penultimate date is less than 0.1 years.

If convergence has not occured in 25 iterations the program switches to the repeated bisection method of solution.

The error is given as the low age and high age calculated on $\pm 2\sigma$ on each of the ratios and put through the iterations again. The 1σ low and high age and range are also presented.

(g) Initial $^{234}U/^{238}U$ ratio is calculated from the equation (Schwarcz and Gascoyne 1984):

$$\left(\frac{^{234}U}{^{238}U}\right)_o = \frac{^{234}U}{^{238}U}_t - 1 \; / \; e^{-\lambda_{234}t} + 1$$

(h) The U and Th concentrations are calculated from the spike and sample weights and the isotopic ratios and masses.

(i) If the $^{230}Th/^{232}Th$ activity ratio is less than 500 then the sample is presumed to have had significant common ^{230}Th of detrital origin to warrent correction of age. The $^{230}Th/^{234}U$ activity ratio is corrected for initial ^{230}Th by assuming an initial $^{230}Th/^{232}Th$ activity ratio of 1.7. The $^{230}Th/^{234}U$ of radiogenic origin is printed out and the corrected age, and error, calculated by iteration with the adjusted ratio. A new initial $^{234}U/^{238}U$ activity is calculated for the new age.

"FRACT.BAS" is applicable if the old spike, WL96, is used. This calculates age by repeated bisection.

A3.2 AGE2.BAS PROGRAM LISTING

```
1 REM: AGE.BAS. (18/9/89) This program corrects for fractionation and calculates
U/Th ages, prints results and saves them on disk.
2 REM: For ST96 Spike
3 REM:-----------------------------------------------
4 PRINT"REMOVE PROGRAM DISK: DATA IS RECORDED ON FLOPPY IN
A: DRIVE. "
5 INPUT "Do you want results saved on disk? (Y/N)";S$
6  IF S$ = "Y" OR S$ = "y" THEN PRINT "Insert disk in A: to collect data"
7  IF S$ = "Y" OR S$ = "y" THEN INPUT"Enter filename for results file";RES$
8 RES$ = "a:" + RES$
9 IF S$ = "Y" OR S$ = "y" THEN OPEN RES$ FOR OUTPUT AS #1
10 INPUT "ENTER SAMPLE NAME"; AAA$
11 LPRINT "SAMPLE       "; AAA$: LPRINT
12 INPUT "Enter sample weight in grams"; WSM
13 INPUT "Enter STAL96 spike weight in grams"; WSP
14 LPRINT: LPRINT "Sample weight  ";WSM;"  ST96 spike weight ";WSP
15 INPUT "Are BOTH uranium and thorium ratios avaliable? Y/N";TR$
16 NASP6 = 3.5E+11: NASP9 = 1.02E+11
17 NA6 = NASP6 * WSP: NA9 = NASP9 * WSP
19 PRINT "Enter the type of chemical extraction:"
20 PRINT "   N means small columns only or no chemistry,"
21 PRINT "   C means large columns (and small ones),"
22 INPUT "   F means Ferric Chloride co-precipitation";CHEM$
23 IF CHEM$ = "C" OR CHEM$ = "c" THEN CORR86 = 1.89E+09 / NA6 AND
CORR56 = 0
24 IF CHEM$ = "C" OR CHEM$ = "c" THEN CORR29 = 2.19E+09 / NA9
25 IF CHEM$ = "F" OR CHEM$ = "f" THEN CORR86 = 9.23E+09 / NA6 AND
CORR56 = 6.26E+07 / NA6
26 IF CHEM$ = "F" OR CHEM$ = "f" THEN CORR29 = 3.61E+09 / NA9
27 IF CHEM$ = "N" OR CHEM$ = "n" THEN CORR86 = 0 AND CORR56 =
0
28 IF CHEM$ = "N" OR CHEM$ = "n" THEN CORR29 = 0
35 INPUT "Are the input values already corrected? (Y/N)";A5$:IF A5$ = "Y" OR
A5$ = "y" THEN GOTO 775
36 INPUT "Was thorium run on a Two Stage Detrital Procedure? Y/N";TH$
37 REM
38 REM: calculates average 235/238 and standard error
39 REM:-----------------------------------------------
40 PRINT "Calculating 235/238, mean and standard error"
42 GOSUB 10034
45 SE58 = SE
50 MR58 = NEWMN:EMR58 = SE58*2
180 REM
190 REM: Calculates average 236/238 and standard deviation
200 REM: -----------------------------------------------
205 PRINT "Calculating 236/238, mean and standard error"
210 GOSUB 10034
215 SE68 = SE
220 R68 = NEWMN:ER68 = SE68*2
```

```
255 R58 = .0072526
256 REM
261 LPRINT : LPRINT "Measured 235/238   "; MR58; "   2 S.E.  "; EMR58
263 FF1 = (R58 / MR58) ^ (1 / 3)
264 LPRINT "      FF 235/238   ";FF1
265 IF (MR58 < .00733) OR (MR58 > .00736) THEN LPRINT "235/238 ratio >
1 sigma from mean"
266 IF (FF1 < .995) OR (FF1 > .9963) THEN LPRINT "FF 235/238 > 1 sigma
from mean"
272 REM
273 REM: calculate true 235/236 and error
274 REM:----------
300 R56 = R53 / R68: ER56 = (ER68/R68) * R56
301 R56 = R56 - CORR56
302 REM
303 REM: calculate corrected 234/236 and error
304 REM:----------
320 INPUT "ENTER MEASURED 234/236 FROM LAST GRAND MEAN AND
THE RELATIVE ERROR "; MR46, EMR46
321 INPUT "ENTER MEASURED 235/236 RATIO FROM LAST GRAND MEAN
AND THE RELATIVE ERROR "; MR56, EMR56
330 FF2 = R56 / MR56
340 LPRINT "      FF 235/236   "; FF2
360 R46 = MR46 * (FF2 ^ 2): ER46 = R46 * ((EMR46/100) * 2)
363 IF TR$ = "N" OR TR$ = "n" THEN GOTO 815
580 IF TH$ = "N" OR TH$ = "n" THEN GOTO 745
585 REM
590 REM: calculates average 229/232 and standard deviation for two stage Th run
595 REM:----------
600 PRINT "Calculating 229/232, mean and standard error"
610 GOSUB 10034
615 SE92 = SE
710 MR92 = NEWMN: ER92 = SE92 * 2
715 R92 = MR92*((229/232)^.5)
716 REM
717 REM: Correct 230/229 for fractionation for two stage Th        run
718 REM:----------
719 REM
720 INPUT "Enter measured 230/229 from last grand mean and relative error
";MR09,EMR09
725 R09 = MR09*((230/229)^.5)
730 ER09 = R09*((EMR09/100)*2)
735 R02 = R92*R09
740 ER02 = R02*(((ER92/R92)^2)+((ER09/R09)^2)^.5): GOTO 815
742 REM
743 REM: Correct Th ratios for fractionation for one stage Th run
744 REM:----------
745 INPUT "ENTER MEASURED 229/232 AND RELATIVE ERROR"; MR92,
EMR92
750 R92 = ((229 / 232) ^ .5) * MR92: ER92 = ((EMR92 / 100) * 2) * R92
752 INPUT "ENTER MEASURED 229/230 AND RELATIVE ERROR"; MR90,
EMR90
```

```
753 R90 =((229/230)^.5)*MR90: ER90 = ((EMR90/100)*2)*R90
755 INPUT "ENTER MEASURED 230/232 AND RELATIVE ERROR"; MR02,
EMR02
760 R02 =((230/232)^.5)*MR02: ER02 = ((EMR02/100)*2)*R02
761 AR09 = 1/R90: AER09 = AR09 * (ER90/R90): BR09 = R02/R92 : BER09
= BR09 * (((ER02/R02)^2 +(ER92/R92)^2) ^.5)
762 LPRINT "aR09 ";AR09;" +/-";AER09;"    bR09 ";BR09;" +/-";BER09
763 IF AER09 < BER09 THEN R09 = AR09
764 IF AER09 > BER09 THEN R09 = BR09
765 IF AER09 < BER09 THEN ER09 = AER09
766 IF AER09 > BER09 THEN ER09 = BER09
769 GOTO 815
770 REM
775 REM: If corrected values are available the program starts here
780 REM:-----------------------------------------------
785 INPUT "Enter corrected 236/238 and 2 S.E. error";R68,ER68
790 INPUT "Enter true 235/236 and 2 S.E. error"; R56, ER56
795 INPUT "Enter corrected 234/236 and 2 S.E. error"; R46,ER46
797 IF TR$ = "N" OR TR$ = "n" THEN GOTO 815
800 INPUT "Enter corrected 230/229 and 2 S.E. error"; R09,ER09
805 INPUT "Enter corrected 229/232 and 2 S.E. error"; R92,ER92
810 INPUT "Enter corrected 230/232 and 2 S.E. error"; R02,ER02
815 LPRINT "True 235/236        "; R56; "      2 S.E. error  "; ER56
820 LPRINT "Corrected 236/238  ";R68;"  2 S.E. error   ";ER68
825 LPRINT "Corrected 234/236    "; R46; "      2 S.E. error  "; ER46
827 IF TR$ = "N" OR TR$ = "n" THEN GOTO 855
830 LPRINT "Corrected 230/229    ";R09;"   2 S.E. error   ";ER09
835 LPRINT "Corrected 229/232    "; R92; "   2 S.E. error   "; ER92
840 LPRINT "Corrected 230/232    "; R02; "   2 S.E. error   "; ER02
844 REM
845 LPRINT
855 REM: provide known information
860 REM:----------------------------
865 DU234 = 2.835E-06: DU238 = 1.55125E-10
870 DTH230 = 9.194999E-06: DTH232 = 4.9475E-11
875 USP = 13.851 : EUSP = .028: THSP = 3.8947 : ETHSP = .0198
880 ASPU = 236.0462: ASPTH = 229.03433#
885 ASMU = 238.028: ASMTH = 232.0382
890 RSP86 = .0003026:ESP86 = 6.377E-05
895 RSP29 = 8.9597E-04: ERSP29 = 3.1792E-05
900 RSP96 = .275497: ESP96 = .000867
915 REM
920 REM: correct R86, R29, R02 and R48 for spike and reagent 238 and 232
925 REM:-----------------------------------------------
930 R86 = 1 / R68: ER86 = R86 * ER68 / R68
935 RSM8K6 = R86 - RSP86 - CORR86: ESM8K6 =((ER86 ^ 2 + ESP86 ^ 2) ^
.5)
937 IF TR$ = "N" OR TR$ = "n" THEN GOTO 1965
940 R29 = 1/R92: ER29 = R29*(ER92/R92)
945 RSM2K9 = R29 - RSP29 - CORR29: ESM2K9 = ((ER29^2 + ERSP29^2)^.5)
950 RSM0M2 = R09/RSM2K9: ESM0M2 = RSM0M2 * ((ER09/R09)^2 +
(ESM2K9/RSM2K9)^2) ^ .5
```

```
955 RSM0K9 = R09: ESM0K9 = ER09
960 RSM4M8 = R46/RSM8K6: ESM4M8 = RSM4M8 *
((ER46/R46)^2+(ESM8K6/RSM8K6)^2) ^ .5
965 R04 = RSM0K9 / R46 * RSP96
970 ER04 = R04 * ((ESM0K9/RSM0K9) ^ 2 + (ER46/R46) ^ 2 + (ESP96/RSP96)
^ 2) ^ .5
975 REM
980 REM: Calculate activity ratios from R02, R04 and R48
985 REM:-----------------------------------------------
990 A04 = DTH230/DU234 * R04: EA04 = A04 * ER04/R04
995 A48 = DU234/DU238 * RSM4M8: EA48 = A48 * ESM4M8 / RSM4M8
1000 A02 = DTH230/DTH232 * RSM0M2: EA02 = A02*ESM0M2/RSM0M2
1002 REM
1004 REM: Print Ratios
1006 REM:--------------
1020 LPRINT "SAMPLE 238 / SPIKE 236 "; RSM8K6; " 2 S.E. "; ESM8K6
1030 LPRINT "SAMPLE 230 / SPIKE 229 "; RSM0K9; " 2 S.E. "; ESM0K9
1040 LPRINT "SAMPLE 232 / SPIKE 229 "; RSM2K9; " 2 S.E. "; ESM2K9
1050 LPRINT
1051 LPRINT "Atomic ratios and 2 S.E. errors:"
1060 LPRINT " 230/234 "; R04; " +/- "; ER04
1070 LPRINT " 234/238 "; RSM4M8; " +/- "; ESM4M8
1100 LPRINT:LPRINT "Activity ratios and 2 S.E. errors:"
1110 LPRINT " Th230/U234 "; A04; " +/- "; EA04
1120 LPRINT " U234/U238 "; A48; " +/- "; EA48
1141 LPRINT " Th230/Th232 ";A02;" +/- ";EA02
1142 LPRINT: GOTO 2025
1960 LPRINT
1965 REM: If only U ratios are available
1966 REM:-----------------------------------
1970 RSM4M8 = R46/RSM8K6: ESM4M8 = RSM4M8 *
((ER46/R46)^2+(ESM8K6/RSM8K6)^2) ^ .5
1975 A48 = DU234/DU238 * RSM4M8: EA48 = A48 * ESM4M8 / RSM4M8
1980 LPRINT "SAMPLE 238 / SPIKE 236 "; RSM8K6; " 2 S.E. "; ESM8K6
1985 LPRINT: LPRINT "Atomic ratios and 2 S.E. errors:"
1990 LPRINT " 234/238 "; RSM4M8; " +/- "; ESM4M8
1995 LPRINT:LPRINT "Activity ratios and 2 S.E. errors:"
2000 LPRINT " U234/U238 "; A48; " +/- "; EA48
2015 GOTO 3000
2020 REM
2025 REM: Age calculations
2028 REM:-----------------
2031 PRINT"Calculating age and error: uncorrected"
2033 GOSUB 12025
2350 LPRINT
2355 LPRINT "Spike 229/236 used ";RSP96
2356 INPUT "Enter N for Thorium run";TH1: INPUT "Enter relative error (1 sigma)
on R02";TH2
2357 LPRINT "Th run: n = ";TH1;", R02 = ";TH2;"% (1 sigma)"
3000 REM
3005 REM: Calculate U and Th concentrations
3010 REM: ---------------------------------
```

```
3012 AMU = 1.66E-16
3015 NA6SK = (3.532388E+11)*WSP :ENA6SK = NA6SK * (3.56E+08 *
2)/3.532388E+11
3020 WTSM5 = R56*NA6SK*235.0439 *AMU: EWTM5 = WTSM5 *
((ER56/R56)^2 + (ENA6SK/NA6SK)^2)^.5
3025 WTSM8 = 1/R68*NA6SK*238.0508*AMU:EWTM8 = WTSM8 *
((ER68/R68)^2 + (ENA6SK/NA6SK)^2)^.5
3030 WTSM4 = R46*NA6SK*234.0409*AMU: EWTM4 = WTSM4 *
((ER46/R46)^2 + (ENA6SK/NA6SK)^2)^.5
3035 WTURSM = (WTSM5 + WTSM8 + WTSM4)/WSM: EURSM =
(((EWTM8)^2 + (EWTM5)^2 + (EWTM4)^2)^.5)/WSM
3040 LPRINT:LPRINT "U conc  ";WTURSM;"ppm  +/- ";EURSM
3045 IF TR$ = "N" OR TR$ = "n" THEN GOTO 3076
3050 NA9SK = (1.023118E+11)*WSP :ENA9SK = NA9SK * (2.61E+08 *
2)/1.023118E+11
3055 WTSM2 = RSM2K9*NA9SK*232.0382 *AMU: EWTM2 = WTSM2 *
((ESM2K9/RSM2K9)^2 + (ENA9SK/NA9SK)^2)^.5
3060 WTSM0 = R09*NA9SK*230.0331*AMU:EWTM0 = WTSM0 *
((ER09/R09)^2 + (ENA9SK/NA9SK)^2)^.5
3070 WTTHSM = (WTSM2 + WTSM0)/WSM: ETHSM = (((EWTM2)^2 +
(EWTM0)^2)^.5)/WSM
3075 LPRINT "Th conc  ";WTTHSM;"ppm  +/- ";ETHSM
3076 REM
3077 REM: Record results on disk
3078 REM:--------------------------
3079 REM
3080 IF S$ = "N" OR S$ = "n" THEN GOTO 3360
3081 REM
3082 P1$ = "SAMPLE    ":PRINT #1, P1$, AAA$
3085 P2$ = "Sample weight    ": P3$ = "ST96 Spike weight  ":PRINT #1, P2$,
WSM, P3$, WSP
3089 P4$ = "Measured 235/238  ":P5$ = " 2 S.E.  ":PRINT #1, P4$ , MR58, P5$,
EMR58
3090 P6$ = "    FF 235/238  ": PRINT #1, P6$, FF1
3093 P7$ = "    FF 235/236  ":PRINT #1, P7$, FF2
3096 P8$ = "True 235/236    ": PRINT #1, P8$, R56, P5$, ER56
3099 P9$ = "Corrected 236/238  ":PRINT #1, P9$, R68, P5$, ER68
3100 P10$ = "Corrected 234/236  ":PRINT #1, P10$, R46, P5$, ER46
3101 P10$ = "Corrected 234/236  ":PRINT #1, P10$, R46, P5$, ER46
3102 IF TR$ = "N" OR TR$ = "n" THEN GOTO 3110
3103 P11$ = "Corrected 230/229  ":PRINT #1, P11$, R09, P5$, ER09
3106 P12$ = "Corrected 229/232  ":PRINT #1, P12$, R92, P5$, ER92
3109 P13$ = "Corrected 230/232  ":PRINT #1, P13$, R02, P5$, ER02
3110 PRINT #1," "
3113 P14$ = "Sample 238 / Spike 236   ":PRINT #1, P14$, RSM8K6, P5$,
ESM8K6: IF TR$ = "N" OR TR$ = "n" THEN GOTO 3120
3116 P15$ = "Sample 230 / Spike 229  ":PRINT #1, P15$, RSM0K9, P5$, ESM0K9

3119 P16$ = "Sample 232 / Spike 229  ":PRINT #1, P16$, RSM2K9, P5$, ESM2K9

3120 PRINT #1, " "
3123 P17$ = "Atomic ratios and 2 S.E. errors:":PRINT #1, P17$: IF TR$ = "N" OR
```

```
TR$ = "n" THEN GOTO 3128
3126 P18$ = "   230/234   ":P19$ = "+/-":PRINT #1, P18$, R04, P19$, ER04
3128 P20$ = "   234/238   ":PRINT #1, P20$, RSM4M8, P19$, ESM4M8
3130 PRINT #1, " "
3133 P21$ = "Activity ratios and 2 S.E. errors:":PRINT #1, P21$: IF TR$ = "N" OR
TR$ = "n" THEN GOTO 3139
3136 PRINT #1, P18$, A04, P19$, EA04
3139 PRINT #1, P20$, A48, P19$, EA48: IF TR$ = "N" OR TR$ = "n" THEN
GOTO 3166
3140 P22$ = "   230/232   ":PRINT #1, P22$, A02, P19$, EA02
3142 PRINT #1, " "
3144 P23$ = "Initial 234/238 Act. ratio   ":PRINT #1, P23$, INA48, P5$, EINA48
3146 PRINT #1, " "
3148 P24$ = "Infinite Age": IF (TM > 600000!) OR (TM < -600000!) THEN
PRINT #1, P24$
3149 P25$ = "Age  ": P26$ = "  -": P27$ = "  +"
3150 IF (HIGH > 600000!) OR (HIGH < -600000!) THEN PRINT #1, P25$, TM,
P26$, LOW, P27$, P24$: GOTO 3162
3152 PRINT #1, P25$, TM, P26$, LOW, P27$, HIGH, P5$
3154 P28$ = "  1 sigma":PRINT #1, P26$, LOW/2, P27$, HIGH/2
3156 P29$ = "Range     ":P30$ = "     to     ":PRINT #1, P29$, TM-(LOW/2),
P30$,TM+(HIGH/2)
3158 PRINT #1," ":P31$ = "        1 sigma % error    ":PRINT #1, P31$,
(((LOW+HIGH)/4)/TM)*100
3162 PRINT #1, " ": P32$ = "Spike 229/236 used    ": PRINT #1, P32$,RSP96
3164 P33$ =  "N for Thorium runs  ": P34$ = "er02, 1 S.E. = ":PRINT #1, P33$,
TH1, P34$, TH2
3166 PRINT #1," ": P35$ = "U conc in ppm    ":P36$ = "  +/- ":PRINT #1, P35$,
WTURSM, P36$,EURSM: IF TR$ = "N" OR TR$ = "n" THEN GOTO 3362
3168 P37$ = "Th conc in ppm    ": P38$ = "   +/- ": PRINT #1, P37$, WTTHSM,
P38$, ETHSM
3360 IF A02 < 500 AND A02 > 0 THEN GOTO 4000
3362 CLOSE #1:END
4000 LPRINT:LPRINT
4005 LPRINT "Corrections for detrital Thorium"
4010 LPRINT "-------------------------------"
4015 LPRINT: REM: Detrital A02 at Time 0 is 1.7
4018     A24 = 1/A02 * A04: T = TM
4020    A04 = A04 - 1.7*(A24)*(EXP(-DTH230*T))
4028 LPRINT "Radiogenic 230/234 Activity ratio  ";A04;"  +/-  ";EA04:LPRINT
4040 GOSUB 12025
4215 LPRINT
4220 LPRINT "Age corrected for detrital thorium"
4225 LPRINT "assuming initial 230/232 activity ratio of 1.7"
4230 IF S$ = "N" OR S$ = "n" THEN GOTO 3362
4233 P39$ = "Corrected for detrital Thorium": PRINT #1, P39$
4234 P40$ = "assuming initial 230/232 activity ratio of 1.7": PRINT #1, P40$
4260 P23$ = "Initial 234/238 Act. ratio   ":PRINT #1, P23$, INA48, P5$, EINA48
4263 PRINT #1, " "
4266 P24$ = "Infinite Age": IF (TM > 600000!) OR (TM < -600000!) THEN
PRINT #1, P24$
4268 P25$ = "Age  ": P26$ = "  -": P27$ = "  +"
```

```
4270 IF (HIGH > 600000!) OR (HIGH < -600000!) THEN PRINT #1, P25$, TM,
P26$, LOW, P27$, P24$: GOTO 4298
4274 PRINT #1, P25$, TM, P26$, LOW, P27$, HIGH, P5$
4277 P28$ = "  1 sigma":PRINT #1, P26$, LOW/2, P27$, HIGH/2
4280 P29$ = "Range     ":P30$ = "     to     ":PRINT #1, P29$, TM-(LOW/2),
P30$,TM+(HIGH/2)
4284 PRINT #1," ":P31$ = "       1 sigma % error   ":PRINT #1, P31$,
(((LOW+HIGH)/4)/TM)*100
4298 GOTO 3362
6977 REM
6988 REM: Bisection Method
6999 REM:-----------------------
7000 PRINT"Bisection Method":TL = 1: TH = 100000000#
7010 T = (TL+TH)/2
7020    IF I = 1 THEN LE = A04
7030    IF I = 2 THEN LE = A04 + EA04
7040    IF I = 3 THEN LE = A04 - EA04
7050    RE1 = 1 - EXP(-DTH230*T)
7060    RE2 = 1 - EXP(-K1*T)
7070    IF I = 1 THEN RE = A84*RE1 + (1 - A84) * K2 * RE2
7080    IF I = 2 THEN RE = (A84+EA84)*RE1 + (1 - (A84 + EA84)) * K2 *
RE2
7090    IF I = 3 THEN RE = (A84-EA84)*RE1 + ((1 - (A84 - EA84)) * K2 *
RE2)
7100 IF ABS(LE / RE - 1) < .001 THEN 12180
7108 IF T = 1E+08 THEN 12180
7150 IF LE > RE THEN TL = T
7160 IF LE < RE THEN TH = T
7170 GOTO 7010
10034 REM:
10035 REM: Subroutine to calculate average and standard error.
10036 REM:---------------------------------------
10040 INPUT "How many ratios are to be entered?";NR
10041 TALLY = 0: NO = 0: DEVMN = 0: DEVSQ = 0
10042 FOR I = 1 TO NR
10045   INPUT "Enter ratio";R(I)
10060   TALLY = TALLY + R(I)
10070   NO = NO + 1
10080 NEXT I
10082 MEAN = TALLY / NO
10090 FOR I = 1 TO NR
10091    DEVMN = (MEAN - R(I))
10100   DEVSQ = DEVSQ + DEVMN*DEVMN
10101 NEXT I
10102 STDEV = (DEVSQ / (NO - 1)) ^ .5
10103 TALLY = 0: DEVSQ = 0: NOR = 0
10104 FOR I = 1 TO NR
10105    IF ABS (R(I) - MEAN) > 1.8 * STDEV THEN GOTO 10128
10120    TALLY = TALLY + R(I)
10125 NOR = NOR + 1
10128 NEXT I
10130 NEWMN = TALLY / NOR
```

```
10135 FOR I = 1 TO NR
10145    IF ABS (R(I) - MEAN) > 1.8 * STDEV THEN GOTO 10165
10150    DEVMN = (NEWMN - R(I))
10160    DEVSQ = DEVSQ + DEVMN*DEVMN
10162    NOR = NOR + 1
10165 NEXT I
10167 NEWSD = (DEVSQ / (NOR - 1))^.5
10168 SE = NEWSD/((NOR)^.5)
10170 MR58 = NEWMN: EMR58 = SE58 * 2
10180 RETURN
10185 REM:
12025 REM: Subroutine: Age calculations
12028 REM:----------
12031 A84 = 1 / A48: EA84 = A84 * EA48 / A48
12033 K1 = DTH230 - DU234: K2 = DTH230 / K1
12036 REM: loop for age, low age and high age
12040  FOR I=1 TO 3
12041  T = 100000!
12042 J = 0: ON OVERFLOW GOTO 12180
12043    REM: iteration loop
12080    IF I = 1 THEN LE = A04
12090    IF I = 2 THEN LE = A04 + EA04
12100    IF I = 3 THEN LE = A04 - EA04
12104    RE1 = 1 - EXP(-DTH230*T)
12106    RE2 = 1 - EXP(-K1*T)
12120    IF I = 1 THEN RE = A84*RE1 + (1 - A84) * K2 * RE2
12130    IF I = 2 THEN RE = (A84+EA84)*RE1 + (1 - (A84 + EA84)) * K2 *
RE2
12135    IF I = 3 THEN RE = (A84-EA84)*RE1 + ((1 - (A84 - EA84)) * K2 *
RE2)
12137    FUNCT# = -LE + RE
12139    IF I = 1 THEN DERIV# = A84 * DTH230 * EXP(-DTH230*T) + K1
* K2 * (1-A84) * EXP(-K1 * T)
12140    IF I = 2 THEN DERIV# = (A84+EA84) * DTH230 * EXP(-DTH230*T)
+ K1 * K2 * (1-(A84 + EA84)) * EXP(-K1 * T)
12142    IF I = 3 THEN DERIV# = (A84-EA84) * DTH230 * EXP(-DTH230*T)
+ K1 * K2 * (1-(A84 - EA84)) * EXP(-K1 * T)
12143 IF DERIV# = 0 THEN PRINT "Deriv = 0": GOTO 7000
12144     DH# = FUNCT#/DERIV#
12146     TEMPT = T
12148     T = T - DH#/2
12150     IF ABS(TEMPT - T) < .1 GOTO 12180
12153 J = J + 1
12154 IF J > 25 THEN GOTO 6988
12155     GOTO 12104
12180  IF I = 1 THEN TM = T
12182  IF I = 2 THEN THIGH = T
12183  IF I = 3 THEN TLOW = T
12184 PRINT "No. of iterations ";J
12185  NEXT I
12186  LOW = TM - TLOW: HIGH = THIGH - TM
12191 REM
```

```
12192 REM: Calculate initial 234/238
12195 REM:-------------------------
12200 INA48 = 1 + (A48 - 1) * EXP(DU234 * TM)
12210 HINA48 = 1 + (A48 - 1) * EXP(DU234 * THIGH)
12220 LINA48 = 1 + (A48 - 1) * EXP(DU234 * TLOW)
12230 EINA48 = (LINA48 - HINA48) / 2
12245 REM
12246 REM: Print age
12247 REM:------------
12255 LPRINT "Initial U234/U238 Act. Rat. "; INA48; "  2 sigma  "; EINA48
12256 LPRINT
12258 IF (TM > 2000000!) OR (TM < -2000000!) THEN LPRINT "Infinite Age
";TM;"  -";LOW;"  +Infinite";HIGH: GOTO 12285
12260 IF (THIGH > 2000000!) OR (THIGH < - 2000000!) THEN LPRINT "Age
";TM;"  -";LOW;"  +Infinite";HIGH: GOTO 2285
12270 LPRINT "AGE  "; TM; "  -"; LOW; "  +"; HIGH;"  2 sigma"
12275 LPRINT "                -";LOW/2;" +";HIGH/2;"  1 sigma"
12277 LPRINT "Range:";TLOW;" to ";THIGH
12280 LPRINT:LPRINT "    1 sigma % error ";(((LOW + HIGH)/4)/TM)*100
12285 LPRINT
12290 RETURN
```

A3.3 ST96UCON.BAS

This is a basic program to calculate the uranium concentration of ST96 spike against the SPEX U standard diluted to 1.02 ppm. It can accept the measured ratios already corrected for fractionation; in this case the program further correctes the ratios for spike ^{238}U and standard ^{236}U contributions. If the ratios are not corrected then an iterative loop is employed to optimise the fractionation correction factor. This method is possible where two ratios are measured and both the spike and standard isotopic composition is known. Because no normalizing ratio is available correction for fractionation has, until now, employed the average correction factor for samples of known normal 235/238. This optimization method is more accurate although, in this case, it makes little difference to the results.

```
1 REM: ST96UCON.BAS Calculates U concentration of ST96 spike
10 REM: with SPEX U standard 1.0211ppm
11 REM:---------------------------------
15 INPUT "Enter sample name";B1$:LPRINT "Sample name ";B1$:LPRINT
20 INPUT "Enter weight of Ur standard in grams";WTST:LPRINT"Wt. U std";WTST

30 INPUT "Enter weight of spike in grams";WTSP:LPRINT"Wt. ST96 spike"; WTSP
40 STCONC = 1.021134
50 F6STWT = 1.4923E-04
60 F8SPWT = .0003052
70 F8STWT = .996678359#
80 F6SPWT = .999695
90 RSP86 = .0003028:EKSP86 = .000111
100 AM8 = 238.0508
110 AM6 = 236.0457
120 AMU = 1.6605E-16
125 DIFF56 = 1.0018
130 DIFF68 = 2.0051
135 SP58 = .281671: SP56 = SP58 * RSP86
140 ST68 = .000151: ST86 = 1 / ST68
145 ST58 = .003201: ST56 = ST58 / ST68
148 F = 0: WW = 0
150 INPUT"Are the ratios already corrected for fractionation? Y/N"; ANS$
155 IF ANS$ = "Y" OR ANS$ = "y" THEN GOTO 244
158 INPUT "ENTER MEASURED 235/238 RATIO";M58:LPRINT "Measured
235/238";M58
160 INPUT "ENTER MEASURED 236/238 RATIO and relative error";M68,E1:E2
= E1*2
162 LPRINT "Measured 236/238: ";M68;"rel.err.: ";E1
163 M86 = 1 / M68: M56 = M58 / M68
```

```
164 P = (M56*(1-DIFF56*F)-SP56)/(ST56-M56*(1-DIFF56*F)):PRINT "P";P
166 P1 = (M86*(1+DIFF68*F)-RSP86)/(ST86-M86*(1+DIFF68*F)):PRINT P1
168 WW = WW+1:PRINT WW
170 F=F-(1-P/P1)/6:PRINT "F";F; "1 - p/p1";ABS(1-P/P1)
172 IF WW = 100 THEN 176
174 IF ABS(1-P/P1)>1/10^6 THEN 164
176 PRINT "NO. ITERATIONS";WW
178 R56 = M56*(1-DIFF56*F): R68 = M68*(1-DIFF68*F): R58 = R56 * R68
180 LPRINT "Corrected 235/236 ";P;" Corrected 236/238 ";R68
184 GOTO 248
244 INPUT "Enter corrected 236/238 and rel. error";R68,E1:E2 = E1*2
246 LPRINT "Corrected 236/238: ";R68;" rel.err.: ";E1
248 ER68 = R68*E2/100
250 UST = WTST * STCONC:LPRINT"Weight Ur in standard ";UST
252 W8ST = UST*F8STWT: LPRINT "Weight 238U in standard ";W8ST
254 AT8ST = W8ST/(AM8*AMU): LPRINT "No. atoms 238U in standard
";AT8ST
260 IF ANS$ = "Y" OR ANS$ = "y" THEN AT6SP = AT8ST / P1: LPRINT
"No.atoms 236U in spike";AT6SP: GOTO 300
280 WT6ST = UST*F6STWT: LPRINT "Weight 236U in standard ";WT6ST
285 AT6ST = WT6ST/(AM6*AMU):LPRINT "No.atoms 236U in standard
";AT6ST
290 AT6ST = WT6ST/(AM6*AMU):LPRINT "No.atoms 236U in standard
";AT6ST
295 AT6SP = (AT6ST-(R68*AT8ST))/((R68*RSP86)-1):LPRINT "No.atoms 236U
in spike ";AT6SP
300 EAT6SP = (2*(ER68/R68)^2)^.5
350 EAT6SP = AT6SP*((2*(ER68/R68)^2)^.5)
355 A6SPGM = AT6SP/WTSP: LPRINT "No.atoms 236U in 1 gm spike
";A6SPGM
360 EA6SPGM = A6SPGM*(EAT6SP/AT6SP):LPRINT"
+/-";EA6SPGM
365 W6SP = AT6SP*(AM6*AMU):LPRINT"Weight 236U in spike ";W6SP
370 EW6SP = W6SP*((EAT6SP/AT6SP))
375 USP = W6SP/F6SPWT:LPRINT "Weight Ur in spike ";USP
380 EUSP = USP*((EW6SP/W6SP))
385 SPCONC = USP/WTSP:LPRINT
390 ESPCONC = SPCONC*((EUSP/USP))
400 LPRINT "Ur conc Stal96 spike ";SPCONC;"ppm +/- ";ESPCONC
410 LPRINT:LPRINT:END
```

A3.4 ST96THCONC.BAS

This is a Basic program to calculate the Th concentration of ST96 spike against the SPEX Th standard diluted to 1.109 ppm.

```
1 REM: ST96THCO.BAS Calculates the Th conc of ST96
10 REM: spike with SPEX Th standard 1.109ppm
15 INPUT "Enter sample name";B1$:LPRINT "Sample name ";B1$:LPRINT
20 INPUT "Enter weight of Th standard in grams";WTST
```

```
30 INPUT "Enter weight of spike in grams";WTSP
40 STCONC = 1.1090232#
70 F2STWT = 1!
100 AM2 = 232.0382
110 AM9 = 229.0316
120 AMU = 1.6605E-16
130 F9SPWT = .99909
160 RSP29 = 8.9512E-04:ERSP29 = 6.395E-06
170 INPUT "Enter measured 229/232 and rel. error";R1,E1:E2 = E1*2
175 LPRINT "Measured 229/232: ";R1;" rel. error: ";E1
180 R92 = R1*((229/232)^.5):ER92 = R92*E2
190 R29 = 1/R92:ER29 = R29*ER92/R92
200 ST2SP9 = R29 - RSP29
205 EST2SP9 = (ER29^2 + ERSP29^2)^.5
210 SP9ST2 = 1/ST2SP9:LPRINT "Sp229/St232   ";SP9ST2
215 ESP9ST2 = SP9ST2*(EST2SP9/ST2SP9)
220 THST = WTST * STCONC:LPRINT"Weight Th in standard  ";THST
230 W2ST = THST*F2STWT: LPRINT "Weight 232Th in standard   ";W2ST
240 AT2ST = W2ST/(AM2*AMU): LPRINT "No. atoms 232Th in standard
";AT2ST
250 AT9SP = AT2ST*SP9ST2: LPRINT "No.atoms 229Th in spike   ";AT9SP
255 EAT9SP = AT9SP*(ESP9ST2/SP9ST2)
260 W9SP = AT9SP*AM9*AMU :LPRINT "Weight 229Th in spike   ";W9SP
265 EW9SP = W9SP*(EAT9SP/AT9SP)
270 THSP = W9SP/F9SPWT: LPRINT "Weight Th in spike   ";THSP
273 A9SPGM = AT9SP/WTSP: LPRINT "No atoms 229Th in 1 gm spike
";A9SPGM
274 EA9SPGM = A9SPGM*(EAT9SP/AT9SP):LPRINT"
+/-";EA9SPGM 275 ETHSP = THSP*(EW9SP/W9SP)
275 ETHSP = THSP*(EW9SP/W9SP)
280 SPCONC = THSP/WTSP:LPRINT
288 ESPCONC = SPCONC*(ETHSP/THSP)
290 LPRINT "Th conc Stal96 spike    ";SPCONC;"ppm      +/- ";ESPCONC
310 END
```

A3.5 SPCALURAN.BAS

This is a Basic program to calculate ST96 spike 229Th/236U ratio against Uraninite in secular equilibrium.

```
1 LPRINT "SPIKE CALIBRATION by URANINITE"
2 LPRINT:LPRINT
3 LPRINT "Uraninite 230/234 activity ratio is assumed to be 1.000"
4 REM: " Spike 229/236 atomic ratio = ":LPRINT "            (Sample 234 / Spike
236) * (Sample 230 / Sample 234)":LPRINT "                                    /
(SAMPLE 230 / SPIKE 229)"
5 INPUT "How many samples?";N1
6 NO = 0: TALLY = 0: MEAN = 0: STDEV = 0: DEVSQ = 0: DEVMN = 0
12 FOR I = 1 TO N1
15    INPUT "Enter Sample Name";SM$
```

```
16    LPRINT:LPRINT "Sample:  ";SM$: LPRINT "----------"
20    INPUT "Enter corrected 234/236 and 2 sigma error";R46,ER46
30    INPUT "Enter Sample 230 / Spike 229 and 2 sigma error";RSMK09,ESMK09
40    R04 = 1!*2.835E-06/9.194999E-06
50    RSP96 = R46*R04/RSMK09
60    ERSP96 = RSP96*(((ER46/R46)^2+(ESMK09/RSMK09)^2)^.5)
160   LPRINT:LPRINT "Spike 229/236 = "; R46;" * ";R04;" / ";RSMK09:LPRINT
170   LPRINT "Spike 229/236 = ";RSP96;" +/- ";ERSP96
175   R(I) = RSP96
176   TALLY = TALLY + R(I)
177   NO = NO + 1
180 NEXT I
185 MEAN = TALLY / NO
190 FOR I = 1 TO N1
200   DEVMN = (MEAN - R(I))
205   DEVSQ = DEVSQ + DEVMN*DEVMN
210 NEXT I
212 STDEV = (DEVSQ / (NO - 1)) ^ .5
220 LPRINT:LPRINT"Average RSP96 from ";N1;" runs:  ";MEAN;" +/- ";STDEV
230 END
```

A3.6 DERIVAGE.BAS

This is a Basic program to calculate ages from 230/234 and 234/238 ratios and their errors. The errors are assumed to be one or two standard deviations and the final error is thus one or two standard deviations.

```
10 REM: DERIVAGE.BAS   This program calculates ages (by Newton's method) from
11 REM: 230/234and 234/238 activity ratios. Results are printed out.
12 REM: ------------------------------------------------
20 INPUT "Enter sample name";A1$: LPRINT"Sample  ";A1$
25 LPRINT "--------------------"
30 INPUT "Enter 230/234 activity ratio, and error";A04,EA04
40 INPUT "Enter 234/238 activity ratio, and error";A48,EA48
50 A84 = 1/A48: EA84 = A84 * EA48/A48
60 DTH230 = 9.194999E-06: DTH232 = 4.9475E-11
70 DU234 =  2.835E-06: DU238 = 1.55125E-10
80 K1 = DTH230 - DU234: K2 = DTH230 / K1
90 REM
100 REM: Loop for (i) age, (ii) high age, (iii) low age
110 REM: ------------------------------------------------
120  FOR I = 1 TO 3
130  T = 1000
140  REM: Iteration loop
170    IF I = 1 THEN LE = A04
180    IF I = 2 THEN LE = A04 + EA04
190    IF I = 3 THEN LE = A04 - EA04
192 RE1 = 1 - EXP(-DTH230*T)
194 RE2 = 1 - EXP(-K1*T)
```

```
200    IF I = 1 THEN RE = A84 * RE1 + (1 - A84)* K2 * RE2
203    IF I = 2 THEN RE = (A84+EA84) * RE1 + (1-(A84+EA84)) * K2 * RE2
206    IF I = 3 THEN RE = (A84 - EA84) * RE1 + ((1-(A84-EA84)) * K2 * RE2)
208 FUNCT# = -LE + RE
209 IF I = 1 THEN DERIV# = A84 * DTH230 * EXP(-DTH230*T) + K1 * K2
* (1-A84) * EXP(-K1 * T)
211 IF I = 2 THEN DERIV# = (A84+EA84) * DTH230 * EXP(-DTH230*T) +
K1 * K2 * (1-(A84+EA84)) * EXP(-K1 * T)
213 IF I = 3 THEN DERIV# = (A84-EA84) * DTH230 * EXP(-DTH230*T) +
K1 * K2 * (1-(A84-EA84)) * EXP(-K1 * T)
215 DH# = FUNCT#/DERIV#
217 TEMPT = T
219 T = T - DH#/2
220 IF ABS(TEMPT - T) < .1 THEN GOTO 250
240 IF T < 0 GOTO 250
245 GOTO 192
250  IF I = 1 THEN TM = T
260  IF I = 2 THEN THIGH = T
270  IF I = 3 THEN TLOW = T
280 NEXT I
285 LOW = TM - TLOW: HIGH = THIGH - TM
290 REM
300 REM: Print results
310 REM: ------------
312 LPRINT
315 IF TM > 600000! OR TM < -600000! THEN LPRINT " Infinite age": GOTO
340
320 IF HIGH > 600000! OR HIGH < -600000! THEN LPRINT "Age  ";TM;"
-";LOW;" +Infinite": GOTO 340
330 LPRINT: LPRINT "Age  ";TM; " -";LOW; " +";HIGH
340 INPUT "Do you want another date on this sample? (Y/N)";A2$
350 IF A2$ = "Y" OR A2$ = "y" THEN GOTO 30
360 INPUT "Do you want to do another sample? (Y/N)";A3$
370 IF A3$ = "Y" OR A3$ = "y" THEN GOTO 20
380 END
```

A3.7 Dating by daughter excess decay: $^{234}U/^{238}U$ dating

If the initial $^{234}U/^{238}U$ ratio is known or can be reasonably accurately estimated, then the extent of restoration of secular equilibrium from the initial ^{234}U excess can give a measure of time. Mass spectrometric measurements of uranium ratios allow this dating to be more precise than by aplha counting. The very real problem which still attends this method is that it is completely dependent on a correct initial $^{234}U/^{238}U$ ratio.

The decay equation used is very simple:

$(234U/238U)_t = (234U/238U)o\ e^{-\lambda 234 * t}$

The activity ratio today (time t) is a simple function of the decay since initiation (time 0).

A BASIC program called "UUDATE.BAS" has been written for this method. It requires inputs of sample name, $^{234}U/^{238}U$ and error (1 or 2 sigma as required) from the "AGE.BAS" output or from alpha counting output and the initial $^{234}U/^{238}U$ estimate and error.

```
50 REM:UUDATE.BAS This program uses the current U/U ratio and its initial
value in "daughter excess" dating.
60 REM:---------- -----
65 REM:
70 INPUT "Enter sample name";AAA$
75 LPRINT "U/U dating on ";AAA$:LPRINT "----------"
80 INPUT "Enter current 234U/238U activity ratio, and error"; A48, EA48
90 INPUT "Enter initial 234U/238U activity ratio, end error"; INA48, EINA48
100 DU234 = 2.835E-06
105 ON ERROR GOTO 190
110 FOR I = 1 TO 3
120     IF I = 1 THEN N1 = A48 - 1: N2 = INA48 - 1
130     IF I = 2 THEN N1 = (A48 + EA48) - 1: N2 = (INA48 - EINA48) - 1
140     IF I = 3 THEN N1 = (A48 - EA48) - 1: N2 = (INA48 + EINA48) - 1
145 IF N1 = 0 THEN N1 = .00001
146 IF N2 = 0 THEN N2 = .00001
150    T = (LOG(N1/N2)) / (-DU234):PRINT T
160 IF I = 1 THEN TM = T
170 IF I = 2 THEN TL = T
180 IF I = 3 THEN TH = T
185 NEXT I
187 GOTO 198
```

```
190 IF TL = 0 THEN LPRINT "Age   ";TM: GOTO 200
195 IF TH = 0 THEN LPRINT "Age  ";TM;"  -";TM-TL: GOTO 200
198 LPRINT "Age   ";TM; "  -";TM - TL; "   +"; TH - TM:LPRINT
200 END
```

Appendix 4

A4.1 LAB REPORTS

This section gives (i) details of sample and spike weights; (ii) some notes on chemical procedures and behaviour of the sample where these were different from normal; (iii) average counts per second on the ^{230}Th ion beam during the main part of the run; (iv) the error on the thorium ratio measurements (see below) and (v) comments on the behaviour of the thorium mass spectrometric runs.

The uranium runs were all quite successful: they ran with a stable ion beam for many hours, with ^{234}U counts at 150 - 200 and the errors on the isotopic ratios lower than 0.2% (1σ).

The thorium runs were much more variable and the errors on the isotopic ratio measurements higher than uranium runs. Thus the quality of the thorium run has a direct effect on the quality of the final age estimate.

The average count per second for the ^{230}Th beam is one indicator of the quality of a thorium run: the higher the number of counts the better the run. For samples of low U content, such as DWBAH, the better runs have counts of 50 - 100. For samples of high U content, such as coral, the counts are usually >100.

The error of the thorium isotopic ratio measurements is another indicator of the quality of the run. The error on the $^{230}Th/^{232}Th$ ratio (referred to below as "Error R02") should be $<1\%$ (1σ) and preferably $<0.3\%$.

The number of scans (in the thorium run) is the final indicator of run quality: the higher the number of scans the better the run. A minimum of 20 scans is usually required in order to consider dating the sample; in the best runs the ion beam is stable for ~ 100 scans.

The comments on the thorium run give an overall evaluation of the quality of the run: "good" means that the beam was relatively stable for some time, and that the number of ^{230}Th counts was acceptable, and that the counting statistics were good (the error on the ratio measurement was low); "poor" means that none of these measures were acceptable

A4.2 BAHAMAS SAMPLES

DWBAH: The major sample of the thesis, large sample of flowstone, taken from -15 m Lucayan Caverns, Grand Bahama Island, Dennis Williams.

7/8/88 Ferric Chloride co-precipitation

Sample name	Weight sample	WL96 spike	No. scans	^{230}Th counts	Error R02	Comment
2b	3.338	0.886	60	~45	0.2%	Good
4b	3.474	0.840	13	~25	1.0%	Poor
6b	3.777	0.792				Died.
10b	3.874	0.837	48	~30	0.5%	Good but centre filament failed
12/13	3.888	0.780	110	~50	0.8%	Very good, high 232, centre filament failed
14b	3.718	0.902	35	~30	0.4%	Poor
16b	3.788	1.018	20	~6	2.0%	Very poor
18b	3.888	0.782				Bead broke.

Sample 12/13 was centrifuged before addition of Ferric Chloride.

30/8/88 Column chemistry only

Sample name	Weight sample	WL96 spike	No. scans	230 counts	Error R02	Comment
2c	2.919	0.932	40	~15	0.7%	Poor
4b	3.618	0.916	50	~50	0.3%	Moderate
6c	3.604	0.874				Died
10bcd	3.967	0.821	60	~20	0.5%	Quite good
12/13	3.611	0.941	56	~20	0.6%	Good but centre filament failed
14	3.416	0.842	88	~30	0.35%	Good, centre filament failed
16c	3.506	0.868	90	~12	0.6%	Quite good
18	3.722	0.825	50	~7	1.7%	Poor

Samples 10, 14, 16 and 18 stuck on the columns the top of which had changed to an orange-brown colour. Addition of further acid rectified the problem but the eluate dried to a white deposit in stead of the usual small drop of yellow deposit. These four were put through the medium columns as well as the small columns.

20/11/88

Sample name	Weight sample	WL96 spike	No. scans	230 counts	Error R02	Comment
1Bah3	5.306	0.703	110	~38	0.23%	Excellent
5Bah3	5.697	0.652	12	~15	2.0%	Very poor
6Bah3	5.162	0.769	109	~100	0.14%	Excellent but centre filament failed
11Bah3	5.216	0.794	50	~40	0.2%	Excellent but centre filament failed
12Bah3	5.446	0.807	95	~70	0.17%	Excellent but centre filament failed
13Bah3	3.823	0.773	76	~50	0.16%	Very good
14Bah3	5.738	0.904				Died.
15Bah3	5.739	0.698	74	~70	0.16%	Excellent
17Bah3	5.363	0.698	20	~12	0.7%	Poor
18Bah3	6.086	0.784	103	~50	0.16%	Excellent

These were run with column chemistry alone. Samples 1, 11, 12, 15 and 18 were cleaned through medium and small columns.

10/1/89

Sample name	Weight sample	WL96 spike	No. scans	230 counts	Error R02	Comment
R	4.332	0.784	100	~50	0.3%	Very good, high 232,
Q	4.585	1.047	80	~12	0.5%	Moderate current too high at 2.9 A
P	4.587	0.892	50	~25	0.7%	Quite good
O	4.709	0.743	60	~5	1.2%	Poor current too high at ~3.2 A
N	4.923	0.875	85	~30	0.2%	Good
M	5.442	1.048	10			Poor, centre filament failed
V	6.486	0.779				Died
W	4.644	0.951	18	~18	1.4%	Very poor
Y	5.306	0.973	70	~70	0.4%	Good, but centre filament failed
X	5.743	0.820				Not run
Z	5.754	0.800	10			Very poor
T4	4.800	0.828	95	~50	0.16%	Very good, but centre filament failed
T2	5.819	0.747				Not run
T1	5.678	0.845	20	~35	0.54%	Moderate
A1	7.194	0.743	30	~15	0.8%	Poor
A2	7.360	0.633				Not run

Column chemistry. The columns were left with 7N HNO_3 for too long and separated (produced air bubbles). The samples were cleaned three times.

15/1/89

Sample name	Weight sample	ST96 spike	Comment
B2	3.288	0.801	Died.
B1	4.812	0.759	Not run
T3	4.684	0.755	Not run
Y	5.127	0.817	Centre filament failed
X	5.676	0.851	Died after 2 scans.
Z	4.549	0.886	No peaks found.
P	3.867	0.699	Not run
L	5.529	0.802	Not run
F	5.666	0.848	Not run
E	5.639	0.936	Not run
D	5.447	0.853	Not run
C	5.985	0.848	Not run
R	2.616	0.836	Not run
O	3.886	0.750	Centre filament failed at start
7	4.849	0.775	Not run
8/9	5.310	0.795	Not run

Note date: this was during the time of detector vacuum problems. Samples were run with large, medium and small columns. First eight ran badly - far too much of this new spike. Next eight were not run.

1/2/89

Sample name	Weight sample	WL96 spike	No. scans	230 counts	Error R02	Comment
I	5.094	0.705	28	~25	0.4%	Poor
H	5.531	0.639	120	~20	0.35%	Very good
T4	4.831	0.756	90	~30	0.25%	Good
G	4.709	0.570	30	~40	0.36%	Moderate
P	3.804	0.785	100	~65	0.11%	Excellent, but centre filament failed
B2	9.290	0.612	86	~45	0.18%	Excellent, but centre filament failed
T3	4.407	0.661	22	~15	0.68%	Poor
B1	3.653	0.756	82	~70	0.16%	Excellent
F	4.652	0.650	70	~90	0.13%	Excellent
O	3.451	0.754				Died
7	5.696	0.710	32	~20	0.86%	Poor
Q	3.726	0.650	70	~15	0.4%	Quite good
T2	4.083	0.603	37	~30	0.34%	Moderately good
3	4.971	0.720	37	~20	1.12%	Moderate
5	4.861	0.611	57	~12	0.5%	Moderately good
8/9	4.497	0.501	17	~40	0.3%	Quite poor, very rapid peak and decay

DWBAH2: Another sample almost identical to DWBAH, also supplied by Dennis Williams. Another attempt to trace deposition through the supposed 40 kyr B.P. rise. It has the same problems of very low U content. The youngest layers, with the least ^{230}Th levels, are to be dated.

11/6/89

Sample name	Weight sample	ST96 spike	No. scans	Error R02	Comment
H5t	6.349	0.316	5		Died
2cm	6.036	0.289	8		Died
1cm	5.873	0.295	13		Died
Below	6.178	0.307	2		Died
Stal	5.133	0.319	60	0.5%	Quite good

H5t is from the topmost layer just underneath the latest erosional hiatus. The next two samples are 2cm and 1 cm above the slight layer of staining which might possibly indicate some kind of flood (but is highly unlikely to indicate a full sea level rise). The next sample was from just below this horizon. The last sample was from the remains of a stalagmite upon which the flowstone had been deposited. It was therefore the oldest part of DWBAH2 and possibly older than the oldest part of DWBAH. All of these samples clogged the columns because they should have been loaded in a larger volume of acid (e.g. 15 ml instead of 10 ml). The mass spectrometer had problems of poor detector vacuum at this time.

Stal sample gave an age of 281 kyr BP. This is within the age of the oldest layer of DWBAH. H5t gave a very rough date of 27 kyr (12 - 46 2σ range) and thus can be taken as very tentative support for continued deposition through the 40 kyr BP period.

A4.3 WIND CAVE WC-MAJ SUB-AQUEOUS CRUST

Run A: 10/4/89 Spike used: ST96

Sample	Sample weight	Spike weight	Comments
WA1	.390	.356	Excess spike,
WA2 .292	.309		V. gentle Th runs, high 230 counts
WA3	.260	.230	(~70) but short-lived
WA4	.271	.253	(40, 50, 15, 30 and 20 scans)
WA5	.292	.217	

Run B: 12/6/89

Sample	Sample weight	Spike weight	Comments
WB1	.300	.207	Good Th run
WB2	.303	.261	Th run failed
WB3	.310	.209	Th run: No peaks found
WB4	.308	.203	Th run failed
WB5	.292	.191	Good Th run

This run was at the beginning of the period of deterioration of the detector vacuum. This explains the highly variable results. Where the Th run was good the 1 σ error on the age was 1 % or less. WB1 ran well for 80 scans at a 230Th count of ~50 and 232Th count of ~500. This sample had relatively high 232Th for thermal deposits. WB5, from close to the base of the crust, gave 100 scans at a 230Th count of ~50 but 232Th counts of only ~35.

Run C: 10/5/89

Sample	Sample weight	Spike weight	Comments
WCa	.391	.290	Th run moderate
WCb	.337	.255	Th run moderate
WCc	.377	.230	Th run failed
WCd	.368	.302	Th run failed
WCe	.358	.260	Th run v. poor
WCf	.387	.228	Th run mediocre
WCg	.408	.275	Th run v. good
WCh	.399	.212	Th run failed
WCi	.388	.256	U run failed, Th run good
WCj	.398	.269	Th run: v. high background
WCk	.398	.246	Th run failed
WCl	.371	.304	Th run: no peaks found

This run was during the period when the detector vacuum was deteriorating. The extraordinary failure of the uranium run on WCi and the high backgrounds on WCj indicate this.

Run D: 12/6/89

Sample	Sample weight	Spike weight	Comments
WD1	.231	.232	Th run v. good
WD2	.236	.267	Th run v. poor
WD3	.212	.267	Th run v. poor
WD4	.205	.283	Th run: No peaks found

WD1 ran for 100 scans at ^{230}Th counts at ~40 and ^{232}Th counts at ~30000. WD3 thorium run was impossible to control with rapid changes in beam stability and size.

Run C repeat: 12/12/89 with added Th standard

Sample	Sample weight	Spike weight	Comments
WCe	.281	.267	Th run excellent
WCf	.312	.273	Th run good
WCg,h	.526	.283	Th run excellent
WCi,j	.292	.312	Th run moderate
WCk	.305	.271	Th run excellent

Two factors contribute to the success of this run and cannot easily be separated. The vacuum pump to the detector unit was running smoothly at this time, and the added thorium standard contributed extra ^{232}Th to help in focusing the beam. The samples with added standard certainly ran extremely well but the improved detector vacuum probably played a greater role than the added ^{232}Th.

A4.4 RAT'S NEST: 881010

18/5/89
E top 1.44 g stal, 0.26 g ST96 spike
G2 top 2.94 g 0.25 g
H1 base D 2.93 g 0.28 g
"D" means "high detrital content".

These were dissolved as normal. H1 base detrital was centrifuged after spiking. E top and G2 top were very slow to run through the columns but did not stick and the thorium fraction did not appear to need another cleaning. E top loaded well on the rhenium filament but G2 top gave a thickish deposit.

E top: U run: normal. Th run: middling, high 230 counts (up to 50) but beam decaying and short lived (20 scans).

G2 top: U run: First stage ran at very high current which reached the limit before the second stage had begun. The second stage was therefore run separately, at ~2.5 A. The ratios from the first stage show a clear change over the course of the run and must be considered to be unreliable because of changing fractionation.
Th run: very poor, very erratic run, rapidly decaying beam, ^{230}Th counts could not be raised above 8 even at current of 3.0 A.

H1 base: U run: halted on division by zero error after 40 scans of second stage. Error good enough to require no repeat run. Th run: used two stage detrital procedure, during first stage there was initially a high background but it burned off in about 15 minutes. Second stage was run separately (because first one stopped inadvertantly). Second stage ran at very high side filament current (2.7 A up to 3.0 A) and 230 counts ~18.

18/6/89 (chemical preparation)
B 2.86 g stal, 0.28 g ST96 spike
C 4.19 g 0.28 g
D 4.33 g 0.31 g
E base 3.65 g 0.30 g
G base 5.53 g 0.27 g
G2 top D 3.55 g 0.28 g

These were run as normal. G2 top detrital was centrifuged before spiking. Samples B and G2 behaved normally throughout chemistry. The larger samples, E, D, G base and C, were very slow on the columns although loaded in 10 ml 7N HNO_3. These were put through the medium sized columns before the final cleaning in the small columns.

23/7/89
G base: U run: second stage stopped on division by zero error. Second stage repeat ran normally. Th run: moderately good, beam decayed but lasted for 50 scans, 230 counts ~25.

18/9/89
E base: U run: normal. Th run: very poor, low 232 counts, beam decayed rapidly,

lasted only 16 scans, 230 counts never above 10.

D: U run: normal. Th run: medium, beam decayed but lasted for 80 scans, 230 counts only ~10 throughout the run in spite of current of 2.5 A.

C: U run: normal. Th run: excellent run, 230 counts up to 170, moderately high 232 (but not enough to warrant the two stage run). Run ended just as beam began to decay slightly because the R array was full, at side filament current of only 2.27 A with an aiming current of 6.3×10^{-14}.

G2 top detrital: U run: normal. Th run: used two stage detrital procedure, very good run, initially high background (up to 190 counts) and ill defined peaks. After about 40 minutes at a current of ~2.7 A it burned off (program was paused). The sample then ran quite well although at a very high side filament current of ~2.7 A in the first stage and up to 3.3 A in the second stage. However, the ratios show no trend over time so changing fractionation is not occurring.

B: U run: normal. Th run: died, beam could not be raised adequately up to current limit of 3.8 A.

9/10/89

E mid	4.29 g stal,		0.40 g ST96 spike.
G2 base D	3.74 g		0.36 g
H1 mid	3.85 g		0.36 g
H1 top	3.17 g		0.34 g
I/J D	2.49 g	0.39 g	
J base	2.35 g	0.39 g	
J mid	5.09 g	0.37 g	
J top	3.40 g	0.37 g	

Except for J mid which stuck on the columns, these samples went through chemistry normally. They were loaded onto the columns in 10 ml 7N HNO_3. The thorium fraction of J mid was put through a second small column. All loaded onto the rhenium filament satisfactorily except for (i) H1 mid thorium fraction which produced a thick black mess. To compound the problem the bead broke so the sample was recovered as well as possible and reloaded onto another filament. (ii) J mid uranium fraction (which had not been cleaned twice) which made a thick black mess. This then fell off the filament so the remainder of the sample was loaded as well.

E mid: U run: normal. Th run: very high centre filament current at 5.8 A (exceptionally high: probably caused by focussing problems). Centre filament failed after a short and very poor run.

G2 base detrital: U run: normal. Th run: used two stage detrital procedure, ran very well although side filament current was rather high, ~ 2.5 A on first stage going up to 2.6 A on second stage. The ratios do not show any clear trend over the course of the run: varying fractionation is not a problem.

H1 mid: U run: normal. Th run: Centre filament current at 5.8 A . Centre filament appeared to be contaminated by the sample, perhaps caused by bubbling of sample during heating. This was left to burn off for 40 minutes but, in spite of the very low

side filament current, there appeared to be little sample left on it. The beam shot out of control a couple of times at a current of more than 3 A and then failed.

H1 top: U run: not so good, very high current reached limit of 2.6 A, run cut short after only 70 scans on the second stage. Th run: Centre filament current at 6.1 A, run promised to be excellent but centre filament failed.

I/J boundary: U run: side filament failed. Th run: used two stage detrital procedure, ran well but at high current 2.5 A for the first stage and ~ 2.8 A for the second. Changing ratios during the course of the run indicate changing fractionation so the final ratios cannot be used for the age calculation. There was a strange "explosion" in the beam after 70 scans in the second stage but the bead was aborted after this because increasing fractionation was obvious.

J base: U run: normal. Th run: good run but very low 230 counts (very young sample) with ill-defined peak, 230 counts up to ~8 at 229 counts of ~ 10000, run failed when aiming current was up to 8.0×10^{-14}.

J mid: U run: did not run at all (the sample fell off the filament), reached current limit of 2.6 A before taking any measuring scans. Th run: very high background counts (~50), left to burn off for 5 minutes. Very high side filament current (2.8 A), 230 counts could not be raised above background, run was aborted after 20 scans.

J top: U run: normal. Th run: quite good run but 230 counts extremely low (sample very young), initially current raised up to 2.8 A before sample "caught" and then was reduced to 2.1 A but after this the beam decayed, 230 counts could not be raised above ~3 at an aiming current of 4.5×10^{-14}.

8/10/89 (chemistry):

E top	2.91 g stal,	0.29 g ST96 spike
G2 top	4.78 g	0.29 g

Chemistry completely normal, loaded onto columns in 10 and 15 ml acid respectively. At final stage converted to the nitrate with 2 drops 7N HNO_3 followed by the usual drop of nitric/phosphoric mixture. This is to see if the thorium fraction dissolves more easily for loading on the filament. These loaded well and the mass spec runs were very good for both samples.

Comments:
1. In general the high detrital samples are the easiest to run because the beams are easy to produce and long lived. However, they seem to run at much higher side filament currents and must be watched carefully for change in ratios over time.
2. The samples from the centre of each deposition horizon are of very white, low uranium and thorium calcite. These need at least 5 g of sample to run adequately.
3. The detrital samples all seem to give too low an age instead of the usual too high an age.

A4.5 CORALS

Sample 75036

24/4/89	Sample wt.	ST96 wt.
1bBA (Boiled in acid)	1.432 g	0.193 g
1dBA (Boiled in acid)	1.627 g	0.229 g
1dNA (No acid treatment)	1.417 g	0.259 g
1fBA (Boiled in acid)	1.530 g	0.199 g

The samples were dissolved as usual, to give a pale yellow clear liquid with no foaming; i.e. the organic content did not appear to be very high. About 2 ml of 16N HNO_3 was added to increase the concentration. This was covered and left to boil under reflux for 6 hours on the hot plates. The colour changed little. They were then spiked and the rest of the chemistry proceeded as normal.

1bBA:
U run: high current up to 2.5A, but otherwise appeared to be quite normal. Th run: good, 230 counts ~35, 120 scans.
1dBA:
U run: normal. Th run: high 230 counts (~50) but beam decayed rapidly. 36 scans, 0.266 % error on 230/232 ratio.
1dNA:
U run: normal. Th run: very good, 230 counts up to 180, sample lasted 120 scans, error on 230/232 ratio 0.052%.
1fBA:
U run: normal. Th run: 230 counts were high early on in the run and stayed around 70, but the beam decayed rapidly and the side filament current rose to 2.5 A. However the high 230 counts gave an error on 230/232 of only .18% after 20 scans.

Sample 790513-2 from Harmon et al 1983

12/6/89
513BA: 0.396 g coral, 0.28 g ST96
513NA: 0.326 g coral, 0.28 g ST96

Chemistry proceeded as normal after acid treatment of first sample.
513BA:
U run: normal. Th run: moderately good, 230 counts only up to ~25 at current of 2.23 A, beam quite good but began to decay after 30 scans and error increased after 50 scans. (Need more sample)
513NA:
Th run: No peaks found at all. (This was during the time when the detector vacuum was turned off).
Comments: Because the second sample failed completely it was impossible to see if the acid treatment made any difference this time.

23/7/89
Note: All these samples were run during the time when the detector vacuum had been turned off.
M1: 0.23 g coral, 0.26 g ST96
M2: 0.35 g 0.28 g
M3: 0.75 g 0.29 g

M4: 1.09 g 0.23 g
M5: 1.77 g 0.27 g
M6: 2.42 g 0.29 g
M7: 2.09 g 0.26 g

This series was intended to find the optimum sample size for coral dating. The thorium fraction from M2 was loaded in 0.5M HCl onto the rhenium filament as a test of loading procedure to see if the chloride form provided better ionization. The samples were treated for organics by the following sequence:-7n HNO_3, dry, conc. HNO_3, dry, aqua regia, dry, 7N HNO_3, dry.

M1 U run: normal. Th run: very poor, 230 counts up to 15 at 2.6 A, beam decayed rapidly, 0.8% error on 230/232 after only 9 scans.
M2 Th run failed
M3 U run: normal. Th run: quite good, 230 counts up to 70 at 2.2 A, beam started to decay after 40 scans, lasted for 100 scans, 0.17% error on 230/232 ratio, 232 counts low.
M4 U run: normal. Th run: moderately poor, 230 counts ~10 at current of 2.6 A, beam decayed for all the 40 scans, 1% error on 230/232.
M5 Th run: No peaks found at all.
M6 U run: normal. Th run: very poor, 230 counts ~15 at current of 2.7 A (far too high for clean samples), beam decayed rapidly, 28 scans, 1.7% error on 230/232.
M7 U run: normal. Th run: very poor, 230 counts only ~5 at current of 2.8 A, beam decayed rapidly, only 20 scans, 2.2% error on 230/232.

Coral samples D3 and VI from Lynton Land to H. P. Schwarcz.

26/6/89
D3: 0.87 g coral, 0.32 g ST96
VI: 0.98 g coral, 0.27 g ST96

The samples were dissolved in 7N HNO_3 to give a pale yellow solution. Both were treated for oxidation of organics until the solution had lost all colour, with the following sequence:- 7N HNO_3, dry, 7N HNO_3, dry, aqua regia, dry, aqua regia, dry. The colour had gone after only three acid-dry cycles. This became the standard treatment for oxidation of organics to be extended as required until the colour disappears. The chemistry proceeded as normal. Loading onto the thorium filament was not very satisfactory. Both made a rather thick mucky residue.
D3: U run: normal. Th run: moderately poor, 230 counts up to 30 but beam decayed rapidly during all scans, reached 40 scans, 0.42% error on 230/232. 232 counts lower than 229 counts. These corals have so little thorium that the normal focus procedure on 232 does not work well.
VI: Th run failed to bring up a beam.

Oct.89
Added thorium standard to one of the samples.

D3A: 0.62 g coral, 0.43 g ST96, 0.35 g Th std.
D3B: 1.04 g 0.37 g
D3C: 1.51 g 0.35 g
VIA: 0.74 g 0.48 g 0.19 g
VIB: 1.07 g 0.47 g
VIC: 1.59 g 0.34 g

All were treated for organics, chemistry normal.
All mass spectrometer runs were good.

A4.6 CARLSBAD LAKE OF CLOUDS
(Samples 87 CLC / JRH -1.0 ft. and 87 CLC / JRH -2.0 ft.)

Run 1 24/4/89: CLC1 7.95 g, ST96 0.252 g.
CLC2 7.85 g, ST96 0.299 g.

Both samples were prepared for mass spectrometry by the Ferric Chloride coprecipitation method. Chemistry was normal.

Uranium ran well for both samples but baseline zero was relatively high at around 17 - 25 counts. Both had extraordinarily high background counts during the thorium runs: 175 counts reducing to 42 counts on CLC1 and 331 down to 178 on CLC2. Only CLC1, the minus 1 ft. sample, had an acceptable thorium run (60 scans) and error margin (0.15% on 230/232). CLC2 only ran 30 scans with a very high error (4.0% on 230/232).

Run 2 2/6/89: 2CLCR 6.38 g, ST96 0.257 g.

The lower sample (minus 2 ft.) was repeated with column chemistry only, on the assumption that the high background was caused by complexing with the ferric chloride. The high background problem was reduced: for the uranium run it varied from 3 to 5 counts and for the thorium run from 10 to 26 counts. The thorium run reached 70 scans with an acceptable error (0.6% on 230/232).

Run 3 10/7/89: 1 CLC 6.49 g, ST96 0.304 g.
2 CLC 7.70 g, ST96 0.216 g.

Both samples were repeated with column chemistry only. The solution was acid treated and dried several times to oxidise organics. Uranium ran normally with background counts less than 5. In both cases the thorium runs failed. 1 CLC began with a high background count. The program was paused to let it burn off at 2.6A but the beam failed soon after. 2CLC did not have a high background but failed after 2 scans.

A4.7 OSTRICH EGGS

Experiments on young shells:

Sample from Neolithic site (6 - 7 kyr?) in Bir Sahara. E-88-10-a

Run 1: Egg1A 1.94544 g shell, .23063 g ST96 spike.
Egg1B 1.75300 g shell, .21369 g ST96 spike.
Dissolution step: Carefully added 7N HNO_3 in small volumes. Strong foaming resulted, fawn in colour. At end of dissolution foam had subsided with residues left on sides of beaker. Solution was a rich yellow-brown colour.

Oxidation step: Added 2 ml 16N HNO_3 to 7N solution. With the lid in place to cause refluxing the solution was heated at close to boiling point for 6 hours. The colour lightened only a little, suggesting that boiling has little effect on organics.

Spiked and continued chemistry as normal with no problems.

Mass spec runs: U runs required very gentle treatment because the sample was very small. This suggested that the unoxidized organics had reduced the yield of uranium. The thorium runs were good: the high 232Th gives a strong Th+ ion beam but no 230Th was detectable.

Egg1A Th run: Very good run. 232Th counts 5 times 229Th counts. Aiming current raised to $1.5x10^{-14}$ A.

Egg1B Th run: 232Th eight times 229Th, good beam at aiming current of $3.0x10^{-14}$.

Results: U concentration around 0.06 ppm.
Th concentration around 2.8 ppb.

Conclusion: U chelated/complexed by organics and lost before loading on column. (Resin from these columns was changed in case the U was trapped in the columns.) A better procedure for oxidation was needed. Decided to try (a) cycles of 7N HNO3 + 6N HCl (aqua regia) dissolution followed by hot lamp evaporation until colour reduced; (b) baking in furnace in oxygen.

Run 2:
1. Tried baking shell at 500 C in oxygen for 12 hours in furnace. Egg shell fragment (not ground) went in pale cream in colour. Disintegrated and dispersed around furnace tube during heating. Emerged black in colour, suggesting that much of the carbon was in a reduced form in spite of the oxygen atmosphere. Dissolution in 7N HNO3 failed to lighten the colour. Oxidation (detectable by yellowing and lightening of colour) achieved through four acid-dry cycles.

2. As a comparison for the baked shell a sample was oxidized only through the acid-dry cycles.

3. Tried large sample to see if 230Th levels high enough to get a date. 6 g egg shell, .25 g spike.

Results:

Baked Egg Th run: 232Th 9 times 229Th. Moderately poor run at aiming current of $4.0x10^{-15}$ A. U run was normal. Run on "U234 for normal samples" procedure with no modifications.

Acid treated egg: 232Th 4 times 229Th. Very similar run to Baked Egg sample. U run also normal.

Large sample Th run: High 232Th (18 times 229Th) but poor run. Baseline zero counts high at 10 - 20. 230Th counts same as interpeak background. Beam died after only 9 scans. U run on normal procedure but beam decayed all the way through and side filament current was high (2.6 A). High background may be unoxidized organics.

Conclusions: 1. Baking does not improve oxidation.
2. Cycles of acid dissolution and hot lamp evaporation seem to release the U well in small samples.

3. Larger samples need much more oxidation to release the U.

Dating of the old egg shells:
Egg 40 Th run: Loaded well. Moderate 232Th (5 times 229Th counts) but poor beam. Beam decayed all through the run: there was no phase of beam growth. Cut all the warm-up sequences short but only got 10 scans at an aiming current of $7.5x10^{-15}$ before the beam died. Error too high at 3.6% on thorium run and 11% on date.
U run: Normal in all respects. Used the U234 procedure for normal samples with no modifications.

Egg 41 Th run: Loaded well. Moderately high 232Th (13 times 229Th counts) gave moderately good thorium beam but low 230Th counts. Raised aiming current to $2.8x10^{-14}$ but side filament current was getting too high to go any further. Got 38 good scans before beam died.
U run: Normal.

Egg 42 Th run : Loaded by etching filament in phosphoric acid first. Sample loaded from the 1 μl of phosphoric/nitric mixture. Did not puff properly and formed a thick source. Moderately high 232Th (8 times 229Th counts) gave moderately good thorium beam at aiming current of $4.2x10^{-15}$ A.
U run: Normal.

Egg 43 Th run: Loaded by etching filament in phosphoric acid first. Sample loaded from the 1 μl of phosphoric/nitric mixture. It did not puff properly and formed a thick source. Strange behaviour but eventually ran quite well. The trace did fall after the rhenium beam was raised but it then shot up out of range. This was probably caused as the side filament heated up the thick sample bubbled up and came into contact with the centre filament. After about 5 minutes the thorium on the centre filament had burned off and the side filament could be turned up. Although some of the sample was lost it ran reasonably well. 232Th counts 5 times 229Th counts. Aiming current reached $6.0x10^{-15}$, 230Th counts approaching 20 for most of the scans.
U run: Normal.

Egg 44 Th run: Loaded well. High 232Th counts (17 times 229Th counts) gave good beam at aiming current of $1.0x10^{-14}$ A.
U run: Normal.

Egg 48 Th run: Loaded by etching filament in phosphoric acid first. Sample loaded from the 1 μl of phosphoric/nitric mixture. It did not outgas properly and formed a thick source High 232Th (160 times 229Th counts) gave good thorium beam. Raised it to $2.0x10^{-13}$ but could find no 230Th.
Did not run the uranium fraction.

APPENDIX 5.1 SPIKE CALIBRATION, WL96

WL96 CALIBRATION BY SPEX STDS (0.99312 ppm U, 1.06209 ppm Th) FF = .9939616

	Weight U std	Weight Th std	Weight WL96	Corrected 236/238	%error 1 sig	Measured 229/232	%error 1 sig	Corrected 229/232	Spike U conc ppb	Spike Th conc ppb	Spike 229/236
1/8'88											
B1	1.6598	1.6267	2.2214	0.006251	0.034	0.002723	0.035	0.002705	4.4839	4.8714	0.47967
B2	1.4350	1.6968	2.1864	0.007088	0.034	0.002563	0.043	0.002546	4.4796	4.8643	0.47951
B3	1.8170	1.7904	2.6569	0.006813	0.030	0.002960	0.043	0.002941	4.4822	4.8755	0.48531
9	0.2717	0.3180	1.9900	0.033462	0.025	0.012303	0.094	0.012223	4.4758	4.8864	0.48032
10	0.1905	0.3042	1.8557	0.044469	0.025	0.012007	0.026	0.011929	4.4772	4.8904	0.48058
								Average	4.4797	4.8776	0.48108
								2 sig	0.0067	0.0215	0.00482

"Corrected 236/238" has been corrected to a normalising 235/238 ratio of 0.003201

Fraction 236U = 0.997689 Fraction 229Th = 0.430950

Average 229/236 (from average sample 229/236)
0.4810789 +/- 0.0048181 Range 0.47626 - 0.48590

Average 229/236 (from average concentrations)
0.4703109 +/- 0.0225198 Range 0.47908 - 0.48142

WL96 CALIBRATION BY URANINITE

	Weight Uraninite	Weight WL96	AtRat 234/236	+/- 2 sig	Sm230 Sp229	+/- 2 sig	230/234 AtRat	+/- 2 sig	234/238 AtRat	+/- 2 sig	230/234 Activity	+/- 2 sig	234/238 Activity	+/- 2 sig	230/232 Activity	+/- 2 sig	U conc ppm	Th conc ppb	Spike 229/236
25/7/88													1.000211	0.004190			2.884		
S	0.28456	0.82540							5.473E-05	2.293E-07			0.997943	0.005888	2458	32	2.883	0.384	0.46200
T	0.33716	0.83503	1.40E-02	5.10E-05	9.36E-03	8.997E-05	0.309995	0.003970	5.461E-05	3.222E-07	1.005432	0.012877	1.001005	0.003440			2.876		
U	0.35961	0.86372							5.477E-05	1.882E-07									
1/8'88																			
6	0.53570	0.89602	2.08E-02	4.58E-05	1.42E-02	1.545E-04	0.316591	0.004272	5.476E-05	1.963E-07	1.026827	0.013850	1.000821	0.003588	3020	41	2.879	0.379	0.45240
7	0.53570	0.89602	1.43E-02	4.52E-05	9.86E-03	7.808E-05	0.319967	0.003664	5.469E-05	2.168E-07	1.037776	0.011880	0.999505	0.003961	2523	28	1.983	0.026	0.44760
8	0.38781	0.77473	1.75E-02	7.00E-05	1.20E-02	8.560E-05	0.318596	0.003567	5.493E-05	2.532E-07	1.033331	0.011568	1.003968	0.004627	2776	29	2.883	0.038	0.45000
3'12/88													1.003974	0.004636			2.898		
G	0.37867	0.71009							5.494E-05	2.537E-07			0.998423	0.004674	2960	30	2.895	0.350	0.45154
H	0.40006	0.70782	1.97E-02	3.71E-05	1.35E-02	7.006E-05	0.317193	0.002992	5.463E-05	2.558E-07	1.028780	0.009704	0.999979	0.005947	2617	30	2.895	0.355	0.45058
J	0.44200	1.00114	1.54E-02	2.65E-05	1.06E-02	6.534E-05	0.317868	0.003172	5.472E-05	3.254E-07	1.030965	0.010289	1.002207	0.003029	2363	26	2.891	0.350	0.45046
L	0.43734	1.24128	1.23E-02	2.37E-05	8.44E-03	6.252E-05	0.317956	0.003439	5.484E-05	1.658E-07	1.031254	0.011154	1.002179	0.005547	3141	33	2.896	0.337	0.45300
P	0.49177	0.78327	2.20E-02	5.02E-05	1.50E-02	7.303E-05	0.316173	0.002955	5.484E-05	3.035E-07	1.025470	0.009585							

Note: Sm230/Sp229 means "Sample 230 / Spike 229" ratio.

Average 229/236 = 0.452198 +/- 0.006579 Range 0.443618 - 0.460776
Sample T is outside this range

Average excluding T = 0.45079 +/- 0.00356 Range 0.44724 - 0.45436

APPENDIX 5.2 SPIKE CALIBRATION, ST96

ST96: ISOTOPIC COMPOSITION FF = .9941656

	Meas. 229/232	%error	Corr. 229/232	Meas. 235/238	1 sig %error	Corr. 235/238	Meas. 236/238	1 sig %error	Corr. 236/238	Meas. 235/236	238/236	232/229
30/12/88												
1	1101.394	0.600	1094.250									9.136E-04
2				0.241190	0.806	0.236992	2766.0202	0.380	2733.838	8.669E-05	3.658E-04	
3	1173.541	2.290	1165.928	0.323639	0.453	0.318007	3841.7078	0.276	3797.010	8.375E-05	2.634E-04	8.577E-04
5	1139.371	0.996	1131.980									8.834E-04
6	1083.506	0.541	1076.477	0.312169	0.617	0.306737	3629.7564	0.276	3587.525	8.550E-05	2.787E-04	9.298E-04
									Average	8.531E-05	3.026E-04	8.960E-04
									2 sig	2.954E-06	1.105E-04	6.358E-05
									2 SE	1.705E-06	6.377E-05	3.179E-05

ST96: CALIBRATION BY SPEX 1.021133 ppm U STD, 1.109023 ppm TH STD

FF = .9941656 Standard 235/238 = .003201

	Weight U std.	Weight Th std.	Weight spike	Meas. 236/238	% error 1 sig	Corr. 236/238	Meas. 235/238	% erro 1 sig	Corr. 235/238	Meas. 229/232	1 sig % error	Number of atoms U236 in 1 g (1)	Correction by iteration FF	Corr. 236/238	Corr. 235/238	Number of atoms U236 in 1 g (2)	Number of atoms Th229 in 1 g	Spike ratio 229/236 (1)	(2)	Average
30/12/88																				
7	0.2628		1.0387	0.054956	0.014	0.054317	3.262E-03	0.065	3.204E-03			3.529E+11	0.99425	0.054329	3.205E-03	3.540E+11				
8	0.3017		1.2635	0.058366	0.020	0.057686	3.270E-03	0.072	3.216E-03			3.538E+11	0.99345	0.057603	3.205E-03	3.542E+11				
9	0.2559		1.2255	0.066669	0.014	0.065892	3.274E-03	0.047	3.217E-03			3.534E+11	0.99311	0.065753	3.206E-03	3.535E+11				
10		0.2959	1.2677							0.015340	0.062						1.024E+11			
11		0.3477	1.2948							0.013190	0.066						1.013E+11			
12		0.3933	1.2351							0.011267	0.072						1.026E+11			
											Average	3.534E+11				3.539E+11	1.021E+11	0.28890	0.28849	0.28869
											2 sig	3.276E+08				6.872E+08	1.059E+09	0.00303	0.00299	0.00426
											2 S.E.	1.891E+08				3.968E+08	6.112E+08			

Continued on next page

ST96: CALIBRATION BY OLD URANINITE

	Weight Uran	Weight ST96	Corr. 234/236	+/- 2 sig	Sm230/ Sp229	+/- 2 sig	230/234 ATrat.	+/- 2 sig	234/238 ATrat.	+/- 2 sig	230/234 Act.rat.	+/- 2 sig	234/238 Act.rat.	+/- 2 sig	230/232 Act.rat.	+/- 2 sig	U conc ppm	Th conc ppb	Spike 229/236
30/12/88																			
14	0.37898	0.78140	0.005477	1.26E-05	0.00607	2.41E-05	0.321124	0.002296	5.486E-05	2.886E-07	1.041529	0.007448	1.002587	0.005274	24959	206	2.8951	0.3628	0.278091
15	0.35532	0.76709	0.005235	1.15E-05	0.00584	6.9E-05	0.323068	0.004267	5.480E-05	1.760E-07	1.047834	0.013840	1.001581	0.003217	25363	336	2.9002	0.3591	0.276817
16	0.37782	0.85079	0.005001	1.08E-05	0.00559	1.92E-05	0.323624	0.002209	5.458E-05	2.236E-07	1.049637	0.007165	0.997471	0.004086	24522	180	2.9017	0.3708	0.275943
15/2/89																			
SU4	0.54493	0.30400	0.020168	4.07E-05	0.02287	0.000229	0.313874	0.004104	5.451E-05	1.764E-07	1.018014	0.013312	0.996262	0.003224	25856	281	2.9018	0.4120	0.271919
									5.480E-05	2.622E-07			1.001580	0.004792			2.8963		
SU5	0.46895	0.20840																	
SU6	0.42244	0.38260	0.012436	2.29E-05	0.01402	8.64E-05	0.312156	0.003242	5.474E-05	1.298E-07	1.012443	0.010515	1.000438	0.002373	25515	184	2.8927	0.4155	0.273415
9/6/89																			
J	0.25886	0.20855	0.013999	2.83E-05	0.01584	9.25E-05	0.313263	0.003205	5.454E-05	2.041E-07	1.016033	0.010393	0.996782	0.003730	25529	161	2.9072	0.4160	0.272449
K	0.23053	0.24795	0.010491	2.1E-05	0.01181	8.7E-05	0.311716	0.003482	5.467E-05	1.024E-06	1.011016	0.011290	0.999109	0.018719	25317	216	2.9019	0.4172	0.273800
																		Average	0.274633
																		2 sigma	0.005028
																		2 S.E.	0.001766

Note: Sm230/Sp229 means "sample 230 / spike 229" ratio.

ST96: CALIBRATION BY AF[illegible] 0.9574 ppm U STD, 1.0212 ppm TH ST FF = .995664 Standard 235/238 = .034633

	Weight U std.	Weight Th std.	Weight spike	Meas. 236/238	%error 1 sig	Corr. 236/238	Meas. 235/238	%error 1 sig	Corr. 235/238	Meas. 229/232	1sig % error		Atoms Th229 in 1 g	Atoms U236 in 1 g	Spike ratio 229/236
20/9/89														3.651E+11	
SS1	0.26350		0.73945	0.04296	0.024	0.042589	0.003510	0.067	0.0034643					3.643E+11	
SS2	0.27167		0.92705	0.052094	0.013	0.051643	0.003504	0.045	0.0034582					3.644E+11	
SS3	0.30416		0.95852	0.048137	0.012	0.047720	0.003516	0.045	0.0034701					3.644E+11	
SS4	0.31153		0.94862	0.046549	0.012	0.046146	0.003508	0.050	0.0034628					3.646E+11	
SSWTh		0.45269	0.80542							0.0067648	0.162		1.009E+11		
SSXTh		0.39062	1.00039							0.0097881	0.250		1.007E+11		
SSZTh		0.40198	1.02195							0.0097436	0.309		1.001E+11		
												Average	1.006E+11	3.646E+11	0.275867
												2 sig	4.942E+08	3.115E+08	0.001376
												2 S.E.	2.853E+08	1.558E+08	0.000791

ST96: CALIBRATION BY NEW URANINITE Ros89

	Weight Uran	Weight ST96	234/236	+/- 2 sig	Sm230/ Sp229	+/- 2 sig	230/234 ATrat.	+/- 2 sig	234/238 ATrat.	+/- 2 sig	230/234 Activity	+/- 2 sig	234/238 Activity	+/- 2 sig	230/232 Activity	+/- 2 sig	U conc ppm	Th conc ppb	Spike 229/236
20/9/89 Dilution B																			
P	0.25597	0.30110	0.04486	0.00012	0.05113	0.00011	0.31550	0.00279	5.37E-05	2.06E-07	1.02328	0.00906	0.98072	0.00376	43712	159	13.826	1.243	0.27052
Q	0.25654	0.22836	0.06026	0.00011	0.06770	0.00015	0.31099	0.00269	5.44E-05	1.96E-07	1.00866	0.00872	0.99370	0.00361	43614	147	13.870	1.247	0.27444
R	0.34402	0.25296	0.07329	0.00013	0.08182	0.00020	0.30901	0.00269	5.45E-05	2.62E-07	1.00223	0.00874	0.99628	0.00478	43677	160	13.899	1.244	0.27620
20/9/89 Dilution C																	2.855		
RJ	0.67383	0.29545							5.45E-05	3.44E-07			0.99658	0.00628			2.853	0.258	0.27720
RK	0.81049	0.30238	0.02973	0.00006	0.03307	0.00006	0.30543	0.00518	5.47E-05	2.46E-07	0.99063	0.01681	0.99887	0.00449	43119	99	2.860	0.262	0.27710
RL	0.77969	0.34209	0.02534	0.00007	0.02820	0.00008	0.30554	0.00525	5.47E-05	2.24E-07	0.99098	0.01704	0.99599	0.00409	42465	317	2.860	0.262	0.27665
RM	0.90763	0.25990	0.03481	0.00007	0.03880	0.00010	0.30604	0.00522	5.47E-05	2.67E-07	0.99260	0.01693	0.99901	0.00488	42497	225	2.860	0.262	0.27873
RN	0.84675	0.34275	0.02601	0.00013	0.03098	0.00005	0.30375	0.00532	5.52E-05	3.03E-07	0.98519	0.01725	1.00875	0.00553	43587	119	2.888	0.260	0.27873
RP	0.89695	0.43998	0.02231	0.00006	0.02502	0.00010	0.30797	0.00537	5.50E-05	2.57E-07	0.99586	0.01742	1.00533	0.00470	44462	272	2.797	0.250	0.27710
													0.99755		43391		2.852	0.258	0.27599
						Average	0.30575		5.48E-05		0.99906		0.00929		1317		0.054	0.009	0.00503
						2 s g	0.00300		4.49E-07		0.01490		0.00310						0.00178
						2 S E.													

APPENDIX 5.3 DATA ON STANDARDS

NBS 005a URANIUM STANDARD

Sample	Sample Weight	WL96 Weight	Measure 235/238	FF 235/238	FF 235/236	True 235/236	Corr. 236/238	Corr. 234/236	SM238/ SK236	Corrected 234/238	+/- 2 sig	U conc ppm
M	0.7592	0.9086	0.00520	0.9931	0.9957	2.2275	0.00229	0.0149	437.63	3.41E-05	1.98E-07	2.283
N	1.0807	1.0614	0.00518	0.9939	0.9941	2.6026	0.00196	0.0175	511.32	3.42E-05	1.72E-07	2.276
O	0.8679	0.9771	0.00519	0.9937	0.9965	2.2804	0.00223	0.0153	448.02	3.42E-05	2.12E-07	2.286

Note: SM238/SK236 means "Sample 238 / Spike 236" ratio

JC1 PRACTISE SAMPLE

Sample	Sample weight	WL96 weight	Age	-2 sig	+2 sig	230/234 At.rat	+/- 2 sig	234/238 At.rat	+/- 2 sig	230/234 Act.rat.	+/- 2 sig	234/238 Act.rat.	+/- 2 sig	Initial 234/238	230/232 Act.rat.	+/- 2 sig	U conc ppm	Th conc ppb
JC1A:C	1.1767	0.9308	403125	37500	65625	0.3016	0.0031	5.51E-05	1.98E-07	0.9781	0.0101	1.0067	0.0036	1.0211	1616	5	0.7589	0.9509
JC1B:C	1.4346	0.8968	356250	37500	56250	0.2973	0.0046	5.51E-05	1.71E-07	0.9643	0.0149	1.0067	0.0031	1.0184	1777	12	0.7442	0.7590
JC1J:F	1.0998	0.7415						5.50E-05	1.87E-07			1.0054	0.0034				0.7411	
JC1K:F	1.6551	0.7080	459375	98437	140625	0.3052	0.0066	5.53E-05	1.66E-07	0.9698	0.0213	1.0112	0.0030	1.0412	1984	24	0.7632	0.7531
JC1H:F	1.2728	0.7175	431250	89062	168750	0.3048	0.0076	5.57E-05	2.39E-07	0.9687	0.0247	1.0187	0.0044	1.0633	1416	19	0.7680	1.4740

Note: The suffix "C" after the sample name means "column chemistry only, "F" means "ferric chloride"

76001 MCMASTER SPELEOTHEM STANDARD

Date	Sample	Weight sample	Weight WL96	Age	-2 sig	+2 sig	%error 1 sigma	At.ratio 230/234	+/- 2 sig	At.ratio 234/238	+/- 2 sig	Act.rat. 230/234	+/- 2 sig	Act.rat. 234/238	+/- 2 sig	Act.rat. 230/232	+/- 2 sig	Initial 234/238	+/- 2 sig	U conc ppm	Th conc ppb	Th run 1 sig %error	Th run No. of scans
1/11/88	E:F	1.68	0.98	47315	1465	1465	1.55	0.11215	0.00290	1.050E-04	2.535E-07	0.36376	0.00941	1.91807	0.00463	360	4	2.0499	0.0097	0.7952	8.2580	0.55	36
1/11/88	D:C	1.26	0.74	42335	1099	1172	1.34	0.10228	0.00230	1.051E-04	4.759E-07	0.33174	0.00746	1.92142	0.00870	393	9	2.0389	0.0132	0.7830	7.1040	0.45	73
	F:F	1.03	0.85	48927	2271	2344	2.36	0.11529	0.00441	1.052E-04	6.740E-07	0.37394	0.01431	1.92305	0.01232	426	17	2.0604	0.0211	0.7919	8.1373	0.71	18
	G:F	1.15	0.79	48634	1025	952	1.02	0.11467	0.00190	1.051E-04	4.585E-07	0.37191	0.00616	1.92008	0.00838	387	6	2.0561	0.0126	0.7915	8.2970	0.29	60
	C:C	1.11	0.76	45411	1318	1392	1.49	0.10848	0.00270	1.053E-04	2.892E-07	0.35184	0.00877	1.92502	0.00528	411	10	2.0521	0.0101	0.7811	7.4460	0.47	73
			ST96																				
16/4/89	X:C	1.63	0.19	47120	733	738	0.78	0.11175	0.00143	1.045E-04	3.643E-07	0.36246	0.00464	1.91043	0.00666	222	3	2.0405	0.0022	0.7786	7.7640	0.61	65
16/4/89	Z:C	1.55	0.20	46226	1338	1353	1.46	0.11002	0.00264	1.054E-04	5.435E-07	0.35684	0.00857	1.92596	0.00993	212	5	2.0556	0.0040	0.7788	8.0570	1.18	39

Average age = 46567 +/- 4477, 2S.E. = 1692

Note: The suffix "C" after the sample name means "column chemistry only, "F" means "ferric chloride"

Continued on next page

REAGENT CONTAMINATION TEST RESULTS

Data required:

Spike	235/236 ratio	235/236 ratio	No.atoms 235U per g	No.atoms 236U per g	No.atoms 238U per g	232/229 ratio	No.atoms 232Th per g	No.atoms 229Th per g
WL96	7.4E-05	0.00224	8.44E+06	1.14E+11	2.55E+08	1.31E+00	7.06E+10	5.4E+10
ST96		0.00296		3.53E+11	1.05E+09	9.09E-04	9.27E+07	1.02E+11

Results:

Treatment	Spike	Weight	No.atoms 235U from spike	No.atoms 236U from spike	No.atoms 238U from spike	Measured 235/236	Measured 238/236	No.atoms 235U from reagent	No.atoms 238U from reagent	No.atoms 229Th from spike	No.atoms 232Th from spike	Measured 232/229	No.atoms 232Th from reagent
FeCl3	WL96	1.9176	1.62E+07	2.19E+11	4.89E+08	0.00036	0.0444	6.26E+07	9.23E+09	1.04E+11	1.358E+11	1.3405	3.61E+09
Columns	ST96	0.5816		2.05E+11	6.07E+08		0.0138		2.22E+09	5.932E+10	5.39E+07	0.0378	2.19E+09

APPENDIX 5.4: BAHAMAS FLOWSTONE DWBAH

Date of run	Sample	Position mm	Age	-2sig	+2sig	Range from	to	%error 1 sig	234/238 Atrat	+/- 2 sig	230/234 Atrat	+/- 2 sig	234/238 Act.	+/- 2 sig	230/234 Act.	+/- 2 sig	230/232 Act.	+/- 2 sig	Initial 234/238	+/- 2 sig	U conc ppm	Th conc ppb	Th run 1 sig % error
1/11/88	1	49	196876	7031	7031	189845	203907	1.8	5.84E-05	2E-07	0.262	0.003	1.068	0.003	0.849	0.011	200	3	1.119	0.008	0.141	3.691	0.23
1/5/88	2	53	176954	9375	11133	167579	188687	2.9	5.84E-05	2E-07	0.251	0.006	1.067	0.003	0.815	0.019	362	9	1.111	0.008	0.130	2.625	0.23
1/6/88	4	60	164063	9961	11719	154102	175782	3.3	5.81E-05	3E-07	0.243	0.007	1.063	0.005	0.789	0.023	1499	44	1.100	0.012	0.115	0.097	0.28
29/3/89	5	64	176954	9961	10547	166993	187501	2.9	5.82E-05	2E-07	0.251	0.006	1.063	0.003	0.814	0.019	682	7	1.104	0.008	0.128	0.757	0.48
1/11/88	6	69	168165	4102	4102	164063	172267	1.2	5.80E-05	2E-07	0.245	0.003	1.061	0.003	0.796	0.009	562	6	1.098	0.006	0.143	1.116	0.14
6/2/89	7	74	94337	8203	8789	86134	103126	4.5	5.82E-05	3E-07	0.180	0.010	1.064	0.005	0.584	0.033	849	19	1.083	0.009	0.146	0.476	1.11
6/2/89	8/9	78	129493	4391	4394	125099	133887	1.7	5.78E-05	2E-07	0.216	0.004	1.057	0.003	0.702	0.012	2202	13	1.083	0.005	0.133	0.015	0.30
1/5/88	10	84	144141	9375	10547	134766	154688	3.5	5.78E-05	2E-07	0.229	0.008	1.056	0.004	0.741	0.025	1466	49	1.084	0.008	0.125	0.056	0.46
1/5/88	10	85	138868	9961	10547	128907	149415	3.7	5.77E-05	2E-07	0.224	0.008	1.055	0.003	0.728	0.027	1635	60	1.082	0.007	0.129	0.138	0.47
1/6/88	11	88	188672	5273	4687	183399	193359	1.4	5.87E-05	2E-07	0.260	0.003	1.073	0.004	0.844	0.009	67	1	1.126	0.012	0.205	15.149	0.20
1/11/88	12	95	133595	2344	2344	131251	135939	0.9	5.85E-05	1E-07	0.220	0.002	1.069	0.003	0.715	0.006	64	1	1.101	0.005	0.276	16.661	0.18
1/11/88	13	100	92579	2637	2344	89942	94923	1.3	5.82E-05	2E-07	0.178	0.003	1.064	0.004	0.577	0.010	196	3	1.084	0.005	0.164	4.348	0.16
1/6/88	14	103	70606	3809	4102	66797	74708	2.8	5.79E-05	3E-07	0.148	0.006	1.058	0.006	0.480	0.019	1459	59	1.071	0.008	0.148	0.077	0.35
1/5/88	14	104	64454	4395	4395	60059	68849	3.4	5.81E-05	2E-07	0.138	0.007	1.062	0.003	0.449	0.023	1395	70	1.074	0.005	0.146	0.098	0.44
1/11/88	15	109	64161	1172	1172	62989	65333	0.9	5.81E-05	2E-07	0.138	0.002	1.061	0.005	0.448	0.006	1250	17	1.073	0.006	0.185	0.215	0.16
1/6/88	16	114	64015	5273	5566	58742	69581	4.2	5.80E-05	2E-07	0.138	0.009	1.061	0.004	0.447	0.003	1236	77	1.073	0.006	0.149	0.192	0.60
1/11/88	17	119	50977	4960	5127	45997	56104	5.0	5.66E-05	2E-07	0.116	0.009	1.023	0.003	0.375	0.029	799	63	1.039	0.004	0.084	0.319	0.67
1/11/88	18	126	39112	1392	1392	37720	40504	1.8	5.75E-05	2E-07	0.093	0.003	1.051	0.004	0.303	0.009	237	7	1.057	0.005	0.116	1.893	0.16
6/2/89	F	83	142970	3516	2930	139454	145900	1.1	5.78E-05	2E-07	0.228	0.002	1.057	0.004	0.738	0.008	1864	5	1.085	0.006	0.158	0.085	0.13
6/2/89	G	78	145899	4688	4688	141211	150587	1.6	5.81E-05	3E-07	0.230	0.004	1.061	0.005	0.746	0.012	2484	18	1.092	0.009	0.182	0.024	0.36
6/2/89	H	71	148829	4102	4688	144727	153517	1.5	5.81E-05	2E-07	0.233	0.003	1.061	0.004	0.754	0.010	2642	18	1.094	0.007	0.204	0.032	0.35
29/3/89	I	66	140040	5859	5272	134181	145313	2.0	5.81E-05	2E-07	0.225	0.004	1.062	0.004	0.731	0.014	2461	21	1.092	0.007	0.201	0.020	0.42
16/1/89	N	26	226173	8203	8203	217970	234376	1.8	5.78E-05	2E-07	0.274	0.003	1.056	0.003	0.887	0.010	228	3	1.106	0.009	0.205	4.535	0.22
6/2/89	P	14	241407	7031	7031	234376	248438	1.5	5.77E-05	2E-07	0.279	0.002	1.054	0.003	0.904	0.007	1567	3	1.107	0.009	0.257	0.366	0.11
29/3/89	Q	8	236719	11718	14062	225001	250781	2.7	5.77E-05	3E-07	0.277	0.004	1.055	0.006	0.899	0.013	854	7	1.108	0.016	0.340	1.331	0.41
10/1/89	Q	9	269532	21094	25781	248438	295313	4.3	5.75E-05	1E-07	0.287	0.006	1.051	0.002	0.929	0.019	963	19	1.110	0.012	0.336	1.196	0.54
10/1/89	R	2	323126	18750	23437	309376	351563	3.2	5.75E-05	2E-07	0.298	0.003	1.052	0.004	0.967	0.010	133	1	1.131	0.018	0.377	12.239	0.32
16/1/89	A1	45	208594	22266	28125	186328	236719	6.0	5.73E-05	3E-07	0.266	0.011	1.046	0.005	0.862	0.034	1285	51	1.084	0.016	0.093	0.191	0.81
10/1/89	T1	41	239063	19922	23437	219141	262500	4.5	5.79E-05	2E-07	0.278	0.007	1.057	0.003	0.902	0.023	1573	40	1.113	0.014	0.144	0.188	0.54
6/2/89	T2	38	225000	11718	15234	213282	240234	3.0	5.78E-05	2E-07	0.273	0.005	1.058	0.003	0.887	0.016	1215	8	1.109	0.011	0.139	0.337	0.34
16/1/89	T4	27	225001	7031	5859	217970	230660	1.4	5.79E-05	3E-07	0.273	0.002	1.059	0.005	0.885	0.008	173	2	1.112	0.012	0.224	1.353	0.16
29/3/89	T4	26	222657	9375	8203	213282	230660	2.0	5.79E-05	1E-07	0.272	0.003	1.058	0.002	0.882	0.010	223	1	1.109	0.007	0.205	4.399	0.25
29/3/89	B1	18	240235	9275	10547	230960	250782	2.1	5.78E-05	2E-07	0.278	0.003	1.057	0.004	0.903	0.010	769	3	1.112	0.011	0.216	1.136	0.17
29/3/89	B2	6	274219	9375	9375	264844	283594	1.7	5.74E-05	3E-07	0.287	0.002	1.050	0.005	0.932	0.007	186	1	1.108	0.015	0.157	3.604	0.18
16/1/89	Y	95	108399	2930	3223	105469	111622	1.4	5.71E-05	2E-07	0.196	0.003	1.044	0.003	0.635	0.011	278	5	1.060	0.004	0.245	3.389	0.32

APPENDIX 5.5 WIND CAVE WALL CRUST, WC-MAJ

Date	Sample	Position mm	Age	-2 sig	+2 sig	Range from	to	% Error 1 sig	Act.rat 230/234	+/- 2 sig	Act.rat 234/238	+/- 2 sig	Act.rat 230/232	+/- 2 sig	Act.rat 234/238	+/- 2 sig	Act.rat 230/232	+/- 2 sig	Init.act 234/238	+/- 2 sig	U conc ppm	Th conc ppb	Th run 1 sig % error	Th run No. of scans
RUN A																								
10/4/89	WA1	19	171249	2049	2085	170224	172291	0.60	0.2649	0.0014	9.08E-05	1.9E-07	0.8591	0.005	1.6601	0.0035	12855	61	2.0727	0.01	4.28	1.62	0.18	47
10/4/89	WA2	15	176579	3805	3924	174676	178541	1.09	0.2689	0.0027	9.14E-05	1.4E-07	0.8721	0.009	1.6707	0.0026	134347	1588	2.1065	0.01	4.11	0.04	0.32	55
10/4/89	WA3	11	194847	3414	3511	193140	196602	0.89	0.2803	0.0020	8.98E-05	1.7E-07	0.9090	0.007	1.6416	0.0031	111719	1804	2.1147	0.01	3.70	0.25	0.21	15
10/4/89	WA4	6	232424	8150	8711	228349	236780	1.81	0.2977	0.0037	8.50E-05	1.3E-07	0.9655	0.012	1.5543	0.0024	51499	796	2.0713	0.03	4.24	0.50	0.53	28
10/4/89	WA5	2	289120	13717	15392	282262	296816	2.52	0.3140	0.0039	7.93E-05	1.5E-07	1.0186	0.013	1.4491	0.0028	334437	11003	2.0192	0.04	4.53	0.05	0.41	9
RUN B																								
12/6/89	WB1	19	161123	2050	2084	160098	162165	0.64	0.2574	0.0016	9.18E-05	1.5E-07	0.8350	0.005	1.6770	0.0028	27386	166	2.0689	0.01	4.26	0.80	0.23	76
12/6/89	WB5	2	255592	9470	10245	250856	260714	1.93	0.3036	0.0035	7.95E-05	1.1E-07	0.9846	0.011	1.4531	0.0020	103643	1185	1.9351	0.03	4.59	0.09	0.39	101
RUN C																								
10/5/89	WCa	20	131023	2706	2766	129670	132406	1.04	0.2303	0.0027	9.09E-05	1.5E-07	0.7469	0.009	1.6617	0.0027	2272	27	1.9593	0.01	4.30	7.59	0.52	24
10/5/89	WCb	18	162810	3683	3794	160969	164707	1.15	0.2588	0.0029	9.20E-05	1.7E-07	0.8395	0.009	1.6808	0.0031	31946	449	2.0802	0.01	4.21	0.69	0.42	36
12/12/89	WCe*	12	176596	2076	2113	174520	178709	0.59	0.2686	0.0014	9.04E-05	2.2E-07	0.8710	0.005	1.6526	0.0040			2.0767	0.01	4.14		0.17	102
10/5/89	WCf	10	209732	7874	8390	205794	213927	1.94	0.2887	0.0043	8.95E-05	1.3E-07	0.9364	0.014	1.6364	0.0023	13901	243	2.1533	0.03	3.40	1.28	0.61	30
12/12/89	WCf*	10	208419	5225	5454	203194	213873	1.28	0.2881	0.0028	8.98E-05	2.4E-07	0.9344	0.009	1.6407	0.0044			2.1569	0.02	3.34		0.45	33
10/5/89	WCg	8	224684	3656	3766	222855	226567	0.83	0.2952	0.0017	8.72E-05	1.1E-07	0.9575	0.006	1.5935	0.0021	37004	236	2.1222	0.01	3.97	0.63	0.18	91
12/12/89	WCg,h*	7	235606	3460	3564	232145	239170	0.75	0.2987	0.0014	8.44E-05	2.1E-07	0.9689	0.005	1.5428	0.0038			2.0586	0.01	4.23		0.13	43
21/11/89	WCi,j*	3	286527	16444	18891	270084	305418	3.08	0.3141	0.0049	8.03E-05	1.5E-07	1.0187	0.016	1.4677	0.0027			2.0539	0.05	4.48		0.84	44
12/12/89	WCk*	1	310743	11565	12806	299178	323549	1.96	0.3199	0.0025	7.97E-05	4.8E-07	1.0374	0.008	1.4562	0.0087			2.1008	0.04	4.27		0.19	153
RUN D																								
12/6/89	WD1	20	147920	1872	1902	146984	148871	0.64	0.2458	0.0016	8.96E-05	1.4E-07	0.7972	0.005	1.6382	0.0026	232	1	1.9707	0.01	3.93	70.65	0.27	92

The asterisk * indicates runs where some thorium standard was added to provide higher levels of Th-232.
The 1 sigma percentage error on the thorium run (229/230 ratio), the number of scans and the % error (1 sigma) on the age indicates the reliability of that run.
Position is shown in mm above the substrate.

APPENDIX 5.6 RAT'S NEST STALACTITE, 881010

Date	Sample	Wt	Age	-2 sig	+2 sig	Range from	to	% Error 1 sig	Actrat 230/234	+/- 2 sig	Actrat 234/238	+/- 2 sig	Actrat 230/234	+/- 2 sig	Actrat 234/235	+/- 2 sig	Actrat 230/232	+/- 2 sig	Initact 234/238	+/- 2 sig	U conc ppm	Th conc ppb	Th run error % 1sig	Th run No. of scans
											6.80E-05	1.26E-07			1.2423	0.0023					0.520			
18/9/89	B	2.56							0.3314	0.0018	6.72E-05	1.46E-07	1.0748	0.0059	1.2278	0.0027	551	2			0.463	3.551	0.20	170
18/9/89	C	4.19	Infinite						0.3415	0.0071	7.06E-05	1.70E-07	1.1078	0.0231	1.2910	0.0031	724	15			0.229	1.431	1.01	64
18/9/89	D	4.33	Infinite						0.3232	0.0130	7.16E-05	1.74E-07	1.0482	0.0421	1.3094	0.0032	1617	65	1.8876	0.3920	0.243	0.663	1.99	16
18/9/89	E base @	3.65	371725	72624	186628	299102	558354	17.44			7.12E-05	1.54E-07			1.3004	0.0028					0.280			
9/10/89	E middle	4.29									7.44E-05	2.00E-07			1.3596	0.0036					0.240			
1/6/89	E top	1.44																						
18/11/89	E top	2.91	385083	25851	32576	359232	417659	3.79	0.3284	0.0033	7.49E-05	2.79E-07	1.0653	0.0108	1.3687	0.0051	690	6	2.0986	0.0920	0.2295	1.552	0.44	72
10/10/89	G2 base *	3.74	212237	6041	6337	209216	215405	1.46	0.2952	0.0034	1.03E-04	2.93E-07	0.9576	0.0109	1.8792	0.0054	13	3	2.6047	0.0282	0.180	82.230	0.53	129
23/7/89	G base	5.53	214546	5277	5500	209269	220045	1.26	0.2975	0.0029	1.06E-04	2.52E-07	0.9649	0.0094	1.9324	0.0046	1912	18	2.7131	0.0262	0.175	0.550	0.44	48
1/6/89	G2 top	2.91									1.06E-04	2.69E-07			1.9377	0.0049					0.195			
18/11/89	G2 top	4.78	211051	2542	2594	208509	213645	0.61	0.2955	0.0014	1.06E-04	2.12E-07	0.9583	0.0045	1.9294	0.0039	1158	4	2.6906	0.0123	0.1973	1.011	0.15	144
18/9/89	G2 top *	3.55	115968	2070	2104	114933	117020	0.90	0.2193	0.0025	1.25E-04	2.86E-07	0.7113	0.0060	2.2929	0.0052	5	5	2.7961	0.0106	0.323	338.000	0.53	111
12/6/89	H1 base *	2.93	157160	1843	1870	155318	159031	0.59	0.2576	0.0015	1.05E-04	2.09E-07	0.8354	0.0049	1.9102	0.0038	5	7	2.4211	0.0075	0.291	296.750	0.23	126
10/10/89	H1 middle	3.85									1.04E-04	2.73E-07			1.9043	0.0050					0.249			
10/10/89	J base	2.35	3843	231	231	3728	3959	3.00	0.0107	0.0006	1.53E-04	3.00E-07	0.0348	0.0021	2.7996	0.0055	33	2	2.8190	0.0012	0.343	326.148	2.96	30
10/10/89	J top	3.40									1.53E-04	3.06E-07			2.7942	0.0056					0.294			

Note: @ indicates a run with high error
* indicates a detrital sample

Sample	U/U AGE	-2 sig	+2 sig
	Initial UU = 2.1		
B	533647	34151	31706
C	555568	34905	32477
D	469045	34558	32123
E base @	447875	34428	31989
E middle	458301	34085	31640
E top	394971	34375	31936
	Initial UU = 2.7		
G2 top *	207753	4419	4409
H1 base *	220437	4038	4026
H1 middl	222771	4503	4495

APPENDIX 5.7 CORALS

Date	Sample	Wt	Age	-2sig	+2sig	Range from	to	% Error 1 sig	Atrat 230/234	+/- 2 sig	Atrat 234/238	+/- 2 sig	Actrat 230/234	+/- 2 sig	Actrat 234/238	+/- 2 sig	Actrat 230/232	+/- 2sig	Initact 234/238	+/- 2sig	U conc ppm	Th conc ppb	No of scans	Th run % error 1 sig
75036 Test sample																								
24/4/89	1bBA	1.43	142943	1981	2019	142677	145606	0.70	0.2294	0.0015	6.06E-05	8.46E-08	0.7441	0.0050	1.1073	0.002	986	6	1.1609	0.0009	2.55	0.68	38	0.27
24/4/89	1dBA	1.63	146794	2138	2181	144656	148975	0.74	0.2326	0.0016	6.08E-05	8.77E-08	0.7543	0.0052	1.1106	0.002	3667	25	1.1677	0.0010	2.41	1.79	33	0.27
24/4/89	1dNA	1.42	199275	2177	2223	197098	201497	0.55	0.2650	0.0010	6.07E-05	9.44E-08	0.8596	0.0032	1.1100	0.002	9571	15	1.1935	0.0012	2.38	0.80	102	0.05
24/4/89	1fBA	1.53	319817	10094	11099	309722	330916	1.66	0.3016	0.0017	6.08E-05	1.06E-07	0.9783	0.0054	1.1119	0.002	2200	11	1.2772	0.0083	1.48	2.36	17	0.18
790513-2 Gascoyne's sample																								
12/6/89	A	0.40	127443	2850	2928	124593	130371	1.13	0.2161	0.0026	6.04E-05	1.2E-07	0.7008	0.0084	1.1037	0.002	13385	164	1.1488	0.0012	2.96	0.58	42	0.54
23/7/89	M3	0.75	117613	934	943	116679	118556	0.40	0.2067	0.0009	6.05E-05	1.0E-07	0.6705	0.0029	1.1051	0.002	26227	98	1.1467	0.0004	2.99	0.31	91	0.17
23/7/89	M4 #	1.09	121163	4826	5047	116337	126210	2.04	0.2102	0.0047	6.06E-05	1.0E-07	0.6819	0.0153	1.1066	0.002	20018	480	1.1504	0.0021	3.02	0.40	28	1.05
23/7/89	M6 @	2.42	123392	7451	7991	115941	131383	3.13	0.2124	0.0072	6.05E-05	1.5E-07	0.6887	0.0235	1.1056	0.003	17215	600	1.1499	0.0033	3.00	0.46	28	1.70
Lynton Land's Corals																								
18/11/89	D3A *	0.62	138467	2745	2817	135722	141284	1.00	0.2266	0.0023	6.21E-05	1.3E-07	0.7351	0.0073	1.1350	0.002			1.1999	0.0016	3.24		79	0.46
21/11/89	D3B	1.04	133032	1323	1342	131709	134374	0.50	0.2218	0.0011	6.18E-05	2.0E-07	0.7195	0.0035	1.1298	0.004	21175	67	1.1893	0.0007	3.20	0.44	61	0.13
18/11/89	D3C	1.51	131817	1508	1532	130309	133349	0.58	0.2208	0.0012	6.18E-05	1.9E-07	0.7160	0.0041	1.1301	0.004	4696	21	1.1890	0.0008	3.20	1.80	78	0.21
26/6/89	VI	0.98	Th failed								6.08E-05	1.2E-07			1.1114	0.002					3.38			
28/10/89	VIA *	0.74	125605	1828	1661	123777	127466	0.73	0.2146	0.0016	6.06E-05	1.4E-07	0.6960	0.0053	1.1117	0.003			1.1592	0.0008	3.48		147	0.34
18/11/89	VIC	1.59	124948	1166	1181	123782	126129	0.47	0.2143	0.0010	6.15E-05	1.9E-07	0.6950	0.0033	1.1231	0.004	41106	110	1.1755	0.0006	3.48	0.26	171	0.08

Abnormal 235/238 measured ratio
* indicates runs where some thorium standard was added
@ indicates a run with high error

APPENDIX 5.8 CARLSBAD LAKE OF CLOUDS, CALCITE RAFT MATERIAL

Date	Sample	Wt.	Age	-2sig	+2sig	Range from	to	% Error 1 sig	Act.rat 230/234	+/- 2 sig	Act.rat 234/238	+/- 2sig	Act.rat 230/234	+/- 2sig	Act.rat 234/238	+/- 2sig	Act.rat 230/232	+/- 2sig	Initial 234/238	+/- 2sig	U conc ppm	Th conc ppb	Th run error % 1sig	Th run No. of scans
24/4/89	CLC1	7.95	115431	1758	1758	113673	117189	0.76	0.2015	0.0018	5.45E-05	1.74E-07	0.6535	0.0058	0.9951	0.0032	1037	3	0.9932	0.0044	0.259	0.519	0.15	55
2.6.89	2CLC	6.38	199219	8203	10547	191016	209766	2.35	0.2586	0.0039	5.42E-05	3.10E-07	0.8389	0.0127	0.9911	0.0057	111	1	0.9843	0.0096	0.272	6.463	1.14	43

APPENDIX 5.9 OSTRICH EGGS

Date	Sample	Wt.	Age	-2 sig	+2 sig	Range from	to	% Error 1 sig	Act.rat 230/234	+/- 2sig	Act.rat 234/238	+/- 2sig	Act.rat 230/234	+/- 2sig	Act.rat 234/238	+/- 2sig	Act.rat 230/232	+/- 2sig	Initial 234/238	+/- 2sig	U conc ppm	Th conc ppb	Th run error % 1sig	Th run No. of scans
26/6/89	Egg 41	0.94	128506	8089	8907	120417	137413	3.31	0.2015	0.0061	4.06E-05	1.15E-07	0.6535	0.0198	0.7420	0.0022	53	2	0.6286	0.0090	0.483	14.223	1.50	34
	corrected		125844	7864	8634	117980	134478						0.6471	0.0198					0.6313	0.0055				
10/7/89	Egg 42	0.50	136004	6171	6654	129833	142658	2.36	0.2065	0.0042	4.04E-05	1.31E-07	0.6698	0.0135	0.7375	0.0024	529	11	0.6141	0.0070	6.939	20.735	1.14	43
10/7/89	Egg 43	0.60	122174	2797	2899	119377	125073	1.42	0.1968	0.0021	4.07E-05	1.55E-07	0.6382	0.0068	0.7437	0.0028	743	7	0.6376	0.0029	4.276	8.745	0.49	76
26/6/89	Egg 44	0.46	134972	4149	4370	130823	139342	1.58	0.2060	0.0027	4.05E-05	1.44E-07	0.6682	0.0069	0.7406	0.0026	279	4	0.6197	0.0046	5.281	29.914	0.63	80
	corrected		134447	4124	4343	130323	138790						0.6670	0.0069					0.6203	0.0007				
10/7/89	Egg 48		No detectab. ; Th230																					

Note: Where a "corrected" age appears it has been corrected assuming an initial 230/232 activity of 1.7